PALEOCOMMUNITY RESPONSE TO EXTINCTION:

AN EXAMPLE FROM THE LATE ORDOVICIAN (MOHAWKIAN) OF

THE APPALACHIAN BASIN OF THE EASTERN UNITED STATES

by

KAREN M. LAYOU

(Under the Direction of Steven M. Holland)

ABSTRACT

A regional extinction occurred among marine macroinvertebrate taxa during the Late Ordovician in eastern North America. Previously unexamined changes to the diversity structure of paleocommunities across the extinction boundary were quantitatively addressed through the development of null models of changes in diversity and evenness metrics as functions of percent extinction. The model results were compared to analyses of field censused paleocommunities from shallow and deep subtidal facies within three regions of the Appalachian Basin, including the Jessamine Dome of central Kentucky, the Nashville Dome of central Tennessee, and the Valley and Ridge of western Virginia.

The null models show that variations in the evenness metric, Pielou's *J*, and variations in the relationship between alpha diversity and the highest level of beta diversity within a sampling hierarchy, are unique to different conditions of extinction selectivity with respect to taxon abundance. Field data from the entire basin suggest this extinction targeted rare taxa, however, at some local scales, abundant taxa appear

to be more affected. The field data also highlight a number of geographic and environmental variations in paleocommunity response to this extinction. Deep subtidal communities in Virginia were most significantly affected during this event. In general, across the extinction boundary, the diversity and evenness metrics decline, the taxonomic composition of paleocommunities shifts, and relative abundances of taxa within ecological guilds varies. Despite these factors, the extinction led to minimal changes in the relative abundance distribution of taxa within paleocommunities, given the small magnitude of change in diversity and evenness metrics. These quantitative analyses highlight the complexity and variability in paleoecological response to the extinction.

INDEX WORDS: Biodiversity, Paleocommunity, Extinction, Selectivity, Recovery, Evenness, Null model, Ordovician, Mohawkian

PALEOCOMMUNITY RESPONSE TO EXTINCTION:
AN EXAMPLE FROM THE LATE ORDOVICIAN (MOHAWKIAN) OF THE APPALACHIAN BASIN OF THE EASTERN UNITED STATES

by

KAREN M. LAYOU

B.S., Pennsylvania State University, 1999

M.S., University of Cincinnati, 2001

A Dissertation Submitted to the Graduate Faculty of The University of Georgia in Partial Fulfillment of the Requirements for the Degree

DOCTOR OF PHILOSOPHY

ATHENS, GEORGIA

2007

PALEOCOMMUNITY RESPONSE TO EXTINCTION:

AN EXAMPLE FROM THE LATE ORDOVICIAN (MOHAWKIAN) OF

THE APPALACHIAN BASIN OF THE EASTERN UNITED STATES

by

KAREN M. LAYOU

Major Professor: Steven M. Holland

Committee: Susan T. Goldstein
Mark E. Patzkowsky
L. Bruce Railsback
Sally E. Walker

Electronic Version Approved:

Maureen Grasso
Dean of the Graduate School
The University of Georgia
May 2007

DEDICATION

To

A and B

For giving me the best motivation possible

ACKNOWLEDGEMENTS

The completion of this degree fulfills a promise I made to myself almost fourteen years ago. Its culmination, however, could not have been possible, or anywhere close to enjoyable, without the support of a myriad of colleagues, friends, and family.

Deep gratitude and thanks are given to my major advisor, Dr. Steve Holland. From our initial email contact, he has been interested in my ideas and supportive of my work. While giving me space to proceed independently, he has consistently been accessible and has offered invaluable direction, not only on this project, but for my career and future as well. Thank you for pushing (and pulling) me as needed (R!).

Thanks to my advisory committee, Drs. Sue Goldstein, Sally Walker, and Bruce Railsback for guidance through various aspects of this project, and offering me a variety of unique research and teaching opportunities throughout my studies at UGA. Special thanks are offered to my non-UGA committee member, Dr. Mark Patzkowsky for stopping to chat with me one October afternoon in 1996 when I was an undergrad at Penn State. His welcoming of me to the Department of Geology, and later advisement and encouragement to try grad school, was integral to where I am today.

To my fellow graduate students, I have enjoyed the companionship and laughs. Infinite thanks to my paleo buddy, Noel Heim, for being my sounding board on productive days and my partner in procrastination on not-so-productive days. I seriously could not have survived the basement without you!

This list would not be complete without mention of my dear friend, Dr. Donna C. Jones. This is the second degree that she has mentored me through, offering a shoulder to lean on when the balance of life gets a bit too wobbly to handle on my own.

Finally, it is almost absurd to try to put into words the appreciation, gratitude, and thanks I offer to my husband, Dann. His constant love has created the strongest of foundations on which I can stand and reach for my dreams.

Financial support for this work was generously awarded by the Geological Society of America, Sigma Xi Grants in Aid of Research, Paleontological Society Stephen J. Gould Student Grant-in-Aid Program, American Museum of Natural History Theodore Roosevelt Memorial Fund and the University of Georgia Department of Geology Wheeler-Watts Fund.

TABLE OF CONTENTS

Page

ACKNOWLEDGEMENTS v

LIST OF TABLES x

LIST OF FIGURES xii

CHAPTER

1 INTRODUCTION AND LITERATURE REVIEW 1

Statement of Objectives 2

Dissertation Structure 3

Literature Cited 5

2 A QUANTITATIVE NULL MODEL OF EXPECTED CHANGES IN PALEOCOMMUNITY EVENNESS FOLLOWING EXTINCTION 7

Abstract 8

Introduction 9

Previous Work 11

Diversity Metrics 12

Model Description 14

Model Results 16

Application of Null Model 19

Conclusions 27

Acknowledgements 28

Literature Cited 29

3 A QUANTITATIVE NULL MODEL OF ADDITIVE DIVERSITY PARTITIONING: EXAMINING THE RESPONSE OF BETA DIVERSITY TO EXTINCTION 52

Abstract 53

Introduction 54

Model Description 60

Results 61

Application of Null Model 65

Conclusions 67

Acknowledgements 68

Literature Cited 69

Appendix 72

4 ECOLOGICAL RESTRUCTURING AFTER EXTINCTION: THE LATE ORDOVICIAN (MOHAWKIAN) OF THE EASTERN UNITED STATES 85

Abstract 86

Introduction 87

Methods 92

Results 97

Discussion 103

Conclusions 106

Acknowledgements 108

Literature Cited 109

Appendix 117

5 CONCLUSIONS 147

APPENDICES

A R CODE 151

B C CODE 155

C FIELD LOCALITY REGISTER 208

D FIELD DATA 214

E COLLECTOR CURVES 245

F DATA ANALYSES WITH BRYOZOANS AND CRINOIDS EXCLUDED 247

G TABLES OF MOST ABUNDANT TAXA BY SEQUENCE FOR BOTH FACIES AND ALL REGIONS 256

LIST OF TABLES

Page

Table 2.1: Summary of variations in diversity and evenness metrics from pre-to post-extinction according to each of model selectivity conditions with respect to taxonomic abundance..... 35

Table 2.2: Number and distribution of samples included in field data analyses indicating subsets of geographic region and environment. 36

Table 2.3: Changes in mean diversity and evenness metrics across a regional extinction boundary based on subsampled subsets of field data. 37

Table 2.4: Summary of variations in diversity and evenness metrics across a regional extinction boundary according to field results 39

Table 2.5: Time bins used in mass extinction analyses. Time bins correspond with the Paleobiology Database (PBDB) “10 million year time bin” scale..... 40

Table 2.6: Changes in mean diversity and evenness metrics across mass extinction boundaries based on subsampled global occurrences of genera. 41

Table 2.7: Summary of variations in diversity and evenness metrics across three mass extinction boundaries..... 43

Table 3.1: Comparisons of pre- and post-extinction beta values as calculated by both multiplicative and additive partitioning definitions of β. 73

Table 3.2: Diversity for pre- and post-extinction data across a regional extinction boundary during the Late Ordovician on the Nashville Dome. 74

Table 4.1: Samples included in field data analyses, subsetted by geographic region and facies 119

Table 4.2: Ecological guilds used in this study 120

Table 4.3: Differences in mean diversity and evenness metrics across a regional extinction boundary based on subsampled subsets of field data 121

Table 4.4: Ten most abundant taxa within each sequence ranked by relative abundance 123

Table 4.5: Beta diversity (Jaccard coefficient) for regional comparisons during the M5 and M6 sequences 124

Table 4.6: Changes in mean diversity and evenness metrics across a regional extinction boundary based on subsampled subsets of field data. 125

LIST OF FIGURES

Page

Figure 2.1: Changes in diversity (*H'*), ln*E*/ln*S*, and evenness (*E*, Pielou's *J*, and *PIE*) metrics with increasing magnitude of extinction for three values of initial taxonomic richness (*S*). 44

Figure 2.2: Regional map of Kentucky, Tennessee, and Virginia. 46

Figure 2.3: Time scale modified from Holland and Patzkowsky (1996). 48

Figure 2.4: Number of genera present in each sequence, and within facies and regions for each sequence 50

Figure 3.1: Hierarchical sampling strategy used in the model and field data to calculate additive partitioning of diversity. 75

Figure 3.2: Decrease in α, β, and γ diversity with increasing percent extinction..... 77

Figure 3.3: Diversity partitioning as a function of percent extinction for different probabilities of taxon occurrence 79

Figure 3.4: Diversity partitioning as a function of percent extinction for different modes of extinction..... 81

Figure 3.5: Diversity partitioning for pre- and post-extinction conditions across a regional extinction boundary in the Late Ordovician Nashville Dome 83

Figure 4.1: Time scale for the Late Ordovician of the Appalachian Basin, indicating the six third-order depositional sequences for the Mohawkian Series, modified from Holland and Patzkowsky (1996) 127

Figure 4.2: Regional map of Kentucky, Tennessee, and Virginia 129

Figure 4.3: Number of genera present in each sequence, and within facies and regions in each sequence 131

Figure 4.4: Diversity and evenness metrics among depositional sequences including the extinction boundary (M4 to M5 transition) and into the following sequence (M5 to M6 transition). 133

Figure 4.5: Diversity and evenness metrics within facies of depositional sequences.. 135

Figure 4.6: Diversity and evenness metrics within regions and depositional sequences. 137

Figure 4.7: Relative abundances of guilds in subsets of the field data. 139

Figure 4.8: MDS ordination of all samples, coded by depositional sequence (A; stress: 27.186) and with centroids of all samples within facies within depositional sequence (B).. 141

Figure 4.9: MDS ordinations of geographic regions by depositional sequence 143

Figure 4.10: MDS ordinations of shallow subtidal samples from Tennessee and Kentucky 145

CHAPTER 1

INTRODUCTION AND LITERATURE REVIEW

Statement of Objectives

Many studies have been done on global mass extinctions throughout the Phanerozoic (e.g. Raup and Sepkoski 1982, 1984; Sepkoski 1986; Jablonski 1995,1996, 2001, 2005), but relatively few have been concerned with the biotic recovery after such an event (Erwin 1996, 1998, 2001; Hart 1996; Hallam and Wignall 1997). Even fewer have focused on the smaller, regional extinction and recovery events within the fossil record that are more comparable in spatial scale to those affecting present-day ecosystems. Although regional events are typically considered as part of "background" extinction, they are responsible for more than 95 percent of all species extinctions during the Phanerozoic (Raup 1992). Additionally, most previous work on extinctions has focused on qualitative taxonomic data, often restricting discussion to a single higher taxonomic group, rather than quantitative paleoecological approaches that incorporate data regarding paleocommunity-level information (but see Droser et al. 2000; Bottjer 2001).

During the Late Ordovician (Mohawkian), a regional extinction occurred among many marine macroinvertebrate taxa within the Appalachian Basin of eastern North America (Patzkowsky and Holland 1993, 1996). This extinction event was concurrent with the onset of physical changes associated with the Taconic orogeny, including an influx of siliciclastic sediment, an increase in phosphate deposition, and a shift from tropical-type to temperate-type carbonate deposition (Holland and Patzkowsky 1997). Although the taxonomic turnover of the biotic extinction has been well-documented (Patzkowsky and Holland 1993, 1996 1997), the paleoecology of not only the extinction,

but also the following recovery period, has not been addressed, specifically in the context of a quantitative, community-level paleoecological approach.

To provide a paleoecological understanding of the Mohawkian extinction and the subsequent recovery interval, the objective of this research is to explore quantitatively how marine macroinvertebrate paleocommunities respond to a regional extinction event, in terms of changes to relative abundance distributions of taxa and the resulting variation to diversity and evenness metrics, changes within and among ecological guilds, and changes in paleocommunity taxonomic composition. These variations are examined in the context of a sequence stratigraphic framework that ensures direct comparison of these paleocommunities within facies and among geographic regions of the Appalachian foreland basin. The coupling of paleocommunity level analyses with paleoenvironmental data shifts the focus away from the compartmentalizing taxonomic approach to understanding biotic response to extinction, and toward a quantitative framework that can be used to make predictions about paleocommunity responses to extinction events on a variety of spatial and temporal scales.

Dissertation Structure

Biotic response to extinction is first presented in a pair of null models that examine the variation in diversity and evenness metrics, and thus, relative abundance distributions (Chapter 2), and the partitioning of beta diversity (Chapter 3), within paleocommunities as a function of percent extinction. These models provide a sense of the magnitude of change expected in these quantitative parameters used to define paleocommunities, and also address the larger question of selectivity with respect to

taxon abundances across extinction boundaries. Each of these models is then applied to field data of macroinvertebrate abundances collected across the Mohawkian extinction boundary to show how these methods may be used to analyze an extinction. Finally, the paleoecology of the Mohawkian extinction and subsequent recovery interval is examined in the context of variation of diversity and evenness metrics, guild structure, and multivariate analyses across the extinction boundary (Chapter 4). Results of all analyses are summarized in the concluding chapter (Chapter 5).

Literature Cited

Bottjer, D. J. 2001. Biotic recovery from mass extinctions. Pp. 202-206 in D. E. G. Briggs and P. R. Crowther, eds. Palaeobiology II. Blackwell Science, Oxford.

Droser, M. L., D. J. Bottjer, P. M. Sheehan, G. R. McGhee, Jr. 2000. Decoupling of taxonomic and ecologic severity of Phanerozoic marine mass extinctions. Geology 28:675-678.

Erwin, D. H. 1996. Understanding biotic recoveries: extinction, survival, and preservation during the End-Permian mass extinction. Pp. 398-418 in D. Jablonski, D. H. Erwin, and J. H. Lipps, eds. Evolutionary Paleobiology. University of Chicago Press, Chicago.

—. 1998. The end and the beginning: recoveries from mass extinctions. Trends in Ecology & Evolution 13:344-349.

—. 2001. Lessons from the past: Biotic recoveries from mass extinctions. Proceedings of the National Academy of Sciences 98:5399-5403.

Hallam, A. and P. B. Wignall. 1997. Mass Extinctions and Their Aftermath. Oxford University Press, Oxford.

Hart, M. B., ed. 1996. Biotic recovery from mass extinction events. Geological Society Special Publication 102. Geological Society of America, Boulder, Colorado.

Holland, S. M. and M. E. Patzkowsky. 1997. Distal orogenic effects on peripheral bulge sedimentation: Middle and Upper Ordovician of the Nashville Dome. Journal of Sedimentary Research 67:250-263.

Jablonski, D. 1995. Extinctions in the fossil record. Pp. 25-44 in J. H. Lawton and R. M. May, eds. Extinction Rates. Oxford University Press, Oxford.

—. 1996. Body Size and Macroevolution. Pp. 256-289 in D. Jablonski, D. H. Erwin, and J. H. Lipps, eds. Evolutionary Paleobiology. University of Chicago Press, Chicago.

—. 2001. Lessons from the past: Evolutionary impacts of mass extinctions. Proceedings of the National Academy of Sciences 98:5393-5398.

—. 2005. Mass extinctions and macroevolution. Paleobiology 31:192-210.

Patzkowsky, M. E. and S. M. Holland. 1993. Biotic response to a Middle Ordovician paleoceanographic event in eastern North America. Geology 21:619-622.

—. 1996. Extinction, invasion, and sequence stratigraphy; patterns of faunal change in the Middle and Upper Ordovician of the Eastern United States. In B. J. Witzke, ed. Paleozoic sequence stratigraphy; views from the North American Craton. Geological Society of America Special Publication 306:131-142. Boulder, CO.

—. 1997. Patterns of turnover in Middle and Upper Ordovician brachiopods of the eastern United States: a test of coordinated stasis. Paleobiology 23:420-443.

Raup, D. M. 1992. Large-body impact and extinction in the Phanerozoic. Paleobiology 18:80-88.

Raup, D. M. and J. J. Sepkoski, Jr. 1982. Mass extinction in the marine fossil record. Science 215:1501-1503.

—. 1984. Periodicity of extinctions in the geologic past. Proceedings of the National Academy of Sciences 81:801-805.

Sepkoski, J.J., Jr. 1986. Phanerozoic overview of mass extinctions. Pp. 277-295 in D. M. Raup and D. Jablonski, eds. Patterns and processes in the history of life. Springer-Verlag, Berlin.

CHAPTER 2

A QUANTITATIVE NULL MODEL OF EXPECTED CHANGES IN PALEOCOMMUNITY EVENNESS FOLLOWING EXTINCTION[1]

[1] Layou, K. M. Submitted to *Paleobiology*, 10/13/06

Abstract

Extinction is typically examined only in light of changes in richness, thus overlooking variations in evenness, the other key component of biodiversity. A quantitative null model of expected changes from pre- to initial post-extinction conditions in two richness metrics (taxonomic richness, *S* and Shannon Index, *H'*) and three evenness metrics (Buzas and Gibson *E*, Pielou's *J*, and Hurlbert's *PIE*) as a function of percent extinction is presented. Several conditions of extinction with respect to taxon abundance are tested, including non-selective extinction, extinction targeting abundant taxa, and extinction targeting rare taxa.

In the model, *S*, *H'*, and *PIE* decline across the extinction boundary with increasing extinction magnitude, regardless of the selectivity of extinction. *E* increases across the extinction boundary with increasing extinction regardless of the selectivity condition; however, the increase will be most substantial for the non-selective condition. Pielou's *J* exhibits unique changes across the extinction boundary for each extinction selectivity condition, with a large increase in Pielou's *J* when abundant taxa are targeted, a decrease in Pielou's *J* when rare taxa are targeted, and a small increase in Pielou's *J* when taxa are not selected with respect to abundance, respectively. These changes in evenness metrics suggest it may be possible to determine whether extinction was selective, and if so, whether rare or abundant taxa were more likely to become extinct, by comparing these metrics from pre- and post-extinction communities.

The model results were compared to data collected across a Late Ordovician regional extinction boundary from the Appalachian Basin of the eastern United States, as well as three global mass extinction boundaries (the end-Ordovician, the end-

Permian, and end-Cretaceous). Field data collected across the regional extinction boundary yield a decrease in Pielou's *J*, which corresponds to extinction that targets rare taxa. Data compiled from the Paleobiology Database reveal different trends in Pielou's *J* for each of the mass extinctions, including a decrease for the end-Ordovician, an increase for the end-Permian, and no change for the end-Cretaceous. The inconsistency of the response of Pielou's *J* across mass extinction boundaries implies there is no common mode of selectivity with respect to taxon abundances during these events.

Introduction

A main goal of many studies in the paleontological literature is to characterize the diversity of biological communities and the factors that influence variability in diversity through geologic time. To sufficiently describe the diversity of a biological community, both components of diversity, taxonomic richness (the number of taxa) and evenness (the proportion of individuals within each taxon), should be determined. However, most assessments of diversity transitions in Phanerozoic paleocommunities solely evaluate changes in taxonomic richness (e.g., Valentine 1969; Bambach 1977; Sepkoski et al. 1981; Alroy et al. 2001). Recent work has argued that abundance data should also be considered to establish trends in evenness through time (Powell and Kowalewski 2002; Olszewski 2004; Peters 2004) to capture variations in community structure that may not be as apparent when examining richness alone.

One well-examined factor affecting biodiversity is extinction and its subsequent impacts on richness patterns (Raup and Sepkoski 1982; Kauffman 1986; Raup and

Boyajian 1988; Donovan 1989; Harries and Kauffman 1990; Jablonski 1995, 2001; Erwin 1996, 1998; Hallam and Wignall 1997; Bottjer 2001; Bambach et al. 2004). Despite this large body of work, evenness patterns with respect to extinction remain unstudied. Evenness is typically examined in the context of community-level analyses. Thus, the lack of attention regarding evenness and extinction may be, in part, due to the fact that much previous work on extinction focuses on differences in richness patterns of a single taxonomic group instead of the changes in richness and abundance patterns of the paleocommunity as a whole.

This paper presents a null model of changes in diversity and evenness metrics across an extinction boundary as a function of percent extinction. The model provides a new perspective on the effects of extinction on biological communities by considering variations in both richness and evenness. Additionally, the model suggests that it may be possible to determine whether extinction is selective or not with respect to taxonomic abundance, and if so, whether the extinction preferentially targeted rare or abundant taxa. The model also offers a direct comparison of changes in community structure from the pre- to post-extinction intervals by determining the null starting conditions during the initial period of recovery from extinction.

The model is not bound by spatial or temporal scales; therefore, the results are also considered in the context of extinction events at two levels, including a regional extinction and three global mass extinctions. Similar variation in diversity and evenness metrics among these events, particularly those of different scales, would suggest a commonality in extinction selectivity.

Previous Work

Many studies have been done on the who, where, and when of global mass extinctions throughout the Phanerozoic (e.g., Raup and Sepkoski 1982; 1984; Sepkoski 1986; Jablonski 1986, 1995,1996, 2001, 2005), yet only recently has the biotic recovery after such events been more fully examined (Erwin 1996; 1998; 2001; Hart 1996; Hallam and Wignall 1997). However, much of this work on recoveries considers a single higher taxonomic group, rather than paleoecological approaches that incorporate data regarding paleocommunity-level information (but see Droser et al. 2000; Bottjer 2001). Also, despite efforts to model different components of extinction (Newman and Palmer 2003, and references therein), including causal mechanisms (Valentine and Walker 1987; Plotnick and Sepkoski 2001), and the role of biogeography (Roy 2001), few models incorporate community-level response to and recovery from extinction (Solè et al. 2002).

The biological response to extinction can be addressed using a more integrative, paleoecological perspective. This approach incorporates analyses of paleocommunity structure both pre- and post-extinction, using features such as taxonomic richness, relative abundance distributions, and evenness patterns (e.g., SHE analysis (Hayek and Buzas 1997; Buzas and Hayek 2005)). Studying taxa in this way allows for predictions to be made regarding their diversity and evenness patterns based on the mathematical relationships among these metrics, without having to infer ecological significance from the fossil record. For example, disaster taxa, which are long-ranging taxa present immediately following the extinction during the survival interval, are often dubbed “opportunists” (Bottjer 2001) because of their high abundances during this earliest

phase of the recovery. Whether these abundances are due to particular life history parameters of the taxa, reduced biotic competition, or the presence of preferred physical conditions is difficult to determine. However, because these taxa are expected to increase in relative abundance in the survival period, potentially to monodominance, the diversity indices and evenness measures of the paleocommunity to which they belong should decrease. Likewise, as diversity rises through the subsequent recovery period and disaster taxa begin to decline, the diversity indices and evenness measures should both increase accordingly.

Diversity Metrics

The model considers several diversity measures: taxonomic richness (*S*), the Shannon diversity index (*H'*), and three evenness metrics (Buzas and Gibson *E*, Pielou's *J*, and Hurlbert's probability of interspecific encounter (*PIE*)). These common diversity measures were chosen from the myriad possible (Olszewski 2004) because of interdependence of *S*, *H'*, *E* and Pielou's *J* as discussed in the context of SHE analysis below, and, the lack of sample-size dependence of *PIE*.

Richness, *S*, is the number of taxa present within the community. The Shannon index, *H'* (Shannon 1948), is defined as

$$H' = -\sum_{i=1}^{S} p_i \ln(p_i) \qquad (2.1)$$

where p_i is equal to the proportional abundance of the *i*th taxon. Thus, abundant taxa contribute proportionally more to the total value of *H'*, and *H'* will increase as richness increases. The relationship among *S*, *H'*, and evenness, *E* (Buzas and Gibson 1969), is expressed as:

$$E = \frac{e^{H'}}{S} \tag{2.2}$$

From this, Hayek and Buzas (1997) derived the following basic equation of SHE analysis:

$$H = \ln S + \ln E \tag{2.3}$$

This characterization of *H* clarifies the separate contributions of richness and evenness to diversity. *H'* will increase as richness increases, and will also increase as taxa become more equally abundant (Shannon 1948; Lande, 1996). Another parameter to consider as part of SHE analysis is the ratio ln*E*/ln*S*, which allows for comparison of the rates of change in evenness and richness and their subsequent effects on diversity. It can be shown that by dividing equation 2.3 by ln*S*, the resulting equation is:

$$\frac{H'}{\ln S} = 1 + \frac{\ln E}{\ln S} \tag{2.4}$$

Since Pielou's *J* (Pielou 1966) is defined as:

$$J = \frac{H'}{\ln S} \tag{2.5}$$

variations in Pielou's *J* should be similar to variations in the ratio of ln*E*/ln*S*.

Finally, Hurlbert's probability of interspecific encounter, *PIE* (Hurlbert 1971), is defined as:

$$PIE = \frac{N}{N-1}(1 - \sum_{i=1}^{S}(p_i)^2) \tag{2.6}$$

where *N* is equal to the number of total individuals in the community. Without the correction for sample size (*N*/(*N*-1)), this metric is equivalent to Simpson's *D* (Lande 1996; Olszewski 2004). *PIE* can be interpreted as the probability that a second

specimen randomly chosen from a sample will be of the same taxon as the first specimen (Hurlbert 1971; Olszewski 2004).

All evenness metrics examined vary from 0 to 1, with 0 representing communities with low evenness (higher dominance of one or a few taxa), and 1 representing communities with high evenness, or similar numbers of individuals among taxa.

Model Description

A quantitative null model describing changes in diversity and evenness as a function of percent extinction is presented here. Individuals within a community are chosen for potential elimination at random, and elimination is based on extinction probabilities assigned to each individual. The model determines extinction of a taxon by elimination of all individuals within that taxon. This procedure is similar to the Field of Bullets scenario used by Raup (1991). Three selectivity conditions with respect to taxon abundance are tested by the model: (1) non-selective extinction, (2) selectivity against abundant taxa, and (3) selectivity against rare taxa. All individuals within a taxon are assigned the same extinction probability based on the selectivity condition being tested by the model. For the non-selective extinction condition, all taxa have the same extinction probability. For all runs with this condition, the extinction probability is set at 1.0 to minimize model run time. Other extinction probabilities (0.2, 0.5, 0.8) were tested for the non-selective extinction condition, and in all cases, the model results did not vary. For selectivity against abundant taxa, the extinction probability for each taxon is set as the percent abundance of the taxon in the initially generated abundance distribution. For selectivity against rare taxa, the extinction probability for each taxon is

set as the reciprocal of the absolute taxon abundance in the initial abundance distribution. Extinction probabilities are calculated in these ways for each selectivity condition such that when an individual within the most abundant or least abundant taxon, respectively, is selected, that individual will have an extremely high probability of being eliminated.

The model begins by generating a lognormal taxonomic abundance distribution for a given *S*. A lognormal was chosen because it is commonly used to fit abundance distributions within ecological communities (Hayek and Buzas 1997; Hubbell 2001). Because a unique abundance distribution was generated for each model run, the total number of individuals present in the initial and post-extinction community varies for each model run. Models were compared for initial *S* values of 10, 30, and 100 taxa, which yielded average initial communities of 160, 475, and 1600 individuals, respectively, among model runs (see below for total number of runs). The extinction begins by randomly choosing an individual and determining whether it should be eliminated by comparing the assigned extinction probability of that individual to a random number from a uniform distribution between 0 and 1. If the assigned extinction probability is greater than the random number, the individual is eliminated and its corresponding taxon abundance is reduced by one; otherwise, a new individual is randomly chosen. This process continues to remove individuals, ultimately eliminating taxa and modifying the initial abundance distribution, until the magnitude of extinction under consideration is reached. The model considers variations in percent extinction from 0 to 95% extinction in 5% increments.

Values of *H'*, *E*, Pielou's *J*, and *PIE* are calculated on the initial and post-extinction abundance distributions. For each magnitude of extinction, mean values for each of these metrics were calculated based on 1000 runs for initial richness values of 10 and 30, but only 100 runs for initial richness of 100 due to computational constraints.

Model Results

Figure 2.1 shows the model results for each of the diversity and evenness metrics and each extinction selectivity condition for the three values of *S* that were tested. In general, the model should be interpreted by comparing the initial, or 0% extinction, metric values to metric values at some higher level of extinction. Table 2.1 summarizes the general direction of change in metric values from pre- to post-extinction conditions for each extinction selectivity condition.

For all metrics, the rare-selective model has the lowest values, followed by the non-selective model, then the abundant-selective model with the highest metric values. The non-selective model is more similar to the rare-selective model at low extinction magnitudes, and more like the abundant-selective model at high extinction magnitudes. Values for the metrics are low for the rare-selective condition because removal of rare taxa eliminates few of the total individuals from the initial abundance distribution, causing minimal change in the abundance distribution of remaining taxa. The opposite relationship is reflected in all abundant-selective evenness metrics (particularly *E*), which show an initial sharp rise in evenness at low magnitudes of extinction (Fig. 2.1, all rows). The increase in evenness is so large at low extinction magnitudes because the process of eliminating the most abundant taxa removes a large number of individuals

from not only the most abundant taxa, but also individuals from other taxa present in the community. Thus, most of the skew of the original abundance distribution curve is removed, creating a more even distribution among remaining taxa. The non-selective model can potentially generate more variable post-extinction abundance distributions that fall between those of the selective models. Because rare taxa are more likely to be eliminated by chance first given their low abundances, the non-selective model produces metric values similar to the rare-selective model at low extinction magnitudes. Likewise, the metrics of the non-selective model are more like the abundant-selective model at high extinction magnitudes because, in each model, the number of individuals per taxon approaches 1.

H' exhibits a decrease with extinction regardless of extinction selectivity (Fig. 2.1, first row). The decrease in *H'* is more pronounced at the highest magnitudes of extinction because at these levels of extinction, both *S* and the number of total individuals are low. The initial values of *H'* vary with the value of *S*, because with more taxa present there are more values in the sum of *H'*.

The various evenness metrics yield results that reflect whether extinction was selective with respect to taxon abundance. The patterns discussed below are present for all values of *S*, despite the increased model variability for lower values of *S*. For the abundant-selective condition, *E* (Fig. 2.1, second row) increases with extinction, exhibiting the greatest increase as the highest extinction levels are reached (85% or higher). The non-selective condition also shows an increase in *E* at all levels of extinction. For the rare-selective condition, *E* declines slightly from the initial value at lower levels of extinction (5-45%) and then increases at moderate to high levels of

extinction. In the context of extinction, with *S* and *H'* declining, it is possible for *E* to either increase or decrease. An increase in *E* across an extinction boundary suggests the post-extinction community has a more similar numbers of individuals among taxa than the initial community, while a decrease in *E* suggests the post-extinction community has most individuals belonging to one or a few dominant taxa. The models indicate that extinction more commonly yields similar numbers of individuals among taxa rather than monodominant communities. Thus, as discussed above, the changes in the abundance distribution under each selectivity condition govern the changes in *E*. In the abundant-selective model, the number of total individuals in the community drops quickly, and once the number of individuals per taxon is relatively low for all taxa, *E* levels off. Similarly, in the rare-selective model, the number of total individuals remains high and the original abundance distribution is maintained through low levels of extinction, thus, *E* does not vary much from its initial pre-extinction value. For the non-selective condition, the potential shape of the post-extinction abundance distribution is much more variable, and therefore exhibits the more constant increase in *E*.

As shown in equations 2.4 and 2.5, the ratio ln*E*/ln*S* and the metric Pielou's *J* reflect the same relationship between richness and evenness. Because ln*E*/ln*S* will always be negative, Pielou's *J* (Fig 2.1., third row) is potentially more useful for comparison since it may be expressed on the same scale as the other evenness metrics (*E*, *PIE*). As percent extinction increases, Pielou's *J* is constant for the abundant-selective model (after the initial large increase), monotonically increases for the non-selective model, and monotonically decreases for the rare-selective model. Pielou's *J* may be the most diagnostic of the evenness metrics, since each selectivity

condition exhibits a different trend. Thus, given a pre- and post-extinction value of Pielou's *J*, a large increase in Pielou's *J* would suggest the extinction was selective with respect to abundant taxa, a small increase in Pielou's *J* would suggest no selectivity with respect to taxon abundance, and a decrease in Pielou's *J* would suggest rare taxa were targeted during the extinction.

Finally, *PIE* (Fig. 2.1, bottom row) decreases with extinction, regardless of extinction selectivity. Because the extinction mechanism in the model eliminates individuals within taxa, the number of individuals per taxon declines at any level of extinction. With fewer individuals per taxon, the likelihood of encountering two individuals of the same taxon decreases.

Application of Null Model

Regional Extinction Event

Background.--The model results were first evaluated against field data collected across a Late Ordovician (Mohawkian) regional extinction boundary within the Appalachian Basin of eastern North America (Patzkowsky and Holland 1993, 1996). Many macroinvertebrate marine taxa were affected by this event, including articulate brachiopods, tabulate and rugose corals, calcareous algae, gastropods, and bryozoans (Patzkowsky and Holland 1996 and references therein). In particular, articulate brachiopods suffered approximately 40% extinction at species and genus levels, with genus- and species-level extinction rates increasing well above both local and global background rates at this extinction boundary (Patzkowsky and Holland 1997). Concomitant with the extinction, a variety of new taxa originate or migrate into the basin.

These faunal changes are concurrent with the onset of physical changes associated with the Taconic orogeny, including, a shift from tropical-type to temperate-type carbonate deposition, an increase in phosphate deposition and an influx of siliciclastic sediment (Holland and Patzkowsky 1997).

Field methods.--Field data were collected at roadcuts in three regions of the Appalachian Basin of eastern North America, including the Nashville Dome of Tennessee, the Jessamine Dome of central Kentucky, and the Valley and Ridge of southwestern and northern Virginia (Figure 2.2). Samples were collected from both shallow subtidal and deep subtidal environments within the sequence stratigraphic framework (Figure 2.3) of Holland and Patzkowsky (1996). Samples from the M3 and M4 sequences are considered together as the pre-extinction samples, while the M5 samples are considered for the post-extinction interval. Lack of exposure or environmental preservation limited sampling in some environments in each region and sequence (Table 2.2). Virginia localities were supplemented with data from Plants (1977) and Springer (1982). The original field data matrix consists of 177 total samples.

Individual samples are based on field censuses of bedding plane surfaces. All macroinvertebrate specimens present were identified to the genus level. Based on an initial set of collector curves, an effort was made to count a minimum of 40 specimens per sample to ensure adequate representation of the community. To find the minimum number of individuals for brachiopods and bivalves, the higher of the counts on unique valves (brachial vs. pedicle for brachiopods, or left vs. right for bivalves) was added to one half of the total number of indeterminate valves. One half of the total number of valves was used for ostracod abundances. One-centimeter lengths of ramose

bryozoans were counted as one individual. Unique morphologies of crinoid columnals were classified as rare (1 specimen per sample), common (2-10 specimens per sample), or abundant (> 10 specimens per sample). For quantitative analyses, these classifications were converted to abundance values 1, 3 and 6 respectively to conservatively estimate the number of individuals present. Runs of all analyses were completed with and without bryozoan and crinoid data. In all cases, identified trends in diversity and evenness metrics did not change, confirming that counting methods for these taxa did not influence the results.

As noted above, the M4/M5 boundary exhibits not only the extinction event, but also a concurrent immigration event to the Appalachian Basin. Thus, taxa within the M5 sequence may be considered as either holdovers from the M4 sequence, or as new taxa. Although holdover richness declines across the M4/M5 boundary for all the field data, including both facies and all regions, total richness remains high due to these new immigrants (Figure 2.4). In order to provide valid comparisons to the model results, diversity and evenness metrics were calculated using data for holdover taxa only.

Because diversity and evenness metrics are dependent on the underlying relative abundance distribution of individuals, the field data for holdover taxa were subsampled to normalize the number of individuals on which the metrics were based to allow for valid comparison of metrics across the extinction boundary and between environments and among the regions. To carry out the subsampling, a subset of the original 177 sample data matrix (e.g., all samples within a facies, or all samples within a region) is selected. Holdover taxon abundances are summed across all samples within the subset to create a single vector of abundances, or a “supersample”. One hundred

individuals from the “supersample” abundance distribution are randomly selected without replacement to create a new sample. This process is repeated 1000 times to create a new data matrix of 1000 samples, each with 100 individuals. Mean diversity and evenness metrics are calculated on the 1000 sample matrix.

Results.— The field data diversity and evenness metrics best match patterns concordant with the rare-selective model. Table 2.3 lists the various metrics based on subsampling for pre- and post-extinction conditions for a number of subsets of the field data. Values of all diversity and evenness metrics decrease across the extinction boundary when comparing all M3/M4 samples to all M5 samples, and this decrease is statistically significant for all metrics. It should be noted, however, that in all cases, the 95% confidence interval on the difference between the metric means from each time interval is relatively small when compared to the value of the metric. This suggests that the exhibited declines in diversity and evenness produced little change to the relative abundance distribution within these paleocommunities. Although substantial changes in paleocommunity diversity structure may not have occurred across this extinction boundary, the general trend of the metrics can be used to determine whether the extinction exhibited selectivity with respect to abundance. The null model predicts declines in *S*, *H’*, and *PIE* across the boundary, and this is observed in the field data; however, these patterns are found for all selectivity conditions. *E* declines across the boundary, which only occurs at lower extinction magnitudes (such as the 40% genus level extinction associated with brachiopods for this particular event) with selection against rare taxa. The other observed decline exhibited by Pielou’s *J* suggests the field

data best corresponds with the rare-selective condition of the null model when using all M3/M4 and M5 samples (Table 2.4).

Further analyses of subsets of the field data by facies consistently show statistically significant declines in all metrics across the extinction boundary (Table 2.3), which also supports selectivity of rare taxa. Again, confidence intervals are small, and there is no indication that either the shallow or deep subtidal environment was more affected by the extinction. However, there are some differences among the regional subsets of data that suggest potential geographic variation in the effects of the extinction on paleocommunity structure. The Kentucky and Virginia subsets are similar to that of the entire dataset, with statistically significant declines in all metrics across the extinction boundary. The Tennessee subset shows statistically significant declines in *S*, *H'*, and *PIE*, but the other evenness metrics (*E* and Pielou's *J*) increase across the boundary. Although statistically significant results may not indicate paleoecologically significant variation, the facies subsets, and the Virginia and Kentucky subsets imply selectivity against rare taxa during this extinction event. The Tennessee data, however, are more consistent with the non-selective null model due to the small increase in Pielou's *J*.

Discussion.—The extinction selectivity predicted by diversity and evenness metrics for the Tennessee data used in this study conflict with prior analyses of this extinction event in Tennessee (Layou, 2007). In this previous work, a portion of the Tennessee data (22 of the 61 total Tennessee samples) was examined using additive diversity partitioning (ADP) (Lande 1996; Veech et al. 2002). The conclusion from

Layou (2007) was that this extinction event targeted abundant taxa, based on trends in alpha and beta diversity across the extinction boundary.

The subsampling routine for diversity and evenness metrics used in this study was carried out on the samples included in the ADP analysis, and an increase in evenness metrics across the extinction boundary was found, including a large increase in Pielou's *J*, which is consistent with the abundant-selective model. As noted above, there appears to be geographic variation in the extinction selectivity based on the regions of Tennessee, Kentucky, and Virginia. Given that two-thirds of the samples used in the ADP subset come from Tennessee localities within 25 miles of each other, it is reasonable to conclude the ADP subset reveals an additional level of geographic variation in extinction selectivity within the Nashville Dome. The ADP subset has rather localized sampling of both shallow and deep subtidal facies during both pre- and post-extinction sequences. The entire Tennessee dataset, however, has expanded spatial coverage of the Nashville Dome (23 localities versus 6 localities in the ADP subset) for both facies before and after the extinction, providing a broader representation of paleocommunity changes across this extinction boundary. Thus, selectivity with respect to taxon abundance varies with spatial scale for this extinction event. At the local level of the ADP subset, the extinction was abundant-selective; regionally in Tennessee, the extinction was non-selective; and basin-wise, the extinction was rare-selective.

Mass Extinctions

Background.—Mass extinctions have clearly affected biodiversity patterns throughout the Phanerozoic, yet the changes in evenness and dominance patterns

among paleocommunities affected by these events have not typically been examined. Here, three global mass extinctions were studied including the end-Ordovician, end-Permian, and end-Cretaceous. These particular events were chosen because the associated depletion in diversity for each of these intervals appears to have been caused by elevated extinction rates, rather than low origination rates (Bambach et al. 2004). Thus, the potential dampening effects of origination on the amount of variation in diversity and evenness metrics during the post-extinction interval as noted above are eliminated.

Methods.—All faunal data for these analyses were downloaded from the Paleobiology Database. Data were downloaded for four time bins for each extinction event to capture pre-extinction conditions, the diversity depletion, and potential recovery of diversity (Table 2.5). For the end-Ordovician and end-Cretaceous events, each time bin represents 10 million years, while the end-Permian bins represent 20 million years to include the Guadalupian extinction the end-Permian diversity decrease. For each time bin, the total number of global occurrences of all marine genera within the following phyla were tabulated and compiled: Arthropoda, Brachiopoda, Bryozoa, Cnidaria, Echinodermata, and Mollusca. The list of total global occurrences of all taxa for each time bin was then subsampled for 500 individuals. This subsampling was repeated 1000 times to create a matrix of equally sized samples for which the mean diversity metrics were calculated. Note the following results are valid assuming that local abundance and global occurrence of a taxon are correlated.

Results.—Despite declines in *S* and *H'* for each of the three mass extinctions, evenness metrics yield varied responses (Table 2.6). As with the regional extinction

data, most changes in metrics were statistically significant, yet the difference in means across the diversity depletion is small. For the end-Ordovician event, all evenness metrics decrease, and thus, signifying an extinction that targeted rare taxa (Table 2.7). For the end-Permian event, all evenness metrics increase (increase in *PIE* is very minimal), and best correspond with an extinction that targeted abundant taxa (Table 2.7). For the end-Cretaceous event, *E* increases, while Pielou's *J* and *PIE* all remain constant (Table 2.7). These results are not found for any of the extinction conditions that were tested with the model, suggesting that this event was driven by processes that do not substantially affect faunal abundance distributions.

Discussion.—An important issue related to extinction is differential survivorship, or selectivity, among taxa. Many factors that are important during background extinction have been shown to not offer the same benefits during mass extinctions (Jablonski 1991, 2001,2005), including species richness and local abundance (McKinney 1997; Lockwood 2003). Each of the three global events examined above produces a different response of Pielou's *J* across the interval of major diversity depletion, indicating different selectivity conditions with respect to global taxon abundances. Thus, global taxon abundance does not seem to be a factor associated with survivorship and mass extinction.

Additionally, the model indicates that at high extinction magnitudes (like those associated with mass extinctions), there should be apparent variation in the values of the evenness metrics when compared to the pre-extinction values. This should be particularly highlighted by abundant-selective extinctions, which should alter the pre-extinction taxon abundance distribution the most. However, both the regional extinction

and mass extinction data, including examples of abundant selectivity, exhibit very small increases or decreases in the evenness metrics across the extinction boundaries. This suggests that although taxonomic richness may decline, the relative abundance of taxa within local paleocommunities or among global distributions of marine macroinvertebrates , does not substantially vary with extinction.

Conclusions

1. The null model predicts diversity metrics *S* and *H'*, and the evenness metric *PIE* to decrease constantly with increasing extinction magnitude, regardless of the selectivity of extinction with respect to taxon abundance. The null model predicts evenness metric *E* to increases constantly with increasing extinction magnitude, regardless of the selectivity for taxon abundance, although the rate of increase is much faster for the case of non-selective extinction. The null model predicts evenness metric Pielou's *J* to have variable, yet distinctive responses to different selectivity conditions, suggesting it may be possible to determine whether extinction is selective with respect to taxon abundance by comparing values of these metrics across an extinction boundary.

2. Field data indicate selectivity with respect to rare taxa did occur across a Late Ordovician regional extinction boundary. The total dataset and most additional subsets based on environment all show changes in diversity and evenness metrics across the extinction boundary that correspond to an extinction that targeted rare taxa. The variation in selectivity based on regional subsets of the data suggests that selectivity is correlated with spatial scale for this extinction event.

3. Each of three mass extinction events indicates different responses of Pielou's *J* across the main interval of diversity depletion. Given the varied outcomes, there does not appear to be a common pattern of selectivity with respect to global taxon abundance associated with mass extinction events.

Acknowledgements

Thanks to S.M. Holland for sharing programming insights and reviewing this work. M.E. Patzkowsky suggested exploration in this direction and provided thoughtful reviews of this paper. This paper was improved by the comments of S.T. Goldstein, L.B. Railsback and S.E. Walker. This work was supported by the Geological Society of America, Sigma Xi Grants in Aid of Research, Paleontological Society Stephen J. Gould Student Grant-in-Aid Program, American Museum of Natural History Theodore Roosevelt Memorial Fund and the University of Georgia Department of Geology Wheeler-Watts Fund.

Literature Cited

Alroy, J., C. R. Marshall, R. K. Bambach, K. Bezusko, M. Foote, F. T. Fursich, T. A. Hansen, S. M. Holland, L. C. Ivany, D. Jablonski, D. K. Jacobs, D. C. Jones, M. A. Kosnik, S. Lidgard, S. Low, A. I. Miller, P. M. Novack-Gotshall, T. D. Olszewski, M. E. Patzkowsky, D. M. Raup, K. Roy, J. J. Sepkoski, Jr., M. G. Sommers, P. J. Wagner, and A. Webber. 2001. Effects of sampling standardization on estimates of Phanerozoic marine diversification. Proceedings of the National Academy of Sciences 98:6261-6266.

Bambach, R. K. 1977. Species richness in marine benthic habitats through the Phanerozoic. Paleobiology 3:152-167.

Bambach, R. K., A. H. Knoll, and S. C. Wang. 2004. Origination, extinction, and mass depletions of marine diversity. Paleobiology 30:522-542.

Bottjer, D. J. 2001. Biotic recovery from mass extinctions. Pp. 202-206 in D. E. G. Briggs and P. R. Crowther, eds. Palaeobiology II. Blackwell Science, Oxford.

Buzas, M.A. and T.G. Gibson. 1969. Species diversity: Benthonic foraminifera in western North Atlantic. Science 163:72-75.

Buzas, M. A. and L. C. Hayek. 2005. On richness and evenness within and between communities. Paleobiology 31:199-220.

Donovan, S. K. 1989. Paleontological criteria for the recognition of mass extinction. Pp. 19-36 in S. K. Donovan, ed. Mass extinctions: processes and evidence. Belhaven Press, London.

Droser, M. L., D. J. Bottjer, P. M. Sheehan, G. R. McGhee, Jr. 2000. Decoupling of taxonomic and ecologic severity of Phanerozoic marine mass extinctions. Geology 28:675-678.

Erwin, D. H. 1996. Understanding biotic recoveries: extinction, survival, and preservation during the End-Permian mass extinction. Pp. 398-418 in D. Jablonski, D. H. Erwin, and J. H. Lipps, eds. Evolutionary Paleobiology. University of Chicago Press, Chicago.

—. 1998. The end and the beginning: recoveries from mass extinctions. Trends in Ecology & Evolution 13:344-349.

—. 2001. Lessons from the past: Biotic recoveries from mass extinctions. Proceedings of the National Academy of Sciences 98:5399-5403.

Hallam, A. and P. B. Wignall. 1997. Mass Extinctions and Their Aftermath. Oxford University Press, Oxford.

Harries, P. J. and E. G. Kauffman. 1990. Patterns of survival and recovery following the Cenomanian-Turonian (Late Cretaceous) mass extinction in the Western Interior Basin, United States. Pp. 277-298 in E. G. Kauffman and G. H. Walliser. eds. Extinction events in Earth history. Springer-Verlag, Berlin.

Hart, M. B., ed. 1996. Biotic recovery from mass extinction events. Geological Society Special Publication 102. Geological Society of America, Boulder, Colorado.

Hayek, L. C. and M. A. Buzas. 1997. Surveying Natural Populations. Columbia University Press, New York.

Holland, S.M. and M. E. Patzkowsky. 1996. Sequence stratigraphy and long-term lithologic change in the Middle and Upper Ordovician of the eastern United

States. In B. J. Witzke, ed. Paleozoic sequence stratigraphy; views from the North American Craton. Geological Society of America Special Publication 306:117-130. Boulder, CO.

—. 1997. Distal orogenic effects on peripheral bulge sedimentation: Middle and Upper Ordovician of the Nashville Dome. Journal of Sedimentary Research 67:250-263.

Hubbell, S. P. 2001. The Unified Neutral Theory of Biodiversity and Biogeography: Monographs in Population Biology 32. Princeton University Press, Princeton.

Hurlbert, S. H. 1971. The nonconcept of species diversity: a critique and alternative parameters. Ecology 52:577-586.

Jablonski, D. 1986. Causes and consequences of mass extinctions: a comparative approach. Pp. 183-229 in D. K. Elliott, ed. Dynamics of extinction. Wiley, New York.

—. 1991. Extinctions: a paleontological perspective. Science 253:754-757.

—. 1995. Extinctions in the fossil record. Pp. 25-44 in J. H. Lawton and R. M. May, eds. Extinction Rates. Oxford University Press, Oxford.

—. 1996. Body Size and Macroevolution. Pp. 256-289 in D. Jablonski, D. H. Erwin, and J. H. Lipps, eds. Evolutionary Paleobiology. University of Chicago Press, Chicago.

—. 2001. Lessons from the past: Evolutionary impacts of mass extinctions. Proceedings of the National Academy of Sciences 98:5393-5398.

—. 2005. Mass extinctions and macroevolution. Paleobiology 31:192-210.

Kauffman, E. G. 1986. High resolution event stratigraphy: regional and global Cretaceous bio-events. Pp. 285-312 in G. H. Walliser, ed. Global bio-events. Springer-Verlag, Berlin.

Lande, R. 1996. Statistics and partitioning of species diversity, and similarity among multiple communities. Oikos 76:5-13.

Layou, K. M. 2007. A quantitative null model of additive diversity partitioning: examining the response of beta diversity to extinction. Paleobiology 33:116-124.

Lockwood, R. 2003. Abundance not linked to survival across the end-Cretaceous mass extinction: patterns in North American bivalves. Proceedings of the National Academy of Sciences USA 100:2478-2482.

McKinney, M. L. 1997. Extinction vulnerability and selectivity: combining ecological and paleontological views. Annual Review of Ecology and Systematics 28:495-516.

Newman, M. E. J. and R. G. Palmer. 2003. Modeling Extinction. Oxford University Press, Oxford.

Olszewski, T. D. 2004. A unified mathematical framework for the measurement of richness and evenness within and among multiple communities. Oikos 104:377-387.

Patzkowsky, M. E. and S. M. Holland. 1993. Biotic response to a Middle Ordovician paleoceanographic event in eastern North America. Geology 21:619-622.

—. 1996. Extinction, invasion, and sequence stratigraphy; patterns of faunal change in the Middle and Upper Ordovician of the Eastern United States. In B. J. Witzke,

ed. Paleozoic sequence stratigraphy; views from the North American Craton. Geological Society of America Special Publication 306:131-142. Boulder, CO.

—. 1997. Patterns of turnover in Middle and Upper Ordovician brachiopods of the eastern United States: a test of coordinated stasis. Paleobiology 23:420-443.

Peters, S. E. 2004. Evenness of Cambrian-Ordovician benthic marine communities in North America. Paleobiology 30:325-346.

Pielou, E. C. 1966. The measurement of diversity in different types of biological collections. Journal of Theoretical Biology 13:131-144.

Plants, H. F. 1977. Paleoecology of the Martinsburg Formation at Catawba Mountain, Virginia. Unpublished Masters thesis, Virginia Polytechnic Institute and State University, Blacksburg, Virginia.

Plotnick, R. E. and J. J. Sepkoski, Jr. 2001. A multiplicative multifractal model for originations and extinctions. Paleobiology 27:126-139.

Powell, M. G. and M. Kowalewski. 2002. Increase in evenness and sampled alpha diversity through the Phanerozoic: comparison of early Paleozoic and Cenozoic marine fossil assemblages. Geology 30:331-334.

Raup, D. M. 1991. Extinction: bad genes or bad luck? W. W. Norton and Company, New York.

Raup, D. M. and G. E. Boyajian. 1988. Patterns of generic extinction in the fossil record. Paleobiology 14:109-125.

Raup, D. M. and J. J. Sepkoski, Jr. 1982. Mass extinction in the marine fossil record. Science 215:1501-1503.

—. 1984. Periodicity of extinctions in the geologic past. Proceedings of the National Academy of Sciences 81:801-805.

Roy, K. 2001. Analyzing temporal trends in regional diversity: a biogeographic perspective. Paleobiology 27:631-645.

Sepkoski, J.J., Jr. 1986. Phanerozoic overview of mass extinctions. Pp. 277-295 in D. M. Raup and D. Jablonski, eds. Patterns and processes in the history of life. Springer-Verlag, Berlin.

Sepkoski, J.J., Jr., R. K. Bambach, D. M. Raup, J. W. Valentine. 1981. Phanerozoic marine diversity and the fossil record. Nature 293:435-437.

Shannon, C. E. 1948. A mathematical theory of communication. Bell System Technical Journal 27:379-423, 623-656.

Solè, R. V., J. M. Montoya, and D. H. Erwin. 2002. Recovery after mass extinction: evolutionary assembly in large-scale biosphere dynamics. Philosophical Transactions of the Royal Society of London B 357:697-707.

Springer, D. A. 1982. Community gradients in the Martinsburg Formation (Ordovician), southwestern Virginia. Unpublished Ph.D. dissertation, Virginia Polytechnic Institute and State University, Blacksburg, Virginia.

Valentine, J. W. 1969. Patterns of taxonomic and ecological structure of the shelf benthos during Phanerozoic time. Palaeontology 12:684-709.

Valentine, J. W. and T. D. Walker. 1987. Extinctions in a model taxonomic hierarchy. Paleobiology 13:193-207.

Veech, J. A., K. S. Summerville, T. O. Crist, and J. C. Gering. 2002. The additive partitioning of species diversity: recent revival of an old idea. Oikos 99:3-9.

Table 2.1. Summary of variations in diversity and evenness metrics from pre-to post-extinction according to each of model selectivity conditions with respect to taxonomic abundance.

	Non-selective	Abundant-selective	Rare-selective
H'	decrease	decrease	decrease
E	increase	increase	decrease (low ext.) increase (high ext.)
Pielou's *J*	small increase	large increase	decrease
PIE	decrease	decrease	decrease

Table 2.2. Number and distribution of samples included in field data analyses indicating subsets of geographic region and facies. First number indicates total samples from sequence, parenthetical numbers reflect distribution of samples per sequence by facies. SS = shallow subtidal facies, DS = deep subtidal facies.

	M3/M4 (pre-extinction)	M5 (post-extinction)
Tennessee	37 (SS: 17, DS: 20)	26 (SS: 17, DS: 9)
Kentucky	10 (SS: 10, DS: 0)	37 (SS: 19, DS: 19)
Virginia	14 (SS: 0, DS: 14)	53 (SS: 0, DS: 53)
All	61 (SS: 27, DS: 34)	116 (SS: 36; DS: 80)

Table 2.3. Changes in mean diversity and evenness metrics across a regional extinction boundary based on subsampled subsets of field data. 95% confidence limit reported is for difference of means. 95%UCL = 95% upper confidence limit; 95%LCL = 95% lower confidence limit; SS = all shallow subtidal samples; DS = all deep subtidal samples.

	S	*H'*	*E*	Pielou's *J*	*PIE*
M3/4 (All)	29.834	2.859	0.589	0.843	0.916
M5 (All)	20.610	2.388	0.534	0.791	0.854
95%UCL	9.439	0.482	0.059	0.054	0.064
95%LCL	9.009	0.460	0.051	0.050	0.060
M3/4 (SS)	28.146	2.918	0.662	0.875	0.934
M5 (SS)	18.203	2.297	0.552	0.794	0.862
95%UCL	10.140	0.630	0.114	0.084	0.073
95%LCL	9.746	0.612	0.106	0.080	0.071
M3/4 (DS)	26.786	2.659	0.538	0.810	0.889
M5 (DS)	16.476	1.974	0.443	0.706	0.760
95%UCL	10.517	0.697	0.099	0.106	0.132
95%LCL	10.103	0.673	0.091	0.101	0.126

M3/4 (Tennessee)	23.969	2.575	0.552	0.812	0.886
M5 (Tennessee)	18.536	2.380	0.592	0.819	0.873
95%UCL	5.624	0.199	-0.035	-0.005	0.015
95%LCL	5.242	0.179	-0.044	-0.010	0.011
M3/4 (Kentucky)	21.422	2.536	0.593	0.828	0.884
M5 (Kentucky)	13.026	1.968	0.556	0.769	0.814
95%UCL	8.540	0.576	0.041	0.061	0.071
95%LCL	8.252	0.559	0.033	0.056	0.068
M3/4 (Virginia)	24.579	2.815	0.683	0.880	0.931
M5 (Virginia)	7.435	1.551	0.640	0.776	0.752
95%UCL	17.282	1.271	0.048	0.107	0.180
95%LCL	17.006	1.257	0.039	0.102	0.177

Table 2.4. Summary of variations in diversity and evenness metrics across a regional extinction boundary according to field results. Field data metrics follow the pattern associated with an extinction that targets rare taxa.

	Field data
H'	decrease
E	small decrease
Pielou's *J*	decrease
PIE	decrease
Extinction selectivity	against rare taxa

Table 2.5. Time bins used in mass extinction analyses. Time bins correspond with the Paleobiology Database (PBDB) "10 million year time bin" scale. Note bins associated with the end-Permian extinction include two 10 My bins.

PBDB time bin	Age (Ma)
Ordovician 4	460.9-450
Ordovician 5	450-443.7
Silurian 1	443.7-428.2
Silurian 2	428.2-416
Permian 1,2	299-270.6
Permian 3,4	270.6-251
Triassic 1,2	251-228
Triassic 3,4	228-199.6
Cretaceous 7	83.5-70.6
Cretaceous 8	70.6-65.5
Cenozoic 1	65.5-55.8
Cenozoic 2	55.8-40.4

Table 2.6. Changes in mean diversity and evenness metrics across mass extinction boundaries based on subsampled global occurrences of genera. 95% confidence limit reported is for difference of means for intervals including the major diversity depletion for each event (Ord 5 to Sil 1; Perm 3,4 to Tri 1,2; Cret 7 to Cret 8; highlighted in italics). 95%UCL = 95% upper confidence limit; 95%LCL = 95% lower confidence limit.

	S	*H'*	*E*	Pielou's *J*	*PIE*
Ord 4	268.646	5.299	0.746	0.947	0.995
Ord 5	272.997	5.335	0.761	0.951	0.995
Sil 1	211.897	4.919	0.647	0.919	0.990
Sil 2	287.494	5.407	0.776	0.955	0.996
95%UCL	61.842	0.420	0.115	0.033	0.005
95%LCL	60.358	0.411	0.112	0.032	0.005
Perm 1,2	233.938	5.116	0.713	0.938	0.993
Perm 3,4	250.403	5.196	0.722	0.941	0.994
Tri 1,2	231.855	5.152	0.746	0.946	0.994
Tri 3,4	235.329	5.116	0.709	0.937	0.993
95%UCL	19.248	0.048	-0.023	-0.005	-0.0003
95%LCL	17.848	0.039	-0.026	-0.006	-0.0004

Cret 7	230.067	5.085	0.703	0.935	0.993
Cret 8	210.772	5.003	0.707	0.935	0.992
Cen 1	289.465	5.356	0.733	0.945	0.994
Cen 2	287.201	5.411	0.780	0.956	0.996
95%UCL	19.988	0.087	-0.002	0.0005	0.0002
95%LCL	18.602	0.078	-0.005	-0.0004	0.00003

Table 2.7. Summary of variations in diversity and evenness metrics across three mass extinction boundaries. Metrics indicate different patterns of selectivity with respect to taxon abundance for each extinction event.

	end-Ordovician	end-Permian	end-Cretaceous
H'	decrease	decrease	decrease
E	decrease	increase	increase
Pielou's *J*	decrease	increase	constant
PIE	decrease	increase	constant
Extinction selectivity	against rare taxa	against abundant taxa	no selectivity with respect to abundance

Figure 2.1. Changes in diversity (*H'*) and evenness (*E*, Pielou's *J*, and *PIE*) metrics with increasing magnitude of extinction for three values of initial taxonomic richness (*S*). Note horizontal axis represents increasing magnitude of extinction, not time.

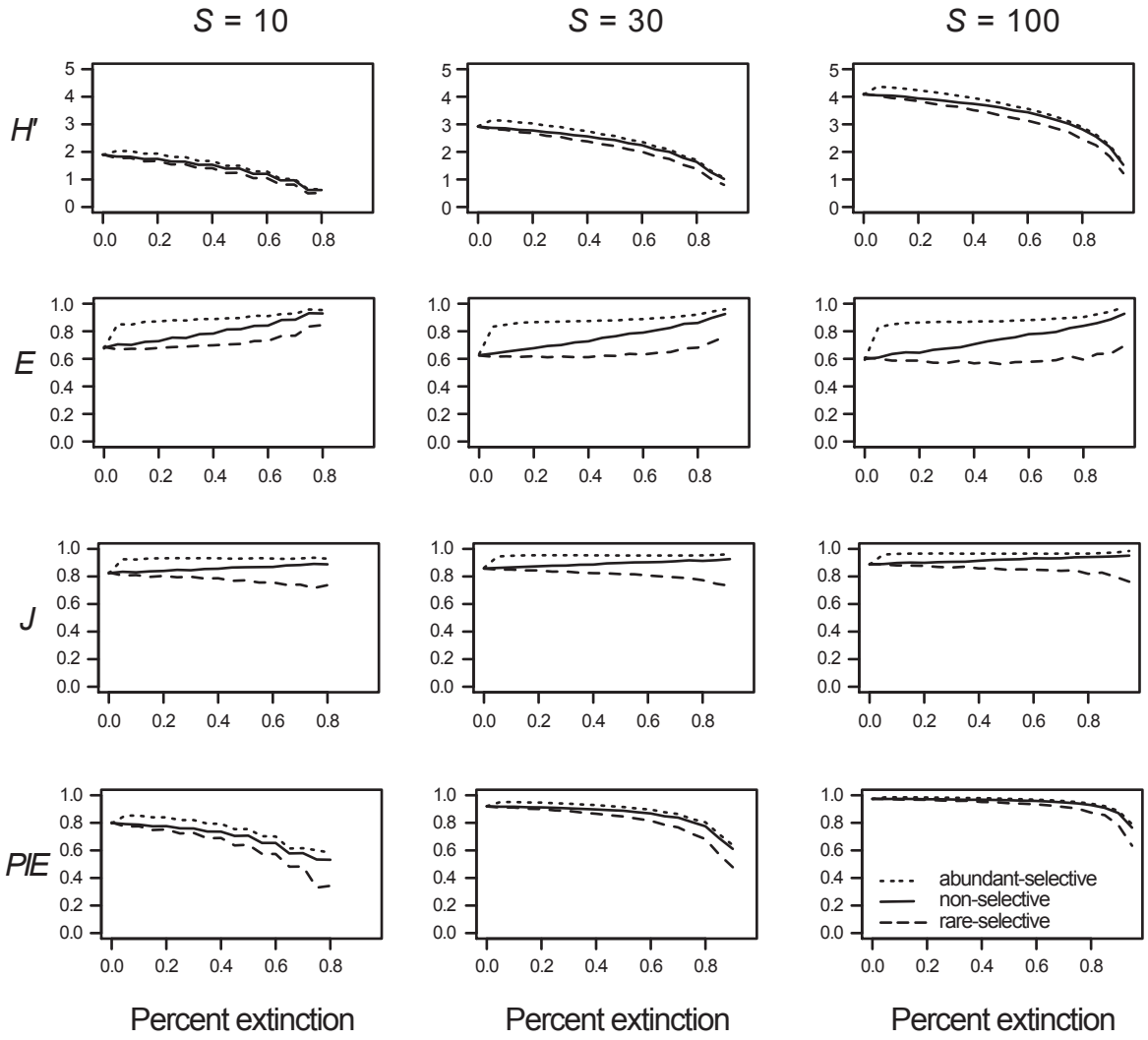
S = 10
S = 30
S = 100
H'
E
J
PIE
abundant-selective
non-selective
rare-selective
Percent extinction
Percent extinction
Percent extinction

Figure 2.2. Regional map of Kentucky, Tennessee, and Virginia. Underlying gray scale reflects geologic bedrock map, with areas of Ordovician bedrock outlined by the heavy black line. White boxes indicate localities of field sample collection.

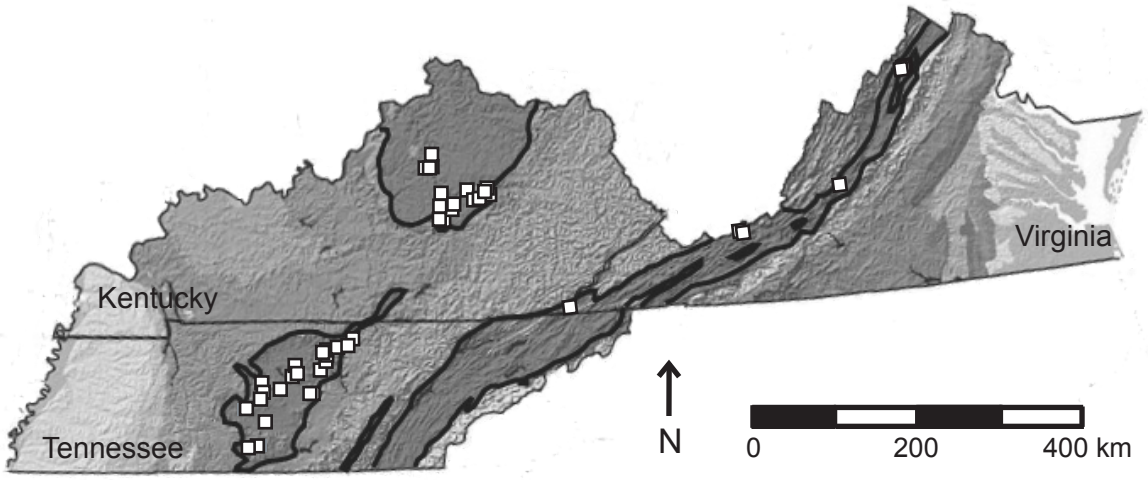
Virginia
Kentucky
Tennessee
N
0
200
400 km

Figure 2.3. Time scale modified from Holland and Patzkowsky (1996).

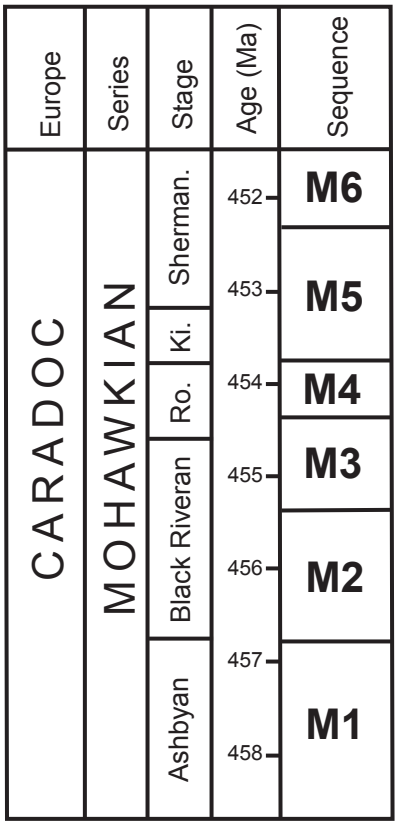
Europe
Series
Stage
Age (Ma)
Sequence
CARADOC
MOHAWKIAN
Ashbyan
Black Riveran
Ro.
Ki.
Sherman.
452
453
454
455
456
457
458
M6
M5
M4
M3
M2
M1

Figure 2.4 Number of genera present in each sequence, and within facies and regions for each sequence. For the M5, black portions of the bar indicate holdover taxa from the M4, and white portions indicate new or immigrant taxa.

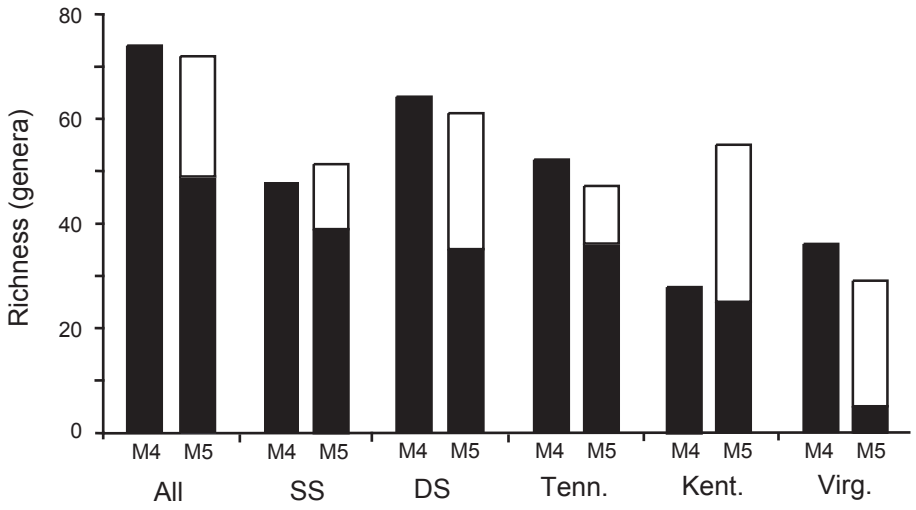
Richness (genera)
80
60
40
20
0
M4
M5
All
SS
DS
Tenn.
Kent.
Virg.

CHAPTER 3

A QUANTITATIVE NULL MODEL OF ADDITIVE DIVERSITY PARTITIONING: EXAMINING THE RESPONSE OF BETA DIVERSITY TO EXTINCTION[1]

[1] Layou, K. M. 2007. *Paleobiology* 33:116-124.
Reprinted here with permission of publisher.

Abstract

Paleobiological diversity is often expressed as α (within sample), β (among samples), and γ (total) diversities. However, when studying the effects of extinction on diversity patterns, only variations in α and γ diversities are typically addressed. A null model that examines changes in β diversity as a function of percent extinction is presented here.

The model examines diversity in the context of a hierarchical sampling strategy that allows for the additive partitioning of γ diversity into mean α and β diversities at varying scales. Here, the sampling hierarchy has four levels: samples, beds, facies, and region; thus, there are four levels of α diversity (α_1, α_2, α_3, α_4) and three levels of β diversity (β_1, β_2, and β_3). Taxa are randomly assigned to samples within the hierarchy based on probability of occurrence, and initial mean α and β values are calculated. A regional extinction is imposed, and the hierarchy is resampled from the remaining extant taxa. Post-extinction mean α and β values are then calculated.

Both non-selective and selective extinctions with respect to taxon abundance yield decreases in α, β, and γ diversities. Non-selective extinction with respect to taxon abundance shows little effect on diversity partitioning except at the highest extinction magnitudes (above 75% extinction), where the contribution of α_1 to total γ increases at the expense of β_3, with β_1 and β_2 varying little with increasing extinction magnitude. The pre-extinction contribution of α_1 to total diversity increases with increased probabilities of taxon occurrence and the number of shared taxa between facies. Both β_1 and β_2 contribute equally to total diversity at low occurrence probabilities, but β_2 is negligible at high probabilities, because individual samples preserve all the taxonomic variation

present within a facies. Selective extinction with respect to rare taxa indicates a constant increase in α_1 and constant decrease in β_3 with increasing extinction magnitudes, while selective extinction with respect to abundant taxa yields the opposite pattern of an initial decrease in α_1 and increase in β_3. Both β_1 and β_2 remain constant with increasing extinction for both cases of selectivity. By comparing diversity partitioning before and after an extinction event, it may be possible to determine whether the extinction was selective with respect to taxon abundances, and if so, whether that selectivity was against rare or abundant taxa.

Field data were collected across a Late Ordovician regional extinction in the Nashville Dome of Tennessee, with a similar sampling hierarchy to that of the model. These data agree with the abundant-selective model, showing declines in α, β, and γ diversities, and a decrease in α_1 and increase in β_3, which suggests this extinction may have targeted abundant taxa.

Introduction

A common method of examining biodiversity trends through geologic time focuses on variation at different scales, which is often expressed as α, β, and γ diversities (Sepkoski 1998; Powell and Kowalewski 2002; Bush and Bambach 2004). Although the spatial scales of α, β, and γ can vary (Whittaker et al. 2001), traditionally in paleobiology, α represents local bed, or outcrop-level diversity, β is regional diversity, and γ is global diversity (Sepkoski 1988). This hierarchical view of paleobiodiversity is based on concepts of diversity partitioning presented in the ecological literature (Whittaker 1960, 1972).

Episodes of extinction in the fossil record are defined by increases in extinction rate that reflect a decline in α or γ diversities, but β diversity is rarely addressed in the context of extinction. The paper presents a null model of changes in β diversity as a function of percent extinction based on an additive partitioning approach. Scenarios allowing for both selective and non-selective extinction with respect to taxon abundance are considered. Examining trends in β with diversity partitioning across an extinction boundary provides a richer view of how paleocommunities respond to extinction events.

A Traditional View of β: the Multiplicative Approach.-The traditional view of β diversity in paleontology is based on the work of Whittaker (1960, 1972). Using data from the forests of the Great Smoky Mountains of the eastern United States and the Siskiyou Mountains of Oregon and California, Whittaker developed a multiplicative definition of γ, such that γ, or total diversity, was the product of β and mean α diversity:

$$\gamma = \alpha\beta \tag{3.1}$$

Whittaker defines β as differences in community composition along environmental gradients, and proposed the use of the Jaccard similarity coefficient to define β:

$$\beta = S_{common} / (S_{sample1} + S_{sample2} - S_{common}) \tag{3.2}$$

where S_{common} is the number of taxa in common between sample 1 and sample 2; $S_{sample1}$ is the total number of taxa present in sample 1; and $S_{sample2}$ is the total number of taxa present in sample 2. By using a similarity coefficient, β becomes a measure of how many taxa two samples (or regions) have in common. Koleff et al. (2003) provide an extensive review of 24 different measures of beta diversity based on similarity measures used in recent ecological analyses, all of which employ presence-absence

data. Defining β with similarity coefficients has also been the primary means of examining diversity patterns in the fossil record (Sepkoski 1988).

The use of similarity coefficients to define β diversity, however, is limiting, because it requires pairwise comparisons of only two units of potentially different spatial scales and because it is based on presence-absence data. This issue is particularly apparent when examining changes in β diversity with respect to extinction events. Intuitively, the null expectation is that β should decrease across an extinction boundary as α and γ do. One major disadvantage to defining β as the Jaccard coefficient in particular is that depending on whether an extinction is selective or non-selective with respect to shared taxa between the two samples, β diversity can either increase or decrease across an extinction boundary. Consider the situation outlined in Table 3.1. Pre-extinction β for the two samples is 0.5 based on the Jaccard coefficient. If shared taxa (A and B) are eliminated during the extinction event, post-extinction β decreases, while if unique taxa (C and D) are eliminated, post-extinction β increases. Elimination of both shared and unique taxa (e.g., A and C) yields no change in β across the extinction boundary. This last case, where shared and unique taxa are eliminated, is particularly misleading, because although similarity between samples has not changed (β remains constant), the total number of shared taxa has decreased, and this is not reflected in the value of β. In most scenarios, it is difficult to assess whether extinction mechanisms are generally selective or non-selective with respect to certain taxa, but it is even more difficult to determine whether shared or unique taxa between two levels of analysis are being targeted. Thus, predicting whether β diversity will increase, decrease, or remain constant as a result of an extinction event is not easy. An approach to β that allows for

testing of these explicit null hypotheses is desirable when considering how β diversity responds to extinction.

A New View of β: Additive Partitioning.-Additive partitioning is a method of quantifying diversity that offers much potential to the study of the fossil record, and has been used to examine diversity patterns in a number of modern ecological studies (e.g., Wagner et al. 2000; Gering and Crist 2002; Crist et al. 2003; Okuda et al. 2004). Although the concept of additive partitioning of diversity has been present in the ecological literature almost as long as the multiplicative approach, only recently have Whittaker's concepts of α, β, and γ been placed in the context of additive partitioning (Veech et al. 2002). Instead of defining β using a quotient, Lande (1996) defined β as the difference between γ and α:

$$\beta = \gamma - \alpha \tag{3.3}$$

Additive partitioning is more intuitive than the multiplicative approach to β diversity because it expresses the total diversity as the sum of within and among sample diversity. Partitioning diversity in this way answers the question of how much more diversity is added to total diversity by counting more samples, or by sampling at a larger spatial scale. Additionally, this method allows for α, β, and γ to be expressed in the same units, facilitating comparisons within and among datasets. Since diversity may be defined as simple taxonomic richness, or with a metric that incorporates abundance information, comparisons of partitioning patterns among different diversity metrics for the same dataset may also be made. Partitioning also presents a clearer picture when considering β in the context of extinction because β diversity can only remain constant or decrease across an extinction boundary when the extinction operates at the scale on

which γ is measured. Consider the response of β to extinction when calculated using the additive partitioning method as shown in Table 3.1. The pre-extinction β diversity equals one. Following the same elimination criteria as with the Jaccard example, if shared taxa (A and B) are eliminated in the extinction event, post-extinction β does not change, because diversity is still gained by looking to other samples. However, if unique taxa (C and D) are eliminated, no new information is gained from the other sample, and thus β decreases to zero. Likewise, eliminating unique and shared taxa (e.g., A and C) reduces the amount of new information in the other sample, so post-extinction β decreases. The additive approach to partitioning implicitly assesses shared and unique taxa to determine β diversity and more accurately reflects changes in diversity when both unique and shared taxa are affected by extinction.

Additive partitioning allows for comparison of β across multiple samples and varying spatial scales if data are collected within a nested sampling hierarchy (e.g., Gering et al. 2003; Okuda et al. 2004). Total diversity, or γ, equals the sum of mean α diversity at the lowest level of sampling (*i*) and β diversity at each additional level within the hierarchy, excluding the highest level (*m*):

$$\gamma = \alpha_1 + \sum_{i=1}^{m-1} \beta_i \tag{3.4}$$

The β diversities are defined as the difference of mean α at adjacent levels within the hierarchy, thus, for each level of the hierarchy from *i* to *m* – 1:

$$\beta_i = \alpha_{i+1} - \overline{\alpha}_i \tag{3.5}$$

Note that at the highest sampling level, γ equals α_m.

The α diversity can be measured using any diversity index that is strictly concave, meaning that the total diversity in a pooled set of samples exceeds or equals the average diversity within samples. Three common diversity indices that meet this criterion include richness (*S*), Shannon information (*H'*), or Simpson's index (Lande 1996). *S* measures diversity based on the presence of a taxon, *H'* measures the frequency of a taxon in a community, and Simpson's index measures the probability that two randomly drawn individuals from a sample are different taxa (Lande 1996). *S* and *H'* are sample-size dependent, thus using a sample-size independent diversity metric may downplay differences in sample size within the hierarchy. Simpson's index, or the equivalent Hurlbert's *PIE*, may be used as sample-size independent metrics. Mean α diversity metrics are calculated either by unweighted arithmetic averages, or by summing the products of a weighting factor and the diversity metric (Crist et al. 2003; Okuda et al. 2004). Use of the weighting factor corrects for sample size variation because larger samples are assumed to be more reliable estimates of diversity, and thus are given more weight. When the weighting factor is used, the mean diversity (α_i) for samples at each hierarchical level *i* is:

$$\alpha_i = \sum_{j=1}^{n_i} D_{ij} q_{ij} \tag{3.6}$$

where n_i is the number of samples taken at level *i* of the sampling hierarchy, D_{ij} represents the diversity metric recorded in each sample *j*, and q_{ij} is the sample weight determined by the proportion of the total number of individuals in each sample *j*. By combining analysis of both spatial scale and abundance into the model, additive partitioning provides a richer view of how all diversity is distributed within the study area. For example, consider the sampling hierarchy used in this study (Fig. 3.1). The

hierarchy includes a regional study area (R), with two distinct facies (F_1, F_2). Within each facies, two individual beds (B_1, B_2) are sampled, and from each of these beds, three collections are obtained (C_1, C_2, C_3). In total, there are four levels to the hierarchy (collection, bed, facies, and region) and thus, there are four α values. Three levels of β diversity may therefore be considered: among collections in a bed (β_1); diversity between beds (β_2); and finally, diversity between facies (β_3). Thus, total diversity is:

$$\gamma = \overline{\alpha}_1 + \overline{\beta}_1 + \overline{\beta}_2 + \beta_3 \quad (3.7)$$

Model Description

To establish some predictions on how additively partitioned β diversity should change across an extinction boundary, a null model is used here. Null models have gained wide use in the development of key concepts of biogeography, community ecology, and paleobiology (e.g., Valentine and Walker 1987; Gotelli and Graves 1996; Hubbell 1997; Gotelli 2001; Plotnick and Sepkoski 2001; Roy 2001; Solé et al. 2002; Crist et al. 2003). The additive partitioning model requires a number of initial inputs including: 1) regional maximum richness; 2) the sampling hierarchy, or number of collections, beds, and facies; 3) a probability of taxon occurrence at the collection level; and, 4) the number of shared taxa between facies. The mode of extinction can be selective or non-selective with respect to taxon abundances. For non-selective extinctions, taxa are eliminated until the proper level of extinction is reached regardless of the total abundance of those taxa in the region. For selective extinctions, all individuals within a taxon are tallied from all collections across the region, and taxa with either the least (for selection against rare taxa) or the most (for selection against

abundant taxa) number of individuals are progressively eliminated until the proper magnitude of extinction is reached.

The model begins by filling each collection in the sampling hierarchy with a unique array of log-normally distributed abundance values for taxa that are present, thus, each taxon will have varying abundances in each collection. Initial α and β values are calculated using richness (*S*) weighted by abundance as the diversity metric. A selective or non-selective extinction that eliminates taxa is then imposed at the regional scale. For every run of the model, different numbers of individuals are lost during the extinction since taxonomic abundances are variable. The hierarchy is then resampled from the remaining taxa and post-extinction α and β values are calculated.

Five different model versions varying probability of taxon occurrence and type of extinction are compared (Appendix). In all models, regional maximum richness is set at 24 taxa; the sampling hierarchy follows the example (Fig. 3.1) with 3 collections, 2 beds and 2 facies; and, there is a 33% taxon overlap between facies. The shared taxa between facies are randomly assigned, and thus, may or may not include the most common or rarest taxa. In each model, the probabilities of taxon occurrence were set either as constant for all taxa, or as a randomly generated value drawn from a uniform distribution between 0 and 1 for all taxa. The probabilities of taxon occurrence are the same for both pre- and post-extinction conditions.

Results

For all versions of the model, regardless of probability of taxon occurrence values or type of extinction, β_1, β_2, and β_3 decrease as percent extinction increases, confirming

the null expectation that β should decrease along with α and γ diversities across an extinction boundary when the extinction occurs among taxa at the highest level of the sampling hierarchy (Fig. 3.2). Note that above 95% extinction, α_1 overlaps γ since the last surviving taxon represents all diversity. Values of β_1 are higher than those of β_2, reflecting high average probabilities of occurrence. Given the construction of the model, there is no defined difference between collections and beds since differences in taxonomic composition are imposed at the facies level. Therefore, collections and beds within facies are random samples of the same community, and β_1 and β_2 ultimately reflect differences in sample size. However, looking at each bed within a facies allows for examination of how much diversity would be added by doubling the sampling intensity within a facies. The low values of β_2 suggest that little additional diversity is captured from sampling additional beds within a facies.

Initial diversity partitioning for extinction that is non-selective with respect to taxon abundance varies for given different probabilities of taxon occurrence (Fig. 3.3). In the plots of Figure 3.3, each line between diversity levels represents an average value for each extinction magnitude based on multiple runs of the model (see Appendix). Variance of these mean values is low for all versions of the model. When these probabilities are low (probability = 0.2) and constant for all taxa (Fig. 3.3A), pre-extinction diversity is evenly partitioned among the various levels of the hierarchy, and there is no major change in partitioning with extinction except at the highest magnitudes for which the model could be run. Above 90% extinction, the model produces average γ values below 1, thus the plot (Fig. 3.3A) is truncated at the highest extinction values. As extinction magnitude increases, β_3 decreases because the facies become more similar

as more taxa are eliminated. Additionally, at high extinction magnitudes, regional diversity is low and the likelihood of producing collections and beds with zero diversity increases. Thus, α_1 is higher, due to not only a response to the decrease in β_3, but also because there is an increased probability of finding the few surviving taxa in only one collection. Although β_1 and β_2 also appear to decrease, their relative proportions remain stable until the highest magnitudes of extinction are reached. When probabilities of taxon occurrence are high (probability = 0.8), β_2 becomes negligible as more diversity is captured by additional collections within a single bed, rather than from additional beds (Fig. 3.3B). Thus, the increased probability of taxon occurrence in samples suggests sampling additional beds within a facies would not be necessary to capture facies-level diversity for these model conditions. Similarly, since β_1 and β_2 reflect differences in sample size, samples approximately three times the size of collections are sufficient for capturing facies-level diversity. The other levels of β diversity, β_1 and β_3, also contribute less to total diversity when the probability of taxon occurrence is high, which is related to the increased contribution of α_1. With higher probabilities of occurrence, there is a high probability of finding the total regional richness at the collection level. At the highest extinction magnitudes, all levels of β diversity become negligible because total remaining regional richness can be found within a single collection.

To address a more realistic scenario, the model was run assuming variable probability of taxon occurrence across facies and taxa. Here, the probability of taxon occurrence was determined using a randomly generated value with a uniform distribution between 0 and 1. As with previous versions of the model, the probability of taxon occurrence does not change across the extinction boundary. Again, there is little

change in how total diversity is divided among its components, except at the very highest extinction magnitudes (Fig. 3.3C). While the relative proportions of both β_1 and β_2 remain constant, α_1 increases and β_3 decreases in response.

Comparison of model results between non-selective and selective extinctions yields results with predictive potential (Fig. 3.4). As in Figure 3.3, the lines between diversity levels on the plots represent mean values based on multiple runs of the model. For non-selective extinction, there is no change in diversity partitioning except at the highest magnitudes of extinction (Fig. 3.4B). However, when the extinction selects rare taxa, there is a general positive slope in diversity components (Fig. 3.4A), and when abundant taxa are selected, there is a general negative slope in diversity components (Fig. 3.4C). Again, for both cases of selective extinction, the plots are truncated at the highest extinction levels because the models produce average γ values below 1. In both cases, this pattern is driven by variation in β_3 and α_1; the other components of β diversity vary little in their contribution to total diversity because both samples and beds are similar due to the construct of the models. For the rare-selective model, the positive slope pattern is driven by a decrease in β_3 and related increase in α_1. As in the previous models, β_3 decreases with increasing magnitude of extinction because the facies become more similar (thus contributing less to total diversity) as more taxa are eliminated. Here, the elimination of taxa is more systematic, leading to a more pronounced pattern. For the abundant-selective model, the negative slope pattern is driven by an initial increase in β_3, which suggests that at lower levels of extinction the facies become more dissimilar. This is expected because taxa present in both facies are more likely to be more abundant at the regional level, and thus are eliminated first.

Given these scenarios, statistical testing for differences from pre- to post-extinction in mean diversity at various levels within the sampling hierarchy may be used to determine if partitioning (particularly at the highest and lowest levels) remains constant (no selectivity with respect to extinction), significantly increases (selection against rare taxa), or significantly decreases (selection against abundant taxa). Methods used to test for differences in mean diversity partitioning in the ecological literature include subsampling (Gering et al. 2003) and ANOVA (Okuda et al. 2004).

Application of Null Model

The goal of null modeling is to establish expected patterns to which empirical data can be compared. To this end, model results were evaluated against field data collected across a Late Ordovician (Mohawkian) regional extinction boundary. This extinction occurred among marine macroinvertebrate taxa within the Appalachian Basin of eastern North America (Patzkowsky and Holland 1993, 1996). The taxa affected by this event include (at least) articulate brachiopods, tabulate and rugose corals, calcareous algae, macluritid gastropods, and possibly some bryozoans (Patzkowsky and Holland 1996 and references therein). In particular, articulate brachiopods suffered approximately 40% extinction at species and genus levels, with genus and species level extinction rates increasing well above both local and global background rates at this extinction boundary (Patzkowsky and Holland 1997). This extinction event was concurrent with the onset of physical changes associated with the Taconic orogeny, including a shift from tropical-type to temperate-type carbonate deposition, an increase

in phosphate deposition, and an influx of siliciclastic sediment (Holland and Patzkowsky 1997).

The pre- and post-extinction partitioning of diversity across this Late Ordovician regional extinction boundary on the Nashville Dome in central Tennessee yields results that are concordant with the abundant-selective model (Fig. 3.5). The sampling hierarchy is identical to that of the model, except that two of the post-extinction beds have only 2 collections. Taxon overlap between facies is similar to that of the model (pre-extinction = 45% shared taxa between facies; post-extinction = 31% shared taxa between facies). Diversity is partitioned similarly to the model with low probabilities of taxon occurrence (Fig. 3.3A), in that all levels of diversity have relatively equal contributions to total diversity (Fig. 3.5). Declines in α, β, and γ diversities are present from pre- to post-extinction conditions (Table 3.2). The small decline in γ is due to the presence of different taxa in the post-extinction interval, however, seventeen taxa present in the pre-extinction interval are not found in the post-extinction interval. There is a change in diversity partitioning from pre- to post-extinction conditions, with an increase in β_3 and decrease in α_1. The other diversity components, β_1 and β_2, remain relatively unchanged. This pattern mirrors that of the abundant-selective model (Fig. 3.4C), suggesting this extinction targeted abundant taxa. The data in this study are limited by both number and geographic extent, which prohibits statistical treatment of these changes in partitioning across the extinction boundary. With a larger data set including more replicates at each level within the sampling hierarchy, testing for variation in diversity at different levels would be possible using subsampling or ANOVA.

Conclusions

1. Null models based on additive partitioning of β diversity indicate that β diversity should decrease as α and γ do with increasing magnitudes of extinction at the highest level of the sampling hierarchy.

2. Variation in probability of taxon occurrence changes the initial distribution of diversity among levels of the sampling hierarchy. Low probabilities of taxon occurrence yield evenly partitioned diversity at all levels of the sampling hierarchy. High probabilities of taxon occurrence increase the contribution of α_1 and all levels of β decline accordingly, with β_2 becoming negligible.

3. Non-selective extinction with respect to taxon abundance suggests that the partitioning of diversity does not vary across an extinction boundary except at the highest magnitudes of extinction. Selective extinction with respect to rare taxa yields positive slopes with increasing extinction magnitude, representing a constant decrease in β_3 and corresponding increase in α_1. Selective extinction with respect to abundant taxa yields negative slopes with increasing extinction magnitude, with an initial increase in β_3 and decline in α_1. These different patterns suggest that it may be possible to determine whether extinction operating at the highest level of the sampling hierarchy is selective or not with respect to taxon abundances.

4. Field data from a Late Ordovician regional extinction event of moderate magnitude corroborate the model results, exhibiting a decrease α, β, and γ diversities. The change in diversity partitioning across this extinction boundary is similar to the abundant-selective model results, with an increase in β_3 and decline in α_1 across the extinction boundary.

Acknowledgments

Thanks to S.M. Holland for sharing programming insights and reviewing this work. T. Olszewski and an anonymous reviewer provided thorough and thoughtful reviews that increased the quality of this paper. This work was supported by the Geological Society of America, Sigma Xi Grants in Aid of Research, Paleontological Society Stephen J. Gould Student Grant-in-Aid Program, American Museum of Natural History Theodore Roosevelt Memorial Fund and the University of Georgia Department of Geology Wheeler-Watts Fund.

Literature Cited

Bush, A. M. and R. K. Bambach. 2004. Did alpha diversity increase during the Phanerozoic? Lifting the veils of taphonomic, latitudinal, and environmental biases. Journal of Geology 112:625-642.

Crist, T. O., J. A. Veech, J. C. Gering, and K. S. Summerville. 2003. Partitioning species diversity across landscapes and regions: a hierarchical analysis of α, β, and γ diversity. The American Naturalist 162:734-743.

Gering, J. C., T. O. Crist, and J. A. Veech. 2003. Additive partitioning of species diversity across multiple scales: implications for regional conservation of biodiversity. Conservation Biology 17:488-499.

Gering, J. C. and T. O. Crist. 2002. The alpha-beta-regional relationship: providing new insights into local-regional patterns of species richness and scale dependence of diversity components. Ecology Letters 5:433-444.

Gotelli, N. J. 2001. Research frontiers in null model analysis. Global Ecology and Biogeography 10:337-343.

Gotelli, N. J. and G.R. Graves. 1996. Null models in ecology. Smithsonian Institution. Washington D.C.

Holland, S. M. and M. E. Patzkowsky. 1997. Distal orogenic effects on peripheral bulge sedimentation: Middle and Upper Ordovician of the Nashville Dome. Journal of Sedimentary Research 67:250-263.

Hubbell, S. P. 1997. A unified theory of biogeography and relative species abundance and its application to tropical rain forests and coral reefs. Coral Reefs 16, Supplement:S9-S21.

Koleff, P., K. J. Gaston, J. L. Lennon. 2003. Measuring beta diversity for presence-absence data. Journal of Animal Ecology 72:367-382.

Lande, R. 1996. Statistics and partitioning of species diversity, and similarity among multiple communities. Oikos 76:5-13.

Okuda, T., T. Noda, T. Yamamoto, N. Ito, and M. Nakaoka. 2004. Latitudinal gradient of species diversity: multi-scale variability in rocky intertidal sessile assemblages along the Northwestern Pacific coast. Population Ecology 46:159-170.

Patzkowsky, M. E. and S. M. Holland. 1993. Biotic response to a Middle Ordovician paleoceanographic event in eastern North America. Geology 21:619-622.

—. 1996. Extinction, invasion, and sequence stratigraphy; patterns of faunal change in the Middle and Upper Ordovician of the Eastern United States. In B. J. Witzke, ed. Paleozoic sequence stratigraphy; views from the North American Craton. Geological Society of America Special Publication 306:131-142. Boulder, CO.

—. 1997. Patterns of turnover in Middle and Upper Ordovician brachiopods of the eastern United States: a test of coordinated stasis. Paleobiology 23:420-443.

Plotnick, R. E. and J. J. Sepkoski, Jr. 2001. A multiplicative multifractal model for originations and extinctions. Paleobiology 27:126-139.

Powell, M. G. and M. Kowalewski. 2002. Increase in evenness and sampled alpha diversity through the Phanerozoic: comparison of early Paleozoic and Cenozoic marine fossil assemblages. Geology 30:331-334.

Roy, K. 2001. Analyzing temporal trends in regional diversity: a biogeographic perspective. Paleobiology 27:631-645.

Sepkoski, Jr., J. J. 1988. Alpha, beta, or gamma: where does all the diversity go? Paleobiology 14:221-234.

Solè, R. V., J. M. Montoya, and D. H. Erwin. 2002. Recovery after mass extinction: evolutionary assembly in large-scale biosphere dynamics. Philosophical Transactions of the Royal Society of London B 357:697-707.

Wagner, H. H., O. Wildi, and K. C. Ewald. 2000. Additive partitioning of plant species diversity in an agricultural mosaic landscape. Landscape Ecology 15:219-227.

Whittaker, R. H. 1960. Vegetation of the Siskiyou Mountains, Oregon and California. Ecological Monographs 30:279-338.

Whittaker, R. H. 1972. Evolution and measurement of species diversity. Taxon 21:213-251.

Whittaker, R. J., K. J. Willis, and R. Field. 2001. Scale and species richness: towards a general hierarchical theory of species diversity. Journal of Biogeography 28:453-470.

Valentine, J. W. and T. D. Walker. 1987. Extinctions in a model taxonomic hierarchy. Paleobiology 13:193-207.

Veech, J. A., K. S. Summerville, T. O. Crist, and J. C. Gering. 2002. The additive partitioning of species diversity: recent revival of an old idea. Oikos 99:3-9.

Appendix. Model versions. All model versions based on sampling hierarchy of one region, two facies, two beds per facies, and three samples per bed.

Model	Taxon overlap between facies	Probability of occurrence	Extinction type	Runs
Low probability	33%	0.2	non-selective	70
High probability	33%	0.8	non-selective	70
Non-selective	33%	random	non-selective	95
Rare-selective	33%	random	rare selected	90
Abundant-selective	33%	random	abundant selected	90

Note: Random probability of occurrence reflects a randomly generated value drawn from a uniform distribution between 0 and 1.

Table 3.1. Comparisons of pre- and post-extinction beta values as calculated by both multiplicative and additive partitioning definitions of β.

Taxon	A	B	C	D
Sample 1	x	x	x	
Sample 2	x	x		x

	Multiplicative (Jaccard)	Additive partitioning
Pre-extinction	0.5	1
Elimination of shared taxa (A and B)	0	1
Elimination of unique taxa (C and D)	1	0
Elimination of shared and unique taxa (e.g., A and C)	0.5	0.5

Table 3.2. Diversity for pre- and post-extinction data across a regional extinction boundary during the Late Ordovician on the Nashville Dome. Values of α and β that are not weighted with respect to abundances are given in parentheses.

	Pre-extinction	Post-extinction
α_1	13.0 (11.6)	10.8 (9.0)
β_1	7.0 (7.7)	5.2 (4.8)
β_2	10.0 (8.8)	8.5 (9.8)
β_3	8.0 (10.0)	11.5 (12.5)
γ	38.0	36.0

Figure 3.1. Hierarchical sampling strategy used in the model and field data to calculate additive partitioning of diversity.

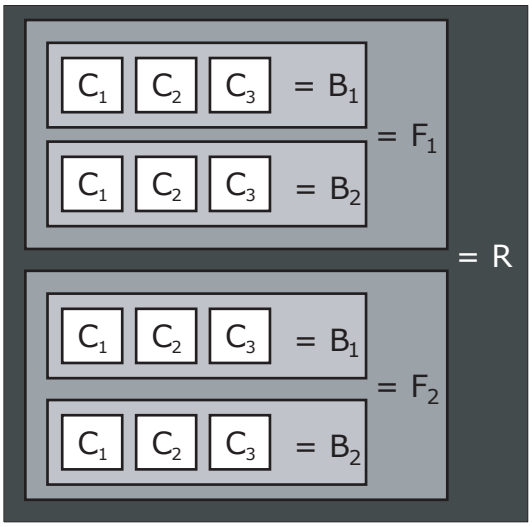
C1 C2 C3 = B1
C1 C2 C3 = B2
= F1
C1 C2 C3 = B1
C1 C2 C3 = B2
= F2
= R

Figure 3.2. Decrease in α, β, and γ diversity with increasing percent extinction. The pattern holds for all probabilities of taxon occurrence and for both non-selective and selective extinction with respect to abundance. Graph based on high-probability model (see Appendix), thus β_2 values are extremely low.

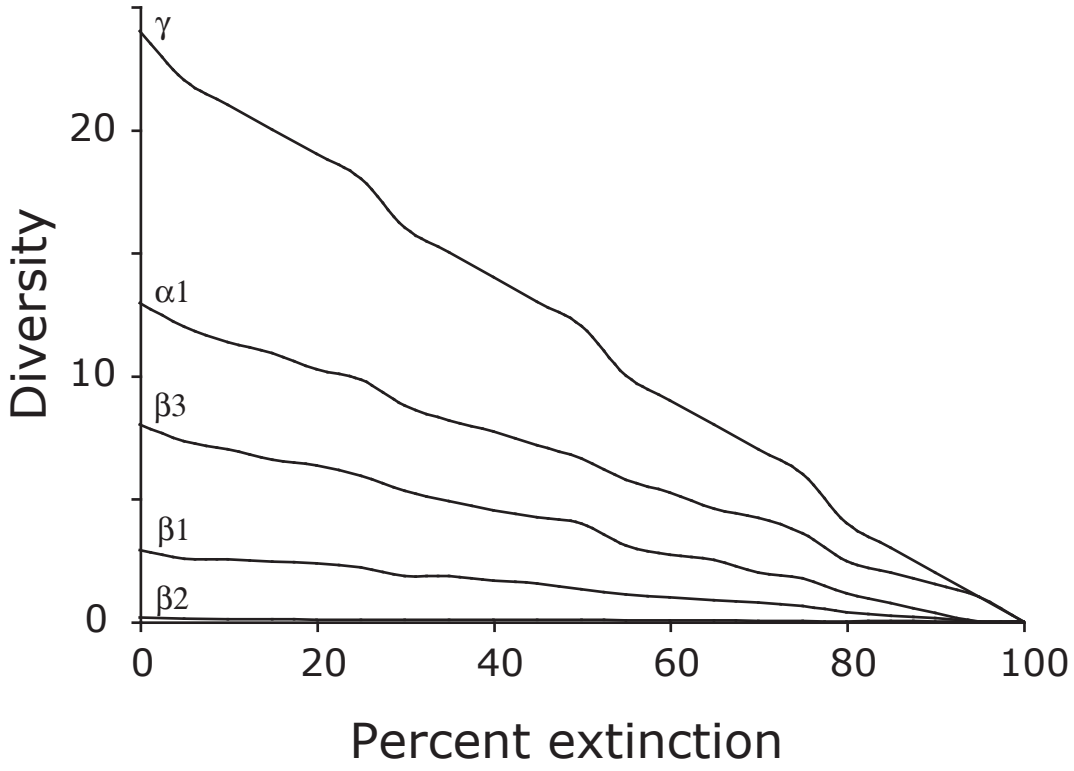
γ
α1
β3
β1
β2
Diversity
0
10
20
0
20
40
60
80
100
Percent extinction

Figure 3.3. Diversity partitioning as a function of percent extinction for different probabilities of taxon occurrence. A, low probability of taxon occurrence (0.2). B, high of taxon occurrence (0.8). C, random probability of taxon occurrence (random number between 0 and 1 drawn from uniform distribution).

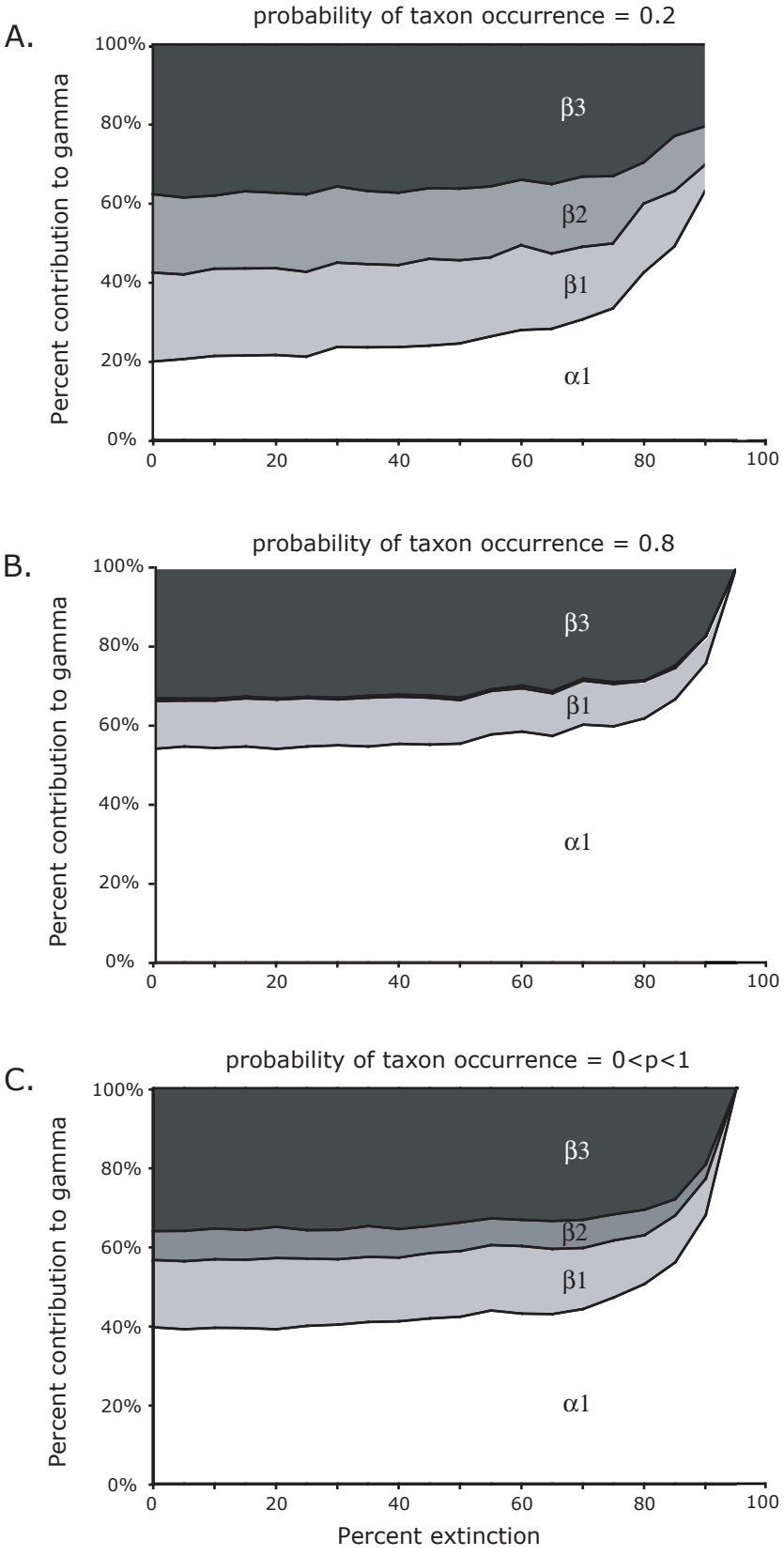
A.
probability of taxon occurrence = 0.2
Percent contribution to gamma
100%
80%
60%
40%
20%
0%
β3
β2
β1
α1
0
20
40
60
80
100
B.
probability of taxon occurrence = 0.8
Percent contribution to gamma
β3
β1
α1
C.
probability of taxon occurrence = 0<p<1
Percent contribution to gamma
β3
β2
β1
α1
Percent extinction

Figure 3.4. Diversity partitioning as a function of percent extinction for different modes of extinction. A, selective extinction targeting rare taxa. B, non-selective extinction with respect to taxon abundance. C, selective extinction targeting abundant taxa. All model trials based on random probability of taxon occurrence. Slight variations in trends due to model noise.

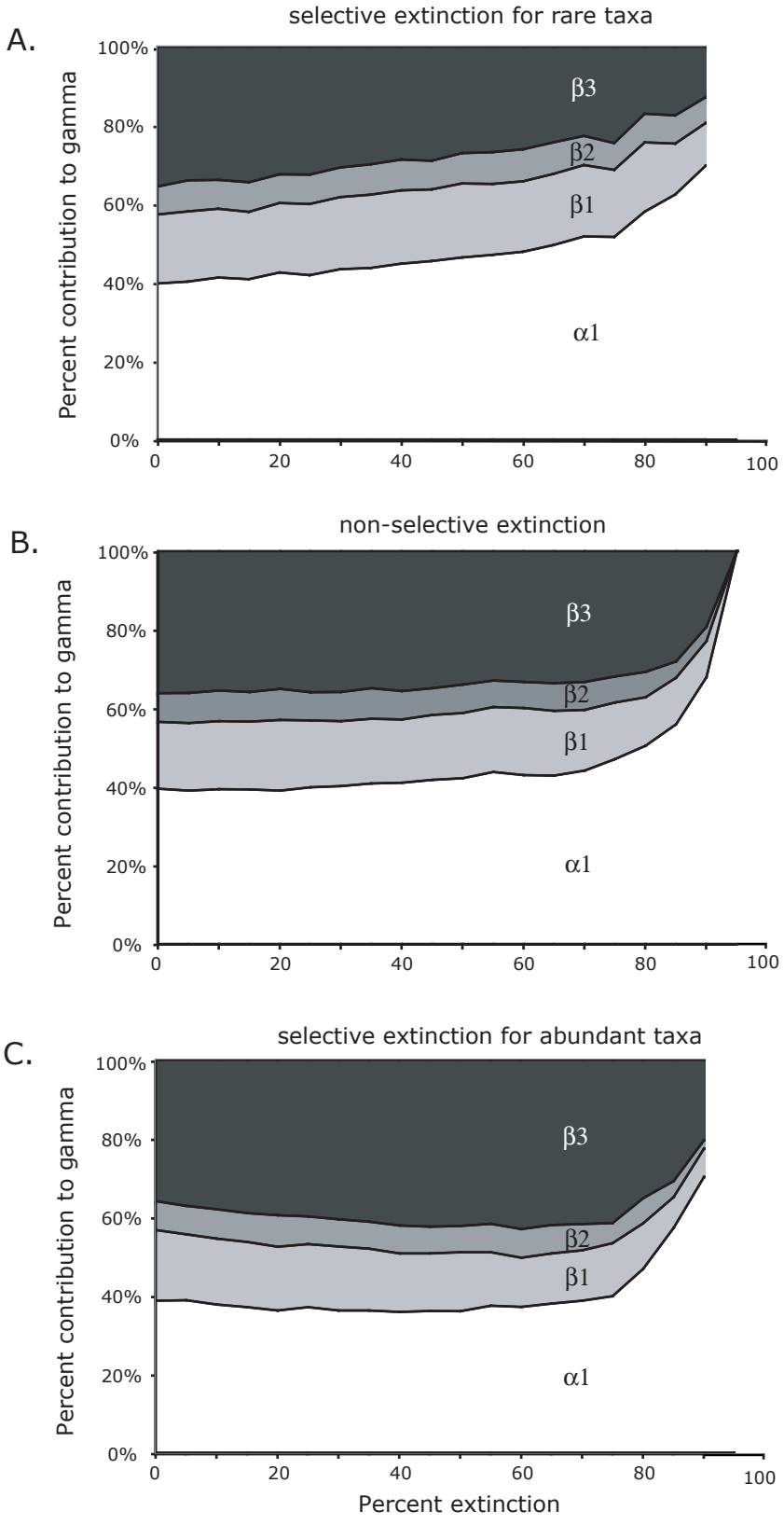
A.
selective extinction for rare taxa
Percent contribution to gamma
100%
80%
60%
40%
20%
0%
β3
β2
β1
α1
0
20
40
60
80
100
B.
non-selective extinction
Percent contribution to gamma
100%
80%
60%
40%
20%
0%
β3
β2
β1
α1
0
20
40
60
80
100
C.
selective extinction for abundant taxa
Percent contribution to gamma
100%
80%
60%
40%
20%
0%
β3
β2
β1
α1
0
20
40
60
80
100
Percent extinction

Figure 3.5. Diversity partitioning for pre- and post-extinction conditions across a regional extinction boundary in the Late Ordovician Nashville Dome.

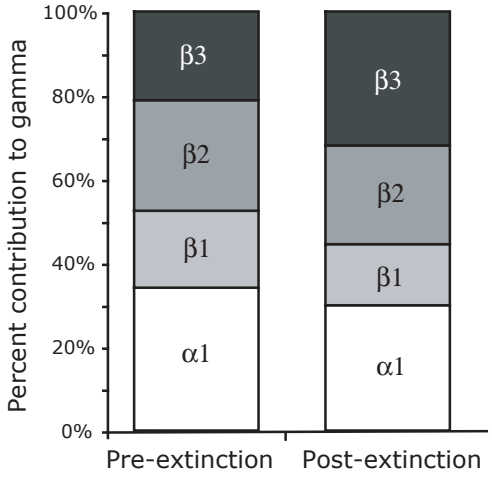
100%
80%
60%
40%
20%
0%
Percent contribution to gamma
β3
β2
β1
α1
β3
β2
β1
α1
Pre-extinction
Post-extinction

CHAPTER 4

ECOLOGICAL RESTRUCTURING AFTER EXTINCTION: THE LATE ORDOVICIAN (MOHAWKIAN) OF THE EASTERN UNITED STATES[1]

[1] Layou, K.M. To be submitted to *Palaios*.

Abstract

Most research regarding ecological response to extinction in the fossil record focuses on qualitative, taxonomically based analyses. By shifting to quantitative analyses that incorporate paleocommunity-level data, a richer ecological perspective on how paleocommunities respond to extinction may be gained.

During the Late Ordovician (Mohawkian), a regional extinction occurred among marine taxa in the Appalachian Basin of eastern North America. To examine community-level paleoecological change across this extinction boundary, field censusing of macroinvertebrate genera was completed for three regions of the Ordovician Appalachian Basin including the Nashville Dome of Tennessee, the Jessamine Dome of central Kentucky, and the Valley and Ridge of western Virginia. In each region, shallow and deep subtidal environments were sampled (when present) in each of four stratigraphic sequences representing pre-extinction (M3 and M4 sequences) and post-extinction (M5 and M6 sequences) intervals.

Diversity and evenness metrics calculated from subsampled field data decline across the extinction boundary and into the M6 sequence. Both shallow and deep subtidal environments exhibit declines in diversity across the extinction boundary, and the metrics for the deep subtidal facies continue to decline into the M6 sequence, unlike those for the shallow subtidal facies. Regionally, the metrics for Virginia decline the most across the extinction boundary, followed by Tennessee, with Kentucky showing no decline. These regional differences reflect geographic variability in not only the effects of the extinction, but also in the extent of immigration of new taxa to different areas of the basin. Variability in guild dominance and in multivariate analyses supports strong

regional differences in ecological response, which may reflect regional variation in environmental change. During deposition of the M4, Virginia paleocommunities were dominated by a unique brachiopod assemblage not seen in Tennessee and Kentucky, namely *Bilobia*, *Christiana*, *Eoplectodonta*, *Paucicrura,* and *Paurorthis*. At this time in Tennessee, shallow and deep subtidal paleocommunities were dominated by ramose bryozoans and articulate brachiopods, while Kentucky shallow subtidal paleocommunities were similar to those of Tennessee, but with locally abundant mollusks and corals. During deposition of the M5, ecological variability among the regions declined, with the emergence of biofacies based primarily on differing proportions of four common articulate brachiopods: *Dalmanella*, *Rafinesquina*, *Sowerbyella*, and *Zygospira*. However, during deposition of the M5 in Tennessee and Kentucky, the previously similar shallow subtidal paleocommunities diverged. During deposition of the M6, paleocommunities in all regions are similar to those of the M5, and Tennessee and Kentucky shallow subtidal communities are compositionally more similar as they were during deposition of the M4. These quantitative analyses highlight the complexity and variability in paleocommunity response to the same extinction event.

Introduction

Extinction is inevitable for all species, and the simultaneous extinction of many taxa is of particular interest to paleobiologists. Indeed, much attention has been paid to mass extinctions and their causal mechanisms (Sepkoski 1986; Donovan 1989; Jablonski 1986, 1995, 2005; Bottjer 2001; Bambach et al. 2004). However, few studies have focused on the smaller, regional extinction events within the fossil record, which

are typically considered “background” extinction, yet are responsible for more than 95 percent of all species extinctions during the Phanerozoic (Raup 1992). Only recently has much attention been given to the aftermath of extinction (Erwin 1996, 1998, 2001; Hart 1996; Hallam and Wignall 1997) at any spatio-temporal scale, and most of this work has focused on taxonomic data, rather than paleoecological approaches that incorporate data regarding paleocommunity-level information (but see Droser et al. 1997, 2000; Bottjer 2001).

This paper explores through a series of quantitative analyses how a marine macroinvertebrate biota responded to a regional extinction. Highlighting changes in diversity structure in the context of paleocommunities offers a richer perspective on the effects of extinction on biodiversity. Other quantitative analyses, such as multivariate ordination, expand this view of paleocommunity response to extinction by highlighting pre- to post-extinction variations in community structure along ecological gradients.

Ecological response to extinction.—The quantitative analyses presented in this paper diverge from the standard methods typically used to examine biological recovery from extinction, which have emphasized qualitative divisions of the history of an extinction episode, and have concentrated on single taxa. Paleontologists have traditionally divided an extinction episode into three phases: 1) the extinction, defined by a rapid decrease in taxonomic diversity; 2) the survival period, during which there is a lag phase of minimal taxonomic diversity; and, 3) the recovery, marked by a rapid increase in taxonomic diversity (Kauffman 1986; Donovan 1989; Harries and Kauffman 1990; Erwin 1996, 1998; Hallam and Wignall 1997; Bottjer 2001). Identification of these phases has highlighted the fact that biotas may not necessarily begin immediate

rebound following extinction. Where lines are drawn between phases can be arbitrary, and methods used to define threshold values for the changes in diversity metrics (e.g., origination and extinction rates) that mark these transitions vary.

Paleontologists have also traditionally studied extinctions through the diversity trajectory of a single higher-order taxon using species counts. Thus, to aid in defining the extinction phases, the responses of these taxa are often categorized using qualitative labels such as Lazarus, holdover, or disaster taxa (Hallam and Wignall 1997; Bottjer 2001). External mechanisms (other than those which caused the extinction) could be responsible for taxonomic patterns observed during the post-extinction interval. For example, consider a Lazarus taxon, which disappears during the extinction, is not present through the survival period, and reappears during the recovery period. Faunal tracking (Brett et al. 1990) or variations in depositional sequence architecture (Holland 1995, 2000) could be responsible for producing a Lazarus taxon, if the taxon's preferred facies is missing from the depositional sequences during the survival period; alternatively, the Lazarus taxon could truly have gone locally extinct. These potential differences have entirely different paleoecological importance.

These previous approaches have left unanswered several important and interesting questions: Do relative abundance distributions within paleocommunities change across extinction boundaries? How does evenness vary with extinction? How is the diversity structure among different ecological guilds affected by the same extinction event? Is there spatial or temporal variation in the response of these parameters among paleocommunities? These questions clarify why more than a

qualitative, taxonomic approach is necessary to understanding biological response to extinction.

Extinctions and their aftermath can be examined using quantitative, ecological approaches that will provide insight on how community-level dynamics change across an extinction boundary. By comparing pre- and post-extinction parameters used to define paleocommunities, such as taxonomic richness, relative abundance distributions, and evenness patterns (e.g., SHE analysis of Hayek and Buzas 1997 and Buzas and Hayek 2005), and by comparing these parameters among ecological guilds (e.g., paleocommunity-level change of Droser et al. 1997, 2000), the response of the community as a whole to extinction may be revealed. Studying extinction in this way allows for predictions to be made based on mathematical relationships among diversity and evenness metrics resulting from changes in the relative abundance structure of communities (Layou 2007; Chapter 2), and allows for examination of changes of resource utilization among taxa. Additionally, the use of multivariate analyses, such as ordination, can assess the extent of taxonomic abundance and compositional change due to extinction.

Finally, quantitative examination of paleoecological changes within a sequence stratigraphic framework is key to understanding not only how faunal assemblages may vary within and among environments through time, but also to what extent preservational biases and stratigraphic architecture influence faunal distributions (Brett 1995; Holland 1995; Patzkowsky and Holland 1997; Holland and Patzkowsky 1999). It is well known that depositional environments heavily affect the taxonomic composition and abundance distributions within faunal assemblages (Dodd and Stanton 1990).

Similarly, specific phases of relative sea level cause the reoccurrence of associated lithofacies. Together, these factors lend enough predictability not only to infer faunal distributions in the stratigraphic record, but also to separate evolutionary from ecological change (i.e., originations and extinctions versus tracking of preferred environments; Holland and Patzkowsky 2002; Holland 2003).

Regional extinction during the Late Ordovician of the Eastern United States.—During the Late Ordovician (Mohawkian), a regional extinction occurred within the Appalachian Basin of the eastern United States. Many macroinvertebrate taxa that were abundant in paleocommunities of the time were affected, including articulate brachiopods, tabulate and rugose corals, calcareous algae, gastropods, and bryozoans (Patzkowsky and Holland 1996 and references therein). For articulate brachiopods, both genus and species level extinction rates increase well above local and global background rates (Patzkowsky and Holland 1997). Based on the sequence stratigraphic framework developed for the Upper Ordovician of the Appalachian Basin by Holland and Patzkowsky (1996, 1998), six depositional sequences have been identified within the Mohawkian Series (Figure 4.1). The regional extinction event occurs predominantly after the M4 sequence—taxa disappear at the M4/M5 boundary and either are absent through the rest of the Mohawkian and the subsequent Cincinnatian Series, or reappear late in the Cincinnatian Series.

The onset of the Taconic orogeny coincides with this extinction, as well as major changes in sedimentation throughout the Appalachian Basin (Holland and Patzkowsky 1996, 1997). Direct and indirect effects of the orogeny include a shift from tropical-type to temperate-type carbonate deposition, an increase in phosphate deposition and an

influx of siliciclastic sediment (Holland and Patzkowsky 1996, 1997). The M4/M5 boundary is also associated with +2-3‰ excursions in $\delta^{13}C$ of micrite, and approximately +4-6‰ for organic carbon in the early M5 for the midcontinent and eastern United States (Hatch et al. 1987; Patzkowsky et al. 1997; Railsback et al. 2003).

These changes in carbonate sedimentation have been attributed to several potentially interacting mechanisms. Because temperature and nutrient levels both control modern carbonate deposition, it has been suggested that a regional zone of upwelling in the distal portions of the Appalachian Basin along the Cincinnati Arch and Nashville Dome may have caused the observed shift to cool-water carbonates and increased occurrence of phosphate (Holland and Patzkowsky 1996, 1997). Recently, it has been argued that regional upwelling alone could not produce the observed carbon isotope shifts in the Appalachian Basin, and that carbon fluxes from bryophyte-dominated terrestrial ecosystems may have played an important role at this time (Panchuk et al. 2005).

Methods

Data collection.—Field samples were collected within a hierarchy of depositional sequences, facies, and regions (Table 4.1). Samples were collected from four depositional sequences: the M3 and M4, which are analyzed together as the pre-extinction interval spanning approximately 1.5 m.y., and the M5 and M6, which represent two post-extinction intervals, and together span 2.0 m.y. Within each sequence, shallow subtidal and deep subtidal facies were sampled to allow for

comparison of paleocommunity response between these environments. Shallow subtidal facies include environments above fair-weather wavebase and are dominated by skeletal packstones and grainstones (Holland and Patzkowsky 1998). Deep subtidal facies are found between fair-weather and storm wavebase, and are predominantly interbedded wackestones, siltstones, and shales (Holland and Patzkowsky, 1998). Exposure of shallow subtidal facies in the M3 is limited, as is the deep subtidal in the M4, thus, samples from these sequences were combined to represent pre-extinction conditions. Samples from both facies within each sequence were collected from three regions within the Appalachian Basin, including the Jessamine Dome in central Kentucky, the Nashville Dome in central Tennessee, and the Valley and Ridge of western Virginia (Figure 4.2). This was done to assess potential variation in paleocommunity response in distal and proximal areas of the basin. Where sufficient exposure was available, both facies in all sequences were sampled at numerous localities within a region, to ensure broad spatial coverage. Lack of exposure precluded sampling from the deep subtidal of the Tennessee M6, the Kentucky M3/M4, and the Virginia shallow subtidal facies for all sequences. Virginia localities were supplemented with data from Plants (1977) and Springer (1982).

Abundances of taxa within samples were obtained by field censusing all macroinvertebrate specimens on bedding-plane surfaces. Specimens were identified to the genus level, since species level identifications for many taxa would require preservation of internal features. Effort was made to count at least 40 specimens per sample, the minimum sampling identified by an initial set of collector curves from each facies and sequence to ensure adequate representation of the paleocommunities. For

brachiopods and bivalves, specimens were identified by individual valve type (brachial, pedicle, or indeterminate for brachiopods; left, right, or indeterminate for bivalves) or as articulated. For both brachiopods and bivalves, the minimum number of individuals was calculated by summing the number of articulated specimens, the larger value of single valves, and half the number of indeterminate valves. One half of the total valves were used for ostracod abundance. One-centimeter lengths were counted as one individual for ramose bryozoans to ensure comparable counts with other similarly abundant taxa. Unique morphologies of crinoid columnals were classified as rare (1 specimen per sample), common (2-10 specimens per sample), or abundant (> 10 specimens per sample). For quantitative analyses, these classifications were converted to abundance values 1, 3 and 6 respectively as a conservative estimate of the number of individuals. Because of the potential difficulty in relating the abundances of bryozoans and crinoids to other more easily counted taxa, runs of all analyses were completed with and without bryozoan and crinoid data. In all cases, identified trends in diversity and evenness metrics and broad patterns in ordinations did not change, confirming that the conclusions are not dependent on counting methods. Prior to any statistical analyses, the five samples bearing only a single taxon were removed from the dataset. Thus, the final total data matrix (Table 4.1) included 317 samples and 107 taxa.

Diversity and evenness analyses.—All samples were evaluated using diversity and evenness metrics that are common in the ecological and paleontological literature, including: *S*, taxonomic richness; Shannon's *H'* (Shannon 1948; also see Hayek and Buzas 1997 for discussion); *E*, Buzas and Gibson's *E* (Buzas and Gibson 1969); Pielou's *J* (Pielou 1966); and Hurlbert's *PIE* (Hurlbert 1971). *S* and *H'* are diversity

metrics, while *E*, Pielou's *J*, and *PIE* are all evenness metrics. When appropriate, beta diversity was calculated using the Jaccard coefficient (e.g. Sepkoski 1988) to compare diversity patterns among sequences and regions. See Appendix for equations for all of these metrics.

Because *S*, *H'*, *E*, and Pielou's *J* are sensitive to sample size, a subsampling routine was used to standardize the total number of individuals per sample to allow for valid comparison of mean metric values for across the extinction boundary for the various facies and regions. The subsampling was carried out on a subset of original 317 sample data matrix using only samples within a single sequence (e.g., all samples per sequence, all shallow subtidal samples per sequence, or all Kentucky samples per sequence). Abundances of each taxon within the data subset were tallied to create a single vector, or supersample, of abundances for all taxa. From this supersample, 100 individuals were randomly chosen without replacement to create a new sample. This process was repeated 1000 times to create a new data matrix of 1000 samples, each with 100 individuals. Mean diversity and evenness metrics (*S*, *H'*, *E*, Pielou's *J*, and *PIE*) and 95% confidence intervals were then calculated based on the matrix of 1000 samples.

Guild analyses.—Ecological guilds offer another perspective on ecological structure in paleocommunities by highlighting potential variation in functional relationships among organisms, including those typically grouped within a taxon. Guilds are generally defined as groups of organisms that use environmental resources in similar ways (Root 1967). The guild designations used here are based on Bambach's (1983) definition of guilds within paleocommunities, which incorporates a three-

dimensional view of ecospace based on food source, space utilization, and organismal bauplan. Ten guilds were recognized among the taxa present within the field samples (Table 4.2), including five guilds that reflect the majority of the fauna, and five that reflect taxa with unique life habits. Taxonomic richness patterns and relative abundance distributions of these guilds were examined across the extinction boundary. 95% confidence intervals for all guild analyses were calculated based on Raup (1991), using a program written by S.M. Holland and available at http://www.uga.edu/~strata/software/Software.html).

Ordination analyses.—Field data were ordinated with nonmetric multidimensional scaling (MDS). Ordination techniques are used to reduce dimensionality of a multivariate dataset to highlight potential ecological gradients within the data (e.g. Springer and Bambach 1985; Webber 2002; Bonelli et al. 2006). All patterns seen in MDS ordinations were also present in detrended correspondence analysis (DCA) ordinations, suggesting robust underlying structure in the data. However, data are reported using MDS because of ease of interpretation due to less gradient distortion (Minchin 1987; Shi 1993 and references therein).

Prior to ordination, data were subjected to a percent transformation on samples, followed by a percent maximum transformation on taxa to correct for differences in sample size and abundances among taxa, respectively (Gower 1987; Miller 1988; Shi 1993). All MDS ordinations were run in R (version 2.2.1) using the metaMDS function of the vegan library, with a Bray-Curtis distance metric and autotransform set to false because data transforms were applied separately prior to ordination.

Results

Diversity and evenness metrics.—Richness (Fig. 4.3, black portions of bars) drops across the M4/M5 sequence boundary in the entire dataset, as well as within each facies and each region. However, in every case, the decline in *S* is mitigated by the appearance of additional taxa in the M5 (Fig. 4.3, white portions of bars). These additional taxa represent true originations and migrations of taxa, as well as first occurrences of these taxa within the collected dataset. Based on taxonomic lists, the extinction is more apparent in deep subtidal environments, and within the proximal areas of the basin (Virginia), yet for both, richness levels are maintained by the immigration of new taxa. Although all regions exhibit an addition of new taxa, Kentucky experiences the greatest influx of new taxa, and total richness in this region is actually higher in the M5 than the M4. This suggests that the Jessamine Dome may have served as an avenue for taxa immigrating into the basin.

Comparison of diversity and evenness metrics among the three depositional sequences reveals declines in richness, but relatively stable evenness across the extinction boundary (Figure 4.4). Although most of these metrics display a statistically significant decline through time (Table 4.3), the changes in most of the metrics are small. Excluding *S*, the difference between means is exceptionally small when compared to the values of the metrics (Fig. 4.4). This suggests that aside from a true decline in taxonomic richness, the variations in the metrics do not have much ecological significance. Both *S* and *H'* decline across the extinction boundary, and continue to drop into the M6. All evenness metrics (*E*, Pielou's *J*, and *PIE*) show very slight declines from the M4 to the M5 and slight increases from the M5 to the M6. Despite the

more substantial decline in richness, the general lack of variability in the evenness metrics implies there was no major restructuring of abundance distributions of taxa within sequences.

Diversity and evenness metrics show different trends in shallow and deep subtidal facies (Figure 4.5). Once again, all tests for differences of means between depositional sequences yield statistically significant results, but the differences in means is much smaller than the metric values (Table 4.3). Both environments show a decline in *S* and *H'* across the extinction boundary, but the deep subtidal environment continues to decline in richness into the M6 while the shallow subtidal gains taxa. This suggests that deep subtidal environments continued to experience the effects of the extinction. In both facies, all evenness metrics (*E*, Pielou's *J*, and *PIE*) decline across the extinction boundary, with a continued decline into the M6 in the shallow environments, and an opposite increase in evenness in the deep subtidal. The different responses of the evenness metrics in the M6 for each facies reflect variations in the diversity metrics. The origination of new taxa or the reappearance of taxa in the shallow subtidal facies is most common during the M6 (Fig. 4.3), which leads to the increases in *S* and *H'*. The new or reappearing taxa are usually found in high abundances. Thus, adding several highly abundant taxa to the paleocommunity causes evenness metrics to decrease. Likewise, declines in *S* and *H'* typically suggest a flattening of the abundance distribution of taxa due to fewer present individuals (Chapter 2), thus, evenness should increase, as is seen in the M6 deep subtidal facies.

Comparison of the metrics across the different regions highlights geographic variability in ecological response to this extinction (Figure 4.6). The results shown are,

again, statistically significant trends with minimal ecological significance (Table 4.3). Tennessee richness slightly declines at the extinction boundary, and does not vary into the M6. Virginia richness substantially drops at the extinction boundary, and continues to decline into the M6. This may, in part, drive the pattern seen in the deep subtidal facies since Virginia samples comprise the majority of the M6 deep subtidal samples. Meanwhile, Kentucky richness is not generally affected at either sequence boundary. In Tennessee and Kentucky, evenness does not substantially vary across either sequence boundary, while in Virginia, evenness declines at the M4/M5 boundary, then rebounds into the M6. Thus, the biological response to the extinction varies geographically. Virginia sustained the most diversity restructuring, while Tennessee experienced lesser major community-level changes, and Kentucky may not have been affected at all by the extinction, most likely because of the substantial influx of taxa to this region (Fig. 4.3).

Guild structure.—At the scale of the entire basin (Figure 4.7A), there are shifts in guild dominance from the pre-extinction to the post-extinction. The M4 guilds include colonial attached suspension feeders (CASF), mobile epifaunal deposit feeders (MEDF), pedunculate epifaunal suspension feeders (PESF), reclining epifaunal suspension feeders (RESF), and solitary attached suspension feeders (SASF). In M5, MEDF, CASF, and SASF decline in relative abundance, while PESF and RESF increase. The relative abundances of guilds change little from the M5 to the M6. Although articulate brachiopods were most affected by this extinction event (Patzkowsky and Holland 1996, 1997), their guilds (PESF and RESF) show marked increases in relative abundance after the extinction. This is due both to the appearance of new brachiopod taxa during the M5, and simultaneous declines in other guilds.

Guild membership varies between facies for the whole basin (Figures 4.7B and 4.7C). CASF (mostly bryozoans) dominate both facies prior to the extinction, however, MEDF and PESF are more abundant in deep subtidal settings than in shallow. A shift in guild dominance occurs after the extinction boundary for both facies. In shallow environments, marked decreases occur in RESF, MEDF, and SASF, and major increases occur in PESF and CASF. Similar declines in MEDF and increases in PESF are found in deep subtidal environments, but CASF decline and RESF increase.

Guild membership also varies among regions during the M4 (Figures 4.7D, 4.7E, and 4.7F), thus, different post-extinction patterns are seen among regions as well. Prior to the extinction, CASF and MEDF dominate Tennessee, along with PESF, RESF, and SASF. After the extinction, MEDF and RESF both decline in relative abundance, while CASF, PESF, and mobile infaunal deposit feeders (MIDF) increase. The patterns exhibited by the brachiopod-dominated guilds (PESF and RESF) agree with those of Patzkowsky and Holland (1999). Kentucky generally follows the same pattern as Tennessee, although post-extinction increases in PESF are much more substantial and CASF decline rather than increase. Virginia pre-extinction paleocommunities are dominated by the PESF and MEDF guilds, with lower but similar abundances of RESF and CASF. In post-extinction Virginia, RESF increases substantially, PESF increases slightly, and MEDF, CASF, and SASF decline.

Ordination.—MDS ordination (Figure 4.8) of all data show a good segregation of the pre-extinction samples (M4) from the M5 and M6 samples (Figure 4.8A), confirming that the pre-extinction paleocommunities differ from the post-extinction communities. While some taxa go regionally extinct at the M4/M5 boundary, over half the taxa present

in the M4 are also present in the M5 and M6 in the dataset used here. Despite little change to either the abundance distributions as seen with the diversity and evenness metrics, or the overall taxonomic list among sequences, there are shifts in which taxa are dominant in each sequence (Table 4.4). The list of the ten most abundant taxa from each sequence shows a clear change from the M4 to the M5. The M4 is dominated by bryozoans, particularly thin ramose taxa, such as *Escharopora* and *Rhindictya*, and articulate brachiopods *Strophomena* and *Pionodema* are particularly abundant. While bryozoans are dominant in the M5 as well, a new group of articulate brachiopods are most abundant. The M5 and the M6 have the same eight most abundant taxa, and the only major difference between the sequences is which brachiopods hold the highest ranks (*Dalmanella* and *Rafinesquina* top the M5, while *Zygospira* and *Sowerbyella* top the M6).

Comparison of the facies among sequences highlights increasing differences between the facies through time (Fig. 4.8B). Using the same axes scores for data shown in Figure 4.8A, only the centroids of both facies within each sequence are plotted for purposes of clarity. Axis 1 reflects a general depth gradient, with high axis 1 scores reflecting deeper water samples. Thus, within each sequence, the deep subtidal facies has a higher mean axis 1 score. The ordering of sequences along axis 1 also corresponds with the overall deepening within the basin from the M4 to the M6. Within the M4, shallow and deep subtidal facies have similar axis 1 scores, while in both post-extinction sequences, facies are better separated along axis 1. This suggests that prior to the extinction, shallow and deep subtidal communities were compositionally more similar, while after the extinction, the communities within these environments became

more disparate.

When regions are considered, the Virginia samples always plot separately from the Tennessee and Kentucky samples (Figure 4.9). During the M4 (Fig. 4.9A) this is due to a unique Virginia brachiopod assemblage, including *Bilobia*, *Christiana*, *Eoplectodonta*, *Paucicrura*, and *Paurorthis*. Given that the faunal lists are so similar for the overall M5 and M6 sequences, beta diversity (Jaccard coefficient based on sequence taxonomic lists) between each of the regions was calculated for these sequences (Table 4.5) to highlight another potential source of faunal variation. For both the M5 and M6, the Jaccard coefficient between Tennessee and Kentucky is significantly higher than that of either region with Virginia. This suggests Tennessee and Kentucky are taxonomically more similar to each other, and is supported by the overlap of Tennessee and Kentucky samples in ordination space for the M5 (Fig. 4.9B) and M6 (Fig. 4.9C). Differences in the length of the faunal list of the Virginia M5 and M6 may also be a result of slightly different counting methods used in this study versus the supplemental data of Plants (1972) and Springer (1985). For example, thin ramose bryozoans were counted based on various morphologies in this study versus one thin ramose category in the supplemental data). However, an avenue to consider is whether the Tennessee and Kentucky samples are as compositionally similar as they initially appear.

Owing to lack of available outcrop for sampling deep subtidal facies in the Kentucky M4 and Tennessee M6, regional comparison of Tennessee and Kentucky is limited to shallow subtidal facies. Ordination of the shallow subtidal samples from Tennessee and Kentucky from the M4 to the M6 captures another aspect of the

geographic variability in ecological response to this extinction event (Figure 4.10). During the M4 (Fig. 4.10A), samples from both regions are similar, and are dominated by articulate brachiopods (*Strophomena*, *Zygospira*) and ramose bryozoans (*Escharopora*, *Rhindictya*), although in Kentucky, gastropods, nautiloids, and corals may be locally abundant. Moving into the M5 (Fig. 4.10B), there is clear separation of Tennessee and Kentucky shallow subtidal samples. This may reflect the variations in diversity and evenness that are seen in Tennessee, but not Kentucky (Fig. 4.6). Tennessee has more abundant *Tetradium* and massive trepostome bryozoans, while Kentucky has more diverse mollusks and crinoids. Finally, in the M6 (Fig. 4.10C), the Tennessee and Kentucky shallow subtidal samples are again much more similar to one another, sharing articulate brachiopods (*Hebertella*, *Rafinesquina*, *Zygospira*) and ramose bryozoans (*Escharopora*, *Rhindictya*, thin ramose 1), perhaps reflecting a recovery in the paleocommunities to a pre-extinction norm. Beta diversity increases slightly across the extinction boundary, and then declines into the M6 (Jaccard coefficient, M4 = 0.479, M5 = 0.472, M6 = 0.491), suggesting that the regions should be more distinct immediately following the extinction.

Discussion

The analyses of this regional extinction event reveal that variation occurs among taxa, between facies, among regions, and within guilds across the extinction boundary, and each level of variation offers another perspective on how variable paleoecological response to extinction may be. Further examination of these quantitative, community-

level parameters can provide insights on the selectivity during this extinction and the extent of environmental change associated with this event.

Selectivity.—Null modelling can be used to predict different responses of the evenness metrics *E*, Pielou's *J*, and *PIE* for extinctions that are selective with respect to taxon abundances (Chapter 2). In general, *E* should increase and *PIE* should decrease across an extinction boundary. Pielou's *J* should increase substantially, increase slightly, or decrease depending on whether the extinction is selective against abundant taxa, not selective with respect to taxon abundance, or selective against rare taxa, respectively. Because the null models of Chapter 2 are based on comparisons of a pre-extinction community with post-extinction survivors, only holdover taxa should be used to calculate evenness metrics to predict selectivity conditions. Table 4.6 compares the subsampled mean diversity and evenness metrics for the M4/M5 boundary using only holdover taxa for the M5 sequence. When compared to mean diversity and evenness metrics for the whole paleocommunity (Figs. 4.4, 4.5, 4.6), the lack of immigrant taxa in the M5 calculations yields a decline in mean diversity metrics (*S* and *H'*), but interestingly, the evenness metrics (*E*, Pielou's *J*, and *PIE*) are very similar. The slight decline in evenness metrics at the sequence level (Table 4.6) suggests selectivity against rare taxa within the basin occurred with this extinction, and this is mirrored in both shallow and deep subtidal facies. However, the three regions examined within the basin have different patterns of evenness variation across the boundary, despite declines in richness in all regions (Table 4.6). In Tennessee, richness slightly declines and evenness (Pielou's *J*) slightly increases, which implies no selectivity with respect to taxon abundances on the Nashville Dome. In Kentucky and Virginia, richness drops

more substantially, and all evenness metrics decline. The decrease in Pielou's *J* across the extinction boundary suggests rare taxa were targeted on the Jessamine Dome and in proximal areas of the basin. The lack of abundance-related selectivity in Tennessee may reflect true geographic variation in selectivity.

The overall selectivity against rare taxa in the basin for this extinction correlates with modern ecological studies that suggest rare taxa are more likely to go extinct than abundant taxa (Gilpin and Soulé 1986). Additionally, the influx of new taxa into the basin may be associated with an increase in immigration that is high enough to accelerate the extinction of rare taxa (Hubbell 2001). However, high abundance has been shown to have no increased benefit on survivorship for the end-Cretaceous extinction (Lockwood 2003). These conflicting results on the importance of abundance on survivorship lend support to the idea that factors that increase survivorship during background extinction, including the regional event examined here, do not offer the same benefits during mass extinctions (Jablonski 1991, 1996, 2001, 2005).

Environmental change.—When changes to the guild abundance structure are examined between facies and among regions, environmental variation within the basin is apparent. Comparison of facies at the M4/M5 boundary (Figs. 4.7B and 4.7C) reveals simultaneous increases among CASF guild members, such as corals and bryozoans, in shallow subtidal facies, and among RESF strophomenid brachiopods in deep subtidal facies. The colonial suspension feeders require firm substrates for colonization and low turbidity within the water column for proper feeding. Strophomenid brachiopods possess wide, flat valves that allow them to "snowshoe" on soft, muddy substrates (Fürsich and Hurst 1974). Thus, these shifts among guilds may reflect

increasing substrate instability, turbidity, and siliciclastic influx (Holland and Patzkowsky 1996, 1997) to the basin during the M5, which may be enhanced by continued deepening of the basin into the M6. Within Tennessee and Kentucky (Figs. 4.7D and 4.7E), there are marked increases in the abundances of pedunculate suspension feeders, and colonial attached suspension feeders gain or maintain high abundances during the M5. Although the orogenic effects of increasing substrate instability and siliciclastic input are present in these regions at this time, the guild compositions suggest the effects were not deleterious enough to limit suspension feeders from paleocommunities. Additionally, increased nutrient availability caused by upwelling (Holland and Patzkowsky 1996, 1997) or increased terrestrial runoff (Panchuk et al. 2005) could potentially support these higher abundances of suspension feeders in distal areas of the basin. Because the Virginia samples (Fig. 4.7F) are more proximal to the orogenic belt, and are dominated by samples from deep subtidal facies, the decline among many attached suspension feeders (CASF, SASF) and major increase in strophomenid brachiopods (RESF) may strongly reflect the changing sedimentological regime in the basin that begins at the M4/M5 boundary.

Conclusions

Quantitative, paleocommunity-level analyses of biotas across a Late Ordovician regional extinction boundary not only offer a more complete view, but also emphasize the variability of ecological response to extinction. Based on these analyses, the following aspects of this event may be highlighted:

1. Although diversity and evenness metrics decline across the extinction boundary, the magnitude of change for these metrics suggests that minimal changes were made to the relative abundance distributions of taxa within paleocommunities of the basin due to the extinction. Deep subtidal paleocommunities, and particularly those in the proximal areas of the Appalachian Basin, were more significantly affected during this event.

2. While guild dominance is quite variable among regions and between facies of the Appalachian Basin, all regions and both facies show major changes in the relative abundances of different guilds across the extinction boundary. Generally, prior to the extinction, paleocommunities are dominated by pedunculate and reclining epifaunal suspension feeders, solitary and colonial attached suspension feeders, and mobile epifaunal deposit feeders. After the extinction, the deposit feeders and attached suspension feeders decline in relative abundance, while the pedunculate and reclining epifaunal suspension feeders increase. These patterns vary by specific facies or region.

3. MDS ordination confirms pre-extinction communities were compositionally different from post-extinction communities, with facies becoming more distinct after the extinction. Regionally, paleocommunities in the proximal portions of the basin are more taxonomically and compositionally distinct throughout the sampled time intervals. The distal areas of the basin are generally more similar, but the response of these paleocommunities varies immediately following the extinction boundary.

Acknowledgements

Thanks to S. M. Holland, L.B. Railsback, S. T. Goldstein, S. E. Walker, and M. E. Patzkowsky for providing thorough and thoughtful reviews of this work. This work was supported by the Geological Society of America, Sigma Xi Grants in Aid of Research, Paleontological Society Stephen J. Gould Student Grant-in-Aid Program, American Museum of Natural History Theodore Roosevelt Memorial Fund and the University of Georgia Department of Geology Wheeler-Watts Fund.

Literature Cited

Bambach, R. K. 1983. Ecospace utilization and guilds in marine communities through the Phanerozoic. Pp. 719-746 in M. J. S. Tevesz and P. L. McCall, eds. Biotic interactions in recent and fossil benthic communities. Plenum Press, New York.

Bambach, R. K., A. H. Knoll, and S. C. Wang. 2004. Origination, extinction, and mass depletions of marine diversity. Paleobiology 30:522-542.

Bonelli, Jr., J. R., C. E. Brett, A. I. Miller, and J. B. Bennington. 2006. Testing for faunal stability across a regional biotic transition: quantifying stasis and variation among recurring coral-rich biofacies in the Middle Devonian Appalachian Basin. Paleobiology 32:20-37.

Bottjer, D. J. 2001. Biotic recovery from mass extinctions. Pp. 202-206 in D. E. G. Briggs and P. R. Crowther, eds. Palaeobiology II. Blackwell Science, Oxford.

Brett, C. E., K. B. Miller, and G. C. Baird. 1990. A temporal hierarchy of paleoecological processes within a Middle Devonian epeiric sea. Pp. 178-209 in W. Miller, III, ed. Paleocommunity temporal dynamics: the long-term development of multispecies assemblies. Paleontological Society Special Publication 5.

Brett, C. E. 1995. Sequence stratigraphy, biostratigraphy, and taphonomy in shallow marine environments. Palaios 10:597-616.

Buzas, M.A. and T.G. Gibson. 1969. Species diversity: Benthonic foraminifera in western North Atlantic. Science 163:72-75.

Buzas, M. A. and L. C. Hayek. 2005. On richness and evenness within and between communities. Paleobiology 31:199-220.

Dodd, J. R. and Stanton, Jr., R. J. 1990. Paleoecology: Concepts and applications. John Wiley & Sons, New York.

Donovan, S. K. 1989. Paleontological criteria for the recognition of mass extinction. Pp. 19-36 in S. K. Donovan, ed. Mass extinctions: processes and evidence. Belhaven Press, London.

Droser, M. L., D. J. Bottjer, and P. M. Sheehan. 1997. Evaluating the ecological architecture of major events in the Phanerozoic history of marine invertebrate life. Geology 25:167-170.

Droser, M. L., D. J. Bottjer, P. M. Sheehan, G. R. McGhee, Jr. 2000. Decoupling of taxonomic and ecologic severity of Phanerozoic marine mass extinctions. Geology 28:675-678.

Erwin, D. H. 1996. Understanding biotic recoveries: extinction, survival, and preservation during the End-Permian mass extinction. Pp. 398-418 in D. Jablonski, D. H. Erwin, and J. H. Lipps, eds. Evolutionary Paleobiology. University of Chicago Press, Chicago.

—. 1998. The end and the beginning: recoveries from mass extinctions. Trends in Ecology & Evolution 13:344-349.

—. 2001. Lessons from the past: Biotic recoveries from mass extinctions. Proceedings of the National Academy of Sciences 98:5399-5403.

Fürsich, F. T. and J. M. Hurst. 1974. Environmental factors determining the distribution of brachiopods. Palaeontology 17:879-900.

Gilpin, M. E. and M. E. Soulé. 1986. Minimum viable populations. Pp. 13-34 in M. E. Gilpin and M. E. Soulé, eds. Conservation Biology: The Science of Scarcity and Diversity. Sinauerr Associates, Sunderland, Massachusetts.

Gower, J. C. 1987. Introduction to ordination techniques. Pp. 3-64 in P. Legendre and L. Legendre, eds. Developments in numerical ecology. Springer, Berlin.

Hallam, A. and P. B. Wignall. 1997. Mass Extinctions and Their Aftermath. Oxford University Press, Oxford.

Harries, P. J. and E. G. Kauffman. 1990. Patterns of survival and recovery following the Cenomanian-Turonian (Late Cretaceous) mass extinction in the Western Interior Basin, United States. Pp. 277-298 in E. G. Kauffman and G. H. Walliser. eds. Extinction events in Earth history. Springer-Verlag, Berlin.

Hart, M. B., ed. 1996. Biotic recovery from mass extinction events. Geological Society Special Publication 102. Geological Society of America, Boulder, Colorado.

Hatch, J. R., S. R. Jacobson, B. J. Witzke, J. B. Risatti, D. E. Ander, W. L. Watney, K. D. Newell, and A. K. Vuletich. 1987. Possible late Middle Ordovician carbon isotope excursion. Evidence from Ordovician oils and hydrocarbon sourcerocks, Mid-Continent and east-central United States: American Association of Petroleum Geologists Bulletin 71:117-129.

Hayek, L. C. and M. A. Buzas. 1997. Surveying Natural Populations. Columbia University Press, New York.

Holland, S. M. 1995. The stratigraphic distribution of fossils. Paleobiology 21:92–109.

Holland, S. M. 1999. The new stratigraphy and its promise for paleobiology. Paleobiology 25:409-416.

Holland, S. M. 2000. The quality of the fossil record: a sequence stratigraphic perspective. Pp. 148-168 in D. H. Erwin, and S. L. Wing, eds. Deep Time: Paleobiology's Perspective. The Paleontological Society, Lawrence, Kansas.

Holland, S. M. 2003. Confidence limits on fossil ranges that account for facies changes. Paleobiology 29:468-479.

Holland, S.M. and M. E. Patzkowsky. 1996. Sequence stratigraphy and long-term lithologic change in the Middle and Upper Ordovician of the eastern United States. In B. J. Witzke, ed. Paleozoic sequence stratigraphy; views from the North American Craton. Geological Society of America Special Publication 306:117-130. Boulder, CO.

—. 1997. Distal orogenic effects on peripheral bulge sedimentation: Middle and Upper Ordovician of the Nashville Dome. Journal of Sedimentary Research 67:250-263.

—. 1998. Sequence stratigraphy and relative sea-level history of the Middle and Upper Ordovician of the Nashville Dome, Tennessee. Journal of Sedimentary Research 68:684-699.

—. 1999. Models for simulating the fossil record. Geology 27:491-494.

—. 2002. Stratigraphic variation in the timing of first and last occurrences. Palaios 17:134-146.

Hubbell, S. P. 2001. The Unified Neutral Theory of Biodiversity and Biogeography: Monographs in Population Biology 32. Princeton University Press, Princeton.

Hurlbert, S. H. 1971. The nonconcept of species diversity: a critique and alternative parameters. Ecology 52:577-586.

Jablonski, D. 1986. Causes and consequences of mass extinctions: a comparative approach. Pp. 183-229 in D. K. Elliott, ed. Dynamics of extinction. Wiley, New York.

—. 1991. Extinctions: a paleontological perspective. Science 253:754-757.

—. 1995. Extinctions in the fossil record. Pp. 25-44 in J. H. Lawton and R. M. May, eds. Extinction Rates. Oxford University Press, Oxford.

—. 1996. Body Size and Macroevolution. Pp. 256-289 in D. Jablonski, D. H. Erwin, and J. H. Lipps, eds. Evolutionary Paleobiology. University of Chicago Press, Chicago.

—. 2001. Lessons from the past: Evolutionary impacts of mass extinctions. Proceedings of the National Academy of Sciences 98:5393-5398.

—. 2005. Mass extinctions and macroevolution. Paleobiology 31:192-210.

Kauffman, E. G. 1986. High resolution event stratigraphy: regional and global Cretaceous bio-events. Pp. 285-312 in G. H. Walliser, ed. Global bio-events. Springer-Verlag, Berlin.

Layou, K. M. 2007. A quantitative null model of additive diversity partitioning: examining the response of beta diversity to extinction. Paleobiology 33:116-124.

Lockwood, R. 2003. Abundance not linked to survival across the end-Cretaceous mass extinction: patterns in North American bivalves. Proceedings of the National Academy of Sciences USA 100:2478-2482.

Miller, A. I. 1988. Spatial resolution in subfossil molluscan remains: implications for paleobiological analysis. Paleobiology 14:91–103.

Minchin, P. R. 1987. An evaluation of the relative robustness of techniques for

ecological ordination. Vegetatio 69:89–107.

Panchuk, K. M., C. Holmden, and L. R. Kump. 2005. Sensitivity of the epeiric sea carbon isotope record to local-scale carbon cycle processes: tales from the Mohawkian Sea. Palaeogeography, Palaeoclimatology, Palaeoecology 228:320-337.

Patzkowsky, M. E. and S. M. Holland. 1993. Biotic response to a Middle Ordovician paleoceanographic event in eastern North America. Geology 21:619-622.

—. 1996. Extinction, invasion, and sequence stratigraphy; patterns of faunal change in the Middle and Upper Ordovician of the Eastern United States. In B. J. Witzke, ed. Paleozoic sequence stratigraphy; views from the North American Craton. Geological Society of America Special Publication 306:131-142. Boulder, CO.

—. 1997. Patterns of turnover in Middle and Upper Ordovician brachiopods of the eastern United States: a test of coordinated stasis. Paleobiology 23:420-443.

—. 1999. Biofacies replacement in a sequence stratigraphic framework: Middle and Upper Ordovician of the Nashville Dome, Tennessee, USA. Palaios 14:301-323.

Patzkowsky, M. E., L. M. Slupik, M. A. Arthur, R. D. Pancost, and K. H. Freeman. 1997. Late Middle Ordovician environmental change and extinction: harbinger of the Late Ordovician or continuation of Cambrian patterns? Geology 10:911-914.

Pielou, E. C. 1966. The measurement of diversity in different types of biological collections. Journal of Theoretical Biology 13:131-144.

Plants, H. F. 1977. Paleoecology of the Martinsburg Formation at Catawba Mountain, Virginia. Unpublished Masters thesis, Virginia Polytechnic Institute and State University, Blacksburg, Virginia.

Railsback, L. B., S. M. Holland, D. M. Hunter, E. M. Jordan, E.M., J. R. Diaz, and D. E. Crowe. 2003. Controls on geochemical expression of subaerial exposure in Ordovician limestones from the Nashville Dome, Tennessee, U.S.A. Journal of Sedimentary Research 73:790-805.

Raup, D. M. 1991. The future of analytical paleobiology. Pp. 207-216 in N. L. Gilinsky and P. W. Signor, eds. Analytical Paleobiology: Short Courses in Paleontology Number 4: Paleontological Society, Knoxville.

—. 1992, Large-body impact and extinction in the Phanerozoic: Paleobiology, v. 18, p. 80-88.

Root, R. B. 1967. The niche exploitation pattern of the blue-gray gnatcatcher. Ecological Monographs 37:317-350.

Sepkoski, J.J., Jr. 1986. Phanerozoic overview of mass extinctions. Pp. 277-295 in D. M. Raup and D. Jablonski, eds. Patterns and processes in the history of life. Springer-Verlag, Berlin.

Sepkoski, Jr., J. J. 1988. Alpha, beta, or gamma: where does all the diversity go? Paleobiology 14:221-234.

Shannon, C. E. 1948. A mathematical theory of communication. Bell System Technical Journal 27:379-423, 623-656.

Shi, G. R. 1993. Multivariate data analysis in palaeoecology and palaeobiogeography—a review. Palaeogeography, Palaeoclimatology, Palaeoecology 105:199–234.

Springer, D. A. 1982. Community gradients in the Martinsburg Formation (Ordovician), southwestern Virginia. Unpublished Ph.D. dissertation, Virginia Polytechnic

Institute and State University, Blacksburg, Virginia.

Springer, D. A. and R. K. Bambach. 1985. Gradient versus cluster analysis of fossil assemblages: a comparison from the Ordovician of southwestern Virginia. Lethaia 18:181–198.

Webber, A. J. 2002. High-resolution faunal gradient analysis and an assessment of the causes of meter-scale cyclicity in the type Cincinnatian Series (Upper Ordovician). Palaios 17:545-555.

Appendix. Equations for diversity and evenness metrics.

1. Richness (*S*) is the number of taxa present within the community.

2. The Shannon index (*H'*, Shannon 1948):

$$H' = -\sum_{i=1}^{S} p_i \ln(p_i)$$

where p_i is equal to the proportional abundance of the ith taxon.

3. Buzas and Gibson evenness (*E*, Buzas and Gibson 1969):

$$E = \frac{e^{H'}}{S}$$

4. Pielou's evenness (*J*, Pielou 1966):

$$J = \frac{H'}{\ln S}$$

5. Hurlbert's probability of interspecific encounter (*PIE*, Hurlbert 1971):

$$PIE = \frac{N}{N-1}(1 - \sum_{i=1}^{S}(p_i)^2)$$

where *N* is equal to the number of total individuals in the community.

6. Beta diversity (Jaccard coefficient, Sepkoski 1988):

$$\beta = \frac{S_S}{S_1 + S_2 - S_S}$$

where S_1 is the richness of sample 1, S_2 is the richness of sample 2, and S_s is the number of shared taxa in samples 1 and 2. Note that this is an inverse measure of beta diversity, such that an increase in the Jaccard value represents a decrease in beta diversity. For calculations in this study, samples represent regional taxonomic lists by sequence (and where applicable, by facies).

Table 4.1. Samples included in field data analyses, subsetted by geographic region and facies. First number indicates total samples from sequence, parenthetical numbers reflect distribution of samples per sequence by facies. SS = shallow subtidal facies, DS = deep subtidal facies.

	M3/M4 (pre-extinction)	M5 (post-extinction)	M6 (post-extinction)
Tennessee	37 (SS: 17, DS: 20)	26 (SS: 17, DS: 9)	37 (SS: 37 , DS: 0)
Kentucky	10 (SS: 10, DS: 0)	37 (SS: 19, DS: 19)	43 (SS: 31, DS: 12)
Virginia	14 (SS: 0, DS: 14)	53 (SS: 0, DS: 53)	60 (SS: 0, DS: 60)
All	61 (SS: 27, DS: 34)	116 (SS: 36; DS:80)	140 (SS: 68; DS:72)

Table 4.2. Ecological guilds used in this study.

Major guilds

Guild	Representative taxa
1. pedunculate epifaunal suspension feeders (PESF)	all non-strophomenid brachiopods, e.g, *Glyptorthis, Zygospira*
2. reclining epifaunal suspension feeders (RESF)	all strophomenid brachiopods, e.g., *Rafinesquina*, *Strophomena*
3. mobile epifaunal deposit feeders (MEDF)	all trilobites and ostracods, most gastropods (see MEP below)
4. colonial attached suspension feeders (CASF)	all bryozoans, colonial corals and sponges
5. solitary attached suspension feeders (SADF)	all crinoids, solitary rugosans

Minor guilds

Guild	Representative taxa
1. mobile infaunal and semi-infaunal deposit feeders (MIDF)	bivalve *Ctenodonta* and burrowing traces
2. epifaunal mobile carnivores (EMC)	nautiloids
3. epibiont suspension feeders (ESF)	encrusting tube organism *Cornulites*
4. mobile epifaunal parasites (MEP)	platycerid gastropod *Cyclonema*
5. byssate suspension feeder (BSF)	bivalves *Ambonychia, Cyrtodonta*

Table 4.3. Differences in mean diversity and evenness metrics across a regional extinction boundary based on subsampled subsets of field data. Difference based on first sequence value – second sequence value. 95% confidence interval is reported. SS = all shallow subtidal samples; DS = all deep subtidal samples.

		S	*H'*	*E*
M4 vs. M5	(All)	5.961 ± 0.227	0.291± 0.011	0.038 ± 0.004
M5 vs. M6	(All)	2.091 ± 0.215	0.051 ± 0.010	-0.023 ± 0.004
M4 vs. M5	(SS)	6.424 ± 0.208	0.369 ± 0.010	0.067 ± 0.004
M5 vs. M6	(SS)	-2.068 ± 0.198	0.020 ± 0.010	0.063 ± 0.004
M4 vs. M5	(DS)	5.733 ± 0.223	0.382 ± 0.012	0.070 ± 0.004
M5 vs. M6	(DS)	7.419 ± 0.179	0.183 ± 0.010	-0.134 ± 0.002
M4 vs. M5	(Tennessee)	2.996 ± 0.196	0.026 ± 0.010	-0.063 ± 0.004
M5 vs. M6	(Tennessee)	-0.344 ± 0.194	0.088 ± 0.010	0.061 ± 0.004
M4 vs. M5	(Kentucky)	-0.390 ± 0.177	0.016 ± 0.009	0.018 ± 0.004
M5 vs. M6	(Kentucky)	-1.323 ± 0.195	0.089 ± 0.011	0.078 ± 0.004
M4 vs. M5	(Virginia)	10.267 ± 0.178	0.928 ± 0.009	0.215 ± 0.004
M5 vs. M6	(Virginia)	2.434 ± 0.137	0.130 ± 0.270	0.170 ±0.345

Table 4.3. Continued.

		Pielou's *J*	*PIE*
M4 vs. M5	(All)	0.032 ± 0.002	0.030 ± 0.002
M5 vs. M6	(All)	-0.008 ± 0.002	-0.007 ± 0.002
M4 vs. M5	(SS)	0.046 ± 0.002	0.039 ± 0.001
M5 vs. M6	(SS)	0.031 ± 0.002	0.014 ± 0.002
M4 vs. M5	(DS)	0.061 ± 0.002	0.055 ± 0.002
M5 vs. M6	(DS)	-0.055 ± 0.003	-0.010 ± 0.002
M4 vs. M5	(Tennessee)	-0.028 ± 0.002	-0.009 ± 0.002
M5 vs. M6	(Tennessee)	0.033 ± 0.002	0.014 ± 0.002
M4 vs. M5	(Kentucky)	0.009 ± 0.002	-0.006 ± 0.002
M5 vs. M6	(Kentucky)	0.044 ± 0.003	0.038 ± 0.002
M4 vs. M5	(Virginia)	0.169 ± 0.002	0.151 ± 0.002
M5 vs. M6	(Virginia)	-0.105 ± 0.033	-0.052 ± 0.002

Table 4.4. Ten most abundant taxa within each sequence ranked by relative abundance. Note the increasing dominance of abundant taxa through time. Thin ramose 1, thin ramose 2 and thick ramose refer to distinct bryozoan morphologies.

M4		M5		M6	
Leperditid ostracod	0.22	*Dalmanella*	0.27	*Zygospira*	0.20
Escharopora	0.14	*Rafinesquina*	0.15	*Sowerbyella*	0.19
Strophomena	0.06	Thick ramose	0.07	Thick ramose	0.12
Rhindictya	0.06	Thin ramose 1	0.06	*Rafinesquina*	0.08
Thin ramose 1	0.05	*Sowerbyella*	0.06	*Dalmanella*	0.07
Thick ramose	0.04	*Zygospira*	0.05	*Isotelus*	0.05
Pionodema	0.03	Thin ramose 2	0.05	Thin ramose 2	0.04
Thin ring crinoid	0.03	*Isotelus*	0.04	Thin ramose 1	0.04
Tetradium	0.02	*Prasopora*	0.02	*Hebertella*	0.03
Hesperorthis	0.02	*Escharopora*	0.02	*Lophospira*	0.02
TOTAL	0.68	TOTAL	0.78	TOTAL	0.83

Table 4.5. Beta diversity (Jaccard coefficient based on sequence taxonomic lists) for regional comparisons during the M5 and M6 sequences.

	M5	M6
Tennessee vs. Kentucky	0.578	0.544
Tennessee vs. Virginia	0.267	0.269
Kentucky vs. Virginia	0.339	0.255

Table 4.6. Changes in mean diversity and evenness metrics across a regional extinction boundary based on subsampled subsets of field data. 95% confidence limit reported is for difference of means. 95%UCL = 95% upper confidence limit; 95%LCL = 95% lower confidence limit; SS = all shallow subtidal samples; DS = all deep subtidal samples.

	S	*H'*	*E*	Pielou's *J*	*PIE*
M3/4 (All)	29.834	2.859	0.589	0.843	0.916
M5 (All)	20.610	2.388	0.534	0.791	0.854
95%UCL	9.439	0.482	0.059	0.054	0.064
95%LCL	9.009	0.460	0.051	0.050	0.060
M3/4 (SS)	28.146	2.918	0.662	0.875	0.934
M5 (SS)	18.203	2.297	0.552	0.794	0.862
95%UCL	10.140	0.630	0.114	0.084	0.073
95%LCL	9.746	0.612	0.106	0.080	0.071
M3/4 (DS)	26.786	2.659	0.538	0.810	0.889
M5 (DS)	16.476	1.974	0.443	0.706	0.760
95%UCL	10.517	0.697	0.099	0.106	0.132
95%LCL	10.103	0.673	0.091	0.101	0.126

M3/4 (Tennessee)	23.969	2.575	0.552	0.812	0.886
M5 (Tennessee)	18.536	2.380	0.592	0.819	0.873
95%UCL	5.624	0.199	-0.035	-0.005	0.015
95%LCL	5.242	0.179	-0.044	-0.010	0.011
M3/4 (Kentucky)	21.422	2.536	0.593	0.828	0.884
M5 (Kentucky)	13.026	1.968	0.556	0.769	0.814
95%UCL	8.540	0.576	0.041	0.061	0.071
95%LCL	8.252	0.559	0.033	0.056	0.068
M3/4 (Virginia)	24.579	2.815	0.683	0.880	0.931
M5 (Virginia)	7.435	1.551	0.640	0.776	0.752
95%UCL	17.282	1.271	0.048	0.107	0.180
95%LCL	17.006	1.257	0.039	0.102	0.177

Figure 4.1. Time scale for the Late Ordovician of the Appalachian Basin, indicating the six third-order depositional sequences for the Mohawkian Series, modified from Holland and Patzkowsky (1996).

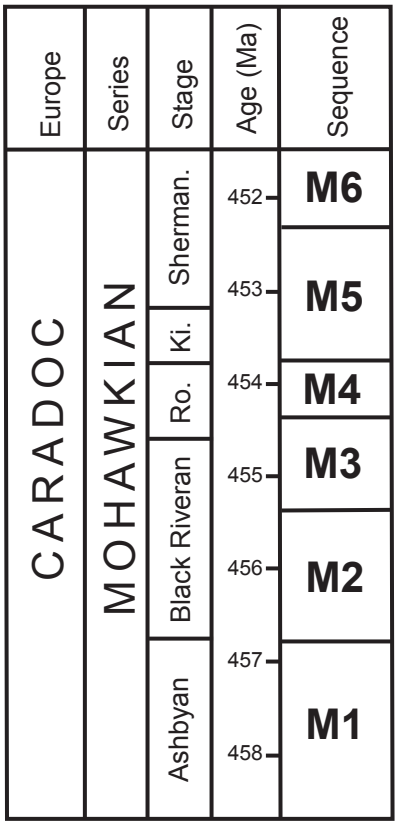
Europe
Series
Stage
Age (Ma)
Sequence
CARADOC
MOHAWKIAN
Ashbyan
Black Riveran
Ro.
Ki.
Sherman.
452
453
454
455
456
457
458
M6
M5
M4
M3
M2
M1

Figure 4.2. Regional map of Kentucky, Tennessee, and Virginia. Underlying gray scale reflects geologic bedrock map, with areas of Ordovician bedrock outlined by the heavy black line. White boxes indicate localities of field sample collection.

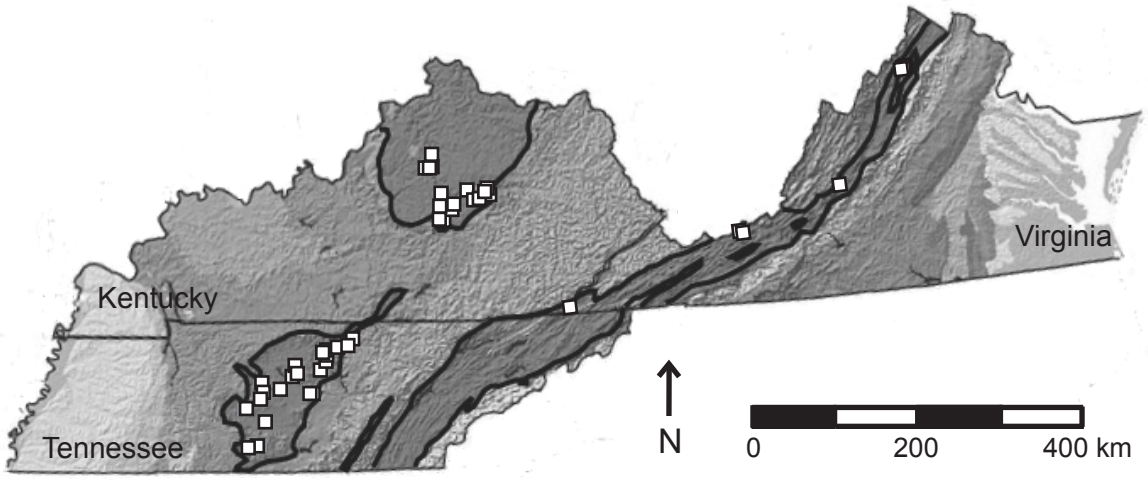
Virginia
Kentucky
Tennessee
N
0
200
400 km

Figure 4.3. Number of genera present in each sequence, and within facies and regions in each sequence. For the M5 and M6, black portions of bars represent holdover taxa from the previous sequence, and white portions represent taxa that occur for the first time in this data set.

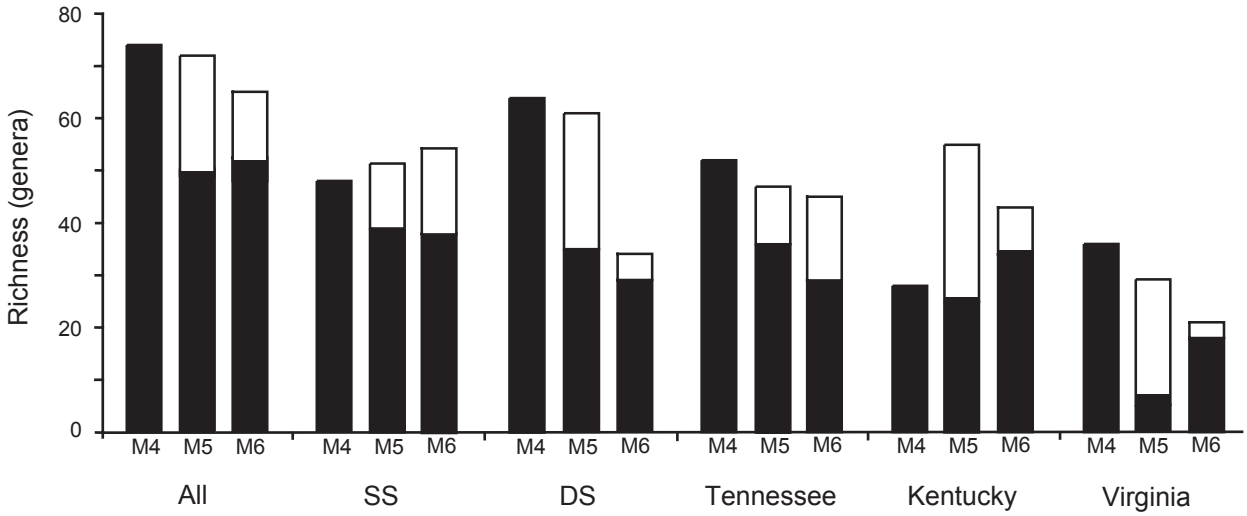
Richness (genera)
80
60
40
20
0
M4 M5 M6
All
SS
DS
Tennessee
Kentucky
Virginia

Figure 4.4. Diversity and evenness metrics among depositional sequences including the extinction boundary (M4 to M5 transition) and into the following sequence (M5 to M6 transition). *S* (taxonomic richness), *H'* (Shannon index), *E* (Buzas and Gibson evenness), *J* (Pielou's evenness), *PIE* (Hurlbert's probability of interspecific encounter). 95% confidence interval indicated.

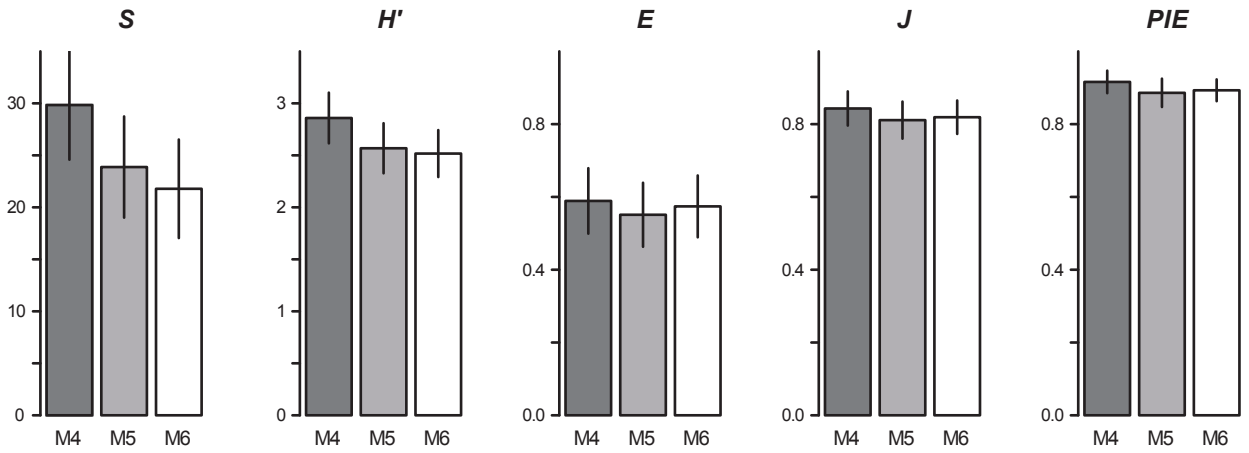
S
H'
E
J
PIE
30
20
10
0
3
2
1
0
0.8
0.4
0.0
0.8
0.4
0.0
0.8
0.4
0.0
M4
M5
M6

Figure 4.5. Diversity and evenness metrics within facies of depositional sequences. *S* (taxonomic richness), *H'* (Shannon index), *E* (Buzas and Gibson evenness), *J* (Pielou's evenness), *PIE* (Hurlbert's probability of interspecific encounter). 95% confidence interval indicated.

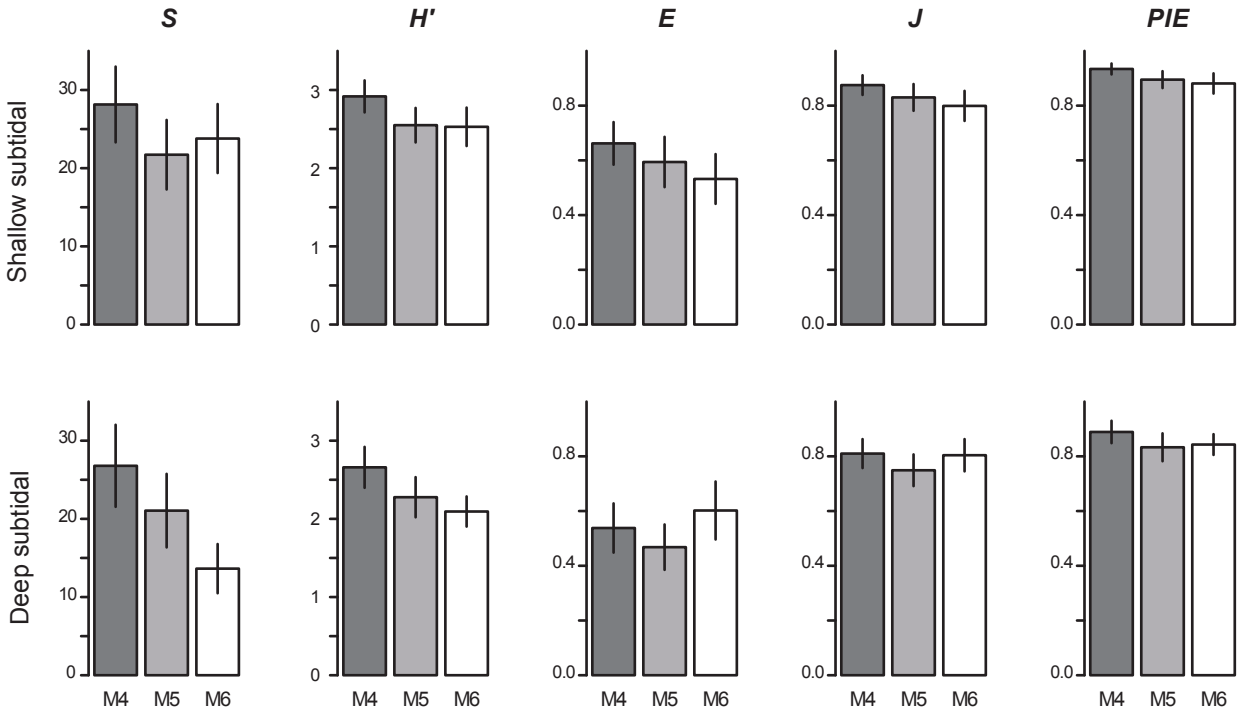
S
H'
E
J
PIE
Shallow subtidal
Deep subtidal
M4
M5
M6

Figure 4.6. Diversity and evenness metrics within regions and depositional sequences. *S* (taxonomic richness), *H'* (Shannon index), *E* (Buzas and Gibson evenness), *J* (Pielou's evenness), *PIE* (Hurlbert's probability of interspecific encounter). 95% confidence interval indicated.

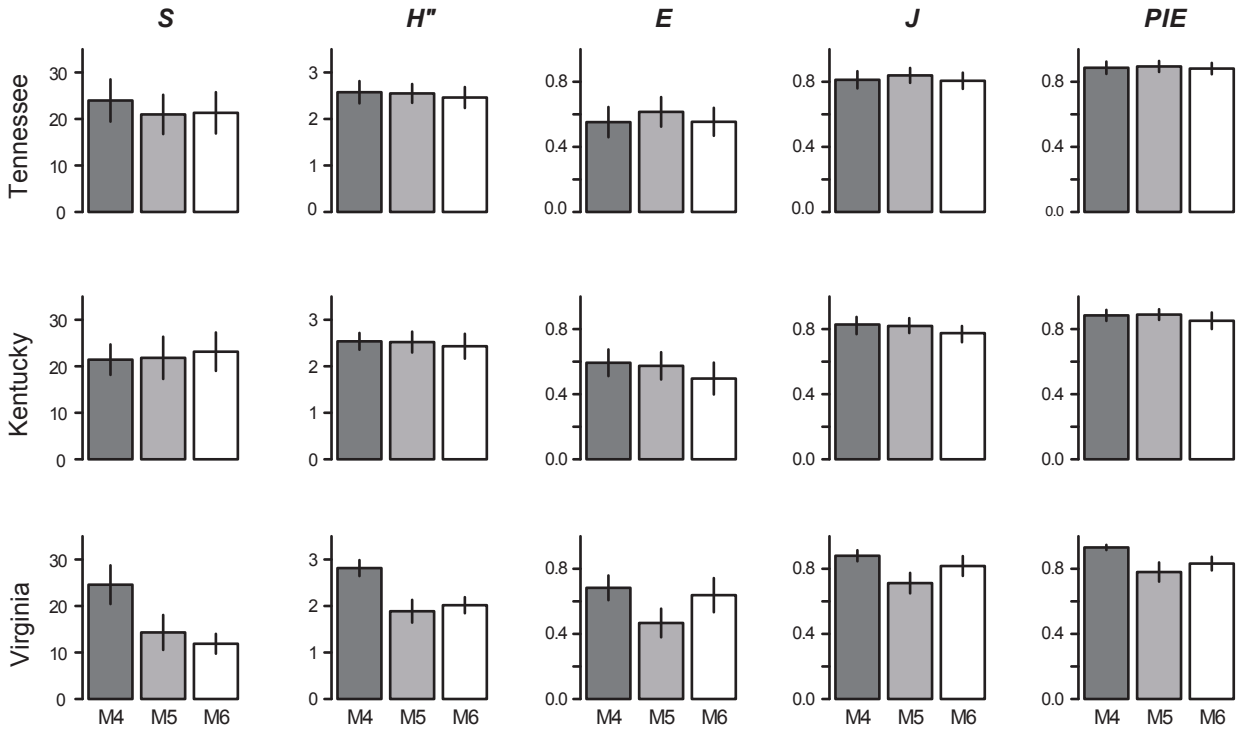
S
H"
E
J
PIE
Tennessee
Kentucky
Virginia
M4
M5
M6

Figure 4.7. Relative abundances of guilds in subsets of the field data. A. All data by sequence, B. All shallow subtidal samples, C. All deep subtidal samples, D. All Tennessee samples, E. All Kentucky samples, F. All Virginia samples. See Table 4.2 for guild abbreviations. 95% confidence interval after Raup (1991); if not shown, value is negligible.

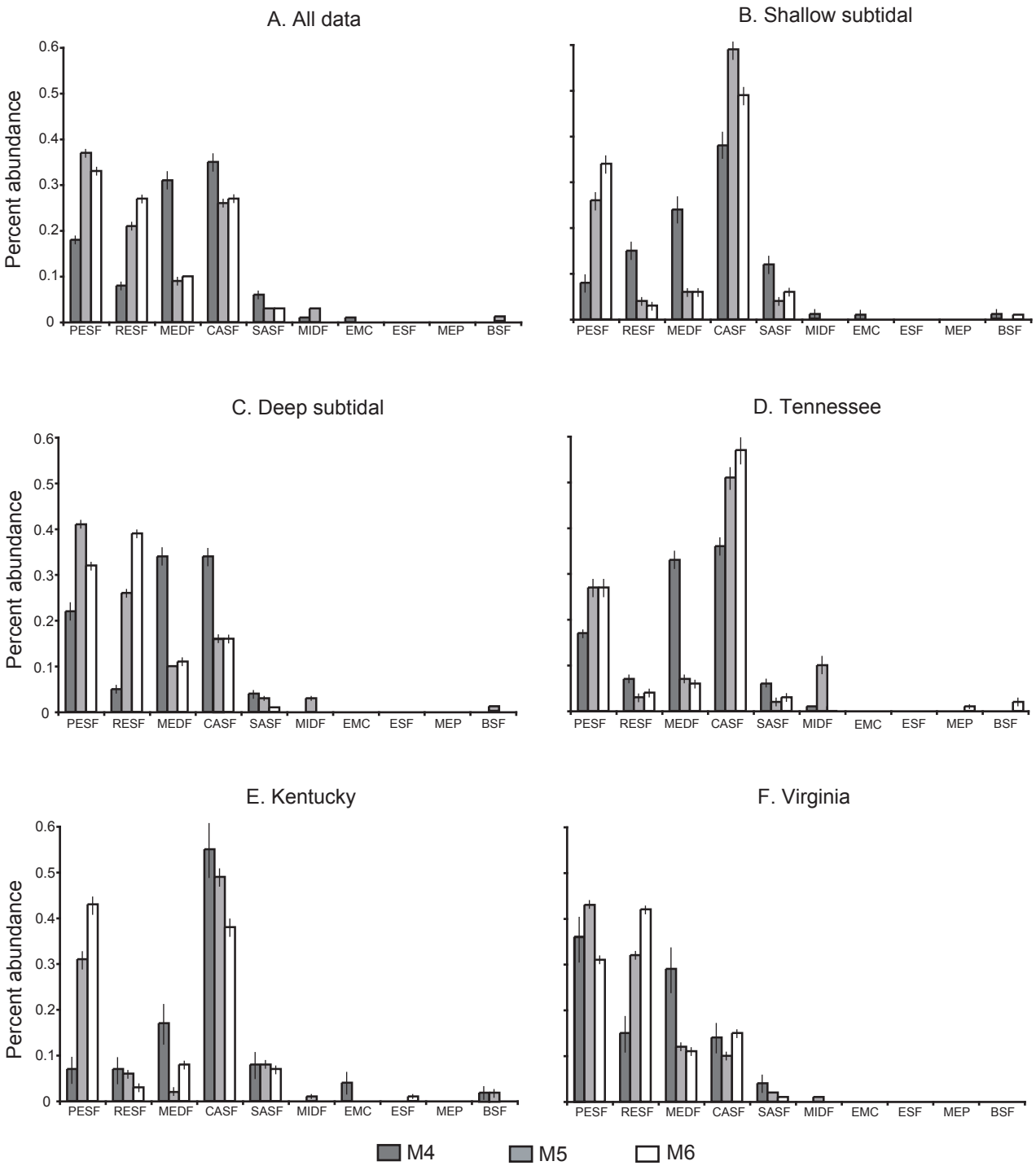
A. All data
B. Shallow subtidal
C. Deep subtidal
D. Tennessee
E. Kentucky
F. Virginia
Percent abundance
0
0.1
0.2
0.3
0.4
0.5
0.6
PESF
RESF
MEDF
CASF
SASF
MIDF
EMC
ESF
MEP
BSF
M4
M5
M6

Figure 4.8. MDS ordination of all samples, coded by depositional sequence (A; stress: 27.186) and with centroids of all samples within facies within depositional sequence (B). SS: shallow subtidal facies, DS: deep subtidal facies.

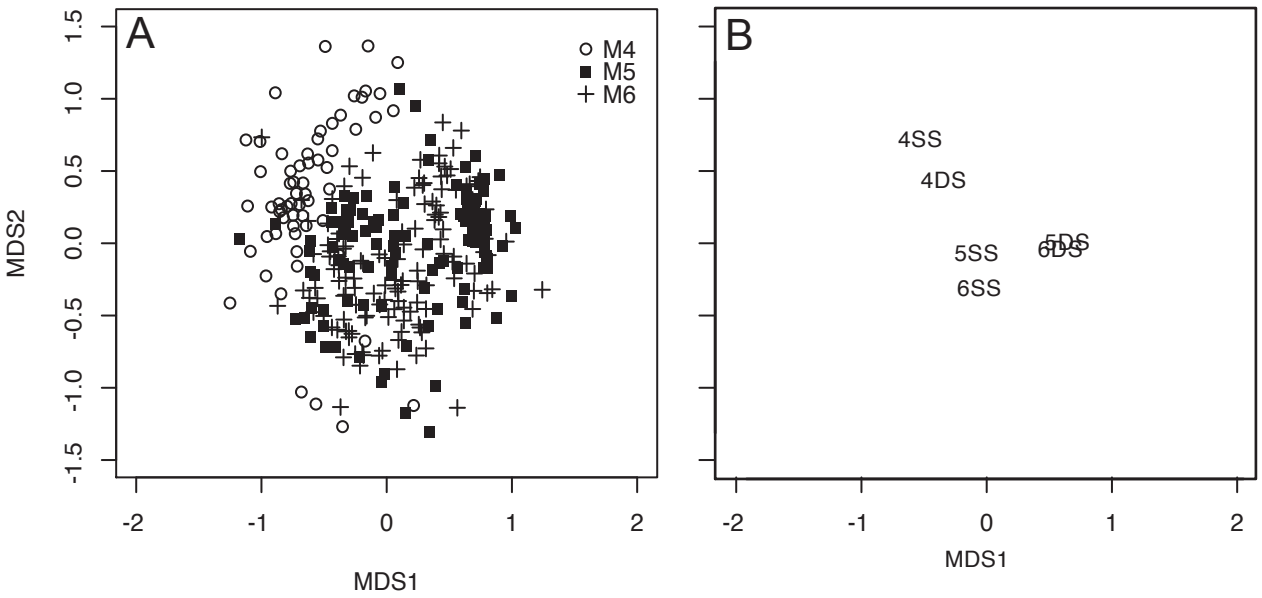
A
M4
M5
M6
MDS2
MDS1
-1.5
-1.0
-0.5
0.0
0.5
1.0
1.5
-2
-1
0
1
2
B
4SS
4DS
5SS
5DS
6DS
6SS
MDS1

Figure 4.9. MDS ordinations of geographic regions by depositional sequence. A. M4 sequence (stress: 25.522), B. M5 sequence (stress: 23.005), C. M6 sequence (stress: 22.450).

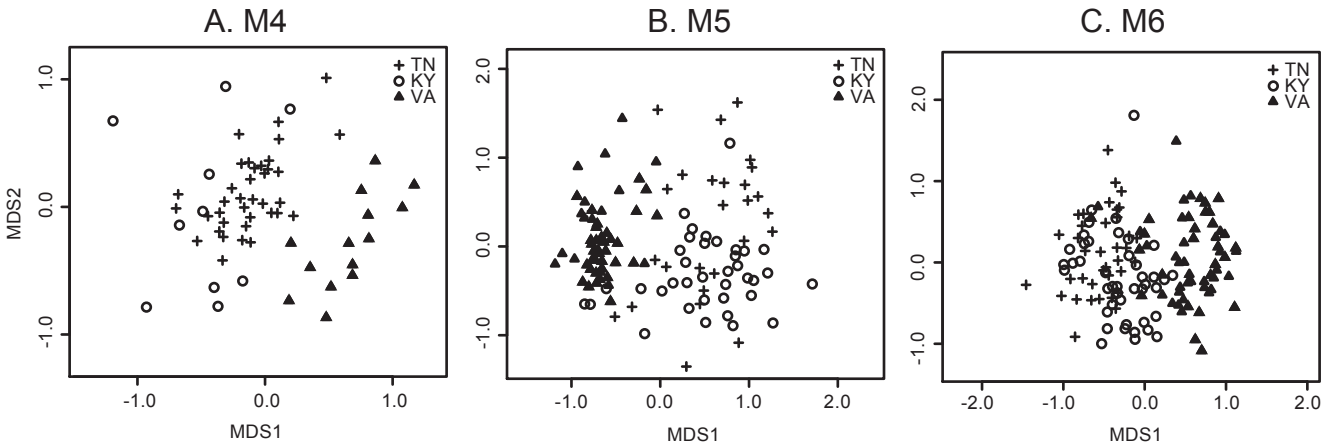
A. M4
B. M5
C. M6
TN
KY
VA
MDS1
MDS2

Figure 4.10. MDS ordinations of shallow subtidal samples from Tennessee and Kentucky. A. M4 sequence (stress: 19.821), B. M5 sequence (stress: 25.370), C. M6 sequence (stress: 24.547).

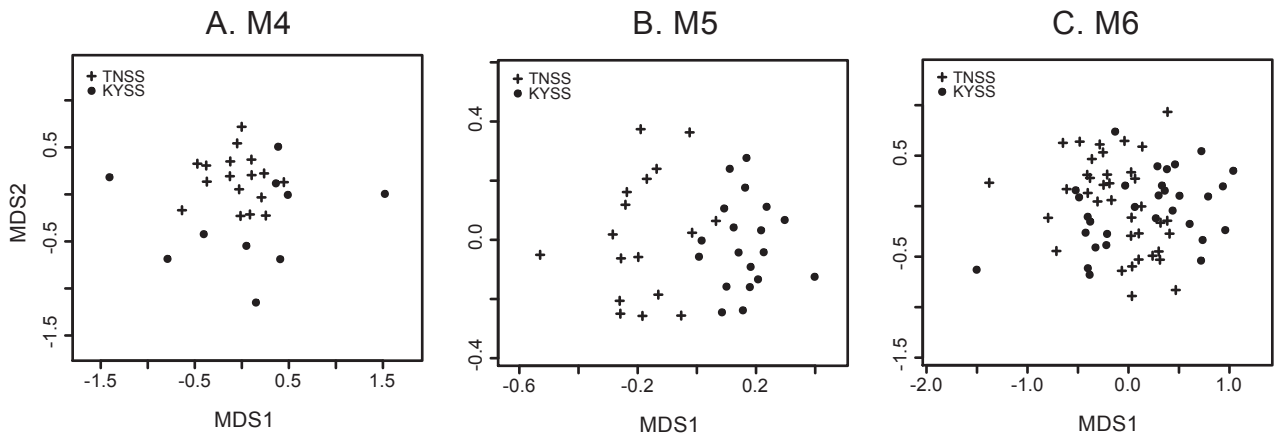
A. M4
B. M5
C. M6
TNSS
KYSS
MDS1
MDS2
-1.5
-0.5
0.5
1.5
-0.6
-0.2
0.2
0.4
0.0
-0.4
-2.0
-1.0
0.0
1.0

CHAPTER 5

CONCLUSIONS

The first null model, which examines changes in diversity and evenness metrics as a function of percent extinction, predicts diversity metrics *S* and *H'*, and the evenness metric *PIE* to decrease constantly with increasing extinction magnitude, regardless of the selectivity of extinction with respect to taxon abundance. This model predicts evenness metric *E* to increases constantly with increasing extinction magnitude, regardless of the selectivity for taxon abundance, although the rate of increase is much faster for the case of non-selective extinction. This model also predicts evenness metric Pielou's *J* to increase substantially for the abundant-selective condition, increase gradually for the non-selective condition, and decrease for the rare-selective condition. These variable, yet distinctive, responses to different selectivity conditions, suggest it may be possible to determine whether extinction is selective with respect to taxon abundance by comparing values of Pielou's *J* across an extinction boundary.

The second set of null models based on additive partitioning of β diversity indicate that β diversity should decrease as α and γ do with increasing magnitudes of extinction at the highest level of a sampling hierarchy. Non-selective extinction with respect to taxon abundance suggests that the partitioning of diversity does not vary across an extinction boundary except at the highest magnitudes of extinction. Selective extinction with respect to rare taxa yields positive slopes with increasing extinction magnitude, representing a constant decrease in β_3 and corresponding increase in α_1. Selective extinction with respect to abundant taxa yields negative slopes with increasing extinction magnitude, with an initial increase in β_3 and decline in α_1. As with Pielou's *J*, these different patterns in partitioning of β diversity suggest that it may be possible to

determine whether extinction operating at the highest level of the sampling hierarchy is selective or not with respect to taxon abundances.

Field data indicate selectivity with respect to rare taxa did occur across a Late Ordovician regional extinction boundary. The total dataset and most additional subsets based on environment all show changes in diversity and evenness metrics across the extinction boundary that correspond to an extinction that targeted rare taxa. However, variation in selectivity based on regional subsets of the data suggests that selectivity is correlated with spatial scale for this extinction event. For example, data collected within a sampling hierarchy from a local area in Tennessee exhibit changes in diversity partitioning across this extinction boundary that are similar to the abundant-selective partitioning model results, with an increase in β_3 and decline in α_1, despite overall decreases in α, β, and γ diversities.

Quantitative, paleocommunity-level analyses of biotas across this same regional extinction boundary emphasizes extensive variability of ecological response to extinction among facies, guilds, and regions. Although diversity and evenness metrics decline across the extinction boundary in most cases, the magnitude of change for these metrics suggests that minimal changes were made to the relative abundance distributions of taxa within paleocommunities of the basin due to the extinction. While guild dominance is quite variable among regions and between facies of the Appalachian Basin, all regions and both facies show major changes in the relative abundances of different guilds across the extinction boundary. Generally, prior to the extinction, paleocommunities are dominated by pedunculate and reclining epifaunal suspension feeders, solitary and colonial attached suspension feeders, and mobile epifaunal

deposit feeders. After the extinction, the deposit feeders and attached suspension feeders decline in relative abundance, while the pedunculate and reclining epifaunal suspension feeders increase. MDS ordination confirms pre-extinction communities were compositionally different from post-extinction communities, with facies becoming more distinct after the extinction. Regionally, paleocommunities in the proximal portions of the basin are more taxonomically and compositionally distinct throughout the sampled time intervals. The distal areas of the basin are generally more similar, but the response of these paleocommunities varies immediately following the extinction boundary. These analyses reveal the underlying complexity of ecological response to extinction.

APPENDIX A

R functions used in analyses of diversity and evenness metrics (Chapter 2).

1. This function calculates the mean and standard deviation of diversity and evenness metrics (S, H, Simpson, E, J, the ratio lnE/lnS, and PIE) for a matrix of samples (x) with taxonomic abundances.

```
mean_div_even_matrix<-function(x)
    {
    diversity_evenness_function<-function(x)
        {
        S<-length(x[x>0])
        total_individuals<-sum(x)
        proportions<-x[x>0]/total_individuals
        H<--sum((proportions*log(proportions)))
        Simpson<-sum((proportions*proportions))
        E<-exp(H)/S
        J<-H/log(S)
        PIE<-(total_individuals/(total_individuals-1))*(1-Simpson)
        LN<-log(E)/log(S)
        results<-c(S,H,Simpson,E,J,PIE,LN)
        results
        }

    div_even_data<-t(apply(x, c(1,),diversity_evenness_function))
    colnames(div_even_data)<-c("S","H","Simpson","E","J","PIE",”LN”)
    results2<-data.frame(div_even_data)
    results2

    average_data<-t(apply(results2, MARGIN=2, mean))
    sd_data<-t(apply(results2,MARGIN=2, sd))
    final<-rbind(average_data,sd_data)
    rownames(final)<-c("mean", "sd")
    final
    }
```

2. This function sums all taxon abundances within samples in a matrix (x) into one vector of occurrences for all taxa, subsamples a specified number of individuals (sample_size), and finds mean diversity and evenness metrics (S, H, Simpson, E, J, the ratio lnE/lnS, and PIE) based on a specified number of trials (trials). Note this function was used for subsampling both field data and data downloaded from the Paleobiology Database (PBDB). For use with the PBDB data, the first line of the function (summing of abundances over matrix) was not needed since the data were downloaded as an occurrence vector.

```
SHEsubsampling<-function(x, trials, sample_size)
        {
        supersample<-apply(x, 2, sum)

        supersample_occurrences<-0
        for (i in 1:length(supersample))
                {
                y<-rep(i,supersample[i])
                supersample_occurrences<-append(supersample_occurrences, y,
                after=length(supersample_occurrences))
                }

        results<-matrix(nrow=1, ncol=ncol(x))
        for (j in 1:trials)
                {
                subsample_occurrences<-sample(supersample_occurrences,
                sample_size, replace=FALSE)
                subsample_abundances<-tabulate(subsample_occurrences,
                nbins=ncol(x))
                results<-rbind(results,subsample_abundances)
                final_results<-results[-1,]
                }

                diversity_evenness_function<-function(final_results)
                        {
                        S<-length(final_results[final_results>0])
                        total_individuals<-sum(final_results)
                        proportions<-final_results[final_results>0]/total_individuals
```

```
                H<--sum((proportions*log(proportions)))
                Simpson<-sum((proportions*proportions))
                E<-exp(H)/S
                LN<-log(E)/log(S)
                J<-H/log(S)
                PIE<-(total_individuals/(total_individuals-1))*(1-Simpson)
                sample_results<-c(S,H,Simpson,E,LN,J,PIE)
                sample_results
                }

        div_even_data<-t(apply(final_results, c(1,), diversity_evenness_function))
        colnames(div_even_data)<-c("S","H","Simpson","E","LN","J","PIE")
        calc_results<-data.frame(div_even_data)
        calc_results
}
```

APPENDIX B

C code for additive diversity partitioning model (Chapter 3).

1. This version of the model uses a set probability of taxon occurrence and includes a non-selective extinction.

```
#include <stdio.h>
#include <stdlib.h>
#include <math.h>
#include "randomNumbers.h"
#include "statistics.h"

#define MAXRICHNESS 24
#define PROBABILITY 0.8
#define SAMPLES 3
#define BEDS 2
#define FACIES 2
#define RUNS 70
#define PERCENTEXTINCTION 0.95

int main()
{

int i;
int n;
int b;
int f;
int r;

double taxon_abundance[RUNS][FACIES][BEDS][SAMPLES][MAXRICHNESS];
double probability[RUNS][FACIES][BEDS][SAMPLES][MAXRICHNESS];
double is_taxa_present;
double count_sample_richness[RUNS][FACIES][BEDS][SAMPLES][MAXRICHNESS];
double total_sample_richness[RUNS][FACIES][BEDS][SAMPLES];
double total_sample_individuals[RUNS][FACIES][BEDS][SAMPLES];
double total_bed_individuals[RUNS][FACIES][BEDS];
double total_bed_richness[RUNS][FACIES][BEDS];
double missing_taxa;
double missing_taxa2;
double total_facies_individuals[RUNS][FACIES];
double total_facies_richness[RUNS][FACIES];
double total_regional_individuals[RUNS];
double missing_taxa3;
double total_regional_richness[RUNS];

double alpha_one_term[RUNS][FACIES][BEDS];
double alpha_one_sum[RUNS][FACIES];
double total_alpha_one[RUNS];
double alpha_two_sum[RUNS][FACIES];
```

```
double total_alpha_two[RUNS];
double total_alpha_three[RUNS];
double total_beta_one[RUNS];
double total_beta_two[RUNS];
double total_beta_three[RUNS];

double post_probability[RUNS][FACIES][BEDS][SAMPLES][MAXRICHNESS];
double extinct_taxa[RUNS];
int dead_taxon;

double post_taxon_abundance[RUNS][FACIES][BEDS][SAMPLES][MAXRICHNESS];
double post_is_taxa_present;
double
post_count_sample_richness[RUNS][FACIES][BEDS][SAMPLES][MAXRICHNESS];
double post_total_sample_richness[RUNS][FACIES][BEDS][SAMPLES];
double post_total_sample_individuals[RUNS][FACIES][BEDS][SAMPLES];
double post_total_bed_individuals[RUNS][FACIES][BEDS];
double post_total_bed_richness[RUNS][FACIES][BEDS];
double post_missing_taxa;
double post_missing_taxa2;
double post_total_facies_individuals[RUNS][FACIES];
double post_total_facies_richness[RUNS][FACIES];
double post_total_regional_individuals[RUNS];
double post_missing_taxa3;
double post_total_regional_richness[RUNS];

double post_alpha_one_term[RUNS][FACIES][BEDS];
double post_alpha_one_sum[RUNS][FACIES];
double post_total_alpha_one[RUNS];
double post_alpha_two_sum[RUNS][FACIES];
double post_total_alpha_two[RUNS];
double post_total_alpha_three[RUNS];
double post_total_beta_one[RUNS];
double post_total_beta_two[RUNS];
double post_total_beta_three[RUNS];

double mean_initial_alpha_one;
double mean_initial_alpha_two;
double mean_initial_alpha_three;
double mean_initial_alpha_four;
double mean_initial_beta_one;
double mean_initial_beta_two;
double mean_initial_beta_three;
double mean_post_alpha_one;
double mean_post_alpha_two;
double mean_post_alpha_three;
```

```
double mean_post_alpha_four;
double mean_post_beta_one;
double mean_post_beta_two;
double mean_post_beta_three;

InitRandNum();

printf("xA1i\t xA2i\t xA3i\t xA4i\t xB1i\t xB2i\t xB3i\t xA1p\t xA2p\t xA3p\t xA4p\t xB1p\t
xB2p\t xB3p\n");

for (r = 0; r < RUNS; ++r)
      {
      total_regional_individuals[r] = 0;
      total_regional_richness[r] = 0;
      for (f = 0; f < 1; ++f)
            {
            total_facies_individuals[r][f] = 0;
            total_facies_richness[r][f] = 0;
            for (b = 0; b < BEDS; ++b)
                  {
                  total_bed_individuals[r][f][b] = 0;
                  total_bed_richness[r][f][b] = 0;
                  for (n = 0; n < SAMPLES; ++n)
                        {
                        total_sample_richness[r][f][b][n] = 0;
                        total_sample_individuals[r][f][b][n] = 0;
                        for (i = 0; i < MAXRICHNESS; ++i)
                              {
                              taxon_abundance[r][f][b][n][i] = 0;
                              count_sample_richness[r][f][b][n][i] = 0;
                              probability[r][f][b][n][i] = PROBABILITY;
                              post_probability[r][f][b][n][i] = PROBABILITY;
                              }

                        for (i = 0; i < MAXRICHNESS * 2/3; ++i)
                              {
                              is_taxa_present = RandNum();
                              if (is_taxa_present > probability[r][f][b][n][i])
                                    {
                                    taxon_abundance[r][f][b][n][i] = LogNormRandNum();
                                    count_sample_richness[r][f][b][n][i] = 1;
                                    }
                              else
                                    {
                                    taxon_abundance[r][f][b][n][i] = 0;
                                    count_sample_richness[r][f][b][n][i] = 0;
```

```
                        }
                    }
                }
            }
        }

for (f = 1; f < FACIES; ++f)
        {
        total_facies_individuals[r][f] = 0;
        total_facies_richness[r][f] = 0;
        for (b = 0; b < BEDS; ++b)
            {
            total_bed_individuals[r][f][b] = 0;
            total_bed_richness[r][f][b] = 0;
            for (n = 0; n < SAMPLES; ++n)
                {
                total_sample_richness[r][f][b][n] = 0;
                total_sample_individuals[r][f][b][n] = 0;

                for (i = 0; i < MAXRICHNESS; ++i)
                    {
                    taxon_abundance[r][f][b][n][i] = 0;
                    count_sample_richness[r][f][b][n][i] = 0;
                    probability[r][f][b][n][i] = PROBABILITY;
                    post_probability[r][f][b][n][i] = PROBABILITY;
                    }

                for (i = MAXRICHNESS * 1/3; i < MAXRICHNESS; ++i)
                    {
                    is_taxa_present = RandNum();
                    if (is_taxa_present >  probability[r][f][b][n][i])
                        {
                        taxon_abundance[r][f][b][n][i] = LogNormRandNum();
                        count_sample_richness[r][f][b][n][i] = 1;
                        }
                    else
                        {
                        taxon_abundance[r][f][b][n][i] = 0;
                        count_sample_richness[r][f][b][n][i] = 0;
                        }
                    }
                }
            }
        }

for (f = 0; f < FACIES; ++f)
```

```
		{
		for (b = 0; b < BEDS; ++b)
			{
			for (n = 0; n < SAMPLES; ++n)
				{
				for (i = 0; i < MAXRICHNESS; ++i)
					{
					total_sample_richness[r][f][b][n] = total_sample_richness[r][f][b][n]
+ count_sample_richness[r][f][b][n][i];
					total_sample_individuals[r][f][b][n] =
total_sample_individuals[r][f][b][n] + taxon_abundance[r][f][b][n][i];
					}

				total_bed_individuals[r][f][b] = total_bed_individuals[r][f][b] +
total_sample_individuals[r][f][b][n];
				}

			for (n = 0; n < SAMPLES - (SAMPLES - 1); ++n)
				{
				missing_taxa = 0;
				for (i = 0; i < MAXRICHNESS; ++i)
					{
					if (taxon_abundance[r][f][b][n][i] == 0 &&
taxon_abundance[r][f][b][n + 1][i] == 0 && taxon_abundance[r][f][b][n + 2][i] == 0)
						missing_taxa++;
					}
				}

			total_bed_richness[r][f][b] = MAXRICHNESS - missing_taxa;
			total_facies_individuals[r][f] = total_facies_individuals[r][f] +
total_bed_individuals[r][f][b];
			}

		for (b = 0; b < BEDS - (BEDS - 1); ++b)
			{
			for (n = 0; n < SAMPLES - (SAMPLES - 1); ++n)
				{
				missing_taxa2 = 0;
				for (i = 0; i < MAXRICHNESS; ++i)
					{
					if (taxon_abundance[r][f][b][n][i] == 0 &&
taxon_abundance[r][f][b][n + 1][i] == 0 && taxon_abundance[r][f][b][n + 2][i] == 0
						&& taxon_abundance[r][f][b + 1][n][i] == 0 &&
taxon_abundance[r][f][b + 1][n + 1][i] == 0 && taxon_abundance[r][f][b + 1][n + 2][i] == 0)
						missing_taxa2++;
					}
```

```
                    }
                }

            total_facies_richness[r][f] = MAXRICHNESS - missing_taxa2;
            total_regional_individuals[r] = total_regional_individuals[r] +
total_facies_individuals[r][f];
        }

        for (f = 0; f < FACIES - (FACIES - 1); ++f)
            {
            for (b = 0; b < BEDS - (BEDS - 1); ++b)
                {
                for (n = 0; n < SAMPLES - (SAMPLES - 1); ++n)
                    {
                    missing_taxa3 = 0;
                    for (i = 0; i < MAXRICHNESS; ++i)
                        {
                        if (taxon_abundance[r][f][b][n][i] == 0 &&
taxon_abundance[r][f][b][n + 1][i] == 0 && taxon_abundance[r][f][b][n + 2][i] == 0
                            && taxon_abundance[r][f][b + 1][n][i] == 0 &&
taxon_abundance[r][f][b + 1][n + 1][i] == 0 && taxon_abundance[r][f][b + 1][n + 2][i] == 0
                            && taxon_abundance[r][f + 1][b][n][i] == 0 &&
taxon_abundance[r][f + 1][b][n + 1][i] == 0 && taxon_abundance[r][f + 1][b][n + 2][i] == 0
                            && taxon_abundance[r][f + 1][b + 1][n][i] == 0 &&
taxon_abundance[r][f + 1][b + 1][n + 1][i] == 0 && taxon_abundance[r][f + 1][b + 1][n +
2][i] == 0)
                            missing_taxa3++;
                        }
                    }
                }
            }

        total_regional_richness[r] = MAXRICHNESS - missing_taxa3;


////****INITIAL ALPHA AND BETA CALCULATIONS****////

        for (f = 0; f < FACIES; ++f)
            {
            for (b = 0; b < BEDS; ++b)
                {
                alpha_one_term[r][f][b] = 0;
                for (n = 0; n < SAMPLES; ++n)
                    {
                    alpha_one_term[r][f][b] = alpha_one_term[r][f][b] +
(total_sample_richness[r][f][b][n] *
```

```
(total_sample_individuals[r][f][b][n]/total_regional_individuals[r]));
                        }
                    }
                }


        for (f = 0; f < FACIES; ++f)
                {
                alpha_one_sum[r][f] = 0;
                alpha_two_sum[r][f] = 0;
                for (b = 0; b < BEDS; ++b)
                    {
                    alpha_one_sum[r][f] = alpha_one_sum[r][f] + alpha_one_term[r][f][b];
                    alpha_two_sum[r][f] = alpha_two_sum[r][f] + (total_bed_richness[r][f][b] *
(total_bed_individuals[r][f][b]/total_regional_individuals[r]));
                    }
                }


        total_alpha_one[r] = 0;
        total_alpha_two[r] = 0;
        total_alpha_three[r] = 0;
        for (f = 0; f < FACIES; ++f)
                {
                total_alpha_one[r] = total_alpha_one[r] + alpha_one_sum[r][f];
                total_alpha_two[r] = total_alpha_two[r] + alpha_two_sum[r][f];
                total_alpha_three[r] = total_alpha_three[r] + (total_facies_richness[r][f] *
(total_facies_individuals[r][f]/total_regional_individuals[r]));
                }


        total_beta_one[r] = total_alpha_two[r] - total_alpha_one[r];
        total_beta_two[r] = total_alpha_three[r] - total_alpha_two[r];
        total_beta_three[r] = total_regional_richness[r] - total_alpha_three[r];
}

////****EXTINCTION****////

for (r = 0; r < RUNS; ++r)
        {
        for (f = 0; f < FACIES; ++f)
                {
                for (b = 0; b < BEDS; ++b)
                    {
                    for (n = 0; n < SAMPLES; ++n)
                        {
```

```
                    for (i = 0; i < MAXRICHNESS; ++i)
                        {
                        while (extinct_taxa[r] < MAXRICHNESS *
PERCENTEXTINCTION)
                            {
                            dead_taxon = RanIntInRange (0, MAXRICHNESS - 1);
                            if (post_probability[r][0][0][0][dead_taxon] > 0)
                                {
                                post_probability[r][0][0][0][dead_taxon] = 0;
                                extinct_taxa[r]++;
                                }
                            }
                        }
                    }
                }
            }
        }


////****POST-EXTINCTION RESAMPLING****////
for (r = 0; r < RUNS; ++r)
    {
    post_total_regional_individuals[r] = 0;
    post_total_regional_richness[r] = 0;
    for (f = 0; f < 1; ++f)
        {
        post_total_facies_individuals[r][f] = 0;
        post_total_facies_richness[r][f] = 0;
        for (b = 0; b < BEDS; ++b)
            {
            post_total_bed_individuals[r][f][b] = 0;
            post_total_bed_richness[r][f][b] = 0;
            for (n = 0; n < SAMPLES; ++n)
                {
                post_total_sample_richness[r][f][b][n] = 0;
                post_total_sample_individuals[r][f][b][n] = 0;
                for (i = 0; i < MAXRICHNESS; ++i)
                    {
                    post_taxon_abundance[r][f][b][n][i] = 0;
                    post_count_sample_richness[r][f][b][n][i] = 0;
                    }

                for (i = 0; i < MAXRICHNESS * 2/3; ++i)
                    {
                    post_is_taxa_present = RandNum();
                    if (post_is_taxa_present > post_probability[r][0][0][0][i] &&
```

```
post_probability[r][0][0][0][i] > 0)
                                {
                                post_taxon_abundance[r][f][b][n][i] = LogNormRandNum();
                                post_count_sample_richness[r][f][b][n][i] = 1;
                                }
                           else
                                {
                                post_taxon_abundance[r][f][b][n][i] = 0;
                                post_count_sample_richness[r][f][b][n][i] = 0;
                                }
                           }
                      }
                 }
            }

       for (f = 1; f < FACIES; ++f)
            {
            post_total_facies_individuals[r][f] = 0;
            post_total_facies_richness[r][f] = 0;
            for (b = 0; b < BEDS; ++b)
                 {
                 post_total_bed_individuals[r][f][b] = 0;
                 post_total_bed_richness[r][f][b] = 0;
                 for (n = 0; n < SAMPLES; ++n)
                      {
                      post_total_sample_richness[r][f][b][n] = 0;
                      post_total_sample_individuals[r][f][b][n] = 0;
                      for (i = 0; i < MAXRICHNESS; ++i)
                           {
                           post_taxon_abundance[r][f][b][n][i] = 0;
                           post_count_sample_richness[r][f][b][n][i] = 0;
                           }

                      for (i = MAXRICHNESS * 1/3; i < MAXRICHNESS; ++i)
                           {
                           post_is_taxa_present = RandNum();
                           if (post_is_taxa_present > post_probability[r][0][0][0][i] &&
post_probability[r][0][0][0][i] > 0)
                                {
                                post_taxon_abundance[r][f][b][n][i] = LogNormRandNum();
                                post_count_sample_richness[r][f][b][n][i] = 1;
                                }
                           else
                                {
                                post_taxon_abundance[r][f][b][n][i] = 0;
                                post_count_sample_richness[r][f][b][n][i] = 0;
```

```
                        }
                    }
                }
            }
        }

    for (f = 0; f < FACIES; ++f)
        {
        for (b = 0; b < BEDS; ++b)
            {
            for (n = 0; n < SAMPLES; ++n)
                {
                for (i = 0; i < MAXRICHNESS; ++i)
                    {
                    post_total_sample_richness[r][f][b][n] =
post_total_sample_richness[r][f][b][n] + post_count_sample_richness[r][f][b][n][i];
                    post_total_sample_individuals[r][f][b][n] =
post_total_sample_individuals[r][f][b][n] + post_taxon_abundance[r][f][b][n][i];
                    }

                post_total_bed_individuals[r][f][b] = post_total_bed_individuals[r][f][b]
+ post_total_sample_individuals[r][f][b][n];
                }

            for (n = 0; n < SAMPLES - (SAMPLES - 1); ++n)
                {
                post_missing_taxa = 0;
                for (i = 0; i < MAXRICHNESS; ++i)
                    {
                    if (post_taxon_abundance[r][f][b][n][i] == 0 &&
post_taxon_abundance[r][f][b][n + 1][i] == 0 && post_taxon_abundance[r][f][b][n + 2][i]
== 0)
                        post_missing_taxa++;
                    }
                }

            post_total_bed_richness[r][f][b] = MAXRICHNESS - post_missing_taxa;
            post_total_facies_individuals[r][f] = post_total_facies_individuals[r][f] +
post_total_bed_individuals[r][f][b];
            }

        for (b = 0; b < BEDS - (BEDS - 1); ++b)
            {
            for (n = 0; n < SAMPLES - (SAMPLES - 1); ++n)
                {
                post_missing_taxa2 = 0;
```

```
                    for (i = 0; i < MAXRICHNESS; ++i)
                        {
                        if (post_taxon_abundance[r][f][b][n][i] == 0 &&
post_taxon_abundance[r][f][b][n + 1][i] == 0 && post_taxon_abundance[r][f][b][n + 2][i]
== 0
                            && post_taxon_abundance[r][f][b + 1][n][i] == 0 &&
post_taxon_abundance[r][f][b + 1][n + 1][i] == 0 && post_taxon_abundance[r][f][b + 1][n
+ 2][i] == 0)
                            post_missing_taxa2++;
                        }
                    }
                }

            post_total_facies_richness[r][f] = MAXRICHNESS - post_missing_taxa2;
            post_total_regional_individuals[r] = post_total_regional_individuals[r] +
post_total_facies_individuals[r][f];
        }

        for (f = 0; f < FACIES - (FACIES - 1); ++f)
            {
            for (b = 0; b < BEDS - (BEDS - 1); ++b)
                {
                for (n = 0; n < SAMPLES - (SAMPLES - 1); ++n)
                    {
                    post_missing_taxa3 = 0;
                    for (i = 0; i < MAXRICHNESS; ++i)
                        {
                        if (post_taxon_abundance[r][f][b][n][i] == 0 &&
post_taxon_abundance[r][f][b][n + 1][i] == 0 && post_taxon_abundance[r][f][b][n + 2][i]
== 0
                            && post_taxon_abundance[r][f][b + 1][n][i] == 0 &&
post_taxon_abundance[r][f][b + 1][n + 1][i] == 0 && post_taxon_abundance[r][f][b + 1][n
+ 2][i] == 0
                            && post_taxon_abundance[r][f + 1][b][n][i] == 0 &&
post_taxon_abundance[r][f + 1][b][n + 1][i] == 0 && post_taxon_abundance[r][f + 1][b][n
+ 2][i] == 0
                            && post_taxon_abundance[r][f + 1][b + 1][n][i] == 0 &&
post_taxon_abundance[r][f + 1][b + 1][n + 1][i] == 0 && post_taxon_abundance[r][f +
1][b + 1][n + 2][i] == 0)
                            post_missing_taxa3++;
                        }
                    }
                }
            }

        post_total_regional_richness[r] = MAXRICHNESS - post_missing_taxa3;
```

```
////****POST-EXTINCTION ALPHA AND BETA CALCULATIONS****////

      for (f = 0; f < FACIES; ++f)
            {
            for (b = 0; b < BEDS; ++b)
                  {
                  post_alpha_one_term[r][f][b] = 0;
                  for (n = 0; n < SAMPLES; ++n)
                        {
                        post_alpha_one_term[r][f][b] = post_alpha_one_term[r][f][b] +
(post_total_sample_richness[r][f][b][n] *
(post_total_sample_individuals[r][f][b][n]/post_total_regional_individuals[r]));
                        }
                  }
            }


      for (f = 0; f < FACIES; ++f)
            {
            post_alpha_one_sum[r][f] = 0;
            post_alpha_two_sum[r][f] = 0;
            for (b = 0; b < BEDS; ++b)
                  {
                  post_alpha_one_sum[r][f] = post_alpha_one_sum[r][f] +
post_alpha_one_term[r][f][b];
                  post_alpha_two_sum[r][f] = post_alpha_two_sum[r][f] +
(post_total_bed_richness[r][f][b] *
(post_total_bed_individuals[r][f][b]/post_total_regional_individuals[r]));
                  }
            }


      post_total_alpha_one[r] = 0;
      post_total_alpha_two[r] = 0;
      post_total_alpha_three[r] = 0;
      for (f = 0; f < FACIES; ++f)
            {
            post_total_alpha_one[r] = post_total_alpha_one[r] + post_alpha_one_sum[r][f];
            post_total_alpha_two[r] = post_total_alpha_two[r] + post_alpha_two_sum[r][f];
            post_total_alpha_three[r] = post_total_alpha_three[r] +
(post_total_facies_richness[r][f] *
(post_total_facies_individuals[r][f]/post_total_regional_individuals[r]));
            }
```

```
	post_total_beta_one[r] = post_total_alpha_two[r] - post_total_alpha_one[r];
	post_total_beta_two[r] = post_total_alpha_three[r] - post_total_alpha_two[r];
	post_total_beta_three[r] = post_total_regional_richness[r] -
post_total_alpha_three[r];
}

mean_initial_alpha_one = mean (total_alpha_one, RUNS);
mean_initial_alpha_two = mean (total_alpha_two, RUNS);
mean_initial_alpha_three = mean (total_alpha_three, RUNS);
mean_initial_alpha_four = mean (total_regional_richness, RUNS);
mean_initial_beta_one = mean (total_beta_one, RUNS);
mean_initial_beta_two = mean (total_beta_two, RUNS);
mean_initial_beta_three = mean (total_beta_three, RUNS);
mean_post_alpha_one = mean (post_total_alpha_one, RUNS);
mean_post_alpha_two = mean (post_total_alpha_two, RUNS);
mean_post_alpha_three = mean (post_total_alpha_three, RUNS);
mean_post_alpha_four = mean (post_total_regional_richness, RUNS);
mean_post_beta_one = mean (post_total_beta_one, RUNS);
mean_post_beta_two = mean (post_total_beta_two, RUNS);
mean_post_beta_three = mean (post_total_beta_three, RUNS);

////****PRINT STATEMENTS****////

printf("%.3f\t%.3f\t%.3f\t%.3f\t%.3f\t%.3f\t%.3f\t%.3f\t%.3f\t%.3f\t%.3f\t%.3f\t%.3f\t%.3f\n
", mean_initial_alpha_one, mean_initial_alpha_two, mean_initial_alpha_three,
mean_initial_alpha_four, mean_initial_beta_one, mean_initial_beta_two,
mean_initial_beta_three, mean_post_alpha_one, mean_post_alpha_two,
mean_post_alpha_three,
mean_post_alpha_four, mean_post_beta_one, mean_post_beta_two,
mean_post_beta_three);

return 0;
}
```

2. This version of the model uses random probabilities of extinction drawn from a uniform distribution between zero and one and includes a non-selective extinction.

```
#include <stdio.h>
#include <stdlib.h>
#include <math.h>
#include "randomNumbers.h"
#include "statistics.h"

#define MAXRICHNESS 24
#define SAMPLES 3
#define BEDS 2
```

```
#define FACIES 2
#define RUNS 70
#define PERCENTEXTINCTION 0.5

int main()
{

int i;
int n;
int b;
int f;
int r;

double taxon_abundance[RUNS][FACIES][BEDS][SAMPLES][MAXRICHNESS];
double probability[RUNS][FACIES][MAXRICHNESS];
double is_taxa_present;
double count_sample_richness[RUNS][FACIES][BEDS][SAMPLES][MAXRICHNESS];
double total_sample_richness[RUNS][FACIES][BEDS][SAMPLES];
double total_sample_individuals[RUNS][FACIES][BEDS][SAMPLES];
double total_bed_individuals[RUNS][FACIES][BEDS];
double total_bed_richness[RUNS][FACIES][BEDS];
double missing_taxa;
double missing_taxa2;
double total_facies_individuals[RUNS][FACIES];
double total_facies_richness[RUNS][FACIES];
double total_regional_individuals[RUNS];
double missing_taxa3;
double total_regional_richness[RUNS];

double alpha_one_term[RUNS][FACIES][BEDS];
double alpha_one_sum[RUNS][FACIES];
double total_alpha_one[RUNS];
double alpha_two_sum[RUNS][FACIES];
double total_alpha_two[RUNS];
double total_alpha_three[RUNS];
double total_beta_one[RUNS];
double total_beta_two[RUNS];
double total_beta_three[RUNS];

double post_probability[RUNS][FACIES][MAXRICHNESS];
double extinct_taxa[RUNS];
int dead_taxon;

double post_taxon_abundance[RUNS][FACIES][BEDS][SAMPLES][MAXRICHNESS];
double post_is_taxa_present;
double
```

```
post_count_sample_richness[RUNS][FACIES][BEDS][SAMPLES][MAXRICHNESS];
double post_total_sample_richness[RUNS][FACIES][BEDS][SAMPLES];
double post_total_sample_individuals[RUNS][FACIES][BEDS][SAMPLES];
double post_total_bed_individuals[RUNS][FACIES][BEDS];
double post_total_bed_richness[RUNS][FACIES][BEDS];
double post_missing_taxa;
double post_missing_taxa2;
double post_total_facies_individuals[RUNS][FACIES];
double post_total_facies_richness[RUNS][FACIES];
double post_total_regional_individuals[RUNS];
double post_missing_taxa3;
double post_total_regional_richness[RUNS];

double post_alpha_one_term[RUNS][FACIES][BEDS];
double post_alpha_one_sum[RUNS][FACIES];
double post_total_alpha_one[RUNS];
double post_alpha_two_sum[RUNS][FACIES];
double post_total_alpha_two[RUNS];
double post_total_alpha_three[RUNS];
double post_total_beta_one[RUNS];
double post_total_beta_two[RUNS];
double post_total_beta_three[RUNS];

double mean_initial_alpha_one;
double mean_initial_alpha_two;
double mean_initial_alpha_three;
double mean_initial_alpha_four;
double mean_initial_beta_one;
double mean_initial_beta_two;
double mean_initial_beta_three;
double mean_post_alpha_one;
double mean_post_alpha_two;
double mean_post_alpha_three;
double mean_post_alpha_four;
double mean_post_beta_one;
double mean_post_beta_two;
double mean_post_beta_three;

InitRandNum();

printf("xA1i\t xA2i\t xA3i\t xA4i\t xB1i\t xB2i\t xB3i\t xA1p\t xA2p\t xA3p\t xA4p\t xB1p\t
xB2p\t xB3p\n");

for (r = 0; r < RUNS; ++r)
      {
      total_regional_individuals[r] = 0;
```

```
total_regional_richness[r] = 0;
for (f = 0; f < 1; ++f)
      {
      total_facies_individuals[r][f] = 0;
      total_facies_richness[r][f] = 0;
      for (b = 0; b < BEDS; ++b)
            {
            total_bed_individuals[r][f][b] = 0;
            total_bed_richness[r][f][b] = 0;
            for (n = 0; n < SAMPLES; ++n)
                  {
                  total_sample_richness[r][f][b][n] = 0;
                  total_sample_individuals[r][f][b][n] = 0;
                  for (i = 0; i < MAXRICHNESS; ++i)
                        {
                        taxon_abundance[r][f][b][n][i] = 0;
                        count_sample_richness[r][f][b][n][i] = 0;
                        probability[r][f][i] = RandNum();
                        post_probability[r][f][i] = probability[r][f][i];
                        }

                  for (i = 0; i < MAXRICHNESS * 2/3; ++i)
                        {
                        is_taxa_present = RandNum();
                        if (is_taxa_present > probability[r][f][i])
                              {
                              taxon_abundance[r][f][b][n][i] = LogNormRandNum();
                              count_sample_richness[r][f][b][n][i] = 1;
                              }
                        else
                              {
                              taxon_abundance[r][f][b][n][i] = 0;
                              count_sample_richness[r][f][b][n][i] = 0;
                              }
                        }
                  }
            }
      }

for (f = 1; f < FACIES; ++f)
      {
      total_facies_individuals[r][f] = 0;
      total_facies_richness[r][f] = 0;
      for (b = 0; b < BEDS; ++b)
            {
            total_bed_individuals[r][f][b] = 0;
```

```
                total_bed_richness[r][f][b] = 0;
                for (n = 0; n < SAMPLES; ++n)
                        {
                        total_sample_richness[r][f][b][n] = 0;
                        total_sample_individuals[r][f][b][n] = 0;

                        for (i = 0; i < MAXRICHNESS; ++i)
                                {
                                taxon_abundance[r][f][b][n][i] = 0;
                                count_sample_richness[r][f][b][n][i] = 0;
                                probability[r][f][i] = RandNum();
                                post_probability[r][f][i] = probability[r][f][i];
                                }

                        for (i = MAXRICHNESS * 1/3; i < MAXRICHNESS; ++i)
                                {
                                is_taxa_present = RandNum();
                                if (is_taxa_present >  probability[r][f][i])
                                        {
                                        taxon_abundance[r][f][b][n][i] = LogNormRandNum();
                                        count_sample_richness[r][f][b][n][i] = 1;
                                        }
                                else
                                        {
                                        taxon_abundance[r][f][b][n][i] = 0;
                                        count_sample_richness[r][f][b][n][i] = 0;
                                        }
                                }
                        }
                }
        }

    for (f = 0; f < FACIES; ++f)
        {
        for (b = 0; b < BEDS; ++b)
                {
                for (n = 0; n < SAMPLES; ++n)
                        {
                        for (i = 0; i < MAXRICHNESS; ++i)
                                {
                                total_sample_richness[r][f][b][n] = total_sample_richness[r][f][b][n]
+ count_sample_richness[r][f][b][n][i];
                                total_sample_individuals[r][f][b][n] =
total_sample_individuals[r][f][b][n] + taxon_abundance[r][f][b][n][i];
                                }
```

```
                    total_bed_individuals[r][f][b] = total_bed_individuals[r][f][b] +
total_sample_individuals[r][f][b][n];
                    }

                for (n = 0; n < SAMPLES - (SAMPLES - 1); ++n)
                    {
                    missing_taxa = 0;
                    for (i = 0; i < MAXRICHNESS; ++i)
                        {
                        if (taxon_abundance[r][f][b][n][i] == 0 &&
taxon_abundance[r][f][b][n + 1][i] == 0 && taxon_abundance[r][f][b][n + 2][i] == 0)
                            missing_taxa++;
                        }
                    }

                total_bed_richness[r][f][b] = MAXRICHNESS - missing_taxa;
                total_facies_individuals[r][f] = total_facies_individuals[r][f] +
total_bed_individuals[r][f][b];
                }

            for (b = 0; b < BEDS - (BEDS - 1); ++b)
                {
                for (n = 0; n < SAMPLES - (SAMPLES - 1); ++n)
                    {
                    missing_taxa2 = 0;
                    for (i = 0; i < MAXRICHNESS; ++i)
                        {
                        if (taxon_abundance[r][f][b][n][i] == 0 &&
taxon_abundance[r][f][b][n + 1][i] == 0 && taxon_abundance[r][f][b][n + 2][i] == 0
                            && taxon_abundance[r][f][b + 1][n][i] == 0 &&
taxon_abundance[r][f][b + 1][n + 1][i] == 0 && taxon_abundance[r][f][b + 1][n + 2][i] == 0)
                            missing_taxa2++;
                        }
                    }
                }

            total_facies_richness[r][f] = MAXRICHNESS - missing_taxa2;
            total_regional_individuals[r] = total_regional_individuals[r] +
total_facies_individuals[r][f];
        }

        for (f = 0; f < FACIES - (FACIES - 1); ++f)
            {
            for (b = 0; b < BEDS - (BEDS - 1); ++b)
                {
                for (n = 0; n < SAMPLES - (SAMPLES - 1); ++n)
```

```
                    {
                    missing_taxa3 = 0;
                    for (i = 0; i < MAXRICHNESS; ++i)
                        {
                        if (taxon_abundance[r][f][b][n][i] == 0 &&
taxon_abundance[r][f][b][n + 1][i] == 0 && taxon_abundance[r][f][b][n + 2][i] == 0
                            && taxon_abundance[r][f][b + 1][n][i] == 0 &&
taxon_abundance[r][f][b + 1][n + 1][i] == 0 && taxon_abundance[r][f][b + 1][n + 2][i] == 0
                            && taxon_abundance[r][f + 1][b][n][i] == 0 &&
taxon_abundance[r][f + 1][b][n + 1][i] == 0 && taxon_abundance[r][f + 1][b][n + 2][i] == 0
                            && taxon_abundance[r][f + 1][b + 1][n][i] == 0 &&
taxon_abundance[r][f + 1][b + 1][n + 1][i] == 0 && taxon_abundance[r][f + 1][b + 1][n +
2][i] == 0)
                            missing_taxa3++;
                        }
                    }
                }
            }

    total_regional_richness[r] = MAXRICHNESS - missing_taxa3;


////****INITIAL ALPHA AND BETA CALCULATIONS****////

    for (f = 0; f < FACIES; ++f)
        {
        for (b = 0; b < BEDS; ++b)
            {
            alpha_one_term[r][f][b] = 0;
            for (n = 0; n < SAMPLES; ++n)
                {
                alpha_one_term[r][f][b] = alpha_one_term[r][f][b] +
(total_sample_richness[r][f][b][n] *
(total_sample_individuals[r][f][b][n]/total_regional_individuals[r]));
                }
            }
        }


    for (f = 0; f < FACIES; ++f)
        {
        alpha_one_sum[r][f] = 0;
        alpha_two_sum[r][f] = 0;
        for (b = 0; b < BEDS; ++b)
            {
            alpha_one_sum[r][f] = alpha_one_sum[r][f] + alpha_one_term[r][f][b];
```

```
                alpha_two_sum[r][f] = alpha_two_sum[r][f] + (total_bed_richness[r][f][b] *
(total_bed_individuals[r][f][b]/total_regional_individuals[r]));
                }
          }


     total_alpha_one[r] = 0;
     total_alpha_two[r] = 0;
     total_alpha_three[r] = 0;
     for (f = 0; f < FACIES; ++f)
          {
          total_alpha_one[r] = total_alpha_one[r] + alpha_one_sum[r][f];
          total_alpha_two[r] = total_alpha_two[r] + alpha_two_sum[r][f];
          total_alpha_three[r] = total_alpha_three[r] + (total_facies_richness[r][f] *
(total_facies_individuals[r][f]/total_regional_individuals[r]));
          }


     total_beta_one[r] = total_alpha_two[r] - total_alpha_one[r];
     total_beta_two[r] = total_alpha_three[r] - total_alpha_two[r];
     total_beta_three[r] = total_regional_richness[r] - total_alpha_three[r];
}

////****EXTINCTION****////

for (r = 0; r < RUNS; ++r)
     {
     for (f = 0; f < FACIES; ++f)
          {
          for (b = 0; b < BEDS; ++b)
               {
               for (n = 0; n < SAMPLES; ++n)
                    {
                    for (i = 0; i < MAXRICHNESS; ++i)
                         {
                         while (extinct_taxa[r] < MAXRICHNESS *
PERCENTEXTINCTION)
                              {
                              dead_taxon = RanIntInRange (0, MAXRICHNESS - 1);
                              if (post_probability[r][0][dead_taxon] > 0)
                                   {
                                   post_probability[r][0][dead_taxon] = 0;
                                   post_probability[r][1][dead_taxon] = 0;
                                   extinct_taxa[r]++;
                                   }
                              }
```

```
                        }
                    }
                }
            }
        }

////****POST-EXTINCTION RESAMPLING****////
for (r = 0; r < RUNS; ++r)
    {
    post_total_regional_individuals[r] = 0;
    post_total_regional_richness[r] = 0;
    for (f = 0; f < 1; ++f)
        {
        post_total_facies_individuals[r][f] = 0;
        post_total_facies_richness[r][f] = 0;
        for (b = 0; b < BEDS; ++b)
            {
            post_total_bed_individuals[r][f][b] = 0;
            post_total_bed_richness[r][f][b] = 0;
            for (n = 0; n < SAMPLES; ++n)
                {
                post_total_sample_richness[r][f][b][n] = 0;
                post_total_sample_individuals[r][f][b][n] = 0;
                for (i = 0; i < MAXRICHNESS; ++i)
                    {
                    post_taxon_abundance[r][f][b][n][i] = 0;
                    post_count_sample_richness[r][f][b][n][i] = 0;
                    }

                for (i = 0; i < MAXRICHNESS * 2/3; ++i)
                    {
                    post_is_taxa_present = RandNum();
                    if (post_is_taxa_present > post_probability[r][f][i] &&
post_probability[r][f][i] > 0)
                        {
                        post_taxon_abundance[r][f][b][n][i] = LogNormRandNum();
                        post_count_sample_richness[r][f][b][n][i] = 1;
                        }
                    else
                        {
                        post_taxon_abundance[r][f][b][n][i] = 0;
                        post_count_sample_richness[r][f][b][n][i] = 0;
                        }
                    }
                }
```

```
                }
            }

        for (f = 1; f < FACIES; ++f)
            {
            post_total_facies_individuals[r][f] = 0;
            post_total_facies_richness[r][f] = 0;
            for (b = 0; b < BEDS; ++b)
                {
                post_total_bed_individuals[r][f][b] = 0;
                post_total_bed_richness[r][f][b] = 0;
                for (n = 0; n < SAMPLES; ++n)
                    {
                    post_total_sample_richness[r][f][b][n] = 0;
                    post_total_sample_individuals[r][f][b][n] = 0;
                    for (i = 0; i < MAXRICHNESS; ++i)
                        {
                        post_taxon_abundance[r][f][b][n][i] = 0;
                        post_count_sample_richness[r][f][b][n][i] = 0;
                        }

                    for (i = MAXRICHNESS * 1/3; i < MAXRICHNESS; ++i)
                        {
                        post_is_taxa_present = RandNum();
                        if (post_is_taxa_present > post_probability[r][f][i] &&
post_probability[r][f][i] > 0)
                            {
                            post_taxon_abundance[r][f][b][n][i] = LogNormRandNum();
                            post_count_sample_richness[r][f][b][n][i] = 1;
                            }
                        else
                            {
                            post_taxon_abundance[r][f][b][n][i] = 0;
                            post_count_sample_richness[r][f][b][n][i] = 0;
                            }
                        }
                    }
                }
            }

        for (f = 0; f < FACIES; ++f)
            {
            for (b = 0; b < BEDS; ++b)
                {
                for (n = 0; n < SAMPLES; ++n)
                    {
```

```
                    for (i = 0; i < MAXRICHNESS; ++i)
                        {
                        post_total_sample_richness[r][f][b][n] =
post_total_sample_richness[r][f][b][n] + post_count_sample_richness[r][f][b][n][i];
                        post_total_sample_individuals[r][f][b][n] =
post_total_sample_individuals[r][f][b][n] + post_taxon_abundance[r][f][b][n][i];
                        }

                    post_total_bed_individuals[r][f][b] = post_total_bed_individuals[r][f][b]
+ post_total_sample_individuals[r][f][b][n];
                    }

                for (n = 0; n < SAMPLES - (SAMPLES - 1); ++n)
                    {
                    post_missing_taxa = 0;
                    for (i = 0; i < MAXRICHNESS; ++i)
                        {
                        if (post_taxon_abundance[r][f][b][n][i] == 0 &&
post_taxon_abundance[r][f][b][n + 1][i] == 0 && post_taxon_abundance[r][f][b][n + 2][i]
== 0)
                            post_missing_taxa++;
                        }
                    }

                post_total_bed_richness[r][f][b] = MAXRICHNESS - post_missing_taxa;
                post_total_facies_individuals[r][f] = post_total_facies_individuals[r][f] +
post_total_bed_individuals[r][f][b];
                }

            for (b = 0; b < BEDS - (BEDS - 1); ++b)
                {
                for (n = 0; n < SAMPLES - (SAMPLES - 1); ++n)
                    {
                    post_missing_taxa2 = 0;
                    for (i = 0; i < MAXRICHNESS; ++i)
                        {
                        if (post_taxon_abundance[r][f][b][n][i] == 0 &&
post_taxon_abundance[r][f][b][n + 1][i] == 0 && post_taxon_abundance[r][f][b][n + 2][i]
== 0
                            && post_taxon_abundance[r][f][b + 1][n][i] == 0 &&
post_taxon_abundance[r][f][b + 1][n + 1][i] == 0 && post_taxon_abundance[r][f][b + 1][n
+ 2][i] == 0)
                            post_missing_taxa2++;
                        }
                    }
                }
```

```
            post_total_facies_richness[r][f] = MAXRICHNESS - post_missing_taxa2;
            post_total_regional_individuals[r] = post_total_regional_individuals[r] +
post_total_facies_individuals[r][f];
      }

      for (f = 0; f < FACIES - (FACIES - 1); ++f)
            {
            for (b = 0; b < BEDS - (BEDS - 1); ++b)
                  {
                  for (n = 0; n < SAMPLES - (SAMPLES - 1); ++n)
                        {
                        post_missing_taxa3 = 0;
                        for (i = 0; i < MAXRICHNESS; ++i)
                              {
                              if (post_taxon_abundance[r][f][b][n][i] == 0 &&
post_taxon_abundance[r][f][b][n + 1][i] == 0 && post_taxon_abundance[r][f][b][n + 2][i]
== 0
                                    && post_taxon_abundance[r][f][b + 1][n][i] == 0 &&
post_taxon_abundance[r][f][b + 1][n + 1][i] == 0 && post_taxon_abundance[r][f][b + 1][n
+ 2][i] == 0
                                    && post_taxon_abundance[r][f + 1][b][n][i] == 0 &&
post_taxon_abundance[r][f + 1][b][n + 1][i] == 0 && post_taxon_abundance[r][f + 1][b][n
+ 2][i] == 0
                                    && post_taxon_abundance[r][f + 1][b + 1][n][i] == 0 &&
post_taxon_abundance[r][f + 1][b + 1][n + 1][i] == 0 && post_taxon_abundance[r][f +
1][b + 1][n + 2][i] == 0)
                                    post_missing_taxa3++;
                              }
                        }
                  }
            }

      post_total_regional_richness[r] = MAXRICHNESS - post_missing_taxa3;


////****POST-EXTINCTION ALPHA AND BETA CALCULATIONS****////

      for (f = 0; f < FACIES; ++f)
            {
            for (b = 0; b < BEDS; ++b)
                  {
                  post_alpha_one_term[r][f][b] = 0;
                  for (n = 0; n < SAMPLES; ++n)
                        {
                        post_alpha_one_term[r][f][b] = post_alpha_one_term[r][f][b] +
```

```
(post_total_sample_richness[r][f][b][n] *
(post_total_sample_individuals[r][f][b][n]/post_total_regional_individuals[r]));
                        }
                    }
                }


        for (f = 0; f < FACIES; ++f)
                {
                post_alpha_one_sum[r][f] = 0;
                post_alpha_two_sum[r][f] = 0;
                for (b = 0; b < BEDS; ++b)
                    {
                    post_alpha_one_sum[r][f] = post_alpha_one_sum[r][f] +
post_alpha_one_term[r][f][b];
                    post_alpha_two_sum[r][f] = post_alpha_two_sum[r][f] +
(post_total_bed_richness[r][f][b] *
(post_total_bed_individuals[r][f][b]/post_total_regional_individuals[r]));
                    }
                }


        post_total_alpha_one[r] = 0;
        post_total_alpha_two[r] = 0;
        post_total_alpha_three[r] = 0;
        for (f = 0; f < FACIES; ++f)
                {
                post_total_alpha_one[r] = post_total_alpha_one[r] + post_alpha_one_sum[r][f];
                post_total_alpha_two[r] = post_total_alpha_two[r] + post_alpha_two_sum[r][f];
                post_total_alpha_three[r] = post_total_alpha_three[r] +
(post_total_facies_richness[r][f] *
(post_total_facies_individuals[r][f]/post_total_regional_individuals[r]));
                }


        post_total_beta_one[r] = post_total_alpha_two[r] - post_total_alpha_one[r];
        post_total_beta_two[r] = post_total_alpha_three[r] - post_total_alpha_two[r];
        post_total_beta_three[r] = post_total_regional_richness[r] -
post_total_alpha_three[r];
}

mean_initial_alpha_one = mean (total_alpha_one, RUNS);
mean_initial_alpha_two = mean (total_alpha_two, RUNS);
mean_initial_alpha_three = mean (total_alpha_three, RUNS);
mean_initial_alpha_four = mean (total_regional_richness, RUNS);
mean_initial_beta_one = mean (total_beta_one, RUNS);
```

```
mean_initial_beta_two = mean (total_beta_two, RUNS);
mean_initial_beta_three = mean (total_beta_three, RUNS);
mean_post_alpha_one = mean (post_total_alpha_one, RUNS);
mean_post_alpha_two = mean (post_total_alpha_two, RUNS);
mean_post_alpha_three = mean (post_total_alpha_three, RUNS);
mean_post_alpha_four = mean (post_total_regional_richness, RUNS);
mean_post_beta_one = mean (post_total_beta_one, RUNS);
mean_post_beta_two = mean (post_total_beta_two, RUNS);
mean_post_beta_three = mean (post_total_beta_three, RUNS);


////****PRINT STATEMENTS****////

printf("%.3f\t%.3f\t%.3f\t%.3f\t%.3f\t%.3f\t%.3f\t%.3f\t%.3f\t%.3f\t%.3f\t%.3f\t%.3f\t%.3f\n
", mean_initial_alpha_one, mean_initial_alpha_two, mean_initial_alpha_three,
mean_initial_alpha_four, mean_initial_beta_one, mean_initial_beta_two,
mean_initial_beta_three, mean_post_alpha_one, mean_post_alpha_two,
mean_post_alpha_three,
mean_post_alpha_four, mean_post_beta_one, mean_post_beta_two,
mean_post_beta_three);

return 0;
}
```

3. This version of the model uses random probabilities of taxon occurrence drawn from a uniform distribution between zero and one and includes an extinction that targets rare taxa.

```
#include <stdio.h>
#include <stdlib.h>
#include <math.h>
#include "randomNumbers.h"
#include "statistics.h"

#define MAXRICHNESS 24
#define SAMPLES 3
#define BEDS 2
#define FACIES 2
#define RUNS 90
#define PERCENTEXTINCTION 0.95

int main()
{

int i;
int n;
int b;
int f;
int r;

double taxon_abundance[RUNS][FACIES][BEDS][SAMPLES][MAXRICHNESS];
double probability[RUNS][FACIES][MAXRICHNESS];
double is_taxa_present;
double count_sample_richness[RUNS][FACIES][BEDS][SAMPLES][MAXRICHNESS];
double total_sample_richness[RUNS][FACIES][BEDS][SAMPLES];
double total_sample_individuals[RUNS][FACIES][BEDS][SAMPLES];
double total_bed_individuals[RUNS][FACIES][BEDS];
double total_bed_richness[RUNS][FACIES][BEDS];
double missing_taxa;
double missing_taxa2;
double total_facies_individuals[RUNS][FACIES];
double total_facies_richness[RUNS][FACIES];
double total_regional_individuals[RUNS];
double missing_taxa3;
double total_regional_richness[RUNS];
double total_taxon_individuals[RUNS][MAXRICHNESS];

double alpha_one_term[RUNS][FACIES][BEDS];
double alpha_one_sum[RUNS][FACIES];
double total_alpha_one[RUNS];
```

```
double alpha_two_sum[RUNS][FACIES];
double total_alpha_two[RUNS];
double total_alpha_three[RUNS];
double total_beta_one[RUNS];
double total_beta_two[RUNS];
double total_beta_three[RUNS];

double post_probability[RUNS][FACIES][MAXRICHNESS];
double extinct_taxa[RUNS];
double rarest_taxon[RUNS];

double post_taxon_abundance[RUNS][FACIES][BEDS][SAMPLES][MAXRICHNESS];
double post_is_taxa_present;
double
post_count_sample_richness[RUNS][FACIES][BEDS][SAMPLES][MAXRICHNESS];
double post_total_sample_richness[RUNS][FACIES][BEDS][SAMPLES];
double post_total_sample_individuals[RUNS][FACIES][BEDS][SAMPLES];
double post_total_bed_individuals[RUNS][FACIES][BEDS];
double post_total_bed_richness[RUNS][FACIES][BEDS];
double post_missing_taxa;
double post_missing_taxa2;
double post_total_facies_individuals[RUNS][FACIES];
double post_total_facies_richness[RUNS][FACIES];
double post_total_regional_individuals[RUNS];
double post_missing_taxa3;
double post_total_regional_richness[RUNS];

double post_alpha_one_term[RUNS][FACIES][BEDS];
double post_alpha_one_sum[RUNS][FACIES];
double post_total_alpha_one[RUNS];
double post_alpha_two_sum[RUNS][FACIES];
double post_total_alpha_two[RUNS];
double post_total_alpha_three[RUNS];
double post_total_beta_one[RUNS];
double post_total_beta_two[RUNS];
double post_total_beta_three[RUNS];

double mean_initial_alpha_one;
double mean_initial_alpha_two;
double mean_initial_alpha_three;
double mean_initial_alpha_four;
double mean_initial_beta_one;
double mean_initial_beta_two;
double mean_initial_beta_three;
double mean_post_alpha_one;
double mean_post_alpha_two;
```

```
double mean_post_alpha_three;
double mean_post_alpha_four;
double mean_post_beta_one;
double mean_post_beta_two;
double mean_post_beta_three;

InitRandNum();

printf("xA1i\t xA2i\t xA3i\t xA4i\t xB1i\t xB2i\t xB3i\t xA1p\t xA2p\t xA3p\t xA4p\t xB1p\t
xB2p\t xB3p\n");

for (r = 0; r < RUNS; ++r)
      {
      total_regional_individuals[r] = 0;
      total_regional_richness[r] = 0;
      for (f = 0; f < 1; ++f)
            {
            total_facies_individuals[r][f] = 0;
            total_facies_richness[r][f] = 0;
            for (b = 0; b < BEDS; ++b)
                  {
                  total_bed_individuals[r][f][b] = 0;
                  total_bed_richness[r][f][b] = 0;
                  for (n = 0; n < SAMPLES; ++n)
                        {
                        total_sample_richness[r][f][b][n] = 0;
                        total_sample_individuals[r][f][b][n] = 0;
                        for (i = 0; i < MAXRICHNESS; ++i)
                              {
                              taxon_abundance[r][f][b][n][i] = 0;
                              count_sample_richness[r][f][b][n][i] = 0;
                              probability[r][f][i] = RandNum();
                              post_probability[r][f][i] = probability[r][f][i];
                              }

                        for (i = 0; i < MAXRICHNESS * 2/3; ++i)
                              {
                              is_taxa_present = RandNum();
                              if (is_taxa_present > probability[r][f][i])
                                    {
                                    taxon_abundance[r][f][b][n][i] = LogNormRandNum();
                                    count_sample_richness[r][f][b][n][i] = 1;
                                    }
                              else
                                    {
                                    taxon_abundance[r][f][b][n][i] = 0;
```

```
                        count_sample_richness[r][f][b][n][i] = 0;
                        }
                    }
                }
            }
        }

for (f = 1; f < FACIES; ++f)
        {
        total_facies_individuals[r][f] = 0;
        total_facies_richness[r][f] = 0;
        for (b = 0; b < BEDS; ++b)
            {
            total_bed_individuals[r][f][b] = 0;
            total_bed_richness[r][f][b] = 0;
            for (n = 0; n < SAMPLES; ++n)
                {
                total_sample_richness[r][f][b][n] = 0;
                total_sample_individuals[r][f][b][n] = 0;

                for (i = 0; i < MAXRICHNESS; ++i)
                    {
                    taxon_abundance[r][f][b][n][i] = 0;
                    count_sample_richness[r][f][b][n][i] = 0;
                    probability[r][f][i] = RandNum();
                    post_probability[r][f][i] = probability[r][f][i];
                    }

                for (i = MAXRICHNESS * 1/3; i < MAXRICHNESS; ++i)
                    {
                    is_taxa_present = RandNum();
                    if (is_taxa_present >  probability[r][f][i])
                        {
                        taxon_abundance[r][f][b][n][i] = LogNormRandNum();
                        count_sample_richness[r][f][b][n][i] = 1;
                        }
                    else
                        {
                        taxon_abundance[r][f][b][n][i] = 0;
                        count_sample_richness[r][f][b][n][i] = 0;
                        }
                    }
                }
            }
        }
```

```
    for (f = 0; f < FACIES; ++f)
        {
        for (b = 0; b < BEDS; ++b)
            {
            for (n = 0; n < SAMPLES; ++n)
                {
                for (i = 0; i < MAXRICHNESS; ++i)
                    {
                    total_sample_richness[r][f][b][n] = total_sample_richness[r][f][b][n]
+ count_sample_richness[r][f][b][n][i];
                    total_sample_individuals[r][f][b][n] =
total_sample_individuals[r][f][b][n] + taxon_abundance[r][f][b][n][i];
                    total_taxon_individuals[r][i] = total_taxon_individuals[r][i] +
taxon_abundance[r][f][b][n][i];
                    }

                total_bed_individuals[r][f][b] = total_bed_individuals[r][f][b] +
total_sample_individuals[r][f][b][n];
                }

            for (n = 0; n < SAMPLES - (SAMPLES - 1); ++n)
                {
                missing_taxa = 0;
                for (i = 0; i < MAXRICHNESS; ++i)
                    {
                    if (taxon_abundance[r][f][b][n][i] == 0 &&
taxon_abundance[r][f][b][n + 1][i] == 0 && taxon_abundance[r][f][b][n + 2][i] == 0)
                        missing_taxa++;
                    }
                }

            total_bed_richness[r][f][b] = MAXRICHNESS - missing_taxa;
            total_facies_individuals[r][f] = total_facies_individuals[r][f] +
total_bed_individuals[r][f][b];
            }

        for (b = 0; b < BEDS - (BEDS - 1); ++b)
            {
            for (n = 0; n < SAMPLES - (SAMPLES - 1); ++n)
                {
                missing_taxa2 = 0;
                for (i = 0; i < MAXRICHNESS; ++i)
                    {
                    if (taxon_abundance[r][f][b][n][i] == 0 &&
taxon_abundance[r][f][b][n + 1][i] == 0 && taxon_abundance[r][f][b][n + 2][i] == 0
                        && taxon_abundance[r][f][b + 1][n][i] == 0 &&
```

```
taxon_abundance[r][f][b + 1][n + 1][i] == 0 && taxon_abundance[r][f][b + 1][n + 2][i] == 0)
                                missing_taxa2++;
                            }
                        }
                    }

            total_facies_richness[r][f] = MAXRICHNESS - missing_taxa2;
            total_regional_individuals[r] = total_regional_individuals[r] +
total_facies_individuals[r][f];
        }

        for (f = 0; f < FACIES - (FACIES - 1); ++f)
            {
            for (b = 0; b < BEDS - (BEDS - 1); ++b)
                {
                for (n = 0; n < SAMPLES - (SAMPLES - 1); ++n)
                    {
                    missing_taxa3 = 0;
                    for (i = 0; i < MAXRICHNESS; ++i)
                        {
                        if (taxon_abundance[r][f][b][n][i] == 0 &&
taxon_abundance[r][f][b][n + 1][i] == 0 && taxon_abundance[r][f][b][n + 2][i] == 0
                                && taxon_abundance[r][f][b + 1][n][i] == 0 &&
taxon_abundance[r][f][b + 1][n + 1][i] == 0 && taxon_abundance[r][f][b + 1][n + 2][i] == 0
                                && taxon_abundance[r][f + 1][b][n][i] == 0 &&
taxon_abundance[r][f + 1][b][n + 1][i] == 0 && taxon_abundance[r][f + 1][b][n + 2][i] == 0
                                && taxon_abundance[r][f + 1][b + 1][n][i] == 0 &&
taxon_abundance[r][f + 1][b + 1][n + 1][i] == 0 && taxon_abundance[r][f + 1][b + 1][n +
2][i] == 0)
                                missing_taxa3++;
                        }
                    }
                }
            }

        total_regional_richness[r] = MAXRICHNESS - missing_taxa3;


////****INITIAL ALPHA AND BETA CALCULATIONS****////

        for (f = 0; f < FACIES; ++f)
            {
            for (b = 0; b < BEDS; ++b)
                {
                alpha_one_term[r][f][b] = 0;
                for (n = 0; n < SAMPLES; ++n)
```

```
                    {
                    alpha_one_term[r][f][b] = alpha_one_term[r][f][b] +
(total_sample_richness[r][f][b][n] *
(total_sample_individuals[r][f][b][n]/total_regional_individuals[r]));
                    }
                }
            }


        for (f = 0; f < FACIES; ++f)
            {
            alpha_one_sum[r][f] = 0;
            alpha_two_sum[r][f] = 0;
            for (b = 0; b < BEDS; ++b)
                {
                alpha_one_sum[r][f] = alpha_one_sum[r][f] + alpha_one_term[r][f][b];
                alpha_two_sum[r][f] = alpha_two_sum[r][f] + (total_bed_richness[r][f][b] *
(total_bed_individuals[r][f][b]/total_regional_individuals[r]));
                }
            }


        total_alpha_one[r] = 0;
        total_alpha_two[r] = 0;
        total_alpha_three[r] = 0;
        for (f = 0; f < FACIES; ++f)
            {
            total_alpha_one[r] = total_alpha_one[r] + alpha_one_sum[r][f];
            total_alpha_two[r] = total_alpha_two[r] + alpha_two_sum[r][f];
            total_alpha_three[r] = total_alpha_three[r] + (total_facies_richness[r][f] *
(total_facies_individuals[r][f]/total_regional_individuals[r]));
            }


        total_beta_one[r] = total_alpha_two[r] - total_alpha_one[r];
        total_beta_two[r] = total_alpha_three[r] - total_alpha_two[r];
        total_beta_three[r] = total_regional_richness[r] - total_alpha_three[r];
}

////****EXTINCTION****////

for (r = 0; r < RUNS; ++r)
        {
        for (f = 0; f < FACIES; ++f)
            {
            for (b = 0; b < BEDS; ++b)
```

```
                {
                for (n = 0; n < SAMPLES; ++n)
                      {
                      while (extinct_taxa[r] < MAXRICHNESS * PERCENTEXTINCTION)
                            {
                            rarest_taxon[r] = nonzero_minimum (total_taxon_individuals[r],
MAXRICHNESS);
                            for (i = 0; i < MAXRICHNESS; ++i)
                                  {
                                  if (rarest_taxon[r] == total_taxon_individuals[r][i])
                                        {
                                        total_taxon_individuals[r][i] = 0;
                                        post_probability[r][0][i] = 0;
                                        post_probability[r][1][i] = 0;
                                        extinct_taxa[r]++;
                                        }
                                  }
                            }
                      }
                }
          }
     }



////****POST-EXTINCTION RESAMPLING****////
for (r = 0; r < RUNS; ++r)
      {
      post_total_regional_individuals[r] = 0;
      post_total_regional_richness[r] = 0;
      for (f = 0; f < 1; ++f)
            {
            post_total_facies_individuals[r][f] = 0;
            post_total_facies_richness[r][f] = 0;
            for (b = 0; b < BEDS; ++b)
                  {
                  post_total_bed_individuals[r][f][b] = 0;
                  post_total_bed_richness[r][f][b] = 0;
                  for (n = 0; n < SAMPLES; ++n)
                        {
                        post_total_sample_richness[r][f][b][n] = 0;
                        post_total_sample_individuals[r][f][b][n] = 0;
                        for (i = 0; i < MAXRICHNESS; ++i)
                              {
                              post_taxon_abundance[r][f][b][n][i] = 0;
```

```
                        post_count_sample_richness[r][f][b][n][i] = 0;
                        }

                    for (i = 0; i < MAXRICHNESS * 2/3; ++i)
                        {
                        post_is_taxa_present = RandNum();
                        if (post_is_taxa_present > post_probability[r][f][i] &&
post_probability[r][f][i] > 0)
                            {
                            post_taxon_abundance[r][f][b][n][i] = LogNormRandNum();
                            post_count_sample_richness[r][f][b][n][i] = 1;
                            }
                        else
                            {
                            post_taxon_abundance[r][f][b][n][i] = 0;
                            post_count_sample_richness[r][f][b][n][i] = 0;
                            }
                        }
                    }
                }
            }

        for (f = 1; f < FACIES; ++f)
            {
            post_total_facies_individuals[r][f] = 0;
            post_total_facies_richness[r][f] = 0;
            for (b = 0; b < BEDS; ++b)
                {
                post_total_bed_individuals[r][f][b] = 0;
                post_total_bed_richness[r][f][b] = 0;
                for (n = 0; n < SAMPLES; ++n)
                    {
                    post_total_sample_richness[r][f][b][n] = 0;
                    post_total_sample_individuals[r][f][b][n] = 0;
                    for (i = 0; i < MAXRICHNESS; ++i)
                        {
                        post_taxon_abundance[r][f][b][n][i] = 0;
                        post_count_sample_richness[r][f][b][n][i] = 0;
                        }

                    for (i = MAXRICHNESS * 1/3; i < MAXRICHNESS; ++i)
                        {
                        post_is_taxa_present = RandNum();
                        if (post_is_taxa_present > post_probability[r][f][i] &&
post_probability[r][f][i] > 0)
                            {
```

```
                                post_taxon_abundance[r][f][b][n][i] = LogNormRandNum();
                                post_count_sample_richness[r][f][b][n][i] = 1;
                                }
                            else
                                {
                                post_taxon_abundance[r][f][b][n][i] = 0;
                                post_count_sample_richness[r][f][b][n][i] = 0;
                                }
                            }
                        }
                    }

        for (f = 0; f < FACIES; ++f)
            {
            for (b = 0; b < BEDS; ++b)
                {
                for (n = 0; n < SAMPLES; ++n)
                    {
                    for (i = 0; i < MAXRICHNESS; ++i)
                        {
                        post_total_sample_richness[r][f][b][n] =
post_total_sample_richness[r][f][b][n] + post_count_sample_richness[r][f][b][n][i];
                        post_total_sample_individuals[r][f][b][n] =
post_total_sample_individuals[r][f][b][n] + post_taxon_abundance[r][f][b][n][i];
                        }

                    post_total_bed_individuals[r][f][b] = post_total_bed_individuals[r][f][b]
+ post_total_sample_individuals[r][f][b][n];
                    }

                for (n = 0; n < SAMPLES - (SAMPLES - 1); ++n)
                    {
                    post_missing_taxa = 0;
                    for (i = 0; i < MAXRICHNESS; ++i)
                        {
                        if (post_taxon_abundance[r][f][b][n][i] == 0 &&
post_taxon_abundance[r][f][b][n + 1][i] == 0 && post_taxon_abundance[r][f][b][n + 2][i]
== 0)
                            post_missing_taxa++;
                        }
                    }

                post_total_bed_richness[r][f][b] = MAXRICHNESS - post_missing_taxa;
                post_total_facies_individuals[r][f] = post_total_facies_individuals[r][f] +
post_total_bed_individuals[r][f][b];
```

```
                }

            for (b = 0; b < BEDS - (BEDS - 1); ++b)
                {
                for (n = 0; n < SAMPLES - (SAMPLES - 1); ++n)
                    {
                    post_missing_taxa2 = 0;
                    for (i = 0; i < MAXRICHNESS; ++i)
                        {
                        if (post_taxon_abundance[r][f][b][n][i] == 0 &&
post_taxon_abundance[r][f][b][n + 1][i] == 0 && post_taxon_abundance[r][f][b][n + 2][i]
== 0
                            && post_taxon_abundance[r][f][b + 1][n][i] == 0 &&
post_taxon_abundance[r][f][b + 1][n + 1][i] == 0 && post_taxon_abundance[r][f][b + 1][n
+ 2][i] == 0)
                            post_missing_taxa2++;
                        }
                    }
                }

            post_total_facies_richness[r][f] = MAXRICHNESS - post_missing_taxa2;
            post_total_regional_individuals[r] = post_total_regional_individuals[r] +
post_total_facies_individuals[r][f];
        }

        for (f = 0; f < FACIES - (FACIES - 1); ++f)
            {
            for (b = 0; b < BEDS - (BEDS - 1); ++b)
                {
                for (n = 0; n < SAMPLES - (SAMPLES - 1); ++n)
                    {
                    post_missing_taxa3 = 0;
                    for (i = 0; i < MAXRICHNESS; ++i)
                        {
                        if (post_taxon_abundance[r][f][b][n][i] == 0 &&
post_taxon_abundance[r][f][b][n + 1][i] == 0 && post_taxon_abundance[r][f][b][n + 2][i]
== 0
                            && post_taxon_abundance[r][f][b + 1][n][i] == 0 &&
post_taxon_abundance[r][f][b + 1][n + 1][i] == 0 && post_taxon_abundance[r][f][b + 1][n
+ 2][i] == 0
                            && post_taxon_abundance[r][f + 1][b][n][i] == 0 &&
post_taxon_abundance[r][f + 1][b][n + 1][i] == 0 && post_taxon_abundance[r][f + 1][b][n
+ 2][i] == 0
                            && post_taxon_abundance[r][f + 1][b + 1][n][i] == 0 &&
post_taxon_abundance[r][f + 1][b + 1][n + 1][i] == 0 && post_taxon_abundance[r][f +
1][b + 1][n + 2][i] == 0)
```

```
                        post_missing_taxa3++;
                    }
                }
            }
        }

    post_total_regional_richness[r] = MAXRICHNESS - post_missing_taxa3;


////****POST-EXTINCTION ALPHA AND BETA CALCULATIONS****////

    for (f = 0; f < FACIES; ++f)
        {
        for (b = 0; b < BEDS; ++b)
            {
            post_alpha_one_term[r][f][b] = 0;
            for (n = 0; n < SAMPLES; ++n)
                {
                post_alpha_one_term[r][f][b] = post_alpha_one_term[r][f][b] +
(post_total_sample_richness[r][f][b][n] *
(post_total_sample_individuals[r][f][b][n]/post_total_regional_individuals[r]));
                }
            }
        }


    for (f = 0; f < FACIES; ++f)
        {
        post_alpha_one_sum[r][f] = 0;
        post_alpha_two_sum[r][f] = 0;
        for (b = 0; b < BEDS; ++b)
            {
            post_alpha_one_sum[r][f] = post_alpha_one_sum[r][f] +
post_alpha_one_term[r][f][b];
            post_alpha_two_sum[r][f] = post_alpha_two_sum[r][f] +
(post_total_bed_richness[r][f][b] *
(post_total_bed_individuals[r][f][b]/post_total_regional_individuals[r]));
            }
        }


    post_total_alpha_one[r] = 0;
    post_total_alpha_two[r] = 0;
    post_total_alpha_three[r] = 0;
    for (f = 0; f < FACIES; ++f)
        {
```

```
            post_total_alpha_one[r] = post_total_alpha_one[r] + post_alpha_one_sum[r][f];
            post_total_alpha_two[r] = post_total_alpha_two[r] + post_alpha_two_sum[r][f];
            post_total_alpha_three[r] = post_total_alpha_three[r] +
(post_total_facies_richness[r][f] *
(post_total_facies_individuals[r][f]/post_total_regional_individuals[r]));
            }


      post_total_beta_one[r] = post_total_alpha_two[r] - post_total_alpha_one[r];
      post_total_beta_two[r] = post_total_alpha_three[r] - post_total_alpha_two[r];
      post_total_beta_three[r] = post_total_regional_richness[r] -
post_total_alpha_three[r];
}

mean_initial_alpha_one = mean (total_alpha_one, RUNS);
mean_initial_alpha_two = mean (total_alpha_two, RUNS);
mean_initial_alpha_three = mean (total_alpha_three, RUNS);
mean_initial_alpha_four = mean (total_regional_richness, RUNS);
mean_initial_beta_one = mean (total_beta_one, RUNS);
mean_initial_beta_two = mean (total_beta_two, RUNS);
mean_initial_beta_three = mean (total_beta_three, RUNS);
mean_post_alpha_one = mean (post_total_alpha_one, RUNS);
mean_post_alpha_two = mean (post_total_alpha_two, RUNS);
mean_post_alpha_three = mean (post_total_alpha_three, RUNS);
mean_post_alpha_four = mean (post_total_regional_richness, RUNS);
mean_post_beta_one = mean (post_total_beta_one, RUNS);
mean_post_beta_two = mean (post_total_beta_two, RUNS);
mean_post_beta_three = mean (post_total_beta_three, RUNS);

////****PRINT STATEMENTS****////

printf("%.3f\t%.3f\t%.3f\t%.3f\t%.3f\t%.3f\t%.3f\t%.3f\t%.3f\t%.3f\t%.3f\t%.3f\t%.3f\t%.3f\n
", mean_initial_alpha_one, mean_initial_alpha_two, mean_initial_alpha_three,
mean_initial_alpha_four, mean_initial_beta_one, mean_initial_beta_two,
mean_initial_beta_three, mean_post_alpha_one, mean_post_alpha_two,
mean_post_alpha_three,
mean_post_alpha_four, mean_post_beta_one, mean_post_beta_two,
mean_post_beta_three);

return 0;
}
```

4. This version of the model uses random probabilities of taxon occurrence drawn from a uniform distribution between zero and one and includes an extinction that targets abundant taxa.

```
#include <stdio.h>
#include <stdlib.h>
#include <math.h>
#include "randomNumbers.h"
#include "statistics.h"

#define MAXRICHNESS 24
#define SAMPLES 3
#define BEDS 2
#define FACIES 2
#define RUNS 2
#define PERCENTEXTINCTION 0.9

int main()
{

int i;
int n;
int b;
int f;
int r;

double taxon_abundance[RUNS][FACIES][BEDS][SAMPLES][MAXRICHNESS];
double probability[RUNS][FACIES][MAXRICHNESS];
double is_taxa_present;
double count_sample_richness[RUNS][FACIES][BEDS][SAMPLES][MAXRICHNESS];
double total_sample_richness[RUNS][FACIES][BEDS][SAMPLES];
double total_sample_individuals[RUNS][FACIES][BEDS][SAMPLES];
double total_bed_individuals[RUNS][FACIES][BEDS];
double total_bed_richness[RUNS][FACIES][BEDS];
double missing_taxa;
double missing_taxa2;
double total_facies_individuals[RUNS][FACIES];
double total_facies_richness[RUNS][FACIES];
double total_regional_individuals[RUNS];
double missing_taxa3;
double total_regional_richness[RUNS];
double total_taxon_individuals[RUNS][MAXRICHNESS];

double alpha_one_term[RUNS][FACIES][BEDS];
double alpha_one_sum[RUNS][FACIES];
double total_alpha_one[RUNS];
```

```
double alpha_two_sum[RUNS][FACIES];
double total_alpha_two[RUNS];
double total_alpha_three[RUNS];
double total_beta_one[RUNS];
double total_beta_two[RUNS];
double total_beta_three[RUNS];

double post_probability[RUNS][FACIES][MAXRICHNESS];
double extinct_taxa;
double most_abundant_taxon[RUNS];

double post_taxon_abundance[RUNS][FACIES][BEDS][SAMPLES][MAXRICHNESS];
double post_is_taxa_present;
double
post_count_sample_richness[RUNS][FACIES][BEDS][SAMPLES][MAXRICHNESS];
double post_total_sample_richness[RUNS][FACIES][BEDS][SAMPLES];
double post_total_sample_individuals[RUNS][FACIES][BEDS][SAMPLES];
double post_total_bed_individuals[RUNS][FACIES][BEDS];
double post_total_bed_richness[RUNS][FACIES][BEDS];
double post_missing_taxa;
double post_missing_taxa2;
double post_total_facies_individuals[RUNS][FACIES];
double post_total_facies_richness[RUNS][FACIES];
double post_total_regional_individuals[RUNS];
double post_missing_taxa3;
double post_total_regional_richness[RUNS];

double post_alpha_one_term[RUNS][FACIES][BEDS];
double post_alpha_one_sum[RUNS][FACIES];
double post_total_alpha_one[RUNS];
double post_alpha_two_sum[RUNS][FACIES];
double post_total_alpha_two[RUNS];
double post_total_alpha_three[RUNS];
double post_total_beta_one[RUNS];
double post_total_beta_two[RUNS];
double post_total_beta_three[RUNS];

double mean_initial_alpha_one;
double mean_initial_alpha_two;
double mean_initial_alpha_three;
double mean_initial_alpha_four;
double mean_initial_beta_one;
double mean_initial_beta_two;
double mean_initial_beta_three;
double mean_post_alpha_one;
double mean_post_alpha_two;
```

```
double mean_post_alpha_three;
double mean_post_alpha_four;
double mean_post_beta_one;
double mean_post_beta_two;
double mean_post_beta_three;

InitRandNum();

printf("xA1i\t xA2i\t xA3i\t xA4i\t xB1i\t xB2i\t xB3i\t xA1p\t xA2p\t xA3p\t xA4p\t xB1p\t
xB2p\t xB3p\n");

for (r = 0; r < RUNS; ++r)
      {
      total_regional_individuals[r] = 0;
      total_regional_richness[r] = 0;
      for (f = 0; f < 1; ++f)
            {
            total_facies_individuals[r][f] = 0;
            total_facies_richness[r][f] = 0;
            for (b = 0; b < BEDS; ++b)
                  {
                  total_bed_individuals[r][f][b] = 0;
                  total_bed_richness[r][f][b] = 0;
                  for (n = 0; n < SAMPLES; ++n)
                        {
                        total_sample_richness[r][f][b][n] = 0;
                        total_sample_individuals[r][f][b][n] = 0;
                        for (i = 0; i < MAXRICHNESS; ++i)
                              {
                              taxon_abundance[r][f][b][n][i] = 0;
                              count_sample_richness[r][f][b][n][i] = 0;
                              probability[r][f][i] = RandNum();
                              post_probability[r][f][i] = probability[r][f][i];
                              }

                        for (i = 0; i < MAXRICHNESS * 2/3; ++i)
                              {
                              is_taxa_present = RandNum();
                              if (is_taxa_present > probability[r][f][i])
                                    {
                                    taxon_abundance[r][f][b][n][i] = LogNormRandNum();
                                    count_sample_richness[r][f][b][n][i] = 1;
                                    }
                              else
                                    {
                                    taxon_abundance[r][f][b][n][i] = 0;
```

```
                        count_sample_richness[r][f][b][n][i] = 0;
                        }
                    }
                }
            }

for (f = 1; f < FACIES; ++f)
        {
        total_facies_individuals[r][f] = 0;
        total_facies_richness[r][f] = 0;
        for (b = 0; b < BEDS; ++b)
            {
            total_bed_individuals[r][f][b] = 0;
            total_bed_richness[r][f][b] = 0;
            for (n = 0; n < SAMPLES; ++n)
                {
                total_sample_richness[r][f][b][n] = 0;
                total_sample_individuals[r][f][b][n] = 0;

                for (i = 0; i < MAXRICHNESS; ++i)
                    {
                    taxon_abundance[r][f][b][n][i] = 0;
                    count_sample_richness[r][f][b][n][i] = 0;
                    probability[r][f][i] = RandNum();
                    post_probability[r][f][i] = probability[r][f][i];
                    }

                for (i = MAXRICHNESS * 1/3; i < MAXRICHNESS; ++i)
                    {
                    is_taxa_present = RandNum();
                    if (is_taxa_present >  probability[r][f][i])
                        {
                        taxon_abundance[r][f][b][n][i] = LogNormRandNum();
                        count_sample_richness[r][f][b][n][i] = 1;
                        }
                    else
                        {
                        taxon_abundance[r][f][b][n][i] = 0;
                        count_sample_richness[r][f][b][n][i] = 0;
                        }
                    }
                }
            }
        }
```

```
    for (f = 0; f < FACIES; ++f)
        {
        for (b = 0; b < BEDS; ++b)
            {
            for (n = 0; n < SAMPLES; ++n)
                {
                for (i = 0; i < MAXRICHNESS; ++i)
                    {
                    total_sample_richness[r][f][b][n] = total_sample_richness[r][f][b][n]
+ count_sample_richness[r][f][b][n][i];
                    total_sample_individuals[r][f][b][n] =
total_sample_individuals[r][f][b][n] + taxon_abundance[r][f][b][n][i];
                    total_taxon_individuals[r][i] = total_taxon_individuals[r][i] +
taxon_abundance[r][f][b][n][i];
                    }

                total_bed_individuals[r][f][b] = total_bed_individuals[r][f][b] +
total_sample_individuals[r][f][b][n];
                }

            for (n = 0; n < SAMPLES - (SAMPLES - 1); ++n)
                {
                missing_taxa = 0;
                for (i = 0; i < MAXRICHNESS; ++i)
                    {
                    if (taxon_abundance[r][f][b][n][i] == 0 &&
taxon_abundance[r][f][b][n + 1][i] == 0 && taxon_abundance[r][f][b][n + 2][i] == 0)
                        missing_taxa++;
                    }
                }

            total_bed_richness[r][f][b] = MAXRICHNESS - missing_taxa;
            total_facies_individuals[r][f] = total_facies_individuals[r][f] +
total_bed_individuals[r][f][b];
            }

        for (b = 0; b < BEDS - (BEDS - 1); ++b)
            {
            for (n = 0; n < SAMPLES - (SAMPLES - 1); ++n)
                {
                missing_taxa2 = 0;
                for (i = 0; i < MAXRICHNESS; ++i)
                    {
                    if (taxon_abundance[r][f][b][n][i] == 0 &&
taxon_abundance[r][f][b][n + 1][i] == 0 && taxon_abundance[r][f][b][n + 2][i] == 0
                        && taxon_abundance[r][f][b + 1][n][i] == 0 &&
```

```
taxon_abundance[r][f][b + 1][n + 1][i] == 0 && taxon_abundance[r][f][b + 1][n + 2][i] == 0)
                                missing_taxa2++;
                            }
                        }
                    }

            total_facies_richness[r][f] = MAXRICHNESS - missing_taxa2;
            total_regional_individuals[r] = total_regional_individuals[r] +
total_facies_individuals[r][f];
        }

        for (f = 0; f < FACIES - (FACIES - 1); ++f)
            {
            for (b = 0; b < BEDS - (BEDS - 1); ++b)
                {
                for (n = 0; n < SAMPLES - (SAMPLES - 1); ++n)
                    {
                    missing_taxa3 = 0;
                    for (i = 0; i < MAXRICHNESS; ++i)
                        {
                        if (taxon_abundance[r][f][b][n][i] == 0 &&
taxon_abundance[r][f][b][n + 1][i] == 0 && taxon_abundance[r][f][b][n + 2][i] == 0
                                && taxon_abundance[r][f][b + 1][n][i] == 0 &&
taxon_abundance[r][f][b + 1][n + 1][i] == 0 && taxon_abundance[r][f][b + 1][n + 2][i] == 0
                                && taxon_abundance[r][f + 1][b][n][i] == 0 &&
taxon_abundance[r][f + 1][b][n + 1][i] == 0 && taxon_abundance[r][f + 1][b][n + 2][i] == 0
                                && taxon_abundance[r][f + 1][b + 1][n][i] == 0 &&
taxon_abundance[r][f + 1][b + 1][n + 1][i] == 0 && taxon_abundance[r][f + 1][b + 1][n +
2][i] == 0)
                                missing_taxa3++;
                        }
                    }
                }
            }

        total_regional_richness[r] = MAXRICHNESS - missing_taxa3;


////****INITIAL ALPHA AND BETA CALCULATIONS****////

        for (f = 0; f < FACIES; ++f)
            {
            for (b = 0; b < BEDS; ++b)
                {
                alpha_one_term[r][f][b] = 0;
                for (n = 0; n < SAMPLES; ++n)
```

```
                        {
                        alpha_one_term[r][f][b] = alpha_one_term[r][f][b] +
(total_sample_richness[r][f][b][n] *
(total_sample_individuals[r][f][b][n]/total_regional_individuals[r]));
                        }
                  }
            }


      for (f = 0; f < FACIES; ++f)
            {
            alpha_one_sum[r][f] = 0;
            alpha_two_sum[r][f] = 0;
            for (b = 0; b < BEDS; ++b)
                  {
                  alpha_one_sum[r][f] = alpha_one_sum[r][f] + alpha_one_term[r][f][b];
                  alpha_two_sum[r][f] = alpha_two_sum[r][f] + (total_bed_richness[r][f][b] *
(total_bed_individuals[r][f][b]/total_regional_individuals[r]));
                  }
            }


      total_alpha_one[r] = 0;
      total_alpha_two[r] = 0;
      total_alpha_three[r] = 0;
      for (f = 0; f < FACIES; ++f)
            {
            total_alpha_one[r] = total_alpha_one[r] + alpha_one_sum[r][f];
            total_alpha_two[r] = total_alpha_two[r] + alpha_two_sum[r][f];
            total_alpha_three[r] = total_alpha_three[r] + (total_facies_richness[r][f] *
(total_facies_individuals[r][f]/total_regional_individuals[r]));
            }


      total_beta_one[r] = total_alpha_two[r] - total_alpha_one[r];
      total_beta_two[r] = total_alpha_three[r] - total_alpha_two[r];
      total_beta_three[r] = total_regional_richness[r] - total_alpha_three[r];
}

////****EXTINCTION****////

//extinct_taxa = 0;
for (r = 0; r < RUNS; ++r)
      {
      extinct_taxa = 0;
      while (extinct_taxa < MAXRICHNESS * PERCENTEXTINCTION)
```

```
            {
            most_abundant_taxon[r] = maximum (total_taxon_individuals[r],
MAXRICHNESS);
            for (i = 0; i < MAXRICHNESS; ++i)
                  {
                  if (most_abundant_taxon[r] == total_taxon_individuals[r][i])
                        {
                        total_taxon_individuals[r][i] = 0;
                        post_probability[r][0][i] = 0;
                        post_probability[r][1][i] = 0;
                        extinct_taxa++;
                        }
                  }
            }
      }




////****POST-EXTINCTION RESAMPLING****////
for (r = 0; r < RUNS; ++r)
      {
      post_total_regional_individuals[r] = 0;
      post_total_regional_richness[r] = 0;
      for (f = 0; f < 1; ++f)
            {
            post_total_facies_individuals[r][f] = 0;
            post_total_facies_richness[r][f] = 0;
            for (b = 0; b < BEDS; ++b)
                  {
                  post_total_bed_individuals[r][f][b] = 0;
                  post_total_bed_richness[r][f][b] = 0;
                  for (n = 0; n < SAMPLES; ++n)
                        {
                        post_total_sample_richness[r][f][b][n] = 0;
                        post_total_sample_individuals[r][f][b][n] = 0;
                        for (i = 0; i < MAXRICHNESS; ++i)
                              {
                              post_taxon_abundance[r][f][b][n][i] = 0;
                              post_count_sample_richness[r][f][b][n][i] = 0;
                              }

                        for (i = 0; i < MAXRICHNESS * 2/3; ++i)
                              {
                              post_is_taxa_present = RandNum();
```

```
                        if (post_is_taxa_present > post_probability[r][f][i] &&
post_probability[r][f][i] > 0)
                            {
                            post_taxon_abundance[r][f][b][n][i] = LogNormRandNum();
                            post_count_sample_richness[r][f][b][n][i] = 1;
                            }
                        else
                            {
                            post_taxon_abundance[r][f][b][n][i] = 0;
                            post_count_sample_richness[r][f][b][n][i] = 0;
                            }
                        }
                    }
                }
            }

    for (f = 1; f < FACIES; ++f)
            {
            post_total_facies_individuals[r][f] = 0;
            post_total_facies_richness[r][f] = 0;
            for (b = 0; b < BEDS; ++b)
                {
                post_total_bed_individuals[r][f][b] = 0;
                post_total_bed_richness[r][f][b] = 0;
                for (n = 0; n < SAMPLES; ++n)
                    {
                    post_total_sample_richness[r][f][b][n] = 0;
                    post_total_sample_individuals[r][f][b][n] = 0;
                    for (i = 0; i < MAXRICHNESS; ++i)
                        {
                        post_taxon_abundance[r][f][b][n][i] = 0;
                        post_count_sample_richness[r][f][b][n][i] = 0;
                        }

                    for (i = MAXRICHNESS * 1/3; i < MAXRICHNESS; ++i)
                        {
                        post_is_taxa_present = RandNum();
                        if (post_is_taxa_present > post_probability[r][f][i] &&
post_probability[r][f][i] > 0)
                            {
                            post_taxon_abundance[r][f][b][n][i] = LogNormRandNum();
                            post_count_sample_richness[r][f][b][n][i] = 1;
                            }
                        else
                            {
                            post_taxon_abundance[r][f][b][n][i] = 0;
```

```
                                post_count_sample_richness[r][f][b][n][i] = 0;
                                }
                        }
                    }
                }

        for (f = 0; f < FACIES; ++f)
            {
            for (b = 0; b < BEDS; ++b)
                {
                for (n = 0; n < SAMPLES; ++n)
                    {
                    for (i = 0; i < MAXRICHNESS; ++i)
                        {
                        post_total_sample_richness[r][f][b][n] =
post_total_sample_richness[r][f][b][n] + post_count_sample_richness[r][f][b][n][i];
                        post_total_sample_individuals[r][f][b][n] =
post_total_sample_individuals[r][f][b][n] + post_taxon_abundance[r][f][b][n][i];
                        }

                    post_total_bed_individuals[r][f][b] = post_total_bed_individuals[r][f][b]
+ post_total_sample_individuals[r][f][b][n];
                    }

                for (n = 0; n < SAMPLES - (SAMPLES - 1); ++n)
                    {
                    post_missing_taxa = 0;
                    for (i = 0; i < MAXRICHNESS; ++i)
                        {
                        if (post_taxon_abundance[r][f][b][n][i] == 0 &&
post_taxon_abundance[r][f][b][n + 1][i] == 0 && post_taxon_abundance[r][f][b][n + 2][i]
== 0)
                            post_missing_taxa++;
                        }
                    }

                post_total_bed_richness[r][f][b] = MAXRICHNESS - post_missing_taxa;
                post_total_facies_individuals[r][f] = post_total_facies_individuals[r][f] +
post_total_bed_individuals[r][f][b];
                }

            for (b = 0; b < BEDS - (BEDS - 1); ++b)
                {
                for (n = 0; n < SAMPLES - (SAMPLES - 1); ++n)
                    {
```

```
                        post_missing_taxa2 = 0;
                        for (i = 0; i < MAXRICHNESS; ++i)
                              {
                              if (post_taxon_abundance[r][f][b][n][i] == 0 &&
post_taxon_abundance[r][f][b][n + 1][i] == 0 && post_taxon_abundance[r][f][b][n + 2][i]
== 0
                                    && post_taxon_abundance[r][f][b + 1][n][i] == 0 &&
post_taxon_abundance[r][f][b + 1][n + 1][i] == 0 && post_taxon_abundance[r][f][b + 1][n
+ 2][i] == 0)
                                    post_missing_taxa2++;
                              }
                        }
                  }

            post_total_facies_richness[r][f] = MAXRICHNESS - post_missing_taxa2;
            post_total_regional_individuals[r] = post_total_regional_individuals[r] +
post_total_facies_individuals[r][f];
      }

      for (f = 0; f < FACIES - (FACIES - 1); ++f)
            {
            for (b = 0; b < BEDS - (BEDS - 1); ++b)
                  {
                  for (n = 0; n < SAMPLES - (SAMPLES - 1); ++n)
                        {
                        post_missing_taxa3 = 0;
                        for (i = 0; i < MAXRICHNESS; ++i)
                              {
                              if (post_taxon_abundance[r][f][b][n][i] == 0 &&
post_taxon_abundance[r][f][b][n + 1][i] == 0 && post_taxon_abundance[r][f][b][n + 2][i]
== 0
                                    && post_taxon_abundance[r][f][b + 1][n][i] == 0 &&
post_taxon_abundance[r][f][b + 1][n + 1][i] == 0 && post_taxon_abundance[r][f][b + 1][n
+ 2][i] == 0
                                    && post_taxon_abundance[r][f + 1][b][n][i] == 0 &&
post_taxon_abundance[r][f + 1][b][n + 1][i] == 0 && post_taxon_abundance[r][f + 1][b][n
+ 2][i] == 0
                                    && post_taxon_abundance[r][f + 1][b + 1][n][i] == 0 &&
post_taxon_abundance[r][f + 1][b + 1][n + 1][i] == 0 && post_taxon_abundance[r][f +
1][b + 1][n + 2][i] == 0)
                                    post_missing_taxa3++;
                              }
                        }
                  }
            }
```

```
	post_total_regional_richness[r] = MAXRICHNESS - post_missing_taxa3;


////****POST-EXTINCTION ALPHA AND BETA CALCULATIONS****////

	for (f = 0; f < FACIES; ++f)
		{
		for (b = 0; b < BEDS; ++b)
			{
			post_alpha_one_term[r][f][b] = 0;
			for (n = 0; n < SAMPLES; ++n)
				{
				post_alpha_one_term[r][f][b] = post_alpha_one_term[r][f][b] +
(post_total_sample_richness[r][f][b][n] *
(post_total_sample_individuals[r][f][b][n]/post_total_regional_individuals[r]));
				}
			}
		}


	for (f = 0; f < FACIES; ++f)
		{
		post_alpha_one_sum[r][f] = 0;
		post_alpha_two_sum[r][f] = 0;
		for (b = 0; b < BEDS; ++b)
			{
			post_alpha_one_sum[r][f] = post_alpha_one_sum[r][f] +
post_alpha_one_term[r][f][b];
			post_alpha_two_sum[r][f] = post_alpha_two_sum[r][f] +
(post_total_bed_richness[r][f][b] *
(post_total_bed_individuals[r][f][b]/post_total_regional_individuals[r]));
			}
		}


	post_total_alpha_one[r] = 0;
	post_total_alpha_two[r] = 0;
	post_total_alpha_three[r] = 0;
	for (f = 0; f < FACIES; ++f)
		{
		post_total_alpha_one[r] = post_total_alpha_one[r] + post_alpha_one_sum[r][f];
		post_total_alpha_two[r] = post_total_alpha_two[r] + post_alpha_two_sum[r][f];
		post_total_alpha_three[r] = post_total_alpha_three[r] +
(post_total_facies_richness[r][f] *
(post_total_facies_individuals[r][f]/post_total_regional_individuals[r]));
		}
```

```
	post_total_beta_one[r] = post_total_alpha_two[r] - post_total_alpha_one[r];
	post_total_beta_two[r] = post_total_alpha_three[r] - post_total_alpha_two[r];
	post_total_beta_three[r] = post_total_regional_richness[r] -
post_total_alpha_three[r];
}

mean_initial_alpha_one = mean (total_alpha_one, RUNS);
mean_initial_alpha_two = mean (total_alpha_two, RUNS);
mean_initial_alpha_three = mean (total_alpha_three, RUNS);
mean_initial_alpha_four = mean (total_regional_richness, RUNS);
mean_initial_beta_one = mean (total_beta_one, RUNS);
mean_initial_beta_two = mean (total_beta_two, RUNS);
mean_initial_beta_three = mean (total_beta_three, RUNS);
mean_post_alpha_one = mean (post_total_alpha_one, RUNS);
mean_post_alpha_two = mean (post_total_alpha_two, RUNS);
mean_post_alpha_three = mean (post_total_alpha_three, RUNS);
mean_post_alpha_four = mean (post_total_regional_richness, RUNS);
mean_post_beta_one = mean (post_total_beta_one, RUNS);
mean_post_beta_two = mean (post_total_beta_two, RUNS);
mean_post_beta_three = mean (post_total_beta_three, RUNS);

////****PRINT STATEMENTS****////

printf("%.3f\t%.3f\t%.3f\t%.3f\t%.3f\t%.3f\t%.3f\t%.3f\t%.3f\t%.3f\t%.3f\t%.3f\t%.3f\t%.3f\n
", mean_initial_alpha_one, mean_initial_alpha_two, mean_initial_alpha_three,
mean_initial_alpha_four, mean_initial_beta_one, mean_initial_beta_two,
mean_initial_beta_three, mean_post_alpha_one, mean_post_alpha_two,
mean_post_alpha_three,
mean_post_alpha_four, mean_post_beta_one, mean_post_beta_two,
mean_post_beta_three);

return 0;
}
```

APPENDIX C

Locality register

Tennessee localities

Alexandria (AL): 36.0842°, -86.0303°. Roadcuts along both sides of TN 53 at Smith/DeKalb county line, just north of Alexandria, TN.

Almaville Rd. (AR): 35.8575°, -86.5914°. Roadcut on south side of TN 840, just west of exit to TN 102 (Almaville Road).

AquaJet Autowash (AW): 36.1897°, -85.9514°. Exposure behind carwash facility on east side of TN 53, just north of intersection of TN 53 with I-40.

Big Bottom (BB): 36.4528, -85.5772°. Roadcut on east side of TN 53, 1.2 miles south of Clay/Jackson County Line and opposite Big Bottom.

Blast Pit (BP): 36.1886°, -85.9508°. Exposures in construction blasting pit, property adjacent to south of AquaJet Autowash on TN 53, just north of intersection of TN 53 with I-40.

Carthage (CAR): 36.2611°, -85.9419°. Roadcuts on both sides of TN 25, along new bypass around town of Carthage.

Columbia North (CN): 35.6167°, -87.0833°. Roadcut on both sides of US 412/US 43, 1.2 miles northeast of overpass over TN 50.

Columbia West (CW): 35.6167°, -87.1000°. Roadcut on both sides of US 412/US 43, 0.3 miles west of overpass over TN 50.

Defeated (DEF): 36.3211°, -85.9419°. Roadcut on north side of TN 85, west of intersection of TN 85 and TN 263.

Fall Creek (FC): 36.0086°, -86.4247°. Roadcut along east side TN 840, approximately 3 miles south of Wilson/Rutherford County line.

Franklin (FR): 35.9333°, -86.8500°. Roadcut on both sides of US 31, 1.2 miles north of intersection with TN 96.

Frankewing (FW): 35.1931°, -86.8700°. Roadcuts along northbound onramp from US 64/TN15 to I-65 at exit 14.

Gladeville (GL): 36.1389°, -86.3836°. Roadcuts on both sides of TN 840, 1 mile north of TN 265/Central Pike overpass, and roadcuts on both sides of southbound exit ramp from TN 840 to TN 265/Central Pike.

Gladdice (GLC): 36.3531°, -85.7906°. Roadcuts on both sides of TN 85, 1.3 miles northeast of bridge over Salt Lick Creek in Gladdice.

Hollis Creek (HC): 35.8142°, -86.1186°. Roadcuts on both sides of US 70S on east side of Hollis Creek valley, 2.3 miles east of intersection with TN 64.

Hollis Creek West (HCW): 35.8083°, -86.1306°. Roadcut on south side of US 70S on west side of Hollis Creek, approximately 2.1 miles east of intersection with TN 64.

Harwell Hollow (HH): 35.1892°, -86.9119°. Exposures along north side of US 64/TN15, just west of intersection of Harwell Hollow Road, approximately 0.75 mile from intersection of US 64/TN 15 with I-65.

Industrial Park Rd. (IPR): 35.6300°, -87.0656°. Roadcut along exit ramp to Industrial Park Rd. from westbound US 412/US 43, northwest of Columbia, TN.

Kennedy Creek (KC): 35.8219°, -86.8303°. Roadcut along south side of TN 840, just east of intersection of TN 840 and I-65.

Lewisburg (LW): 35.4728°, -86.8017°. Roadcuts on both sides of TN 417, 0.1 mile southwest of intersection with US 431/TN 50.

Marathon Gas Station (MGS): 36.3656°, -85.6511°. Exposure behind gas station on east side of TN 53, approximately 1 mile north of Gainesboro, TN

Monoville (MV): 36.2886°, -85.9892°. Roadcut on south side of TN 80, just east of intersection of TN 80 with TN 25, north of Tanglewood, TN.

Peaks Hill (PH): 35.8000°, -86.2000°. Exposures northwest of Woodbury Rd., just north of intersection with US 70S, approximately 7 miles east of outskirts of Murfreesboro, TN.

Richland Creek (RC): 35.1672°, -87.0406°. Roadcut on north side of US 64 bypass, 0.7 miles east of intersection with TN 166 and 1.5 miles west of intersection with US 31 on south side of Pulaski, TN.

Roaring River (RR): 36.3733°, -85.6439°. Exposures along TN 135, just east of intersection with TN 53, approximately 2 miles northeast of Gainesboro, TN.

70S outcrop 1 (SA): 35.8083°, -86.1308°. Exposure on north side of US 70S, approximately 1 mile east of Rutherford/Cannon County Line.

70S outcrop 2 (SB): 35.8078°, -86.1761°. Exposure on north side of US 70S, approximately 1 mile east of Rutherford/Cannon County Line.

Tanglewood (TW): 36.2931°, -85.9972°. Roadcut on northeast side of TN 25 along Petty Bluff, 0.5 miles northwest of intersection with TN 80.

Williamson County Line (WCL): 35.7411°, -86.8694°. Exposure near intersection of TN 396 and I-65 at Williamson/Maury County Line.

Whippoorwill Rd. (WWR): 36.0433°, -86.3528°. Roadcuts on both sides of US 231/TN 10, 0.1 mile north of Whippoorwill Rd. in Vine, TN.

Kentucky localities

Athens-Boonesborough Rd. (AB): 37.9822°, -84.4236°. Small outcrop on west side of KY 418 (4200 block), just north of Aphids Way and Walnut Creek subdivision.

Bananas on the River (BA): 37.8981°, -84.2614°. Outcrop on KY 1924, about 0.5 mile south of intersection with KY 627, south of and adjacent to restaurant parking lot along the Kentucky River.

Boyle County Fire Department (BCFD): 37.6722°, -84.7092°. Exposures along both sides of KY 34, just west of western intersection of Old KY 34.

Clay's Ferry (CF): 37.8808°, -84.3408°. Roadcut on south side of KY 2328, 1.0 mile north of intersection with US 25/US 421 at Clay's Ferry.

Camp Nelson (CNL): 37.7836°, -84.6083°. Exposures immediately before and after 1 mile marker north of Kentucky River on west side of US 27.

Dry Fork Rd. (DF): 37.9356°, -84.1436°. Exposure on Dry Ford Rd. just south of intersection with KY 974, approximately 4.5 miles south of Winchester, KY.

Devil's Hollow Rd. (DH): 38.2069°, -84.9372°. Roadcut on north side of KY 1005 (Devil's Hollow Rd.), west of Frankfort, KY.

Danville (DN): 37.6833°, -84.7639°. Small exposure long both sides of KY 33, north of Danville, just immediately south of Spears Lane.

Downtown Winchester (DW): 38.0019°, -84.1744°. Exposure along east side of Maple St. in Winchester, just south of intersection with Magnolia St.

Fort Boonesborough (FB): 37.8956°, -84.2714°. Outcrop immediately south of Fort entrance on west side of ; also outcrop immediately north of State Park entrance on E side of .

Frankfort West (FFW): 38.1994°, -84.8936°. Roadcuts on both sides of US 127, west of Frankfort, KY.

Ford's Mill Rd. (FM): 37.9492°, -84.7419°. Small exposure along KY 1965 (Ford's Mill Rd.) near crossing of Clear Creek.

Frankfort North (FN): 38.2203°, -84.8536°. Roadcuts on both sides of US 127, beginning at intersection with Cove Spring Road, 0.2 miles north of intersection of US 127 and US 421 north of Frankfort, KY and continuing northward to intersection with KY 1900 (Peaks Mill Rd.).

Frankfort 421 (FT): 38.2078°, -84.8847°. Roadcuts on northeast side of US 421, 0.1 miles northwest of intersection with US 127 on northwest side of Frankfort, KY.

Owenton (OW): 38.3467°, -84.8583°. Roadcuts on both sides of US 127, beginning 1.3 miles north of intersection with KY 2919 near Swallowfield, KY, and extending about 1.0 mile to the north.

Southwind Golf Course (SGC): 37.9667°, -84.2050°. Exposure on east side of KY 627, near entrance to Southwind Golf Course.

Shaker Village (SV): 37.8164°, -84.7575°. Exposure on south side of US 68, about 1 mile west of Shaker Village.

Vineyard (VY): 37.8381°, -84.5853°. Exposures along west and east sides of US 27, near town of Vineyard.

Virginia localities

Arby's (AR): 39.0047°, -78.3408°. Construction excavation float piles, behind Arby's parking lot, just east of I-81 at exit 298 in northern VA.

Catawba (CA): 37.3803°, -80.8572°. Roadcuts along VA 311, on northwest slope of Catawba Mtn., 1.1 miles east of the intersection of VA 311, VA 698, and VA 779 at Catawba.

Narrows (DNR): 37.3531°, -80.8100°. Roadcuts on US 460 westbound, 1.0 mile west of Narrows.

Exit 298 (ET): 39.0083°, -78.3367°. Roadcuts at both northbound exit 298 and southbound entrance ramp of exit 298 to Strasburg from I-81.

Gordon's Run (GR): 37.7608°, -79.4231°. Exposure along US 60, 0.1 mile east of Stonewall Jackson House marker and 0.1 mile west of intersection of Wesley Chapel Rd. and US 360.

Hagan (HMB): 36.6981°, -83.2872°. Exposures along spur of Louisville and Nashville Railroad, parallel to Hagan-Smiley Rd., at town of Hagan.

Oranda (OR): 38.9975°, -78.3625°. Exposure near intersection of VA 55 and Colley Block Rd., outcrop on north side of VA 55.

Tumbling Run (TR): 38.9747°, -78.3986°. Roadcuts along both westbound and eastbound lanes of US 11, approximately 1.5 miles west of Strasburg.

Walker Mountain (WK): 36.89°, -81.55°. Roadcuts and exposures along VA 16, along northeast slope of Walker Mountain, Smyth County, VA.

APPENDIX D

Field data. Sample labels include year of data collection, collection locality, stratigraphic sequence, depositional environment, and replicate letter. For example, 04WWR3Db indicates the sample was collected in 2004 (04) at Whippoorwill Rd. (WWR) from sequence M3 (3) , from a deep subtidal environment (D), and represents the second sample from this environment and sequence at this locality (b). First row of database below taxa indicate guild assignments for each taxon. Guild abbreviations are as follows: pedunculate epifaunal suspension feeders (PESF), reclining epifaunal suspension feeders (RESF), mobile epifaunal deposit feeders (MEDF), colonial attached suspension feeders (CASF), solitary attached suspension feeders (SADF), mobile infaunal and semi-infaunal deposit feeders (MIDF), epifaunal mobile carnivores (EMC), epibiont suspension feeders (ESF), mobile epifaunal parasites (MEP), byssate suspension feeder (BSF).

GUILD	*Anazyga* PESF	*Bilobia* PESF	*Camerella* PESF	*Christiana* PESF	*Dalmanella* PESF	*Dinorthis* PESF	*Doleroides* PESF	*Eoplectodonta* PESF	*Glyptorthis* PESF	*Hebertella* PESF	*Hesperorthis* PESF	*Heterorthina* PESF	*Leptaena* RESF	*Lingula* PESF	*Multicostella* PESF	*Oepikina* RESF	*Orthorhyncula* PESF	*Oxoplecia* PESF	*Paucicrura* PESF	*Paurorthis* PESF	*Pionodema* PESF	*Platystrophia* PESF	*Plectocamara* PESF	*Rafinesquina* RESF
03PH4S	0	0	0	0	1	0	0	0	2	0	0	0	0	0	0	0	0	0	0	0	0	0	0	0
03AL3Da	1	0	0	0	0	2	0	0	0	0	0	0	0	0	1	0	0	0	0	0	0	0	0	0
03AL3Db	0	0	0	0	0	7	0	0	0	0	0	0	0	0	0	0	0	0	0	0	0	0	0	0
03CW5Sa	1	0	0	0	0	0	0	0	0	7	0	0	0	0	0	0	0	0	0	0	0	0	0	5
03CW5Sb	1	0	0	0	0	0	0	0	0	7	0	0	0	0	0	0	0	0	0	0	0	0	0	6
03TW5Sa	0	0	0	0	0	0	0	0	0	5	0	0	0	0	0	0	0	0	0	0	0	0	0	0
03TW5Sb	0	0	0	0	0	0	0	0	0	17	0	0	0	0	0	0	0	0	0	0	0	1	0	0
03TW5Sc	1	0	0	0	1	0	0	0	0	0	1	0	0	0	0	0	0	0	0	0	0	0	0	0
03TW5D	0	0	0	0	7	0	0	0	0	0	0	0	0	0	0	0	0	0	0	0	0	0	0	4
03HCW5Da	0	0	0	0	0	0	0	0	0	0	0	0	0	0	0	0	0	0	0	0	0	0	0	0
03HCW5Db	0	0	0	0	0	0	0	0	0	0	0	0	0	0	0	0	0	0	0	0	0	0	0	0
03HCW4Sa	1	0	0	0	0	0	1	0	0	0	0	0	0	0	1	0	0	0	0	0	0	0	0	0
03HCW4Sb	0	0	0	0	1	0	0	0	0	0	0	0	0	0	2	0	0	0	0	0	0	0	0	0
03HCW4Sc	0	0	0	0	0	0	0	0	0	0	0	0	0	0	6	0	0	0	0	0	0	0	0	0
03GL4Da	2	0	0	0	1	0	0	0	0	0	0	0	0	0	0	0	0	0	0	0	0	0	0	0
03GL4Db	2	0	0	0	1	0	0	0	0	0	0	0	0	0	0	0	0	0	0	0	0	0	0	0
03GL4Dc	0	0	0	0	0	0	0	0	0	0	0	0	0	0	0	0	0	0	0	0	0	0	0	0
03GL4Sa	0	0	0	0	0	0	0	0	0	0	0	0	0	0	0	0	0	0	0	0	0	0	0	0
03GL4Sb	0	0	0	0	0	0	0	0	0	0	0	0	0	0	0	0	0	0	0	0	0	0	0	0
03GL4Sc	0	0	0	0	0	0	0	0	0	0	0	0	0	0	0	0	0	0	0	0	0	0	0	0
03GL3D	0	0	0	0	0	0	0	0	0	0	15	0	0	0	0	0	0	0	0	0	0	0	0	0
03CN5D	0	0	0	0	54	0	0	0	0	0	0	0	0	0	0	0	0	0	0	0	0	0	0	0
03FW5S	2	0	0	0	0	1	0	0	0	0	0	0	0	0	0	0	0	0	0	0	0	0	0	0
03LW3Da	0	0	0	0	0	0	0	0	1	0	3	0	0	0	6	0	0	0	0	0	62	0	0	0
03LW3Db	0	0	0	0	0	0	41	0	0	0	2	0	0	0	0	0	0	0	0	0	0	0	0	0
03LW3Dc	7	0	0	0	0	0	0	0	2	0	4	0	0	0	2	0	0	0	0	0	0	0	0	0
03HC3D	0	0	0	0	0	0	0	0	0	0	6	0	0	0	0	0	0	0	0	0	4	0	0	0
03HC5Da	6	0	0	0	6	1	0	0	0	1	0	0	0	0	0	0	0	0	0	0	0	0	0	2
03HC5Db	1	0	0	0	11	0	0	0	0	1	0	0	0	0	0	0	0	0	0	0	0	0	0	3
03HC5Dc	2	0	0	0	5	0	0	0	0	2	0	0	0	0	0	0	0	0	0	0	0	0	0	3
03SA3Da	4	0	0	0	0	0	0	0	1	0	0	0	0	0	0	0	0	0	0	0	17	0	0	0
03SA3Db	0	0	0	0	0	0	0	0	0	0	0	0	0	0	0	0	0	0	0	0	14	0	0	0
03SB3Da	0	0	0	0	0	0	0	0	0	0	7	0	0	0	2	0	0	0	0	0	1	0	0	0
03SB3Db	0	0	0	0	0	0	0	0	0	0	35	0	0	0	0	0	0	0	0	0	0	0	0	0
04WWR3Da	0	0	0	0	0	0	0	0	0	0	0	0	0	0	0	0	0	0	0	0	2	0	0	0
04WWR3Db	0	0	0	0	0	0	0	0	1	0	0	0	0	0	0	0	0	0	0	0	1	0	0	0
04WWR3Dc	0	0	0	0	0	0	0	0	1	0	0	0	0	0	0	0	0	0	0	0	1	0	0	0
04FC3Da	0	0	0	0	0	0	3	0	0	0	0	0	0	0	1	0	0	0	0	0	10	0	0	0
04FC3Db	0	0	0	0	0	0	0	0	0	0	0	0	0	0	9	0	0	0	0	0	0	0	0	0
04FC3Dc	0	0	0	0	0	0	2	0	1	0	2	0	0	0	0	0	0	0	0	0	0	0	0	0
04AR4Sa	2	0	0	0	0	0	0	0	0	0	3	0	0	0	0	0	0	0	0	0	0	0	0	0
04AR4Sb	0	0	0	0	0	0	0	0	0	0	0	0	0	0	0	0	0	0	0	0	0	0	0	0
04AR4Sc	4	0	0	0	0	0	5	0	0	0	0	0	0	0	0	0	0	0	0	0	0	0	0	0
04AR4Sd	4	0	0	0	0	2	1	0	0	0	0	0	0	0	0	0	0	0	0	0	0	0	0	0
04WCL4S	0	0	0	0	0	0	0	0	0	0	0	0	0	0	0	0	0	0	0	0	0	0	0	0
04AW4Sa	0	0	0	0	0	0	0	0	0	0	0	0	0	0	0	0	0	0	0	0	0	0	0	0
04AW4Sb	0	0	0	0	1	0	1	0	0	0	0	0	0	0	0	0	0	0	0	0	0	0	0	0
04AW4Sc	0	0	0	0	2	0	2	0	0	0	0	0	0	0	0	0	0	0	0	0	0	0	0	0
04BP4Sa	0	0	0	0	0	0	0	0	2	0	0	0	0	0	0	0	0	0	0	0	0	0	0	0
04BP4Sb	0	0	0	0	0	0	0	0	0	0	0	0	0	0	0	0	0	0	0	0	0	0	0	0
04MV5Da	0	0	0	0	8	0	0	0	0	0	0	0	0	0	0	0	0	0	0	0	0	0	0	5
04MV5Db	0	0	0	0	20	0	0	0	0	0	0	0	0	0	0	0	0	0	0	0	0	0	0	0
04MV5Dc	0	0	0	0	21	0	0	0	0	0	0	0	0	0	0	0	0	0	0	0	0	0	0	0
04MV5Sa	0	0	0	0	0	6	0	0	0	15	0	0	0	0	0	0	0	0	0	0	0	0	0	0

GUILD	*Rhynchotrema*	*Rostricellula*	*Schizotreta*	*Strophomena*	*Sowerbyella*	*Zygospira*	*Inarticulata indet.*	*rhynchonellid indet.*	*Brachiopoda indet.*	*Ceraurus*	*Cryptolithus*	*Eomonorachus*	*Flexicalymene*	*Gravicalymene*	*Isotelus*	*Pterygometopus*	*Trilobita A*	*Trilobita indet.*	*Isotelus spines*	*Bellerophon*	*Bucania*	*Cyclonema*	*Hormotoma*	*Liospira*
	PESF	PESF	PESF	RESF	RESF	PESF	PESF	PESF	PESF	MEDF	MEDF	MEDF	MEDF	MEDF	MEDF	MEDF	MEDF	MEDF	MEDF	MEDF	MEDF	MEP	MEDF	MEDF
03PH4S	0	0	0	16	0	0	0	0	0	0	0	0	0	0	0	0	0	0	0	0	0	0	1	2
03AL3Da	0	13	0	0	0	0	0	0	0	0	0	0	0	0	0	0	0	0	0	0	0	0	0	0
03AL3Db	0	11	0	0	0	0	0	0	0	0	0	0	0	0	0	0	0	3	0	0	0	0	1	0
03CW5Sa	0	1	0	0	0	0	0	0	0	0	0	0	0	0	0	0	0	0	0	0	0	0	0	0
03CW5Sb	0	0	0	0	0	3	0	0	0	0	0	0	0	0	0	0	0	0	0	0	0	0	0	0
03TW5Sa	3	0	0	0	0	1	0	0	0	0	0	0	0	0	0	0	0	0	0	0	0	0	0	0
03TW5Sb	6	0	0	0	0	2	0	0	0	0	0	0	0	0	0	0	0	0	0	0	0	0	0	0
03TW5Sc	0	0	0	0	0	0	0	0	0	0	0	0	0	0	0	0	0	1	0	0	0	0	0	0
03TW5D	10	0	0	0	0	0	0	0	0	0	0	0	0	0	0	0	0	0	0	0	0	0	0	0
03HCW5Da	0	0	0	0	0	3	0	0	0	0	0	0	0	0	0	0	0	0	0	0	0	0	0	0
03HCW5Db	0	0	0	0	0	0	0	0	0	0	0	0	0	0	0	0	0	0	0	0	0	0	0	0
03HCW4Sa	0	0	0	12	0	0	0	0	0	0	0	0	0	0	1	0	0	1	0	0	0	0	0	0
03HCW4Sb	0	0	0	4	0	0	0	0	0	0	0	0	0	0	2	0	0	1	0	0	0	0	0	0
03HCW4Sc	0	0	0	4	0	0	0	0	0	0	0	0	0	0	0	0	0	12	0	0	0	0	0	0
03GL4Da	0	0	0	1	0	0	0	0	0	0	0	0	0	0	1	0	0	5	0	0	0	0	0	0
03GL4Db	0	0	0	4	0	2	0	0	0	1	0	0	0	0	1	0	0	0	0	0	0	0	1	0
03GL4Dc	0	0	0	1	0	2	0	0	0	0	0	0	0	0	0	0	0	0	0	0	0	0	0	0
03GL4Sa	0	0	0	8	0	0	0	0	0	0	0	0	0	0	2	0	0	0	0	0	0	0	1	0
03GL4Sb	0	0	0	15	0	0	0	0	0	0	0	0	0	0	0	0	0	0	0	0	0	1	1	0
03GL4Sc	0	0	0	25	0	0	0	0	0	0	0	0	0	0	0	0	0	0	0	0	0	0	0	1
03GL3D	0	0	0	5	0	1	0	0	0	0	0	0	0	0	0	1	0	0	0	0	0	0	0	0
03CN5D	0	0	0	0	0	0	0	0	0	0	0	0	0	0	0	0	0	0	0	0	0	0	0	0
03FW5S	4	0	0	0	0	1	0	0	0	0	0	0	0	0	0	0	0	0	0	0	0	0	0	0
03LW3Da	0	1	0	1	0	0	0	0	0	0	0	0	0	0	1	0	0	1	0	0	0	0	0	0
03LW3Db	0	0	0	16	0	4	0	0	0	1	0	0	0	0	2	0	0	0	0	0	0	0	0	0
03LW3Dc	0	0	0	1	0	0	0	0	0	0	0	0	0	0	0	0	0	2	0	0	0	0	0	0
03HC3D	0	1	0	14	0	4	0	0	0	0	0	0	0	0	0	0	0	1	0	0	0	0	0	0
03HC5Da	2	0	0	0	0	6	1	0	0	4	0	0	1	0	0	0	0	0	0	0	0	0	0	0
03HC5Db	7	0	0	0	0	10	0	0	0	0	0	0	2	0	0	0	0	6	0	0	0	0	0	0
03HC5Dc	1	0	0	0	0	2	0	0	0	0	0	0	0	0	2	0	0	2	0	0	0	0	0	0
03SA3Da	0	0	0	0	0	0	0	0	0	0	0	0	0	0	2	3	0	4	0	0	0	0	0	0
03SA3Db	0	0	0	0	0	10	0	0	0	0	0	0	0	0	0	0	0	4	0	0	0	0	0	0
03SB3Da	0	2	0	7	0	0	0	0	0	0	0	0	0	0	0	0	0	1	0	0	0	0	0	0
03SB3Db	0	0	0	9	0	1	0	0	0	0	0	0	0	0	0	0	0	1	0	0	0	0	1	0
04WWR3Da	0	12	0	0	0	1	0	0	0	0	0	0	0	0	0	0	0	1	2	0	0	0	0	0
04WWR3Db	0	9	0	0	0	3	0	0	0	0	0	0	0	0	0	0	0	0	0	0	0	0	0	0
04WWR3Dc	0	10	0	0	0	13	0	0	0	0	0	0	0	0	1	0	0	0	3	0	0	0	0	0
04FC3Da	0	0	0	0	0	6	0	0	0	0	0	0	0	0	0	1	0	0	0	0	0	0	0	0
04FC3Db	0	0	0	0	0	0	0	0	0	0	0	0	0	0	0	0	0	0	2	0	0	0	0	0
04FC3Dc	0	0	0	1	0	1	0	0	0	0	0	0	0	0	0	0	0	1	1	0	0	0	0	0
04AR4Sa	0	0	0	8	0	0	0	0	0	2	0	0	0	0	0	0	0	0	0	0	0	0	0	0
04AR4Sb	0	0	0	4	0	0	0	0	0	0	0	0	0	0	0	0	0	0	2	0	0	0	0	0
04AR4Sc	0	4	0	1	0	0	0	0	0	0	0	0	0	0	1	0	0	1	0	0	0	0	0	0
04AR4Sd	0	3	0	3	0	0	0	0	0	1	0	0	0	0	5	0	0	0	0	0	0	0	0	0
04WCL4S	0	0	0	6	0	0	0	0	0	0	0	0	0	0	0	0	0	0	0	0	0	0	0	0
04AW4Sa	0	0	0	8	0	0	0	0	0	0	0	0	0	0	0	1	0	0	0	0	0	0	0	0
04AW4Sb	1	0	0	3	0	0	0	0	0	0	0	0	0	0	0	0	0	0	0	0	0	0	0	0
04AW4Sc	0	3	0	7	0	0	0	0	0	0	0	0	0	0	0	2	0	0	6	0	0	0	0	0
04BP4Sa	0	0	0	2	0	0	0	0	0	0	0	0	0	0	0	1	0	0	0	0	0	0	0	0
04BP4Sb	0	5	0	13	0	2	0	0	0	0	0	0	0	0	0	1	0	0	1	0	0	0	0	0
04MV5Da	0	0	0	0	0	1	0	0	0	0	0	0	0	0	0	0	0	3	0	0	0	0	0	0
04MV5Db	0	0	0	0	0	0	0	0	0	0	0	0	0	0	0	0	0	0	0	0	0	0	0	0
04MV5Dc	0	0	0	0	0	0	0	0	0	0	0	0	0	0	0	0	0	0	0	0	0	0	0	0
04MV5Sa	0	0	0	0	0	0	0	0	0	0	0	0	0	0	0	0	0	0	0	0	0	0	0	0

GUILD	*Lophospira* MEDF	*Maclurites* MEDF	*Sinuites* MEDF	*Gastropoda indet.* MEDF	*Cyclora* MEDF	*Ambonychia* BSF	*Ctenodonta* M1DF	*Cunemya* BSF	*Cyrtodonta* BSF	*Cyrtodontula* BSF	*Deceptrix* M1DF	*Ischyrodonta* M1DF	*modiomorph* BSF	*Lyrodesma* M1DF	*Paleoneilo* M1DF	*Whitella* BSF	*Bivalvia indet.* M1DF	*Ieperditid ostracod* MEDF	*Columnaria* CASF	*Streptelasma* CASF	*Tetradium* CASF	*Stromatoporoidea* CASF	*Chasmatopora* CASF	*Constellaria* CASF
03PH4S	1	0	0	0	0	0	0	0	0	0	0	0	0	0	0	0	0	0	0	0	0	0	2	0
03AL3Da	0	0	0	0	0	0	0	0	0	0	0	0	0	0	0	0	0	0	0	0	0	0	0	0
03AL3Db	0	0	0	0	0	0	0	0	0	0	0	0	0	0	0	0	0	1	0	0	0	0	0	0
03CW5Sa	19	0	0	0	0	0	0	0	0	0	0	0	0	0	0	0	0	0	0	0	0	0	0	0
03CW5Sb	0	0	0	0	0	0	0	0	0	0	0	0	0	0	0	0	0	0	0	0	6	0	0	0
03TW5Sa	0	0	0	0	0	0	0	0	0	0	0	0	0	0	0	0	0	0	0	1	0	0	0	0
03TW5Sb	0	0	0	0	0	0	0	0	0	0	0	0	0	0	0	0	0	0	0	0	0	0	0	0
03TW5Sc	0	0	0	0	0	0	0	0	0	0	0	0	0	0	0	0	1	2	0	1	23	0	0	0
03TW5D	0	0	0	0	0	0	0	0	0	0	0	0	0	0	0	0	0	0	0	0	0	0	0	0
03HCW5Da	0	0	0	0	0	0	0	0	0	0	97	0	0	0	0	0	0	0	0	0	1	0	0	0
03HCW5Db	0	0	0	0	0	1	0	0	0	0	27	0	0	0	0	0	0	0	0	0	0	0	0	0
03HCW4Sa	2	0	0	0	0	0	0	0	0	0	0	0	0	0	0	0	0	1	0	0	1	0	0	0
03HCW4Sb	0	0	0	0	0	0	0	0	0	0	0	0	0	0	0	0	0	0	0	0	0	0	1	0
03HCW4Sc	0	0	0	0	0	0	0	0	0	0	0	0	0	0	0	0	0	0	0	0	0	0	0	0
03GL4Da	0	0	0	0	0	0	0	0	0	0	0	0	0	0	0	0	0	240	0	1	0	0	0	0
03GL4Db	0	0	0	0	0	0	0	0	0	0	0	0	0	0	0	0	0	120	0	0	0	0	3	0
03GL4Dc	0	0	0	0	0	0	0	0	0	0	0	0	0	0	0	0	0	63	0	0	0	0	1	0
03GL4Sa	4	0	0	0	0	0	0	0	0	0	0	0	0	0	0	0	0	0	0	0	0	0	0	0
03GL4Sb	10	0	0	0	0	0	0	1	0	0	0	0	0	0	0	0	0	0	0	0	0	0	0	0
03GL4Sc	9	0	0	0	0	0	0	0	0	0	0	0	0	0	0	0	0	0	0	0	0	0	2	0
03GL3D	0	0	0	0	0	0	0	0	0	0	0	0	0	0	0	0	0	0	0	1	0	0	0	0
03CN5D	0	0	0	0	0	0	0	0	0	0	0	0	0	0	0	0	0	0	0	0	0	0	0	0
03FW5S	0	0	0	0	0	0	0	0	0	0	0	0	0	0	0	0	0	0	0	0	0	0	0	0
03LW3Da	0	0	0	0	0	0	0	0	0	0	0	0	0	0	0	0	0	0	0	0	0	0	0	0
03LW3Db	0	1	0	0	0	0	0	0	0	0	0	0	0	0	0	0	0	2	0	1	0	0	0	0
03LW3Dc	0	0	0	0	0	0	0	0	0	0	0	0	0	0	0	0	0	0	0	0	0	0	0	0
03HC3D	0	0	0	0	0	0	0	0	0	0	1	0	0	0	0	0	0	1	0	1	2	0	0	0
03HC5Da	0	0	0	0	0	0	0	0	0	0	0	0	0	0	0	0	0	1	0	0	0	0	0	0
03HC5Db	0	0	0	0	0	0	0	0	0	0	0	0	0	0	0	0	0	0	0	0	0	0	0	0
03HC5Dc	0	0	0	0	0	0	0	0	0	0	0	0	0	0	0	1	0	0	0	0	40	0	0	0
03SA3Da	0	3	0	0	0	0	0	0	0	0	0	0	0	0	0	0	0	61	0	0	0	0	0	0
03SA3Db	0	0	0	0	0	0	0	0	0	0	0	0	0	0	0	0	0	47	0	0	0	0	0	0
03SB3Da	3	0	0	0	0	0	0	0	0	0	0	0	0	0	0	0	0	13	0	0	0	0	0	0
03SB3Db	0	1	0	0	0	0	0	0	0	0	0	0	0	0	0	0	0	6	0	1	0	0	0	0
04WWR3Da	0	0	0	0	0	0	0	0	0	0	0	0	0	0	0	0	0	0	0	0	0	0	5	0
04WWR3Db	0	0	0	1	0	0	0	0	0	0	0	0	0	0	0	0	0	1	0	0	0	0	3	0
04WWR3Dc	2	0	0	0	0	0	0	0	0	0	0	0	0	0	0	0	0	0	0	0	0	0	1	0
04FC3Da	0	0	0	0	0	0	0	0	0	0	0	0	0	0	0	0	0	41	0	0	0	0	2	0
04FC3Db	0	1	0	0	0	0	0	0	0	0	0	0	0	0	0	0	0	22	0	0	0	0	0	0
04FC3Dc	2	6	0	0	0	0	0	0	0	0	0	0	0	0	0	0	0	7	0	0	0	0	2	0
04AR4Sa	0	0	0	0	0	0	0	0	0	0	0	0	0	0	0	0	0	42	0	0	0	0	4	0
04AR4Sb	0	18	0	0	0	0	0	0	0	0	0	0	0	0	0	0	0	25	0	0	0	0	13	0
04AR4Sc	0	0	0	0	0	0	0	0	0	0	0	0	0	0	0	0	0	6	0	0	0	0	0	0
04AR4Sd	0	1	0	0	0	0	0	0	0	0	0	0	0	0	0	0	0	23	0	0	0	0	0	0
04WCL4S	0	0	0	0	0	0	0	0	0	0	0	0	0	0	0	0	0	0	0	0	0	0	0	0
04AW4Sa	3	1	0	0	0	0	0	0	0	0	0	0	0	0	0	0	0	2	0	0	0	0	0	0
04AW4Sb	0	0	0	0	0	0	0	0	0	0	0	0	0	0	0	0	0	0	0	1	0	0	0	0
04AW4Sc	3	0	0	0	0	0	0	0	0	0	0	0	0	0	0	0	0	2	0	1	4	0	0	0
04BP4Sa	0	0	0	0	0	0	0	0	0	0	0	0	0	0	0	0	0	0	0	0	0	0	0	0
04BP4Sb	1	0	0	0	0	0	0	0	0	0	0	0	0	0	0	0	0	0	0	0	1	0	0	0
04MV5Da	0	0	0	0	0	0	0	0	0	0	0	0	0	0	0	0	0	0	0	0	0	0	0	0
04MV5Db	0	0	0	0	0	0	0	0	0	0	0	0	0	0	0	0	0	0	0	0	0	0	0	0
04MV5Dc	0	0	0	0	0	0	0	0	0	0	0	0	0	0	0	0	0	0	0	0	0	0	0	0
04MV5Sa	2	0	0	0	0	0	0	0	0	0	0	0	0	0	0	0	0	0	0	0	0	0	0	0

GUILD	*Escharopora* CASF	*Heterotrypa* CASF	*Prasopora* CASF	*Rhindictya* CASF	*massive trepostome* CASF	*bifoliate bryozoan* CASF	*bumpy ramose* CASF	*encrusting bryozoan* CASF	*thick ramose* CASF	*thin ramose 1* CASF	*thin ramose 2* CASF	*cog crinoid* SASF	*cog star crinoid* SASF	*thin ring crinoid* SASF	*thick ring crinoid* SASF	*flower crinoid* SASF	*pentagonal crinoid* SASF	*stacked crinoid* SASF	*star crinoid* SASF	*inner star crinoid* SASF	*striped crinoid* SASF	*striped flower crinoid* SASF	*striped star crinoid* SASF	*crinoidea indet.* SASF
03PH4S	10	0	0	5	0	0	0	0	0	1	0	0	0	0	0	0	0	0	0	0	0	0	0	0
03AL3Da	0	0	0	0	0	0	0	0	0	0	0	0	0	0	0	0	0	0	0	0	0	0	0	0
03AL3Db	0	0	0	0	0	0	0	1	2	0	0	0	0	0	0	0	0	0	0	0	0	0	0	0
03CW5Sa	0	0	0	0	51	0	0	0	62	0	0	1	0	0	1	0	0	0	0	0	0	0	0	0
03CW5Sb	0	0	0	0	0	0	0	0	0	0	0	0	0	0	0	0	0	0	0	0	0	0	0	0
03TW5Sa	0	0	0	0	0	0	0	0	0	0	0	0	0	0	0	0	0	0	0	0	0	0	0	0
03TW5Sb	0	0	0	0	0	0	0	0	0	0	0	0	0	0	0	0	0	0	0	0	0	0	0	0
03TW5Sc	0	0	0	0	0	0	0	0	4	0	0	0	0	0	0	0	0	0	0	0	0	0	0	0
03TW5D	2	0	0	0	0	0	0	0	3	10	0	0	0	0	0	0	0	0	0	0	0	0	0	0
03HCW5Da	0	0	0	0	0	0	0	0	1	0	0	0	0	0	0	0	0	0	0	0	0	0	0	0
03HCW5Db	0	0	0	0	0	0	0	0	0	0	0	0	0	0	0	0	0	0	0	0	0	0	0	0
03HCW4Sa	5	0	0	3	0	14	0	1	0	2	0	0	0	0	0	0	0	0	0	0	0	0	0	0
03HCW4Sb	12	0	0	3	0	2	0	4	1	0	0	0	0	0	0	0	0	0	0	0	0	0	0	0
03HCW4Sc	9	0	0	5	0	0	0	0	0	0	0	0	0	0	0	0	0	0	0	0	0	0	0	0
03GL4Da	55	0	0	26	0	0	0	2	38	9	0	0	0	3	0	3	0	0	0	0	0	0	0	0
03GL4Db	73	0	0	17	0	0	0	0	75	0	0	0	0	3	0	3	0	0	0	0	0	0	0	0
03GL4Dc	30	0	0	2	11	0	0	0	0	25	0	0	0	1	0	1	0	0	0	0	0	0	0	0
03GL4Sa	5	0	0	8	0	0	0	1	0	4	0	0	0	1	1	0	0	0	0	0	0	0	0	0
03GL4Sb	0	0	0	8	0	1	0	1	0	5	0	0	0	1	1	0	0	0	0	0	0	0	0	0
03GL4Sc	0	0	0	3	0	0	0	4	0	11	0	0	0	0	1	0	0	0	0	0	0	0	0	0
03GL3D	5	0	0	1	0	0	0	0	0	2	0	0	0	3	1	0	0	0	0	1	1	0	0	0
03CN5D	0	0	0	0	0	0	0	0	0	0	0	0	0	0	0	0	0	0	0	0	0	0	0	0
03FW5S	0	0	0	0	31	0	0	0	2	2	0	0	0	0	1	0	0	0	0	0	0	0	0	0
03LW3Da	50	0	0	12	0	0	0	0	0	9	7	0	0	0	1	0	0	0	0	0	0	0	0	0
03LW3Db	35	0	0	10	0	0	0	0	0	21	0	0	0	3	3	1	1	0	0	0	1	0	0	0
03LW3Dc	22	0	0	22	0	0	0	0	0	12	0	0	0	0	3	0	0	0	0	0	0	0	0	0
03HC3D	3	0	0	7	0	0	0	0	1	0	4	0	0	0	1	0	0	0	0	0	1	0	0	0
03HC5Da	2	0	2	0	0	0	0	0	0	17	0	0	0	0	1	0	1	0	1	0	0	0	0	0
03HC5Db	18	0	2	0	0	0	0	0	7	17	0	0	0	0	1	0	1	1	0	0	1	0	0	0
03HC5Dc	9	0	5	1	0	0	0	0	0	24	0	0	0	0	1	0	1	3	1	0	0	0	0	0
03SA3Da	10	0	0	3	0	0	0	0	0	8	0	0	0	0	0	0	0	0	0	0	0	0	0	0
03SA3Db	0	0	0	2	0	0	0	0	0	0	0	0	0	0	0	0	0	0	0	0	0	0	0	0
03SB3Da	3	0	0	0	0	0	0	0	0	0	1	0	0	0	1	0	0	0	0	0	0	0	0	0
03SB3Db	9	0	0	3	0	0	0	0	0	0	4	0	0	0	1	0	0	0	0	0	0	1	0	0
04WWR3Da	7	0	0	4	0	0	0	0	0	5	0	0	0	1	1	0	0	0	0	0	0	0	0	0
04WWR3Db	10	0	0	2	0	0	0	0	0	3	0	0	0	3	3	0	0	0	0	0	0	0	0	0
04WWR3Dc	11	0	1	2	0	0	0	0	0	8	0	0	0	3	6	0	0	0	0	0	0	0	0	0
04FC3Da	9	0	0	1	0	0	0	0	0	1	0	1	0	3	3	3	0	0	0	1	3	0	0	0
04FC3Db	3	0	0	2	0	0	0	0	0	0	0	0	0	0	0	0	0	0	0	0	0	0	0	0
04FC3Dc	6	0	0	3	0	0	0	0	0	9	0	3	0	6	1	0	1	0	0	0	0	0	0	0
04AR4Sa	15	0	0	2	0	0	0	0	0	3	0	1	0	3	6	0	0	0	0	0	1	0	0	0
04AR4Sb	1	0	0	0	0	0	0	0	0	0	0	1	0	6	0	0	0	0	0	0	0	0	0	0
04AR4Sc	2	0	0	0	0	0	0	0	0	1	0	0	0	3	0	0	0	0	0	0	1	0	0	0
04AR4Sd	10	0	0	1	0	0	0	0	6	0	0	0	0	3	3	0	0	0	0	0	1	0	0	0
04WCL4S	0	0	0	0	0	0	0	0	2	0	0	0	0	1	1	3	0	0	3	0	1	0	0	0
04AW4Sa	0	0	0	0	0	0	0	0	1	0	0	0	0	1	0	0	0	0	0	0	3	0	0	0
04AW4Sb	5	0	0	3	0	0	0	0	0	5	0	0	0	6	6	3	0	0	0	0	1	0	1	0
04AW4Sc	16	0	0	2	0	0	0	0	0	0	0	0	0	3	3	1	1	0	0	0	0	0	0	0
04BP4Sa	6	0	0	8	0	0	0	0	0	0	0	0	0	6	6	0	0	0	3	0	0	0	0	0
04BP4Sb	3	0	0	0	0	0	0	0	0	0	1	0	0	6	6	0	0	0	0	0	0	0	0	0
04MV5Da	1	0	1	1	0	0	0	0	5	1	0	0	0	1	0	0	0	0	0	0	0	0	0	0
04MV5Db	0	0	0	0	0	0	0	0	0	0	0	0	0	0	0	0	0	0	0	0	0	0	0	0
04MV5Dc	1	0	0	2	0	0	0	0	3	0	0	0	0	0	0	0	0	0	0	0	0	0	0	0
04MV5Sa	6	0	0	0	0	0	0	0	5	0	0	0	0	0	0	0	0	0	0	0	0	0	0	0

GUILD	*Echinodermata indet.*	*orthoconic nautiloids*	*algal coating*	*Solenopora*	*Stromatoporoids*	*Chondrites*	*Diplocriterion*	*Cornulites*	*alga(Hindia?)*	*rhombiferan plate*	*graptolites*
	SASF	EMC	ESF	CASF	CASF	MIDF	MIDF	ESF	ESF	SASF	EMC
03PH4S	0	1	0	0	0	0	0	0	0	0	0
03AL3Da	0	0	0	0	0	0	0	0	0	0	0
03AL3Db	0	0	0	0	0	0	0	0	0	0	0
03CW5Sa	0	0	0	0	0	0	0	0	0	0	0
03CW5Sb	0	0	0	0	0	0	0	0	0	0	0
03TW5Sa	0	0	0	0	0	0	0	0	0	0	0
03TW5Sb	0	0	0	0	0	0	0	0	0	0	0
03TW5Sc	0	0	0	0	0	0	0	0	0	0	0
03TW5D	0	0	0	0	0	0	0	0	0	0	0
03HCW5Da	0	0	0	0	0	0	0	0	0	0	0
03HCW5Db	0	0	0	0	0	0	0	0	0	0	0
03HCW4Sa	0	0	0	0	0	0	0	0	0	0	0
03HCW4Sb	0	2	0	0	0	0	0	0	0	0	0
03HCW4Sc	0	0	0	0	0	0	0	0	0	0	0
03GL4Da	0	0	0	0	0	0	0	0	0	0	0
03GL4Db	0	0	0	0	0	0	0	0	0	0	0
03GL4Dc	0	0	0	0	0	0	0	0	0	0	0
03GL4Sa	0	0	0	0	0	0	0	0	0	0	0
03GL4Sb	0	0	0	0	0	3	0	0	0	0	0
03GL4Sc	0	0	0	0	0	0	0	0	0	0	0
03GL3D	0	0	0	0	0	0	3	0	0	0	0
03CN5D	0	0	0	0	0	0	0	0	0	0	0
03FW5S	0	0	0	0	0	0	0	0	0	0	0
03LW3Da	0	0	0	0	0	0	0	0	0	0	0
03LW3Db	0	0	0	0	0	0	0	0	0	0	0
03LW3Dc	0	0	0	0	0	0	0	0	0	0	0
03HC3D	0	0	0	0	0	0	0	0	0	0	0
03HC5Da	1	0	0	0	0	0	0	0	0	0	0
03HC5Db	0	0	0	0	0	0	0	0	0	0	0
03HC5Dc	0	0	0	0	0	0	0	0	0	0	0
03SA3Da	0	2	0	0	0	0	0	0	0	0	0
03SA3Db	0	0	0	0	0	0	0	0	0	0	0
03SB3Da	0	0	0	0	0	0	0	0	0	0	0
03SB3Db	0	1	0	0	0	0	0	0	0	0	0
04WWR3Da	0	1	0	0	0	0	0	0	0	0	0
04WWR3Db	0	1	0	0	0	0	1	1	0	0	0
04WWR3Dc	0	0	0	0	0	3	0	1	0	0	0
04FC3Da	0	0	0	0	0	0	0	0	0	0	0
04FC3Db	0	0	0	0	0	0	0	0	0	0	0
04FC3Dc	0	0	0	0	0	0	0	0	0	0	0
04AR4Sa	0	0	0	0	0	0	0	0	0	0	0
04AR4Sb	0	0	0	0	0	0	0	0	0	0	0
04AR4Sc	0	0	0	0	0	0	0	0	0	0	0
04AR4Sd	0	0	0	0	0	0	0	0	0	0	0
04WCL4S	0	0	0	0	0	0	0	0	0	0	0
04AW4Sa	0	0	0	0	0	6	0	0	0	0	0
04AW4Sb	0	0	0	0	0	0	0	0	0	0	0
04AW4Sc	0	0	0	0	0	3	0	0	0	0	0
04BP4Sa	0	0	0	0	0	0	0	0	0	0	0
04BP4Sb	0	0	0	0	0	0	0	0	0	0	0
04MV5Da	0	0	0	0	0	0	0	0	0	0	0
04MV5Db	0	0	0	0	0	0	0	0	0	0	0
04MV5Dc	0	0	0	0	0	0	0	0	0	0	0
04MV5Sa	0	0	0	0	0	0	0	0	0	0	0

	Anazyga	*Bilobia*	*Camerella*	*Christiana*	*Dalmanella*	*Dinorthis*	*Doleroides*	*Eoplectodonta*	*Glyptorthis*	*Hebertella*	*Hesperorthis*	*Heterorthina*	*Leptaena*	*Lingula*	*Multicostella*	*Oepikina*	*Orthorhyncula*	*Oxoplecia*	*Paucicrura*	*Paurorthis*	*Pionodema*	*Platystrophia*	*Plectocamara*	*Rafinesquina*
04MV5Sb	0	0	0	0	0	0	0	0	0	4	0	0	0	0	0	0	0	0	0	0	0	0	0	0
04IPR5D	0	0	0	0	63	0	0	0	0	0	0	0	0	0	0	0	0	0	0	0	0	0	0	0
04DEF5S	0	0	0	0	0	0	0	0	0	13	0	0	0	0	0	0	0	0	0	0	0	0	0	2
04FR5Sa	0	0	0	0	0	0	0	0	0	0	0	0	0	0	0	0	0	0	0	0	0	0	0	0
04FR5Sb	0	0	0	0	0	0	1	0	0	1	0	0	0	0	0	0	0	0	0	0	0	0	0	3
04CAR5Sa	0	0	0	0	0	2	0	0	4	5	0	0	0	0	0	0	0	0	0	0	0	0	0	0
04CAR5Sb	0	0	0	0	0	0	0	0	0	3	0	0	0	0	0	0	0	0	0	0	0	0	0	0
04CAR5Sc	0	0	0	0	0	0	0	0	0	1	0	0	0	0	0	0	0	0	0	0	0	0	0	0
04CAR5Sd	0	0	0	0	0	6	0	0	0	8	0	0	0	0	0	0	0	0	0	0	0	0	0	0
04CAR5Se	0	0	0	0	0	0	0	0	0	5	0	0	0	0	0	0	0	0	0	0	0	0	0	0
04CAR5Sf	0	0	0	0	0	0	0	0	0	0	0	0	0	0	0	0	0	0	0	0	0	0	0	2
04MV6S	0	0	0	0	0	0	0	0	0	4	4	0	0	0	0	0	0	0	0	0	0	0	0	0
04KC6Sa	0	0	0	0	0	0	0	0	0	0	0	0	0	0	0	0	0	0	0	0	0	4	0	1
04KC6Sb	0	0	0	0	0	1	0	0	0	1	0	0	0	0	0	0	0	0	0	0	0	7	0	0
04KC6Sc	0	0	0	0	0	0	0	0	0	2	0	0	0	0	0	0	0	0	0	0	0	0	0	1
04KC6Sd	0	0	0	0	0	0	0	0	0	3	0	0	0	0	0	0	0	0	0	0	0	1	0	0
04DEF6Sa	0	0	0	0	0	1	0	0	0	1	0	0	0	0	0	0	0	0	0	0	0	0	0	0
04DEF6Sb	0	0	0	0	0	0	0	0	0	3	0	0	0	0	0	0	0	0	0	0	0	1	0	1
04DEF6Sc	0	0	0	0	0	0	0	0	0	0	0	0	0	0	0	0	0	0	0	0	0	5	0	1
04DEF6Sd	0	0	0	0	0	0	0	0	0	2	0	0	0	0	0	0	0	0	0	0	0	2	0	5
04DEF6Se	0	0	0	0	0	0	0	0	0	6	0	0	0	0	0	0	0	0	0	0	0	1	0	2
04DEF6Sf	0	0	0	0	0	0	0	0	0	0	0	0	0	0	0	0	0	0	0	0	0	0	0	0
04DEF6Sg	0	0	0	0	0	0	0	0	0	2	0	0	0	0	0	0	0	0	0	0	0	0	0	0
04DEF6Sh	0	0	0	0	0	0	0	0	0	8	0	0	0	0	0	0	0	0	0	0	0	0	0	0
04GLC6Sa	0	0	0	0	0	0	0	0	0	1	0	0	0	0	0	0	0	0	0	0	0	0	0	13
04GLC6Sb	0	0	0	0	0	0	0	0	1	3	0	0	0	0	0	0	0	0	0	0	0	5	0	6
04GLC6Sc	0	0	0	0	0	0	0	0	0	1	0	0	0	0	0	0	0	0	0	0	0	6	0	3
04GLC6Sd	0	0	0	0	0	0	1	0	0	4	0	0	0	0	0	0	0	0	0	0	0	10	0	1
04GLC6Se	0	0	0	0	0	0	0	0	0	0	0	0	0	0	0	0	0	0	0	0	0	2	0	4
04BB6Sa	0	0	0	0	0	0	0	0	0	6	0	0	0	0	0	0	0	0	0	0	0	0	0	5
04BB6Sb	0	0	0	0	0	0	0	0	0	3	0	0	0	0	0	0	0	0	0	0	0	0	0	0
04BB6Sc	2	0	0	0	0	0	0	0	0	4	0	0	0	0	0	0	0	0	0	0	0	0	0	3
04BB6Sd	0	0	0	0	0	0	0	0	0	1	0	0	0	0	0	0	0	0	0	0	0	0	0	0
04BB6Se	0	0	0	0	0	0	0	0	1	5	0	0	0	0	0	0	0	0	0	0	0	1	0	2
04HH6Sa	0	0	0	0	0	0	0	0	0	6	0	0	0	0	0	0	0	0	0	0	0	2	0	0
04HH6Sb	0	0	0	0	0	0	0	0	0	16	0	0	0	0	0	0	0	0	0	0	0	1	0	0
04RC6Sa	0	0	0	0	0	0	0	0	0	2	0	0	0	0	0	0	0	0	0	0	0	2	0	0
04RC6Sb	0	0	0	0	0	0	0	0	0	0	0	0	0	0	0	0	0	0	0	0	0	0	0	0
04RC6Sc	0	0	0	0	0	0	0	0	0	0	0	0	0	0	0	0	0	0	0	0	0	0	0	0
04RC6Sd	0	0	0	0	0	0	0	0	0	0	0	0	0	0	0	0	0	0	0	0	0	0	0	0
04RC6Se	0	0	0	0	0	0	0	0	0	0	0	0	0	0	0	0	0	0	0	0	0	0	0	0
04RR6Sa	0	0	0	0	0	0	0	0	0	4	0	0	0	0	0	0	0	0	0	0	0	0	0	4
04RR6Sb	0	0	0	0	0	0	0	0	1	6	0	0	0	0	0	0	0	0	0	0	0	0	0	1
04RR6Sc	0	0	0	0	0	0	0	0	2	5	0	0	0	0	0	0	0	0	0	0	0	0	0	2
04RR6Sd	0	0	0	0	0	0	0	0	0	0	0	0	0	0	0	0	0	0	0	0	0	0	0	0
04MGS6Sa	0	0	0	0	0	0	1	0	0	12	1	0	0	0	0	0	0	0	0	0	0	0	0	0
04MGS6Sb	0	0	0	0	0	0	0	0	0	4	0	0	0	0	0	0	0	0	0	0	0	1	0	4
04MGS6Sc	0	0	0	0	0	0	0	0	0	0	0	0	0	0	0	0	0	0	0	0	0	0	0	0
04FM5D	0	0	0	0	16	0	0	0	0	0	1	0	0	0	0	0	0	0	0	0	0	0	0	0
04FM4S	0	0	0	0	0	0	0	0	0	0	0	0	0	0	0	0	0	0	0	0	0	0	0	0
04AB6Sa	0	0	0	0	0	0	0	0	0	11	0	0	0	0	0	0	4	0	0	0	0	0	0	1
04AB6Sb	0	0	0	0	0	0	0	0	0	3	0	0	0	0	0	0	5	0	0	0	0	0	0	0
04AB6Sc	0	0	0	0	0	0	0	0	0	5	0	0	0	0	0	0	8	0	0	0	0	12	0	1
04SGC6Sa	0	0	0	0	0	0	0	0	0	1	0	0	0	0	0	0	5	0	0	0	0	1	0	0
04SGC6Sb	0	0	0	0	0	0	0	0	0	7	0	0	0	0	0	0	1	0	0	0	0	0	0	0
04DW6S	0	0	0	0	0	0	0	0	0	1	0	0	0	0	0	0	2	0	0	0	0	0	0	13
04DF6Sa	0	0	0	0	0	0	0	0	0	1	0	0	0	0	0	0	2	0	0	0	0	0	0	3

	Rhynchotrema	*Rostricellula*	*Schizotreta*	*Strophomena*	*Sowerbyella*	*Zygospira*	*Inarticulata indet.*	*rhynchonellid indet.*	*Brachiopoda indet.*	*Ceraurus*	*Cryptolithus*	*Eomonorachus*	*Flexicalymene*	*Gravicalymene*	*Isotelus*	*Pterygometopus*	*Trilobita A*	*Trilobita indet.*	*Isotelus spines*	*Bellerophon*	*Bucania*	*Cyclonema*	*Hormotoma*	*Liospira*
04MV5Sb	1	0	0	0	0	0	0	0	0	0	0	0	0	0	0	0	0	0	0	0	0	3	0	
04IPR5D	0	0	0	0	0	0	0	0	0	0	0	0	0	0	0	0	0	0	0	0	0	0	0	
04DEF5S	0	0	0	0	0	1	0	0	0	0	0	0	0	0	0	0	0	0	0	0	0	0	0	
04FR5Sa	0	0	0	0	0	1	0	0	0	0	0	0	0	0	0	0	0	0	0	0	0	0	0	
04FR5Sb	1	0	0	0	0	0	0	0	0	0	0	0	0	0	0	0	1	0	0	0	0	0	0	
04CAR5Sa	4	0	0	0	0	4	0	0	0	0	0	0	0	0	0	0	3	0	0	0	0	0	0	
04CAR5Sb	3	0	0	0	0	14	0	0	0	0	0	0	0	0	0	0	3	2	0	0	0	0	0	
04CAR5Sc	0	0	0	0	0	0	0	0	0	0	0	0	0	0	0	0	0	2	0	0	4	0	0	
04CAR5Sd	1	0	0	0	0	2	0	0	0	0	0	0	0	0	0	0	0	0	0	0	0	0	0	
04CAR5Se	3	0	0	0	0	1	0	0	0	0	0	0	0	0	0	0	0	0	0	0	0	0	0	
04CAR5Sf	3	0	0	0	0	0	0	0	0	0	0	0	0	0	0	0	0	0	0	0	0	0	0	
04MV6S	2	0	0	0	0	3	0	0	0	0	0	0	0	0	0	0	0	0	1	0	0	2	0	
04KC6Sa	0	0	0	0	0	5	0	0	0	0	0	0	0	0	0	0	0	0	0	0	0	0	0	
04KC6Sb	1	0	0	3	0	9	0	0	0	0	0	0	0	2	0	0	0	1	0	0	0	0	0	
04KC6Sc	0	0	0	0	0	27	0	0	0	0	0	0	0	0	0	0	0	2	0	0	0	0	0	
04KC6Sd	0	0	0	0	0	2	0	0	0	0	0	0	0	0	0	0	0	0	0	0	0	0	0	
04DEF6Sa	6	0	0	0	0	0	0	0	0	0	0	0	0	0	0	0	0	1	0	0	0	0	0	
04DEF6Sb	0	0	0	0	0	6	0	0	0	0	0	0	0	0	0	0	1	0	0	0	0	0	0	
04DEF6Sc	0	0	0	0	0	5	0	0	0	0	0	0	0	0	0	0	4	1	0	0	0	0	0	
04DEF6Sd	0	0	0	0	0	0	0	0	0	0	0	0	0	0	0	0	0	0	0	0	0	0	0	
04DEF6Se	0	0	0	0	0	3	0	0	0	0	0	0	0	0	0	0	0	0	0	0	0	0	0	
04DEF6Sf	0	0	0	0	0	13	0	0	0	0	0	0	0	0	0	0	0	0	0	0	0	0	0	
04DEF6Sg	0	0	0	0	0	17	0	0	0	0	0	0	0	0	0	0	0	0	0	0	0	0	0	
04DEF6Sh	0	0	0	0	0	27	0	0	0	0	0	0	0	0	0	0	0	0	0	0	0	0	0	
04GLC6Sa	0	0	0	0	0	3	0	0	0	0	0	0	0	0	0	0	0	0	0	0	0	0	0	
04GLC6Sb	0	0	0	0	0	0	0	0	0	0	0	0	0	0	0	0	0	0	0	0	0	0	0	
04GLC6Sc	1	0	0	0	0	0	0	0	0	0	0	0	0	0	0	0	1	0	0	0	0	0	0	
04GLC6Sd	0	0	0	0	0	1	0	0	0	0	0	0	0	0	0	0	0	1	0	0	0	0	0	
04GLC6Se	0	0	0	0	0	2	0	0	0	0	0	0	0	0	0	0	0	0	0	0	0	0	0	
04BB6Sa	0	0	0	0	0	0	0	0	0	0	0	0	0	0	0	0	0	0	0	0	0	0	0	
04BB6Sb	0	0	0	0	0	0	0	0	0	0	0	0	0	0	0	0	0	0	0	0	1	0	0	
04BB6Sc	4	0	0	0	0	0	0	0	0	0	0	0	0	0	0	0	0	0	0	0	1	0	0	
04BB6Sd	2	0	0	0	0	0	0	0	0	0	0	0	0	0	0	0	0	0	0	0	0	0	0	
04BB6Se	0	0	0	0	0	0	0	0	0	0	0	0	0	0	0	0	0	0	0	0	2	0	0	
04HH6Sa	0	0	0	0	0	0	0	0	0	0	0	0	0	0	0	0	1	0	0	0	0	0	0	
04HH6Sb	1	0	0	0	0	6	0	0	0	0	0	0	0	0	0	0	0	0	0	0	0	0	0	
04RC6Sa	4	0	0	0	0	6	0	0	0	0	0	0	0	0	0	0	0	1	0	0	0	0	0	
04RC6Sb	0	0	0	0	0	1	0	0	0	0	0	0	0	0	0	0	0	0	0	0	0	0	0	
04RC6Sc	0	0	0	0	0	0	0	0	0	0	0	0	0	0	0	0	0	0	0	0	0	0	0	
04RC6Sd	0	0	0	0	0	3	0	0	0	0	0	0	0	0	0	0	0	0	0	0	0	0	0	
04RC6Se	5	0	0	0	0	0	0	0	0	0	0	0	0	0	0	0	0	0	0	0	0	0	0	
04RR6Sa	0	0	0	0	0	2	0	0	0	0	0	0	0	0	1	0	0	4	0	0	0	0	0	
04RR6Sb	0	0	0	0	0	5	0	0	0	0	0	0	0	0	0	0	0	2	0	0	0	0	0	
04RR6Sc	1	0	0	0	0	0	0	0	0	0	0	0	0	0	0	0	0	3	0	0	0	0	0	
04RR6Sd	0	0	0	0	0	0	0	0	0	0	0	0	0	0	0	0	0	0	0	0	0	4	0	0
04MGS6Sa	1	0	0	0	0	9	0	0	0	0	0	0	0	0	0	0	0	0	0	0	0	0	0	
04MGS6Sb	0	0	0	0	0	21	0	0	0	0	0	0	0	0	0	0	0	1	0	0	0	0	0	
04MGS6Sc	2	0	0	0	0	3	0	0	0	0	0	0	0	0	0	0	0	0	0	0	0	0	0	
04FM5D	0	0	0	0	0	0	0	0	0	0	0	0	0	0	0	0	0	0	0	0	0	0	0	
04FM4S	0	0	0	0	0	0	0	0	0	0	0	0	0	0	0	0	0	0	0	0	0	0	0	
04AB6Sa	0	0	0	0	0	9	0	0	0	0	0	0	0	0	0	0	0	0	0	0	0	0	0	
04AB6Sb	0	0	0	0	0	4	0	0	0	0	0	0	0	0	0	0	2	0	0	0	0	0	0	
04AB6Sc	0	0	0	0	0	1	0	0	0	0	0	0	0	0	0	0	0	0	0	0	0	0	0	
04SGC6Sa	0	0	0	0	0	10	0	0	0	0	0	0	0	0	0	0	0	0	0	0	0	0	0	
04SGC6Sb	0	0	0	0	0	1	0	0	0	0	0	0	0	0	0	0	0	0	0	0	1	0	0	
04DW6S	0	0	0	0	0	0	0	0	0	0	0	0	0	0	0	0	0	0	0	0	0	0	0	
04DF6Sa	0	0	0	0	0	1	0	0	0	0	0	0	0	0	0	0	0	0	0	0	0	0	0	

	Lophospira	*Maclurites*	*Sinuites*	*Gastropoda indet.*	*Cyclora*	*Ambonychia*	*Ctenodonta*	*Cunemya*	*Cyrtodonta*	*Cyrtodontula*	*Deceptrix*	*Ischyrodonta*	*modiomorph*	*Lyrodesma*	*Paleoneilo*	*Whitella*	*Bivalvia indet.*	*Ieperditid ostracod*	*Columnaria*	*Streptelasma*	*Tetradium*	*Stromatoporoidea*	*Chasmatopora*	*Constellaria*
04MV5Sb	13	0	0	0	0	0	0	0	0	0	0	0	0	0	0	0	0	0	0	0	0	0	0	0
04IPR5D	0	0	0	0	0	0	0	0	0	0	0	0	0	0	0	0	0	0	0	0	0	0	0	0
04DEF5S	0	0	0	0	0	0	0	0	0	0	0	0	0	0	0	0	0	0	0	0	0	0	0	0
04FR5Sa	0	0	0	0	0	0	0	0	0	0	0	0	0	0	0	0	0	0	0	0	0	0	0	0
04FR5Sb	0	0	0	0	0	0	0	0	0	0	0	0	0	0	0	0	0	0	0	0	0	0	0	0
04CAR5Sa	0	0	0	0	0	0	0	0	0	0	0	0	0	0	0	0	0	3	0	0	0	0	0	0
04CAR5Sb	0	0	0	0	0	0	0	0	0	0	0	0	0	0	0	0	0	0	0	0	0	0	0	0
04CAR5Sc	12	0	0	0	0	0	0	0	0	0	0	0	0	0	0	0	0	0	0	0	0	0	0	0
04CAR5Sd	3	0	0	1	0	0	0	0	0	0	0	0	0	0	0	0	0	0	0	0	0	0	0	0
04CAR5Se	0	0	0	0	0	0	0	0	0	0	0	0	0	0	0	0	0	0	0	0	0	0	0	0
04CAR5Sf	0	0	0	0	0	0	0	0	0	0	0	0	0	0	0	1	0	3	0	0	0	0	0	0
04MV6S	5	0	0	0	0	0	0	0	15	0	0	0	0	5	0	0	0	0	0	0	0	0	0	0
04KC6Sa	0	0	0	0	0	0	0	0	0	0	0	0	0	0	0	0	0	0	0	0	0	0	0	0
04KC6Sb	0	0	0	0	0	0	0	0	0	0	0	0	0	0	0	0	0	0	0	0	0	0	0	0
04KC6Sc	0	0	0	0	0	0	0	0	0	0	0	0	0	0	0	0	0	0	0	0	0	0	0	0
04KC6Sd	0	0	0	0	0	0	0	0	0	0	0	0	0	0	0	0	0	0	18	0	0	0	0	0
04DEF6Sa	0	0	0	0	0	0	0	0	0	0	0	0	0	0	0	0	0	0	0	0	0	0	0	0
04DEF6Sb	0	0	0	0	0	0	0	0	0	0	0	0	0	0	0	0	0	0	0	0	0	0	0	0
04DEF6Sc	0	0	0	0	0	0	0	0	0	0	0	0	0	0	0	0	0	0	0	0	0	0	0	5
04DEF6Sd	0	0	0	0	0	0	0	0	0	0	0	0	0	0	0	0	0	0	0	0	0	0	0	0
04DEF6Se	0	0	0	0	0	0	0	0	0	0	0	0	0	0	0	0	0	0	0	0	0	0	0	0
04DEF6Sf	0	0	0	0	0	0	0	0	0	0	0	0	0	0	0	0	0	0	0	0	0	0	0	0
04DEF6Sg	0	0	0	0	0	0	0	0	0	0	0	0	0	0	0	0	0	0	0	0	0	0	0	0
04DEF6Sh	0	0	0	0	0	0	0	0	0	0	0	0	0	0	0	0	0	0	0	0	0	0	0	0
04GLC6Sa	1	0	0	0	0	0	0	0	0	0	0	0	0	0	0	0	0	0	0	0	0	0	0	0
04GLC6Sb	0	0	0	0	0	0	0	0	0	0	0	0	0	0	0	0	0	0	0	0	0	0	0	0
04GLC6Sc	0	0	0	0	0	0	0	0	0	0	0	0	0	0	0	0	0	0	0	0	0	0	0	0
04GLC6Sd	0	0	0	0	0	0	0	0	0	0	0	0	0	0	0	0	0	1	0	0	0	0	0	0
04GLC6Se	0	0	0	0	0	0	0	0	0	0	0	0	0	0	0	0	0	0	0	0	0	0	0	0
04BB6Sa	0	0	0	0	0	0	0	0	0	0	0	0	0	0	0	0	0	0	0	0	0	0	0	0
04BB6Sb	0	0	0	0	0	0	0	0	0	0	0	0	0	0	0	0	0	2	0	0	0	0	0	0
04BB6Sc	0	0	0	0	0	0	0	0	0	0	0	0	0	0	0	0	0	0	0	0	0	2	1	0
04BB6Sd	0	0	0	0	0	0	0	0	0	0	0	0	0	0	0	0	0	0	0	0	0	0	0	0
04BB6Se	0	0	0	0	0	0	0	0	0	0	0	0	0	0	0	0	0	0	0	0	0	0	0	0
04HH6Sa	0	0	0	0	0	0	0	0	0	0	0	0	0	0	0	0	0	0	0	0	0	0	0	0
04HH6Sb	0	0	0	0	0	0	0	0	0	0	0	0	0	0	0	0	0	0	0	0	0	0	0	0
04RC6Sa	2	0	0	0	0	0	0	0	0	0	0	0	0	0	0	0	0	0	0	0	0	0	0	0
04RC6Sb	0	0	0	0	0	0	0	0	0	0	0	0	0	0	0	0	0	0	0	0	0	0	0	14
04RC6Sc	0	0	0	0	21	0	0	0	0	0	0	0	0	0	0	0	0	0	0	0	0	0	0	0
04RC6Sd	0	0	0	0	0	0	0	0	0	0	0	0	0	0	0	0	0	0	0	0	0	0	0	0
04RC6Se	0	0	0	0	0	0	0	0	0	0	0	0	0	0	0	0	0	0	0	0	0	0	0	0
04RR6Sa	1	0	0	0	0	0	0	0	0	0	0	0	0	0	0	0	0	0	0	0	0	0	0	0
04RR6Sb	0	0	0	0	0	0	0	0	0	0	0	0	0	0	0	0	0	0	0	0	0	0	0	0
04RR6Sc	0	0	0	0	0	0	0	0	0	0	0	0	0	0	0	0	0	0	0	0	0	0	0	0
04RR6Sd	25	0	0	0	0	0	0	0	0	0	0	0	0	0	0	0	0	0	0	0	0	0	0	0
04MGS6Sa	0	0	0	0	0	1	0	0	0	0	0	0	0	0	0	0	0	0	0	0	0	0	0	0
04MGS6Sb	0	0	0	0	0	0	0	0	0	0	0	0	0	0	0	0	0	0	0	0	0	0	0	0
04MGS6Sc	0	0	0	0	0	13	0	1	0	0	0	0	1	0	0	0	0	0	0	0	0	0	0	23
04FM5D	0	0	0	0	0	0	0	3	1	1	0	0	0	0	0	0	1	0	0	0	0	0	0	0
04FM4S	2	5	0	0	0	0	0	0	0	0	0	0	0	0	0	0	0	2	0	0	3	0	0	0
04AB6Sa	0	0	0	0	0	0	0	0	0	0	0	0	0	0	0	0	0	0	0	0	0	0	0	0
04AB6Sb	0	0	0	0	0	0	0	0	0	0	0	0	0	0	0	0	0	0	0	0	0	0	0	0
04AB6Sc	0	0	0	0	0	0	0	0	0	0	0	0	0	0	0	0	0	0	0	0	0	0	0	0
04SGC6Sa	0	0	0	0	0	0	0	0	0	0	0	0	0	0	0	0	0	0	0	0	0	0	0	0
04SGC6Sb	0	0	0	0	0	0	0	0	0	0	0	0	0	0	0	0	0	0	0	0	0	0	0	0
04DW6S	0	0	0	0	0	0	0	0	0	0	0	0	0	0	0	0	0	0	0	0	0	0	0	0
04DF6Sa	0	0	0	0	0	0	0	0	0	0	0	0	0	0	0	0	0	0	0	0	0	0	0	0

	Escharopora	*Heterotrypa*	*Prasopora*	*Rhindictya*	*massive trepostome*	*bifoliate bryozoan*	*bumpy ramose*	*encrusting bryozoan*	*thick ramose*	*thin ramose 1*	*thin ramose 2*	*cog crinoid*	*cog star crinoid*	*thin ring crinoid*	*thick ring crinoid*	*flower crinoid*	*pentagonal crinoid*	*stacked crinoid*	*star crinoid*	*inner star crinoid*	*striped crinoid*	*striped flower crinoid*	*striped star crinoid*	*crinoidea indet.*
04MV5Sb	2	0	0	0	0	0	0	0	3	1	0	0	0	0	0	0	0	0	0	0	0	0	0	0
04IPR5D	3	0	0	0	0	0	0	10	0	0	0	0	0	0	0	0	0	0	0	0	0	0	0	0
04DEF5S	2	0	0	0	0	0	0	1	0	0	0	0	0	3	0	0	0	0	0	0	0	0	0	0
04FR5Sa	3	0	0	0	0	0	0	0	167	0	0	0	0	1	0	0	0	0	0	0	0	0	0	0
04FR5Sb	1	0	2	0	0	0	0	0	11	17	0	0	0	3	0	0	0	0	0	0	0	0	0	0
04CAR5Sa	0	0	0	0	0	0	0	0	3	0	1	0	0	0	0	0	0	0	0	0	0	0	0	0
04CAR5Sb	3	0	0	1	0	0	0	0	10	10	0	0	0	0	1	0	0	0	0	0	0	0	0	0
04CAR5Sc	0	2	0	0	0	0	0	0	0	0	2	0	0	0	0	0	0	0	0	0	0	0	0	0
04CAR5Sd	0	0	0	0	0	0	0	0	0	0	0	0	0	1	0	0	0	0	0	0	0	0	0	0
04CAR5Se	0	0	0	0	0	0	0	0	42	0	0	0	0	0	0	0	0	0	0	0	0	0	0	0
04CAR5Sf	0	0	0	0	0	0	0	0	5	0	0	0	0	0	0	0	0	0	0	0	0	0	0	0
04MV6S	0	0	1	0	0	0	0	0	10	6	0	0	0	0	0	0	0	0	0	0	0	0	0	0
04KC6Sa	4	0	0	8	0	0	0	0	3	18	0	0	0	0	6	0	0	0	0	0	0	0	0	0
04KC6Sb	27	0	0	0	0	0	0	0	16	21	0	3	0	3	3	1	0	0	0	0	0	0	0	0
04KC6Sc	4	0	0	4	0	0	0	0	9	12	0	1	0	3	0	0	0	0	0	0	1	0	0	0
04KC6Sd	1	0	0	0	0	0	0	0	6	0	0	0	0	0	0	0	0	0	0	0	0	0	0	0
04DEF6Sa	0	0	0	0	0	0	0	0	0	0	0	0	0	1	0	0	0	0	0	0	0	0	0	0
04DEF6Sb	0	0	0	0	0	0	0	0	11	13	0	0	0	0	3	0	0	0	0	0	0	0	0	0
04DEF6Sc	0	0	0	0	0	0	0	0	10	10	5	0	0	0	3	0	0	0	0	0	0	0	0	0
04DEF6Sd	0	0	0	0	0	0	0	0	7	0	0	0	0	0	0	0	0	0	0	0	0	0	0	0
04DEF6Se	1	0	0	0	0	0	0	3	2	10	0	0	0	1	0	0	0	0	0	0	0	0	0	0
04DEF6Sf	3	0	0	0	0	0	0	0	7	1	0	1	0	1	0	0	0	0	0	0	0	0	0	0
04DEF6Sg	20	0	0	0	0	0	0	0	8	45	0	0	0	0	0	0	0	0	0	0	0	0	0	0
04DEF6Sh	15	0	0	0	0	0	0	5	0	27	0	0	0	0	0	0	0	0	0	0	0	0	0	0
04GLC6Sa	0	0	1	0	0	0	0	0	8	0	0	0	0	1	0	0	0	0	0	0	0	0	0	0
04GLC6Sb	0	0	0	0	0	0	0	0	4	0	0	0	0	0	0	0	0	0	0	0	0	0	0	0
04GLC6Sc	0	0	0	0	0	0	0	0	2	0	0	0	0	0	0	0	0	0	0	0	0	0	0	0
04GLC6Sd	0	0	0	0	0	0	0	0	3	0	0	0	0	0	3	0	0	0	0	1	0	0	0	0
04GLC6Se	0	0	0	0	0	0	0	0	2	11	0	0	0	0	0	0	0	0	0	0	0	0	0	0
04BB6Sa	1	0	0	1	0	0	0	0	32	0	0	0	0	0	0	0	0	0	0	0	0	0	0	0
04BB6Sb	0	0	0	0	0	0	0	0	8	0	0	0	0	0	0	0	0	0	0	0	0	0	0	0
04BB6Sc	0	0	0	0	0	0	0	0	2	0	0	0	0	0	0	0	0	0	0	0	0	0	0	0
04BB6Sd	0	0	7	0	0	0	0	0	112	0	0	0	0	0	0	0	0	0	0	0	0	0	0	0
04BB6Se	0	0	0	0	0	0	0	0	1	0	0	0	0	0	0	0	0	0	0	0	0	0	0	0
04HH6Sa	0	0	0	0	0	0	0	0	11	0	0	0	0	0	0	0	0	0	0	0	0	0	0	0
04HH6Sb	5	0	0	1	0	0	0	0	21	0	0	0	0	0	0	0	0	0	0	0	0	0	0	0
04RC6Sa	0	0	0	0	0	0	0	0	3	0	0	0	0	0	0	0	0	0	0	0	0	0	0	0
04RC6Sb	1	0	0	0	0	0	0	0	6	7	0	0	0	0	0	0	0	0	0	0	0	0	0	0
04RC6Sc	8	0	0	0	0	0	0	0	0	7	2	1	0	0	3	0	0	0	0	0	0	0	0	0
04RC6Sd	11	0	0	6	0	0	0	0	15	4	5	0	0	0	1	0	0	0	0	0	0	0	0	0
04RC6Se	8	0	0	1	0	0	0	0	14	11	10	0	0	0	0	0	0	0	0	0	0	0	0	0
04RR6Sa	0	0	0	0	0	0	0	0	11	1	0	0	0	0	0	0	0	0	0	0	0	0	0	0
04RR6Sb	0	0	1	0	0	0	0	0	14	0	0	0	0	0	0	0	0	0	0	0	0	0	0	0
04RR6Sc	0	0	0	0	0	0	0	0	2	0	0	0	0	0	0	0	0	0	0	0	0	0	0	0
04RR6Sd	0	0	0	0	0	0	0	0	1	0	0	0	0	0	0	0	0	0	0	0	0	0	0	0
04MGS6Sa	0	0	1	0	0	2	0	0	2	1	0	0	0	0	0	0	0	0	0	0	0	0	0	0
04MGS6Sb	0	0	0	0	0	0	0	0	9	0	0	0	0	0	0	0	0	0	0	0	0	0	0	0
04MGS6Sc	5	0	1	0	0	0	0	0	9	11	0	0	0	0	0	0	0	0	0	0	0	0	0	0
04FM5D	0	0	0	0	0	0	0	0	10	1	0	0	0	0	1	0	1	0	0	0	0	0	0	0
04FM4S	0	0	0	0	0	0	0	0	0	0	0	0	0	0	0	0	0	0	0	0	0	0	0	0
04AB6Sa	0	0	0	0	0	0	0	0	6	12	0	0	0	0	3	0	0	0	0	0	0	0	0	0
04AB6Sb	1	0	0	0	0	0	6	0	22	3	0	0	0	0	3	0	0	0	0	0	0	0	0	0
04AB6Sc	0	0	0	0	0	9	0	0	3	0	0	0	0	0	0	0	0	0	0	0	0	0	0	0
04SGC6Sa	0	0	0	0	0	5	0	0	3	3	0	0	0	0	0	0	0	0	0	0	0	0	0	0
04SGC6Sb	0	0	0	0	0	0	0	0	26	0	0	0	0	0	0	0	0	0	0	0	0	0	0	0
04DW6S	1	0	0	0	0	0	0	0	13	0	0	0	0	0	0	0	0	0	0	0	0	0	0	0
04DF6Sa	0	0	0	0	0	0	0	0	55	19	0	0	0	0	3	0	0	0	0	0	0	0	0	0

	Echinodermata indet.	*orthoconic nautiloids*	*algal coating*	*Solenopora*	*Stromatoporoids*	*Chondrites*	*Diplocriterion*	*Cornulites*	*alga(Hindia?)*	*rhombiferan plate*	*graptolites*
04MV5Sb	0	0	0	0	0	0	0	0	0	0	0
04IPR5D	0	0	0	0	0	0	0	0	0	0	0
04DEF5S	0	0	0	0	0	3	0	0	0	0	0
04FR5Sa	0	0	0	0	0	0	0	0	0	0	0
04FR5Sb	0	0	0	0	0	0	0	0	0	0	0
04CAR5Sa	0	0	0	0	0	0	0	0	0	0	0
04CAR5Sb	0	0	0	0	0	0	0	0	0	0	0
04CAR5Sc	0	0	0	0	0	0	0	0	0	0	0
04CAR5Sd	0	0	0	0	0	0	0	0	0	0	0
04CAR5Se	0	0	0	0	0	0	0	0	0	0	0
04CAR5Sf	0	0	0	0	0	0	0	0	0	0	0
04MV6S	0	0	0	0	0	0	0	0	0	0	0
04KC6Sa	0	0	0	0	0	0	0	0	0	0	0
04KC6Sb	0	0	0	0	0	0	0	0	0	0	0
04KC6Sc	0	0	0	0	0	0	0	0	0	0	0
04KC6Sd	0	0	0	0	0	0	0	0	0	0	0
04DEF6Sa	0	2	0	0	0	0	0	0	0	0	0
04DEF6Sb	0	1	0	0	0	0	0	0	0	0	0
04DEF6Sc	0	0	0	0	0	0	0	0	0	0	0
04DEF6Sd	0	0	0	0	0	0	0	0	0	0	0
04DEF6Se	0	0	0	0	0	0	0	0	0	0	0
04DEF6Sf	0	0	0	0	0	0	0	0	0	0	0
04DEF6Sg	0	0	0	0	0	0	0	0	0	0	0
04DEF6Sh	0	0	0	0	0	0	0	0	0	0	0
04GLC6Sa	0	0	0	0	0	0	0	0	0	0	0
04GLC6Sb	0	0	0	0	0	0	0	0	0	0	0
04GLC6Sc	0	0	0	0	0	0	0	0	0	0	0
04GLC6Sd	0	0	0	0	0	0	0	0	0	0	0
04GLC6Se	0	0	0	0	0	0	0	0	0	0	0
04BB6Sa	0	0	0	0	0	0	0	0	0	0	0
04BB6Sb	0	0	0	0	0	0	0	0	0	0	0
04BB6Sc	0	0	0	0	0	0	0	0	0	0	0
04BB6Sd	0	0	0	0	0	0	0	0	0	0	0
04BB6Se	0	0	0	0	0	0	0	0	0	0	0
04HH6Sa	0	0	0	0	0	0	0	0	0	0	0
04HH6Sb	0	0	0	0	0	0	0	0	0	0	0
04RC6Sa	0	0	0	0	0	0	0	0	0	0	0
04RC6Sb	0	0	0	0	0	0	0	0	0	0	0
04RC6Sc	0	0	0	0	0	0	0	0	0	0	0
04RC6Sd	0	0	0	0	0	0	0	0	0	0	0
04RC6Se	0	0	0	0	0	0	0	0	0	0	0
04RR6Sa	0	0	0	0	0	0	0	0	0	0	0
04RR6Sb	0	0	0	0	0	0	0	0	0	0	0
04RR6Sc	0	0	0	0	0	0	0	0	0	0	0
04RR6Sd	0	0	0	0	0	0	0	0	0	0	0
04MGS6Sa	0	0	0	0	0	0	0	0	0	0	0
04MGS6Sb	0	0	0	0	0	0	0	0	0	0	0
04MGS6Sc	0	0	0	0	0	0	0	0	0	0	0
04FM5D	0	0	0	0	0	0	0	0	0	0	0
04FM4S	0	0	0	0	0	0	0	0	0	0	0
04AB6Sa	0	0	0	0	0	0	0	0	0	0	0
04AB6Sb	0	0	0	20	0	0	0	0	0	0	0
04AB6Sc	0	0	0	0	0	0	0	0	0	0	0
04SGC6Sa	0	0	0	0	0	0	0	0	0	0	0
04SGC6Sb	0	0	0	0	0	0	0	0	0	0	0
04DW6S	0	0	0	0	0	0	0	0	0	0	0
04DF6Sa	0	0	0	0	60	0	0	0	0	0	0

	Anazyga	*Bilobia*	*Camerella*	*Christiana*	*Dalmanella*	*Dinorthis*	*Doleroides*	*Eoplectodonta*	*Glyptorthis*	*Hebertella*	*Hesperorthis*	*Heterorthina*	*Leptaena*	*Lingula*	*Multicostella*	*Oepikina*	*Orthorhyncula*	*Oxoplecia*	*Paucicrura*	*Paurorthis*	*Pionodema*	*Platystrophia*	*Plectocamara*	*Rafinesquina*
04DF6Sb	0	0	0	0	0	0	0	0	0	5	0	0	0	0	0	0	0	0	0	0	0	0	0	1
04FB4S	0	0	0	0	0	0	0	0	0	0	0	0	0	0	0	0	0	0	0	0	0	0	0	0
04FB5Da	0	0	0	0	0	0	0	0	0	0	0	0	0	0	0	0	0	0	0	0	0	0	0	4
04FB5Db	0	0	0	0	0	0	0	0	0	0	0	0	0	0	0	0	0	0	0	0	0	0	0	0
04FB5Dc	0	0	0	0	0	0	0	0	0	0	1	0	0	0	0	0	0	0	0	0	0	0	0	0
04FB5Dd	0	0	0	0	0	0	0	0	0	0	0	0	0	0	0	0	0	0	0	0	0	0	0	0
04OW6Sa	0	0	0	0	0	0	0	0	0	0	0	0	0	0	0	0	0	0	0	0	0	0	0	0
04OW6Sb	0	0	0	0	0	0	0	0	0	0	0	0	0	0	0	0	0	0	0	0	0	0	0	0
04OW6Sc	0	0	0	0	0	0	0	0	0	3	0	0	0	0	0	0	11	0	0	0	0	0	0	0
04OW6Sd	0	0	0	0	0	0	0	0	0	0	0	0	0	0	0	0	0	0	0	0	0	0	0	0
04OW6Se	0	0	0	0	0	0	0	0	0	1	0	0	0	0	0	0	11	0	0	0	0	0	0	0
04OW6Sf	0	0	0	0	0	0	0	0	0	4	0	0	0	0	0	0	2	0	0	0	0	0	0	0
04OW6Sg	0	0	0	0	0	0	0	0	0	1	1	0	0	0	0	0	0	0	0	0	0	0	0	0
04OW6Da	0	0	0	0	0	0	0	0	0	0	0	0	0	0	0	0	0	0	0	0	0	0	0	0
04OW6Db	0	0	0	0	0	0	0	0	0	0	0	0	0	0	0	0	0	0	0	0	0	0	0	0
04OW6Dc	0	0	0	0	0	0	0	0	0	1	0	0	0	0	0	0	0	0	0	0	0	0	0	4
04FN6S	0	0	0	0	0	0	0	0	0	1	0	0	0	0	0	0	0	0	0	0	0	0	0	0
04FN5Da	0	0	0	0	30	0	0	0	0	0	0	0	0	0	0	0	0	0	0	0	0	0	0	0
04FN5Db	0	0	0	0	14	0	0	0	0	0	0	0	0	0	0	0	0	0	0	0	0	0	0	1
04FN5Dc	0	0	0	0	9	0	0	0	0	0	0	0	0	0	0	0	0	0	0	0	0	0	0	2
04FN5Dd	0	0	0	0	4	0	0	0	0	2	0	0	0	0	0	0	0	0	0	0	0	0	0	2
04FN5De	0	0	0	0	3	0	0	0	1	1	0	0	0	0	0	0	0	0	0	0	0	0	0	11
04FN5Df	0	0	0	0	5	0	5	0	0	0	0	0	0	0	0	0	0	0	0	0	0	0	0	2
04FN5Dg	0	0	0	0	0	0	0	0	0	0	0	0	0	0	0	0	0	0	0	0	0	0	0	2
04FFW6Sa	0	0	0	0	0	0	0	0	0	0	0	0	0	0	0	0	0	0	0	0	0	0	0	0
04FFW6Sb	0	0	0	0	0	0	0	0	1	0	0	0	0	0	0	0	0	0	0	0	0	0	0	0
04FFW6Sc	0	0	0	0	0	0	0	0	0	0	1	0	0	0	0	0	0	0	0	0	0	1	0	0
04FFW6Sd	0	0	0	0	0	0	0	0	3	0	0	0	0	0	0	0	0	0	0	0	0	0	0	2
04FFW6Se	0	0	0	0	0	0	0	0	0	0	0	0	0	0	0	0	0	0	0	0	0	0	0	0
04FFW6Sf	0	0	0	0	0	0	0	0	0	0	0	0	0	0	0	0	0	0	0	0	0	0	0	0
04FFW6Sg	0	0	0	0	0	0	0	0	0	0	0	0	0	0	0	0	0	0	0	0	0	0	0	0
04DH5Da	0	0	0	0	8	0	0	0	0	0	0	0	0	0	0	0	0	0	0	0	0	0	0	0
04DH5Db	0	0	0	0	1	0	0	0	0	0	0	0	0	0	0	0	0	0	0	0	0	0	0	0
04DH5Sa	0	0	0	0	0	0	0	0	0	0	0	0	0	0	0	0	0	0	0	0	0	0	0	5
04DH5Sb	0	0	0	0	0	0	0	0	1	0	0	9	0	0	0	0	0	0	0	0	0	0	0	0
04DH5Sc	0	0	0	0	0	0	0	0	1	0	0	1	0	0	0	0	0	0	0	0	0	0	0	0
04DH6Sa	0	0	0	0	0	0	0	0	0	0	0	0	0	0	0	0	0	0	0	0	0	0	0	0
04DH6Sb	0	0	0	0	4	0	0	0	0	0	1	0	0	0	0	0	0	0	0	0	0	0	0	2
04FT6S	0	0	0	0	0	0	0	0	0	0	0	0	0	0	0	0	0	0	0	0	0	0	0	0
04FT5Da	0	0	0	0	24	0	0	0	0	1	0	1	0	0	0	0	0	0	0	0	0	0	0	2
04FT5Db	0	0	0	0	14	0	0	0	0	0	0	0	0	0	0	0	0	0	0	0	0	0	0	1
04FT5Dc	0	0	0	0	13	0	0	0	0	0	0	0	0	0	0	0	0	0	0	0	0	0	0	2
04FT5Dd	0	0	0	0	1	0	0	0	0	0	0	0	0	0	0	0	0	0	0	0	0	0	0	2
04FT5De	0	0	0	0	0	0	0	0	0	1	0	9	0	0	0	0	0	0	0	0	0	0	0	0
04FT5Sa	0	0	0	0	2	0	0	0	0	1	0	0	0	0	0	0	0	0	0	0	0	0	0	0
04FT5Sb	0	0	0	0	8	0	0	0	0	2	0	0	0	0	0	0	0	0	0	0	0	0	0	0
04FT5Sc	0	0	0	0	0	0	0	0	0	0	0	0	0	0	0	0	0	0	0	0	0	0	0	0
04FT5Sd	0	0	0	0	4	0	0	0	0	0	0	0	0	0	0	0	0	0	0	0	0	0	0	0
04VY5Sa	0	0	0	0	0	0	0	0	0	0	0	0	0	0	0	0	0	0	0	0	0	0	0	4
04VY5Sb	0	0	0	0	0	0	0	0	0	0	0	0	0	0	0	0	0	0	0	0	0	0	0	5
04VY5Sc	0	0	0	0	0	0	0	0	0	1	0	0	0	0	0	0	0	0	0	0	0	0	0	1
04VY5Sd	0	0	0	0	0	0	0	0	0	0	0	0	0	0	0	0	0	0	0	0	0	0	0	3
04VY5Se	0	0	0	0	4	0	0	0	0	0	0	0	0	0	0	0	0	0	0	0	0	0	0	2
04BCFD4Sa	0	0	0	0	0	0	0	0	0	0	2	0	0	0	0	0	0	0	0	0	0	0	0	0
04BCFD4Sb	0	0	0	0	0	0	0	0	0	0	1	0	0	0	0	0	0	0	0	0	0	0	0	0
04BCFD4Sc	0	0	0	0	0	0	0	0	0	0	3	0	0	0	0	0	0	0	0	0	0	0	0	0
04CNL4Sa	0	0	0	0	0	0	0	0	0	0	0	0	0	0	0	0	0	0	0	0	0	0	0	0

	Rhynchotrema	*Rostricellula*	*Schizotreta*	*Strophomena*	*Sowerbyella*	*Zygospira*	*Inarticulata indet.*	*rhynchonellid indet.*	*Brachiopoda indet.*	*Ceraurus*	*Cryptolithus*	*Eomonorachus*	*Flexicalymene*	*Gravicalymene*	*Isotelus*	*Pterygometopus*	*Trilobita A*	*Trilobita indet.*	*Isotelus spines*	*Bellerophon*	*Bucania*	*Cyclonema*	*Hormotoma*	*Liospira*
04DF6Sb	0	0	0	0	0	2	0	0	0	0	0	0	0	0	0	0	0	0	0	0	0	0	0	0
04FB4S	0	0	0	0	0	0	0	0	0	0	0	0	0	0	0	0	0	0	0	0	0	0	0	0
04FB5Da	0	0	0	0	0	1	0	0	0	0	0	0	0	0	0	0	0	0	0	0	0	0	0	0
04FB5Db	0	0	0	3	0	0	0	0	0	0	0	0	0	0	1	0	0	0	0	0	0	0	0	0
04FB5Dc	0	0	0	2	0	0	0	0	0	0	0	0	0	0	0	0	0	0	0	0	0	0	0	0
04FB5Dd	3	0	0	8	0	30	0	0	0	0	0	0	0	0	0	0	0	0	4	0	0	1	0	0
04OW6Sa	0	0	0	0	0	19	0	0	0	0	0	0	0	0	0	0	0	0	7	0	0	0	0	0
04OW6Sb	0	0	0	0	0	30	0	0	0	0	0	0	0	0	0	0	0	11	0	0	0	0	0	0
04OW6Sc	0	0	0	0	0	19	0	0	0	0	0	0	0	0	0	0	0	1	0	0	0	0	0	0
04OW6Sd	0	0	0	0	0	22	0	0	0	0	0	0	0	0	0	0	0	7	1	0	0	0	0	0
04OW6Se	0	0	0	0	0	20	0	0	0	0	0	0	0	0	0	0	0	1	0	0	0	0	0	0
04OW6Sf	0	0	0	0	0	20	0	0	0	0	0	0	0	0	0	0	0	1	0	0	0	0	0	0
04OW6Sg	0	0	0	0	0	11	0	0	0	0	0	0	0	0	0	0	0	0	0	0	0	0	0	0
04OW6Da	0	0	0	0	0	17	0	0	0	0	0	0	0	0	0	0	0	0	10	0	0	0	0	0
04OW6Db	0	0	0	0	0	68	0	0	0	0	0	0	0	0	0	0	0	0	5	0	0	1	0	0
04OW6Dc	0	0	0	0	0	3	0	0	0	0	0	0	0	0	0	0	0	0	4	0	0	0	0	0
04FN6S	2	0	0	0	0	2	0	0	0	0	0	0	0	0	0	0	0	0	0	0	0	0	0	0
04FN5Da	0	0	0	0	0	0	0	0	0	0	0	0	0	0	0	0	0	0	0	0	0	0	0	0
04FN5Db	0	0	0	0	0	2	0	0	0	0	0	0	0	0	0	0	0	0	0	0	0	0	0	0
04FN5Dc	0	0	0	0	0	0	0	0	0	0	0	0	0	0	0	0	0	0	0	0	0	0	0	0
04FN5Dd	0	0	0	0	0	0	0	0	0	0	0	0	0	0	0	0	0	0	0	0	0	0	0	0
04FN5De	0	0	0	0	0	0	0	0	0	0	0	0	0	0	0	0	0	1	0	0	0	0	0	0
04FN5Df	0	0	0	0	0	4	0	0	0	0	0	0	0	0	0	0	0	0	0	0	0	0	0	0
04FN5Dg	0	0	0	0	0	41	0	0	0	0	0	0	0	0	0	0	0	0	1	0	0	0	0	0
04FFW6Sa	0	0	0	0	0	0	0	0	0	0	0	0	0	0	0	0	0	0	0	0	0	1	1	0
04FFW6Sb	0	0	0	0	0	20	0	0	0	0	0	0	0	0	0	0	0	0	0	0	0	0	0	0
04FFW6Sc	2	0	0	0	0	56	0	0	0	0	0	0	0	0	0	0	0	0	2	0	0	0	0	0
04FFW6Sd	0	0	0	0	0	7	0	0	0	0	0	0	0	0	0	0	0	0	0	0	0	0	0	0
04FFW6Se	0	0	0	0	0	4	0	0	0	0	0	0	0	0	0	0	0	0	0	0	0	0	0	0
04FFW6Sf	31	0	0	0	0	2	0	0	0	0	0	0	0	0	0	0	0	0	0	0	0	0	0	0
04FFW6Sg	25	0	0	0	0	2	0	0	0	0	0	0	0	0	0	0	0	0	0	0	0	0	0	0
04DH5Da	0	0	0	0	0	19	0	0	0	0	0	0	0	0	0	0	0	0	3	0	0	0	0	0
04DH5Db	0	0	0	0	0	0	0	0	0	0	0	0	0	0	0	0	0	0	0	0	0	0	0	0
04DH5Sa	0	0	0	0	0	1	0	0	0	0	0	0	0	0	0	0	0	0	0	0	0	0	0	0
04DH5Sb	0	0	0	0	0	5	0	0	0	0	0	0	0	0	0	0	0	0	0	0	0	0	0	0
04DH5Sc	1	0	0	0	0	5	0	0	0	0	0	0	0	0	0	0	0	0	0	0	0	0	0	0
04DH6Sa	1	0	0	0	0	1	0	0	0	0	0	0	0	0	0	0	0	0	0	0	0	0	0	0
04DH6Sb	0	0	0	0	0	6	0	0	0	0	0	0	0	0	0	0	0	0	0	0	0	0	0	0
04FT6S	0	0	0	0	0	3	0	0	0	0	0	0	0	0	0	0	0	1	0	0	0	0	0	0
04FT5Da	0	0	0	0	0	0	0	0	0	0	0	0	0	0	0	0	0	0	0	0	0	0	0	0
04FT5Db	0	0	0	0	0	0	0	0	0	0	0	0	0	0	0	0	0	0	0	0	0	0	0	0
04FT5Dc	0	0	0	0	0	0	2	0	0	0	0	0	0	0	0	0	0	0	0	0	0	0	0	0
04FT5Dd	0	0	0	0	0	3	0	0	0	0	0	0	0	0	0	0	0	0	0	0	0	0	0	0
04FT5De	0	0	0	0	0	3	0	0	0	0	0	0	0	0	0	0	0	0	0	0	0	0	0	0
04FT5Sa	0	0	0	0	0	0	0	0	0	0	0	0	0	0	0	0	0	0	0	0	0	0	0	0
04FT5Sb	0	0	0	0	0	15	0	0	0	1	0	0	0	0	0	0	0	1	0	0	0	0	0	0
04FT5Sc	0	0	0	0	0	0	0	0	0	0	0	0	0	0	0	0	0	0	0	0	0	0	0	0
04FT5Sd	0	0	0	0	0	1	0	0	0	0	0	0	0	0	0	0	0	0	0	0	0	0	0	0
04VY5Sa	0	0	0	0	0	1	0	0	0	0	0	0	0	0	0	0	0	1	0	0	0	0	0	0
04VY5Sb	18	0	0	0	0	4	0	0	0	0	0	0	0	0	0	0	0	0	0	0	0	0	0	0
04VY5Sc	0	0	0	0	0	13	0	0	0	0	0	0	0	0	0	0	0	0	0	0	0	0	0	0
04VY5Sd	0	0	0	0	0	3	0	0	0	0	0	0	0	0	0	0	0	0	0	0	0	0	0	0
04VY5Se	0	0	0	0	0	20	0	0	0	0	0	0	0	0	0	0	0	1	0	0	0	0	0	0
04BCFD4Sa	0	0	0	1	0	10	0	0	0	0	0	0	0	0	1	0	0	0	0	0	0	0	0	0
04BCFD4Sb	0	0	0	6	0	0	0	0	0	0	0	0	0	0	0	0	0	0	0	0	0	0	0	0
04BCFD4Sc	0	0	0	11	0	1	0	0	0	0	0	0	0	0	0	0	0	0	0	0	0	0	0	0
04CNL4Sa	0	0	0	1	0	0	0	0	0	0	0	0	0	0	0	0	0	0	0	0	0	0	1	0

	Lophospira	*Maclurites*	*Sinuites*	*Gastropoda indet.*	*Cyclora*	*Ambonychia*	*Ctenodonta*	*Cunemya*	*Cyrtodonta*	*Cyrtodontula*	*Deceptrix*	*Ischyrodonta*	*modiomorph*	*Lyrodesma*	*Paleoneilo*	*Whitella*	*Bivalvia indet.*	*leperditid ostracod*	*Columnaria*	*Streptelasma*	*Tetradium*	*Stromatoporoidea*	*Chasmatopora*	*Constellaria*
04DF6Sb	1	0	0	0	0	0	0	0	0	0	0	0	0	0	0	0	0	0	0	0	0	0	0	22
04FB4S	0	0	0	2	0	0	0	0	0	0	0	0	0	0	0	0	0	5	0	0	0	0	0	0
04FB5Da	0	0	0	0	0	0	5	0	0	0	0	0	0	0	0	0	0	0	0	0	0	0	0	0
04FB5Db	4	0	0	0	0	1	0	0	0	0	0	0	0	0	0	0	0	0	0	0	0	0	0	0
04FB5Dc	0	0	0	0	0	1	0	0	0	0	0	0	1	0	0	0	0	0	0	0	0	0	0	0
04FB5Dd	0	0	0	0	0	0	0	0	0	0	0	0	0	0	0	0	0	0	0	0	0	0	0	0
04OW6Sa	3	0	0	0	0	0	0	0	0	0	0	0	0	0	0	0	0	0	0	0	0	0	0	0
04OW6Sb	0	0	0	0	0	0	0	0	0	0	0	0	0	0	0	0	0	0	0	0	0	0	0	0
04OW6Sc	0	0	0	0	0	0	0	0	0	0	0	0	0	0	0	0	0	0	0	0	0	0	0	0
04OW6Sd	0	0	0	0	0	0	0	0	0	0	0	0	0	0	0	1	0	0	0	0	0	0	0	0
04OW6Se	0	0	0	0	0	0	0	0	0	0	0	0	0	0	0	0	0	0	0	0	0	0	0	0
04OW6Sf	0	0	0	0	0	0	0	0	0	0	0	0	0	0	0	0	0	0	0	0	0	0	0	0
04OW6Sg	2	0	0	0	0	0	0	0	0	0	0	0	0	0	0	0	0	0	0	0	0	0	0	0
04OW6Da	30	0	0	0	0	0	0	0	0	0	0	0	0	0	0	0	0	0	0	0	0	0	0	0
04OW6Db	2	0	0	0	0	0	0	0	0	0	0	0	0	0	0	0	0	0	0	0	0	0	0	0
04OW6Dc	1	0	0	0	0	0	0	0	0	0	0	0	0	0	0	0	0	0	0	0	0	0	0	0
04FN6S	0	0	0	0	0	0	0	0	0	0	0	0	0	0	0	0	0	0	0	0	0	0	0	6
04FN5Da	0	0	0	0	0	0	0	0	0	0	0	0	0	0	0	0	0	0	0	0	0	0	0	0
04FN5Db	0	0	0	0	0	0	0	0	0	0	0	0	0	0	0	0	0	0	0	0	0	0	0	0
04FN5Dc	0	0	0	0	0	0	0	0	0	0	0	0	0	0	0	0	0	0	0	0	0	0	0	0
04FN5Dd	0	0	0	0	0	0	0	0	0	0	0	0	9	0	0	0	0	0	0	0	0	0	0	0
04FN5De	0	0	0	0	0	0	0	0	0	0	0	0	0	0	0	0	0	0	0	0	0	0	0	0
04FN5Df	0	0	0	0	0	0	0	0	0	0	0	0	0	0	0	0	0	0	0	0	0	0	0	0
04FN5Dg	0	0	2	1	0	0	0	0	0	0	0	0	0	0	0	0	0	0	0	0	0	0	0	0
04FFW6Sa	7	0	1	0	0	0	0	0	0	0	0	0	0	0	0	0	0	32	0	0	0	0	0	0
04FFW6Sb	0	0	0	0	0	0	0	0	0	0	0	0	0	0	0	0	0	0	0	0	0	0	0	0
04FFW6Sc	0	0	0	0	0	0	0	0	0	0	0	0	0	0	0	0	0	0	0	0	0	0	0	0
04FFW6Sd	0	0	0	0	0	1	0	0	0	0	0	0	0	0	0	0	0	0	0	0	0	0	0	0
04FFW6Se	0	0	0	0	0	0	0	0	0	0	0	0	0	0	0	0	0	0	0	0	0	0	0	0
04FFW6Sf	0	0	0	0	0	0	0	0	0	0	0	0	0	0	0	0	0	6	0	0	0	0	0	0
04FFW6Sg	0	0	0	0	0	0	0	0	0	0	0	0	0	0	0	0	0	7	0	0	0	0	0	0
04DH5Da	0	0	0	0	0	0	0	0	0	0	0	0	0	0	0	0	0	0	0	0	0	0	0	0
04DH5Db	0	0	0	0	0	0	0	0	0	0	0	0	0	0	0	0	0	0	0	0	0	0	0	0
04DH5Sa	0	0	0	0	0	0	0	0	0	0	0	0	0	0	0	0	0	0	0	0	0	0	0	0
04DH5Sb	1	0	0	0	0	0	0	0	0	0	2	0	0	0	0	0	0	0	0	0	0	0	0	0
04DH5Sc	0	0	0	0	0	0	0	0	0	0	0	0	0	0	0	0	0	0	0	0	0	0	0	0
04DH6Sa	0	0	0	0	0	0	0	0	0	0	0	0	0	0	0	0	0	0	0	0	0	0	0	0
04DH6Sb	0	0	0	0	0	0	0	0	0	0	0	0	0	0	0	0	0	0	0	0	0	0	0	0
04FT6S	0	0	0	0	0	0	0	0	0	0	0	0	0	0	0	0	0	0	0	0	0	0	0	15
04FT5Da	0	0	0	0	0	0	0	0	0	0	0	0	0	0	0	0	0	0	0	0	0	0	0	0
04FT5Db	0	0	0	0	0	0	0	2	0	0	1	0	0	0	0	0	1	0	0	0	0	0	0	0
04FT5Dc	0	0	0	0	0	0	0	2	0	0	0	0	0	0	0	0	0	0	0	0	0	0	0	0
04FT5Dd	0	0	0	0	0	0	0	0	0	0	0	0	0	0	0	0	0	0	0	0	0	0	0	0
04FT5De	0	0	0	0	0	0	0	0	0	0	0	0	7	0	0	1	4	0	0	0	0	0	0	0
04FT5Sa	0	0	0	0	0	0	0	0	0	0	0	0	0	0	0	0	0	0	0	0	0	0	0	0
04FT5Sb	0	0	0	0	0	0	0	0	0	0	0	0	0	0	0	0	0	0	0	0	0	0	0	0
04FT5Sc	0	0	0	0	0	0	0	0	0	0	0	0	0	0	0	0	0	0	0	0	0	0	0	0
04FT5Sd	0	0	0	0	0	0	0	0	0	0	0	0	0	0	0	0	0	0	0	0	0	0	0	0
04VY5Sa	0	0	0	0	0	0	0	0	0	0	0	0	0	0	0	0	0	0	0	0	0	0	0	0
04VY5Sb	0	0	0	0	0	0	0	0	0	0	0	0	0	0	0	0	0	0	0	0	0	0	0	0
04VY5Sc	0	0	0	0	0	0	0	0	0	0	0	0	0	0	0	0	0	0	0	0	0	0	0	0
04VY5Sd	1	0	1	0	0	0	0	0	0	0	0	0	0	0	0	0	0	1	0	0	0	0	0	0
04VY5Se	1	0	4	0	0	0	0	0	0	0	0	0	0	0	0	0	0	0	0	0	0	0	0	0
04BCFD4Sa	0	0	0	0	0	0	0	0	0	0	0	0	0	0	0	0	0	0	0	1	0	0	0	0
04BCFD4Sb	0	0	0	0	0	0	0	0	0	0	0	0	0	0	0	0	0	0	0	0	0	0	0	0
04BCFD4Sc	0	0	0	0	0	0	0	0	0	0	0	0	0	0	0	0	0	0	0	0	0	0	0	0
04CNL4Sa	5	2	0	0	0	0	0	0	0	0	0	0	0	0	0	0	0	0	0	1	73	0	0	0

	Escharopora	*Heterotrypa*	*Prasopora*	*Rhindictya*	*massive trepostome*	*bifoliate bryozoan*	*bumpy ramose*	*encrusting bryozoan*	*thick ramose*	*thin ramose 1*	*thin ramose 2*	*cog crinoid*	*cog star crinoid*	*thin ring crinoid*	*thick ring crinoid*	*flower crinoid*	*pentagonal crinoid*	*stacked crinoid*	*star crinoid*	*inner star crinoid*	*striped crinoid*	*striped flower crinoid*	*striped star crinoid*	*crinoidea indet.*
04DF6Sb	0	0	0	0	0	0	0	0	44	0	0	0	0	0	3	0	0	0	0	0	0	0	0	0
04FB4S	0	0	0	0	0	0	0	0	0	0	0	0	0	0	0	0	0	0	0	0	0	0	0	0
04FB5Da	1	0	0	0	0	0	0	0	16	4	0	0	0	0	0	0	0	0	0	0	0	0	0	0
04FB5Db	0	0	0	0	0	0	0	0	7	2	0	0	0	3	3	1	0	0	0	0	0	0	0	0
04FB5Dc	0	0	0	0	0	0	0	0	0	0	0	0	0	3	3	0	0	0	0	0	0	0	0	0
04FB5Dd	3	0	0	0	0	0	0	13	0	8	0	0	0	0	1	0	0	0	0	0	0	0	0	0
04OW6Sa	3	0	0	0	0	0	0	0	0	8	0	0	0	0	0	0	0	0	0	0	0	0	0	0
04OW6Sb	0	0	0	0	0	0	0	0	0	1	0	3	0	6	6	0	0	0	0	0	0	0	0	0
04OW6Sc	0	0	0	0	0	0	0	0	7	1	0	3	0	1	0	0	0	0	0	0	0	0	0	0
04OW6Sd	2	0	0	0	0	0	0	0	0	0	0	0	0	0	0	0	0	0	0	0	0	0	0	0
04OW6Se	0	0	0	0	0	0	0	0	14	0	0	0	0	3	3	0	0	0	0	0	0	0	0	0
04OW6Sf	0	0	0	0	0	0	0	0	0	15	0	3	0	3	3	0	0	0	0	0	0	0	0	0
04OW6Sg	2	0	0	18	0	0	0	5	3	1	0	0	3	6	0	6	3	0	6	0	0	0	0	0
04OW6Da	0	0	0	0	0	0	0	0	0	5	0	0	0	0	0	0	0	0	0	0	0	0	0	0
04OW6Db	0	0	0	1	0	0	0	0	0	3	0	0	0	0	0	0	0	0	0	0	0	0	0	0
04OW6Dc	0	0	0	0	0	0	0	0	7	0	0	0	0	0	0	0	0	0	0	0	0	0	0	0
04FN6S	0	0	0	0	0	0	0	0	22	0	0	0	0	0	1	0	0	0	0	0	0	0	0	0
04FN5Da	0	0	0	0	0	0	0	0	0	0	0	0	0	0	0	0	0	0	0	0	0	0	0	0
04FN5Db	1	0	0	0	0	0	0	0	0	11	0	0	0	0	1	0	0	0	0	0	0	0	0	0
04FN5Dc	3	0	0	2	0	0	0	2	0	1	0	0	0	0	0	0	0	0	0	0	0	0	0	0
04FN5Dd	2	0	1	0	0	0	0	2	5	7	0	3	0	3	0	0	1	1	3	0	0	0	0	0
04FN5De	2	0	3	0	0	0	0	0	0	23	0	3	0	0	3	0	0	1	0	0	0	0	0	0
04FN5Df	1	0	0	1	0	0	0	8	0	23	0	6	0	3	6	0	6	0	0	0	0	0	0	0
04FN5Dg	4	0	0	7	0	0	0	0	0	5	0	0	0	0	3	0	3	0	0	0	0	0	0	0
04FFW6Sa	0	0	0	0	0	0	0	0	0	0	0	0	0	0	0	0	0	0	0	0	0	0	0	0
04FFW6Sb	0	0	0	0	0	0	0	0	17	7	0	0	0	6	6	0	0	0	0	0	0	0	0	0
04FFW6Sc	1	0	0	0	0	0	0	0	18	1	0	3	0	3	0	0	0	0	0	0	1	0	0	0
04FFW6Sd	1	0	0	0	0	0	0	0	1	3	0	1	0	6	6	0	0	0	0	0	0	0	0	0
04FFW6Se	0	0	0	0	0	0	0	0	28	0	0	6	0	0	6	0	0	0	0	0	0	0	0	0
04FFW6Sf	1	0	0	0	0	0	0	0	6	0	0	0	0	1	0	0	0	0	0	0	0	0	0	0
04FFW6Sg	0	0	0	0	0	0	0	0	4	3	0	0	0	0	0	0	0	0	0	0	0	0	0	0
04DH5Da	0	0	2	0	0	0	0	0	2	2	0	0	0	0	0	0	0	0	0	0	0	0	0	0
04DH5Db	2	0	0	3	0	0	0	0	10	32	0	0	0	0	0	0	0	0	0	0	0	0	0	0
04DH5Sa	0	0	5	1	0	0	0	0	5	7	0	0	0	0	0	0	0	0	0	0	0	0	0	0
04DH5Sb	1	0	1	4	0	0	0	0	2	18	0	0	0	1	0	0	0	0	0	0	0	0	0	0
04DH5Sc	0	0	12	2	0	0	0	0	1	13	0	0	0	1	0	0	0	0	0	0	0	0	0	0
04DH6Sa	0	0	0	0	0	0	0	0	20	2	0	0	0	0	0	0	0	0	0	0	0	0	0	0
04DH6Sb	0	0	0	0	0	0	0	0	0	0	0	0	0	1	0	0	0	0	0	0	0	0	0	0
04FT6S	0	0	0	0	0	8	0	0	0	2	8	1	0	3	3	1	0	0	0	0	0	0	0	0
04FT5Da	0	0	0	0	0	0	0	0	0	0	0	0	0	0	0	0	0	0	0	0	0	0	0	0
04FT5Db	0	0	0	0	0	0	0	0	0	0	0	0	0	0	0	0	0	0	0	0	0	0	0	0
04FT5Dc	0	0	0	0	0	0	0	0	0	0	0	0	0	0	0	0	0	0	0	0	0	0	0	0
04FT5Dd	1	0	5	0	0	0	4	0	9	21	0	1	0	3	3	0	1	0	0	0	0	0	0	0
04FT5De	0	0	0	0	0	0	0	0	0	0	0	0	0	0	0	0	0	0	0	0	0	0	0	0
04FT5Sa	1	0	27	0	0	0	0	0	7	10	0	0	0	0	0	0	0	0	0	0	0	0	0	0
04FT5Sb	1	0	0	1	0	0	0	1	0	3	0	0	0	1	1	0	0	0	0	0	0	0	0	0
04FT5Sc	0	0	3	0	0	0	0	0	12	40	0	0	0	0	0	0	0	0	0	0	0	0	0	0
04FT5Sd	6	0	2	18	0	0	0	0	5	4	0	0	0	0	0	0	0	0	0	0	0	0	0	0
04VY5Sa	6	0	1	19	0	0	0	0	3	2	0	0	0	0	1	0	1	0	0	0	0	0	0	0
04VY5Sb	0	0	1	2	0	0	0	0	7	3	0	0	0	1	3	0	0	0	0	0	0	0	0	0
04VY5Sc	9	0	2	9	0	0	0	0	0	14	0	0	0	3	0	0	0	0	0	0	0	0	0	0
04VY5Sd	7	0	0	6	0	0	0	0	0	0	0	1	0	3	3	0	0	0	0	0	0	0	0	0
04VY5Se	0	0	0	7	0	0	0	0	0	35	0	1	0	3	6	0	0	0	0	0	0	0	0	0
04BCFD4Sa	5	0	0	0	0	0	0	0	10	0	0	0	0	1	1	0	0	0	0	0	0	0	0	0
04BCFD4Sb	0	0	0	0	0	0	0	0	4	0	0	0	0	3	0	0	0	0	0	0	0	0	0	0
04BCFD4Sc	0	0	0	0	0	0	0	0	5	2	0	0	0	3	3	0	0	0	1	0	0	0	0	0
04CNL4Sa	0	0	0	4	0	0	0	4	0	0	2	1	0	3	0	1	0	0	0	0	0	0	0	0

	Echinodermata indet.	*orthoconic nautiloids*	*algal coating*	*Solenopora*	*Stromatoporoids*	*Chondrites*	*Diplocriterion*	*Cornulites*	*alga(Hindia?)*	*rhombiferan plate*	*graptolites*
04DF6Sb	0	0	0	0	0	0	0	0	0	0	0
04FB4S	0	0	0	0	0	0	0	0	0	0	0
04FB5Da	0	0	0	0	0	0	0	0	0	0	0
04FB5Db	0	0	0	0	0	0	0	0	0	0	0
04FB5Dc	0	0	0	0	0	0	3	0	0	0	3
04FB5Dd	0	0	0	0	0	0	0	0	0	0	0
04OW6Sa	0	0	0	0	0	0	0	4	0	0	0
04OW6Sb	0	0	0	0	0	0	0	0	0	0	0
04OW6Sc	0	0	0	0	0	0	0	0	0	0	0
04OW6Sd	0	0	0	0	0	0	0	4	0	0	0
04OW6Se	0	0	0	0	0	0	0	0	0	0	0
04OW6Sf	0	0	0	0	0	0	0	0	0	0	0
04OW6Sg	0	0	0	0	0	0	0	0	0	0	0
04OW6Da	0	0	0	0	0	0	0	7	0	0	0
04OW6Db	0	0	0	0	0	0	0	4	0	0	0
04OW6Dc	0	0	0	0	0	0	0	1	0	0	0
04FN6S	0	0	0	0	0	0	0	0	0	0	0
04FN5Da	0	0	0	0	0	0	0	0	0	0	0
04FN5Db	0	1	0	0	0	0	0	0	0	0	0
04FN5Dc	0	0	0	0	0	0	0	0	0	0	0
04FN5Dd	0	0	0	0	0	0	0	0	0	0	0
04FN5De	0	0	0	0	0	0	0	0	0	0	0
04FN5Df	0	0	0	0	0	0	0	0	0	0	0
04FN5Dg	0	0	0	0	0	0	0	0	0	0	0
04FFW6Sa	0	0	0	0	0	0	0	0	0	0	0
04FFW6Sb	0	0	0	0	0	0	0	0	0	0	0
04FFW6Sc	0	0	0	0	0	0	0	0	0	0	0
04FFW6Sd	0	0	0	0	0	0	0	0	0	0	0
04FFW6Se	0	0	0	0	0	0	0	0	0	0	0
04FFW6Sf	0	0	0	0	0	0	0	0	0	0	0
04FFW6Sg	0	0	0	0	0	0	0	0	0	0	0
04DH5Da	0	0	0	0	0	0	0	0	0	0	0
04DH5Db	0	0	0	0	0	0	0	0	0	0	0
04DH5Sa	0	0	0	0	0	0	0	0	0	0	0
04DH5Sb	0	0	3	0	0	0	0	0	0	0	0
04DH5Sc	0	0	0	0	0	0	0	0	0	0	0
04DH6Sa	0	0	0	0	0	0	0	0	0	0	0
04DH6Sb	0	0	0	0	0	0	0	0	0	0	0
04FT6S	0	0	0	0	0	0	0	0	0	0	0
04FT5Da	0	0	0	0	0	0	0	0	0	0	0
04FT5Db	0	0	0	0	0	0	0	0	0	0	0
04FT5Dc	0	0	0	0	0	0	0	0	0	0	0
04FT5Dd	0	0	0	0	0	0	0	0	0	0	0
04FT5De	0	0	0	0	0	0	0	0	0	0	0
04FT5Sa	0	0	0	0	0	0	0	0	0	0	0
04FT5Sb	0	0	0	0	0	0	0	0	0	0	0
04FT5Sc	0	0	0	0	0	0	0	0	0	0	0
04FT5Sd	0	0	0	0	0	0	0	0	0	0	0
04VY5Sa	0	0	0	0	0	0	0	0	0	0	0
04VY5Sb	0	0	0	0	0	0	0	0	0	0	0
04VY5Sc	0	0	0	0	0	0	0	0	0	0	0
04VY5Sd	0	1	0	0	0	0	0	0	0	0	0
04VY5Se	0	0	0	0	0	0	0	0	0	0	0
04BCFD4Sa	0	0	0	0	0	0	0	0	0	0	0
04BCFD4Sb	0	0	0	0	0	0	0	0	0	0	0
04BCFD4Sc	0	0	0	0	0	0	0	0	0	0	0
04CNL4Sa	0	0	0	0	0	0	0	0	0	0	0

	Anazyga	*Bilobia*	*Camerella*	*Christiana*	*Dalmanella*	*Dinorthis*	*Doleroides*	*Eoplectodonta*	*Glyptorthis*	*Hebertella*	*Hesperorthis*	*Heterorthina*	*Leptaena*	*Lingula*	*Multicostella*	*Oepikina*	*Orthorhyncula*	*Oxoplecia*	*Paucicrura*	*Paurorthis*	*Pionodema*	*Platystrophia*	*Plectocamara*	*Rafinesquina*
04CNL4Sb	0	0	0	0	0	0	0	0	0	0	0	0	0	0	0	0	0	0	0	0	0	0	0	0
04CNL4Sc	0	0	0	0	0	0	0	0	0	0	0	0	0	0	0	0	0	0	0	0	0	0	0	0
04BA5Sa	0	0	0	0	0	0	0	0	0	0	0	0	0	0	0	0	0	0	0	0	0	0	0	5
04BA5Sb	0	0	0	0	0	0	0	0	0	0	0	0	0	0	0	0	0	0	0	0	0	0	0	2
04BA5Sc	0	0	0	0	0	0	0	0	0	0	0	0	0	0	0	0	0	0	0	0	0	0	0	7
04BA5Sd	0	0	0	0	0	1	0	0	0	0	0	0	0	0	0	0	0	0	0	0	0	0	0	19
04BA5Se	0	0	0	0	0	0	0	0	0	0	0	0	0	0	0	0	0	0	0	0	0	0	0	2
04DN5Sb	1	0	0	0	0	0	0	0	1	0	0	0	0	0	0	0	0	0	0	0	0	0	0	0
04DN5Sc	0	0	0	0	0	0	4	0	0	0	0	0	0	0	0	0	0	0	0	0	0	0	0	0
05CF6Da	0	0	0	0	0	0	0	0	0	0	0	0	0	0	0	0	2	0	0	0	0	0	0	2
05CF6Db	0	0	0	0	0	0	1	0	0	0	0	0	0	0	0	0	0	0	0	0	0	0	0	1
05CF6Dc	0	0	0	0	0	0	1	0	0	0	0	0	0	0	0	0	0	0	0	0	0	0	0	2
05CF6Dd	0	0	0	0	0	0	3	0	0	0	0	0	0	0	0	0	0	0	0	0	0	0	0	0
05CF6De	0	0	0	0	0	1	0	0	0	0	0	0	0	0	0	0	0	0	0	0	0	1	0	3
05CF6Df	0	0	0	0	0	0	0	0	0	0	0	0	0	0	0	0	0	0	0	0	0	1	0	4
05CF6Dg	0	0	0	0	0	0	0	0	0	0	0	0	0	0	0	0	0	0	0	0	0	0	0	3
05CF6Dh	0	0	0	0	0	0	0	0	0	0	0	0	0	0	0	0	0	0	0	0	0	0	0	8
05CF6Di	0	0	0	0	0	0	1	0	0	0	0	0	0	0	0	0	0	0	0	0	0	2	0	3
05FN6Sa	0	0	0	0	0	0	0	0	0	5	0	0	0	0	0	0	0	0	0	0	0	4	0	0
05FN6Sb	0	0	0	0	0	0	0	0	0	5	0	0	0	0	0	0	0	0	0	0	0	1	0	1
05FN6Sc	0	0	0	0	0	0	0	0	0	3	0	0	0	0	0	0	0	0	0	0	0	3	0	3
05FN6Sd	0	0	0	0	0	0	0	0	0	3	0	0	0	0	0	0	0	0	0	0	0	0	0	1
05FN6Se	0	0	0	0	0	0	0	0	0	0	0	0	0	0	0	0	0	0	0	0	0	0	0	0
05SV4Sa	0	0	0	0	0	0	0	0	0	0	0	0	0	0	0	0	0	0	0	0	0	0	0	0
05SV4Sb	0	0	0	0	0	0	0	0	0	0	0	0	0	0	0	0	0	0	0	0	0	0	0	0
05SV4Sc	0	0	0	0	0	0	0	0	0	0	0	0	0	0	0	0	0	0	0	0	0	0	0	0
05ET3Da	0	0	0	0	0	0	0	0	0	0	0	0	0	0	0	0	0	0	0	0	0	0	0	0
05ET3Db	0	0	0	1	0	0	0	8	0	0	0	0	3	0	0	1	0	0	0	2	0	0	0	0
05ET3Dc	0	0	0	1	0	0	0	8	0	0	0	0	0	0	0	0	0	1	2	0	0	0	0	0
05ET3Dd	0	0	0	0	0	0	0	0	0	0	0	0	1	0	0	2	0	2	0	4	0	0	0	0
05ET3De	0	1	0	1	0	0	0	0	0	0	0	0	0	0	0	4	0	0	0	0	0	0	1	0
05AB3D	0	0	0	0	0	0	0	4	0	0	0	0	0	0	0	0	0	0	0	0	0	0	1	0
05OR4Da	0	7	0	5	0	0	0	0	0	0	0	0	0	0	0	0	0	1	0	0	0	0	0	0
05OR4Db	0	0	0	4	0	0	0	0	0	0	0	0	0	0	0	0	0	0	0	0	0	0	0	0
05TR3Da	0	0	2	0	0	0	0	0	0	0	0	0	0	0	0	0	0	0	0	3	0	0	0	0
05TR3Db	0	0	0	0	0	0	0	1	0	0	0	0	1	0	0	0	0	0	15	0	0	0	0	0
05TR3Dc	0	0	0	4	0	0	0	1	0	0	0	0	0	0	0	0	0	0	0	0	0	0	0	0
05TR4Dd	0	4	0	3	0	0	0	0	0	0	0	0	0	0	0	0	0	0	0	0	0	0	0	0
05TR4De	0	9	0	2	0	0	0	1	0	0	0	0	0	0	0	0	0	0	0	0	0	0	0	0
05GR4D	0	0	0	0	0	0	0	1	0	0	0	0	0	0	0	0	0	1	0	0	0	0	0	0
77CA75D	0	0	0	0	0	0	0	0	0	0	0	0	0	1	0	0	0	0	0	0	0	0	0	31
77CA65D	0	0	0	0	0	0	0	0	0	0	0	0	0	1	0	0	0	0	0	0	0	0	0	21
77CA55D	0	0	0	0	0	0	0	0	0	0	0	0	0	3	0	0	0	0	0	0	0	0	0	3
77CA45D	0	0	0	0	0	0	0	0	0	0	0	0	0	0	0	0	0	0	0	0	0	0	0	1
77CA35D	0	0	0	0	0	0	0	0	0	0	0	0	0	0	0	0	0	0	0	0	0	0	0	1
77CA25D	0	0	0	0	0	0	0	0	0	0	0	0	0	0	0	0	0	0	0	0	0	0	0	3
77CA15D	0	0	0	0	0	0	0	0	0	0	0	0	0	35	0	0	0	0	0	0	0	0	0	0
77CA536D	0	0	0	0	0	0	0	0	0	0	0	0	0	0	0	0	0	0	0	0	0	0	0	0
77CA526D	0	0	0	0	0	0	0	0	0	0	0	0	0	0	0	0	0	0	0	0	0	0	0	0
77CA516D	0	0	0	0	0	0	0	0	0	0	0	0	0	0	0	0	0	0	0	0	0	0	0	0
77CA506D	0	0	0	0	0	0	0	0	0	0	0	0	0	0	0	0	0	0	0	0	0	0	0	0
77CA496D	0	0	0	0	0	0	0	0	0	0	0	0	0	0	0	0	0	0	0	0	0	0	0	0
77CA486D	0	0	0	0	0	0	0	0	0	0	0	0	0	0	0	0	0	0	0	0	0	0	0	2
77CA476D	0	0	0	0	0	0	0	0	0	0	0	0	0	0	0	0	0	0	0	0	0	0	0	1
82WK105D	0	0	0	0	0	0	0	0	0	0	0	0	0	0	0	0	0	0	0	0	0	0	0	0
82WK20A5D	0	0	0	0	14	0	0	0	0	0	0	0	0	0	0	0	0	0	0	0	0	0	0	0
82WK255D	0	0	0	0	112	0	0	0	0	0	0	0	0	0	0	0	0	0	0	0	0	0	0	5

	Rhynchotrema	*Rostricellula*	*Schizotreta*	*Strophomena*	*Sowerbyella*	*Zygospira*	*Inarticulata indet.*	*rhynchonellid indet.*	*Brachiopoda indet.*	*Ceraurus*	*Cryptolithus*	*Eomonorachus*	*Flexicalymene*	*Gravicalymene*	*Isotelus*	*Pterygometopus*	*Trilobita A*	*Trilobita indet.*	*Isotelus spines*	*Bellerophon*	*Bucania*	*Cyclonema*	*Hormotoma*	*Liospira*
04CNL4Sb	0	0	0	0	0	0	0	0	0	0	0	0	0	0	0	0	0	0	0	0	0	0	2	0
04CNL4Sc	0	0	0	0	0	2	0	0	0	0	0	0	0	0	0	0	0	0	0	0	0	0	0	0
04BA5Sa	0	0	0	0	0	24	1	0	0	0	0	0	0	0	0	0	0	0	0	0	0	0	0	0
04BA5Sb	0	0	0	0	0	14	0	0	0	0	0	0	0	0	0	0	0	0	0	0	0	0	0	0
04BA5Sc	0	0	0	0	0	18	0	0	0	0	0	0	0	0	1	0	0	2	0	0	0	1	0	0
04BA5Sd	1	0	0	0	0	29	0	0	0	0	0	0	0	0	0	0	0	0	0	0	0	0	0	0
04BA5Se	0	0	0	0	0	42	0	0	0	0	0	0	0	0	0	0	0	2	0	0	0	0	0	0
04DN5Sb	0	0	0	1	0	1	0	0	0	0	0	0	0	0	1	0	0	0	1	0	0	0	0	0
04DN5Sc	0	0	0	1	0	0	0	0	0	0	0	0	0	0	0	0	0	0	0	0	0	0	0	0
05CF6Da	0	0	0	0	0	2	0	0	0	0	0	0	0	0	0	0	0	0	0	0	0	0	0	0
05CF6Db	0	0	0	0	0	21	0	0	0	0	0	0	0	0	1	0	0	1	0	0	0	0	0	0
05CF6Dc	0	0	0	0	0	4	0	0	0	0	0	0	0	0	0	0	0	0	0	0	0	0	0	0
05CF6Dd	0	0	0	0	0	7	0	0	0	0	0	0	0	0	0	0	0	0	0	0	0	0	0	0
05CF6De	0	0	0	0	0	21	0	0	0	0	0	0	0	0	0	0	0	0	8	0	0	0	0	0
05CF6Df	0	0	0	0	0	18	0	0	0	0	0	0	0	0	1	0	0	0	2	0	0	0	0	0
05CF6Dg	0	0	0	0	0	20	0	0	0	0	0	0	0	0	1	0	0	1	0	0	0	0	0	0
05CF6Dh	0	0	0	0	0	42	0	0	0	0	0	0	0	0	0	0	0	0	0	0	0	2	0	0
05CF6Di	0	0	0	0	0	7	0	0	0	0	0	0	0	0	0	0	0	0	0	0	0	4	0	0
05FN6Sa	1	0	0	0	0	23	0	0	0	0	0	0	0	0	0	0	0	0	0	0	0	0	0	0
05FN6Sb	0	0	0	0	0	20	0	0	0	0	0	0	0	0	0	0	0	0	0	0	0	0	0	0
05FN6Sc	0	0	0	0	0	12	0	0	0	0	0	0	0	0	0	0	0	0	0	0	0	0	0	0
05FN6Sd	0	0	0	0	0	24	0	0	0	0	0	0	0	0	0	0	0	1	0	0	0	0	0	0
05FN6Se	0	0	0	0	0	71	0	0	0	0	0	0	0	0	0	0	0	0	0	0	0	0	0	0
05SV4Sa	0	0	0	0	0	0	0	0	0	0	0	0	0	0	0	0	0	0	1	0	0	0	0	0
05SV4Sb	0	0	0	0	0	0	0	0	0	0	0	0	0	0	0	0	0	0	0	0	0	0	0	0
05SV4Sc	0	0	0	0	0	0	0	0	0	0	0	0	0	0	0	0	0	0	0	0	0	0	0	0
05ET3Da	0	0	0	0	1	0	0	0	3	0	0	0	0	0	0	0	0	0	0	0	0	0	0	0
05ET3Db	0	0	0	0	4	0	0	0	0	0	0	0	0	0	0	0	0	1	0	0	0	0	0	0
05ET3Dc	0	0	0	0	2	0	0	0	0	0	0	0	0	0	0	0	0	0	0	0	0	0	0	0
05ET3Dd	0	0	0	0	16	0	0	0	0	0	0	0	0	0	0	0	0	1	0	0	0	0	0	0
05ET3De	0	0	0	0	6	0	0	0	3	0	0	0	0	0	0	1	0	7	0	0	0	0	0	0
05AB3D	0	0	0	0	1	0	0	0	3	0	0	0	0	0	0	0	0	0	0	0	0	0	0	0
05OR4Da	0	0	0	0	0	0	1	0	1	0	0	0	0	0	0	0	0	0	0	0	0	0	0	0
05OR4Db	0	0	0	0	0	0	1	2	0	0	0	0	0	0	0	0	0	1	0	0	0	0	0	0
05TR3Da	0	0	0	0	3	0	1	0	3	0	0	0	0	0	0	0	0	15	3	0	0	0	0	0
05TR3Db	0	0	0	0	2	0	0	0	2	0	0	0	0	0	0	0	0	2	0	0	0	0	0	0
05TR3Dc	0	0	7	0	0	0	0	1	0	0	0	0	0	0	0	0	0	1	0	0	0	0	0	0
05TR4Dd	0	0	0	0	3	0	0	0	2	0	0	0	0	0	0	0	0	4	0	0	0	0	0	0
05TR4De	0	0	0	0	0	0	0	0	0	0	0	0	0	0	0	0	0	1	0	0	0	0	0	0
05GR4D	0	0	0	0	4	0	0	0	2	2	0	0	0	0	0	0	1	6	0	0	0	0	0	0
77CA75D	0	0	0	0	0	0	0	0	0	8	0	4	0	0	0	0	0	0	0	0	0	0	0	0
77CA65D	0	0	0	0	6	0	0	0	0	0	0	2	0	0	0	0	0	0	0	0	0	0	0	0
77CA55D	0	0	0	0	0	3	0	0	0	1	0	0	0	0	0	0	0	0	0	0	0	0	0	0
77CA45D	0	0	0	0	0	2	0	0	0	0	0	0	0	0	0	0	0	0	0	0	0	0	0	0
77CA35D	0	0	0	0	0	0	0	0	0	0	0	0	0	0	0	0	0	1	0	0	1	0	0	0
77CA25D	0	0	0	0	1	0	0	0	0	0	7	0	0	0	3	0	0	84	0	0	47	0	0	0
77CA15D	0	0	0	0	0	0	0	0	0	0	0	0	0	0	0	0	0	0	0	0	0	0	0	0
77CA536D	0	0	0	0	125	34	0	0	0	0	1	0	0	0	0	0	0	0	0	0	0	0	0	0
77CA526D	0	0	0	0	8	0	0	0	0	0	0	0	0	0	0	0	0	0	0	0	0	0	0	0
77CA516D	0	0	0	0	3	18	0	0	0	0	0	0	0	0	0	0	0	0	0	0	0	0	0	0
77CA506D	0	0	0	0	27	30	0	0	0	0	0	0	0	0	0	0	0	1	0	0	2	0	0	0
77CA496D	0	0	0	0	6	16	0	0	0	0	0	0	0	0	0	0	0	0	0	0	0	0	0	0
77CA486D	0	0	0	0	51	47	0	0	0	0	0	1	0	0	0	0	0	2	0	0	0	0	0	0
77CA476D	0	0	0	0	2	7	0	0	0	0	0	0	0	0	1	0	0	2	0	0	0	0	0	0
82WK105D	0	0	0	0	0	0	0	0	0	0	0	0	0	0	1	0	0	0	0	0	0	0	0	0
82WK20A5D	0	0	0	0	20	0	0	0	0	0	0	0	0	0	0	0	0	0	0	0	0	0	0	0
82WK255D	0	0	0	0	17	0	0	0	0	0	0	0	0	0	0	0	0	0	0	0	0	0	0	0

	Lophospira	*Maclurites*	*Sinuites*	*Gastropoda indet.*	*Cyclora*	*Ambonychia*	*Ctenodonta*	*Cunemya*	*Cyrtodonta*	*Cyrtodontula*	*Deceptrix*	*Ischyrodonta*	*modiomorph*	*Lyrodesma*	*Paleoneilo*	*Whitella*	*Bivalvia indet.*	*leperditid ostracod*	*Columnaria*	*Streptelasma*	*Tetradium*	*Stromatoporoidea*	*Chasmatopora*	*Constellaria*
04CNL4Sb	6	2	0	0	0	0	0	0	0	0	0	0	0	0	0	0	0	0	0	0	0	0	0	0
04CNL4Sc	0	0	0	0	0	0	1	0	4	0	0	0	0	0	0	1	0	0	0	0	0	0	0	0
04BA5Sa	0	0	0	0	0	0	0	0	0	0	0	0	0	0	0	0	0	0	0	0	0	0	0	0
04BA5Sb	0	0	0	0	0	0	0	0	0	0	0	0	0	0	0	0	0	0	0	0	0	0	0	0
04BA5Sc	0	0	0	0	0	2	0	0	0	0	0	0	0	0	0	0	0	0	0	0	0	0	0	0
04BA5Sd	0	0	0	0	0	1	0	0	0	0	0	0	0	0	0	0	0	0	0	0	0	0	0	0
04BA5Se	0	0	0	0	0	0	0	0	0	0	0	0	0	0	0	0	0	0	0	0	0	0	0	0
04DN5Sb	0	2	0	0	0	0	0	0	0	0	0	0	0	0	0	0	0	0	0	0	0	0	0	0
04DN5Sc	0	0	0	0	0	0	0	0	0	0	0	0	0	0	0	0	0	0	0	0	0	0	0	0
05CF6Da	0	0	0	0	0	0	0	0	0	0	0	0	0	0	0	0	0	0	0	0	0	0	0	0
05CF6Db	0	0	0	0	0	0	0	0	0	0	0	0	0	0	0	0	0	0	0	0	0	0	0	0
05CF6Dc	0	0	0	0	0	0	0	0	0	0	0	0	0	0	0	0	0	0	0	0	0	0	0	0
05CF6Dd	0	0	0	0	0	0	0	0	0	0	0	0	0	0	0	0	0	0	0	0	0	0	0	0
05CF6De	0	0	0	0	0	0	0	0	0	0	0	0	0	0	0	0	0	0	0	0	0	0	0	0
05CF6Df	0	0	0	0	0	0	0	0	0	0	0	0	0	0	0	0	0	0	0	0	0	0	0	0
05CF6Dg	0	0	0	0	0	0	0	0	0	0	0	0	0	0	0	0	0	0	0	0	0	0	0	0
05CF6Dh	0	0	0	0	0	0	0	0	0	0	0	0	0	0	0	0	0	0	0	0	0	0	0	0
05CF6Di	0	0	0	0	0	0	0	0	0	0	0	0	0	0	0	0	0	0	0	0	0	0	0	0
05FN6Sa	0	0	0	0	0	0	0	0	0	0	0	0	0	0	0	0	0	0	0	0	0	0	0	0
05FN6Sb	0	0	0	0	0	0	0	0	0	0	0	0	0	0	0	0	0	0	0	0	0	0	0	0
05FN6Sc	0	0	0	0	0	0	0	0	0	0	0	0	0	0	0	0	0	0	0	0	0	0	0	0
05FN6Sd	1	0	0	0	0	0	0	0	0	0	0	0	0	0	0	0	0	0	0	0	0	0	0	0
05FN6Se	0	0	0	0	0	0	0	0	0	0	0	0	0	0	0	0	0	0	0	0	0	0	0	0
05SV4Sa	4	0	0	0	0	0	0	0	0	0	0	0	0	0	0	0	0	0	0	0	0	0	0	0
05SV4Sb	11	0	0	0	0	0	0	0	0	0	0	0	0	0	0	0	0	0	0	0	0	0	0	0
05SV4Sc	4	0	0	0	0	0	0	0	0	0	0	0	0	0	0	0	0	0	0	0	0	0	0	0
05ET3Da	0	0	0	1	0	0	0	0	0	0	0	0	0	0	0	0	0	0	0	0	0	0	0	0
05ET3Db	0	0	0	0	0	0	0	0	0	0	0	0	0	0	0	0	0	0	0	0	0	0	0	0
05ET3Dc	0	0	0	3	0	0	0	0	0	0	0	0	0	0	0	0	0	0	0	0	0	0	0	0
05ET3Dd	0	0	0	0	0	0	0	0	0	0	0	0	0	0	0	0	0	0	0	0	0	0	0	0
05ET3De	0	0	0	37	0	0	0	0	0	0	0	0	0	0	0	0	0	1	0	0	0	0	0	0
05AB3D	0	0	0	0	0	0	0	0	0	0	0	0	0	0	0	0	0	0	0	0	0	0	0	0
05OR4Da	0	0	0	1	0	0	0	0	0	0	0	0	0	0	0	0	0	0	0	0	0	0	0	0
05OR4Db	0	0	0	0	0	0	0	0	0	0	0	0	0	0	0	0	0	0	0	0	0	0	0	0
05TR3Da	0	0	0	0	0	0	0	0	0	0	0	0	0	0	0	0	0	0	0	0	0	0	0	0
05TR3Db	0	0	0	1	0	0	0	0	0	0	0	0	0	0	0	0	0	0	0	0	0	0	0	0
05TR3Dc	0	0	0	0	0	0	0	0	0	0	0	0	0	0	0	0	0	1	0	0	0	0	0	0
05TR4Dd	0	0	0	0	0	0	0	0	0	0	0	0	0	0	0	0	0	0	0	0	0	0	0	0
05TR4De	0	0	0	0	0	0	0	0	0	0	0	0	0	0	0	0	0	2	0	0	0	0	0	0
05GR4D	0	0	0	9	0	0	0	0	0	0	0	0	0	0	0	0	0	5	0	0	0	0	0	0
77CA75D	0	0	0	0	0	0	0	0	0	0	0	1	0	0	0	0	0	1	0	0	0	0	0	0
77CA65D	0	0	0	0	0	0	1	0	0	0	0	0	1	0	0	0	0	0	0	0	0	0	0	0
77CA55D	0	0	0	0	0	0	0	1	0	0	0	0	2	0	0	0	0	0	0	0	0	0	0	0
77CA45D	0	0	0	0	0	0	0	0	0	0	0	0	6	0	3	0	0	0	0	0	0	0	0	0
77CA35D	0	0	0	0	0	0	0	0	0	0	0	0	0	0	0	0	6	0	0	0	0	0	0	0
77CA25D	17	0	0	0	0	0	25	0	0	0	0	1	0	0	0	0	0	0	0	0	0	0	0	0
77CA15D	0	0	0	0	0	0	0	0	0	0	0	14	0	0	0	0	0	0	0	0	0	0	0	0
77CA536D	0	0	0	0	0	0	0	0	0	0	0	0	0	0	0	0	0	0	0	0	0	0	0	0
77CA526D	0	0	0	0	0	0	0	0	0	0	0	0	0	0	0	0	0	0	0	0	0	0	0	0
77CA516D	0	0	0	0	0	0	0	0	0	0	0	0	0	0	0	0	0	0	0	0	0	0	0	0
77CA506D	1	0	0	0	0	0	0	0	0	0	0	0	0	0	0	0	0	0	0	0	0	0	0	0
77CA496D	0	0	0	0	0	0	0	0	0	0	0	0	0	0	0	0	0	0	0	0	0	0	0	0
77CA486D	0	0	0	0	0	0	0	0	0	0	0	0	0	0	0	0	0	0	0	0	0	0	0	0
77CA476D	0	0	0	32	0	0	0	0	0	0	0	0	0	0	0	0	0	0	0	0	0	0	0	0
82WK105D	0	0	0	0	0	0	0	0	0	0	0	0	0	0	0	0	0	0	0	0	0	0	0	0
82WK20A5D	0	0	0	0	0	0	0	0	0	0	0	0	0	0	0	0	0	0	0	0	0	0	0	0
82WK255D	0	0	0	0	0	0	0	0	0	0	0	0	0	0	0	0	0	0	0	0	0	0	0	0

	Escharopora	*Heterotrypa*	*Prasopora*	*Rhindictya*	*massive trepostome*	*bifoliate bryozoan*	*bumpy ramose*	*encrusting bryozoan*	*thick ramose*	*thin ramose 1*	*thin ramose 2*	*cog crinoid*	*cog star crinoid*	*thin ring crinoid*	*thick ring crinoid*	*flower crinoid*	*pentagonal crinoid*	*stacked crinoid*	*star crinoid*	*inner star crinoid*	*striped crinoid*	*striped flower crinoid*	*striped star crinoid*	*crinoidea indet.*
04CNL4Sb	2	0	0	2	25	0	0	0	0	0	1	0	0	3	0	0	0	0	0	0	0	0	0	0
04CNL4Sc	0	0	0	0	0	0	0	0	0	0	0	0	0	0	0	0	0	0	0	0	0	0	0	0
04BA5Sa	0	0	0	0	0	0	0	0	13	11	3	0	0	0	0	0	0	0	0	0	0	0	0	0
04BA5Sb	0	0	0	0	0	0	0	0	0	4	0	0	0	0	3	0	0	0	0	0	0	0	0	0
04BA5Sc	1	0	0	0	0	0	0	15	0	23	0	0	0	0	1	0	0	0	0	0	0	0	0	0
04BA5Sd	1	0	0	1	0	0	0	5	2	0	0	0	0	0	3	0	0	0	0	0	0	0	0	0
04BA5Se	0	0	0	0	0	0	0	12	0	19	0	1	0	0	1	0	0	0	0	0	0	0	0	0
04DN5Sb	20	0	1	5	0	2	0	0	7	15	0	0	0	3	3	0	0	0	0	0	0	0	0	0
04DN5Sc	0	0	1	5	0	0	0	0	0	5	0	1	0	6	6	0	0	0	3	0	1	0	0	0
05CF6Da	0	0	0	0	0	6	0	0	26	0	2	0	0	0	0	0	0	0	0	0	0	0	0	0
05CF6Db	0	0	0	0	0	10	0	0	6	0	0	0	0	0	0	0	0	0	0	0	0	0	0	0
05CF6Dc	0	0	0	0	0	15	1	0	2	0	1	0	0	0	0	0	0	0	0	0	0	0	0	0
05CF6Dd	0	0	0	0	0	0	0	0	1	0	0	0	0	0	0	0	0	0	0	0	0	0	0	0
05CF6De	0	0	0	1	0	0	0	5	0	0	4	0	0	0	0	0	0	0	0	0	0	0	0	0
05CF6Df	0	0	0	0	0	1	0	0	0	0	4	0	0	0	0	0	0	0	0	0	0	0	0	0
05CF6Dg	0	0	0	0	0	2	0	0	0	5	6	0	0	0	0	0	0	0	0	0	0	0	0	0
05CF6Dh	0	0	0	0	0	0	0	0	3	0	13	0	0	3	0	0	0	0	0	0	0	0	0	0
05CF6Di	0	0	0	0	0	0	0	3	5	0	7	0	0	1	1	0	0	0	0	0	0	0	0	0
05FN6Sa	0	0	0	0	0	0	0	0	0	0	1	0	0	0	1	0	0	0	0	0	0	0	0	0
05FN6Sb	0	0	0	0	0	6	0	0	0	0	2	0	0	3	0	0	0	0	0	0	0	0	0	0
05FN6Sc	0	0	0	0	0	0	0	0	15	0	0	0	0	0	0	0	0	0	0	0	0	0	0	0
05FN6Sd	0	0	0	0	0	0	0	1	1	0	2	0	0	0	0	0	0	0	0	0	0	0	0	0
05FN6Se	0	0	0	0	0	0	0	0	0	0	0	0	0	1	0	0	0	0	0	0	0	0	0	0
05SV4Sa	0	0	0	0	0	0	0	0	0	0	0	0	0	0	0	0	0	0	0	0	0	0	0	0
05SV4Sb	0	0	0	0	0	0	0	0	0	0	0	0	0	0	0	0	0	0	0	0	0	0	0	0
05SV4Sc	0	0	0	0	0	0	0	0	0	0	1	0	0	1	0	0	0	0	0	0	0	0	0	0
05ET3Da	0	0	0	1	0	0	0	0	0	0	2	0	0	1	0	0	0	1	0	0	0	0	0	0
05ET3Db	2	0	0	12	0	0	0	0	0	0	0	0	0	3	0	0	0	0	0	0	0	0	0	0
05ET3Dc	5	0	0	13	0	0	0	0	0	5	0	0	0	0	3	0	0	0	0	0	0	0	0	0
05ET3Dd	1	0	0	3	0	0	0	0	0	0	0	0	0	0	0	0	0	0	0	0	0	0	0	0
05ET3De	2	0	0	0	0	0	0	0	0	0	0	0	0	1	1	0	0	0	0	0	0	0	0	0
05AB3D	0	0	0	1	0	0	0	0	0	0	0	0	0	0	0	0	0	0	0	0	0	0	0	0
05OR4Da	0	0	0	0	0	0	0	0	1	0	0	0	0	0	0	0	0	0	0	0	0	0	0	0
05OR4Db	0	0	0	0	0	0	0	0	0	0	0	0	0	0	0	0	0	0	0	0	0	0	0	0
05TR3Da	0	0	0	0	0	0	0	0	0	0	0	0	0	1	0	0	0	0	0	0	1	0	0	0
05TR3Db	0	0	0	0	0	0	0	0	0	2	2	0	0	0	0	0	0	0	0	0	0	0	0	0
05TR3Dc	0	0	0	0	0	0	0	0	0	0	0	0	0	1	0	0	0	0	0	0	0	0	0	0
05TR4Dd	0	0	0	0	0	0	0	0	0	0	0	0	0	1	0	0	0	0	0	1	0	0	0	0
05TR4De	0	0	0	0	0	0	0	0	0	0	0	0	0	0	0	0	0	0	0	0	0	0	0	0
05GR4D	1	0	0	0	0	0	0	0	0	0	0	0	0	0	0	0	0	0	0	0	0	0	0	0
77CA75D	0	0	0	0	0	0	0	0	0	0	1	0	0	0	0	0	0	0	0	0	0	0	0	1
77CA65D	0	0	0	0	0	0	0	0	0	0	19	0	0	0	0	0	0	0	0	0	0	0	0	0
77CA55D	0	0	0	0	0	0	0	0	0	0	2	0	0	0	0	0	0	0	0	0	0	0	0	0
77CA45D	0	0	0	0	0	0	0	0	0	0	1	0	0	0	0	0	0	0	0	0	0	0	0	0
77CA35D	0	0	0	0	0	0	0	0	0	0	0	0	0	0	0	0	0	0	0	0	0	0	0	0
77CA25D	0	0	0	0	0	0	0	0	0	0	0	0	0	0	0	0	0	0	0	0	0	0	0	0
77CA15D	0	0	0	0	0	0	0	0	0	0	0	0	0	0	0	0	0	0	0	0	0	0	0	0
77CA536D	0	0	0	0	0	0	0	0	0	0	10	0	0	0	0	0	0	0	0	0	0	0	0	0
77CA526D	0	0	5	0	0	0	0	0	0	0	34	0	0	0	0	0	0	0	0	0	0	0	0	0
77CA516D	0	0	3	0	0	0	0	0	0	0	3	0	0	0	0	0	0	0	0	0	0	0	0	0
77CA506D	0	0	5	0	0	0	0	0	0	0	24	0	0	0	0	0	0	0	0	0	0	0	0	8
77CA496D	0	0	4	0	0	0	0	0	0	0	16	0	0	0	0	0	0	0	0	0	0	0	0	1
77CA486D	0	0	0	0	0	0	0	0	0	0	1	0	0	0	0	0	0	0	0	0	0	0	0	1
77CA476D	0	0	0	0	0	0	0	0	0	0	100	0	0	0	0	0	0	0	0	0	0	0	0	0
82WK105D	0	0	0	0	0	0	0	0	0	0	0	0	0	0	0	0	0	0	0	0	0	0	0	0
82WK20A5D	0	0	0	0	0	0	0	0	0	0	44	0	0	0	0	0	0	0	0	0	0	0	0	0
82WK255D	0	0	0	0	0	0	0	0	0	0	1	0	0	0	0	0	0	0	0	0	0	0	0	0

	Echinodermata indet.	*orthoconic nautiloids*	*algal coating*	*Solenopora*	*Stromatoporoids*	*Chondrites*	*Diplocriterion*	*Cornulites*	*alga(Hindia?)*	*rhombiferan plate*	*graptolites*
04CNL4Sb	0	3	0	0	0	0	0	0	0	0	0
04CNL4Sc	0	6	0	0	0	0	0	0	0	0	0
04BA5Sa	0	0	0	0	0	0	0	0	0	0	0
04BA5Sb	0	0	0	0	0	0	0	0	0	0	0
04BA5Sc	0	0	0	0	0	0	0	0	0	0	0
04BA5Sd	0	0	0	0	0	0	0	1	0	0	0
04BA5Se	0	0	0	0	0	0	0	0	0	0	0
04DN5Sb	0	0	0	0	0	0	0	0	0	0	0
04DN5Sc	0	0	0	0	0	0	0	0	0	0	0
05CF6Da	0	0	0	0	0	0	0	0	0	0	0
05CF6Db	0	0	0	0	0	0	0	0	0	0	0
05CF6Dc	0	0	0	0	0	0	0	0	0	0	0
05CF6Dd	0	0	0	0	0	6	0	0	0	0	0
05CF6De	0	0	0	0	0	0	0	0	0	0	0
05CF6Df	0	0	0	0	0	0	0	0	0	0	0
05CF6Dg	0	0	0	0	0	0	0	0	0	0	0
05CF6Dh	0	0	0	0	0	0	0	0	0	0	0
05CF6Di	0	0	0	0	0	0	0	0	0	0	0
05FN6Sa	0	0	0	0	0	0	0	0	0	0	0
05FN6Sb	0	0	0	0	0	0	0	0	0	0	0
05FN6Sc	0	0	0	0	0	0	0	0	0	0	0
05FN6Sd	0	0	0	0	0	0	0	0	0	0	0
05FN6Se	1	0	0	0	0	0	0	0	0	0	0
05SV4Sa	0	0	0	0	0	0	0	0	0	0	0
05SV4Sb	0	0	0	0	0	0	0	0	0	0	0
05SV4Sc	0	1	0	0	0	0	0	0	0	0	0
05ET3Da	0	0	0	0	0	0	0	0	0	0	0
05ET3Db	0	0	0	0	0	0	0	0	0	0	0
05ET3Dc	0	0	0	0	0	0	0	0	0	1	0
05ET3Dd	0	0	0	0	0	0	0	0	0	0	0
05ET3De	0	0	0	0	0	0	0	0	0	0	0
05AB3D	0	0	0	0	0	0	0	0	0	0	0
05OR4Da	0	0	0	0	0	0	0	0	0	0	0
05OR4Db	0	0	0	0	0	0	0	0	0	0	0
05TR3Da	0	0	0	0	0	0	0	0	0	0	0
05TR3Db	0	0	0	0	0	0	0	0	0	0	0
05TR3Dc	0	0	0	0	0	1	0	0	0	0	0
05TR4Dd	0	0	0	0	0	0	0	0	1	0	0
05TR4De	0	1	0	0	0	0	0	0	0	0	0
05GR4D	0	0	0	0	0	0	0	0	0	0	0
77CA75D	0	0	0	0	0	0	0	0	0	0	0
77CA65D	0	0	0	0	0	0	0	0	0	0	0
77CA55D	0	0	0	0	0	0	0	0	0	0	0
77CA45D	0	0	0	0	0	0	0	0	0	0	0
77CA35D	0	0	0	0	0	0	0	0	0	0	0
77CA25D	0	0	0	0	0	0	0	0	0	0	0
77CA15D	0	0	0	0	0	0	0	0	0	0	0
77CA536D	0	0	0	0	0	0	0	0	0	0	0
77CA526D	0	0	0	0	0	0	0	0	0	0	0
77CA516D	0	0	0	0	0	0	0	0	0	0	0
77CA506D	0	0	0	0	0	0	0	0	0	0	0
77CA496D	0	0	0	0	0	0	0	0	0	0	0
77CA486D	0	1	0	0	0	0	0	0	0	0	0
77CA476D	0	0	0	0	0	0	0	0	0	0	0
82WK105D	0	0	0	0	0	0	0	0	0	0	0
82WK20A5D	0	0	0	0	0	0	0	0	0	0	0
82WK255D	0	0	0	0	0	0	0	0	0	0	0

	Anazyga	*Bilobia*	*Camerella*	*Christiana*	*Dalmanella*	*Dinorthis*	*Doleroides*	*Eoplectodonta*	*Glyptorthis*	*Hebertella*	*Hesperorthis*	*Heterorthina*	*Leptaena*	*Lingula*	*Multicostella*	*Oepikina*	*Orthorhyncula*	*Oxoplecia*	*Paucicrura*	*Paurorthis*	*Pionodema*	*Platystrophia*	*Plectocamara*	*Rafinesquina*
82WK305D	0	0	0	0	11	0	0	0	0	0	0	0	0	0	0	0	0	0	0	0	0	0	0	42
82WK375D	0	0	0	0	43	0	0	0	0	0	0	0	0	0	0	0	0	0	0	0	0	0	0	144
82WK425D	0	0	0	0	24	0	0	0	0	0	0	0	0	0	0	0	0	0	0	0	0	0	0	22
82WK785D	0	0	0	0	71	0	0	0	0	0	0	0	0	0	0	0	0	0	0	0	0	0	0	13
82WK1305D	0	0	0	0	5	0	0	0	0	0	0	0	0	0	0	0	0	0	0	0	0	0	0	48
82WK1325D	0	0	0	0	109	0	0	0	0	0	0	0	0	0	0	0	0	0	0	0	0	0	0	23
82WK1405D	0	0	0	0	5	0	0	0	0	0	0	0	0	0	0	0	0	0	0	0	0	0	0	42
82W175A5D	0	0	0	0	3	0	0	0	0	0	0	0	0	0	0	0	0	0	0	0	0	0	0	2
82WK1856D	0	0	0	0	17	0	0	0	0	0	0	0	0	0	0	0	0	0	0	0	0	0	0	10
82WK2046D	0	0	0	0	10	0	0	0	0	0	0	0	0	0	0	0	0	0	0	0	0	0	0	18
82WK2116D	0	0	0	0	30	0	0	0	0	0	0	0	0	0	0	0	0	0	0	0	0	0	0	30
82WK2306D	0	0	0	0	14	0	0	0	0	0	0	0	0	0	0	0	0	0	0	0	0	0	0	17
82WK2506D	0	0	0	0	46	0	0	0	0	0	0	0	0	0	0	0	0	0	0	0	0	0	0	4
82W260S6D	0	0	0	0	1	0	0	0	0	0	0	0	0	0	0	0	0	0	0	0	0	0	0	2
82WK2606D	0	0	0	0	1	0	0	0	0	0	0	0	0	0	0	0	0	0	0	0	0	0	0	16
82WK2706D	0	0	0	0	22	0	0	0	0	0	0	0	0	0	0	0	0	0	0	0	0	0	0	10
82W270S6D	0	0	0	0	55	0	0	0	0	0	0	0	0	0	0	0	0	0	0	0	0	0	0	2
82WK3006D	0	0	0	0	0	0	0	0	0	0	0	0	0	0	0	0	0	0	0	0	0	0	0	126
82WK3126D	0	0	0	0	73	0	0	0	0	0	0	0	0	0	0	0	0	0	0	0	0	0	0	1
82WK3506D	0	0	0	0	31	0	0	0	0	0	0	0	0	0	0	0	0	0	0	0	0	0	0	1
82WK3656D	0	0	0	0	6	0	0	0	0	0	0	0	0	0	0	0	0	0	0	0	0	0	0	1
82WK3836D	0	0	0	0	0	0	0	0	0	0	0	0	0	0	0	0	0	0	0	0	0	0	0	69
82WM40B6D	0	0	0	0	20	0	0	0	0	0	0	0	0	0	0	0	0	0	0	0	0	0	0	3
82WM496D	0	0	0	0	1	0	0	0	0	0	0	0	0	0	0	0	0	0	0	0	0	0	0	1
82HMB15D	0	0	0	0	2	0	0	0	0	0	0	0	0	0	0	0	0	0	0	0	0	0	0	9
82HMB25D	0	0	0	0	81	0	0	0	0	0	0	0	0	0	0	0	0	0	0	0	0	0	0	6
82HMB35D	0	0	0	0	15	0	0	0	0	0	0	0	0	0	0	0	0	0	0	0	0	0	0	18
82HMB4A5D	0	0	0	0	29	0	0	0	0	0	0	0	0	0	0	0	0	0	0	0	0	0	0	13
82HMB4B5D	0	0	0	0	84	0	0	0	0	0	0	0	0	0	0	0	0	0	0	0	0	0	0	14
82HMB5A5D	0	0	0	0	10	0	0	0	0	0	0	0	0	0	0	0	0	0	0	0	0	0	0	5
82HMB5B5D	0	0	0	0	17	11	0	0	0	0	0	0	0	0	0	0	0	0	0	0	0	0	0	0
82HMB6A5D	0	0	0	0	58	1	0	0	0	0	0	0	0	0	0	0	0	0	0	0	0	0	0	9
82HMB6B5D	0	0	0	0	16	0	0	0	0	0	0	0	0	0	0	0	0	0	0	0	0	0	0	29
82HMB75D	0	0	0	0	12	5	0	0	0	0	0	0	0	0	0	0	0	0	0	0	0	0	0	7
82HMB8A5D	0	0	0	0	18	0	0	0	0	0	0	0	0	0	0	0	0	0	0	0	0	0	0	5
82HMB8B5D	0	0	0	0	12	7	0	0	0	0	0	0	0	0	0	0	0	0	0	0	0	0	0	3
82HMB8C5D	0	0	0	0	160	1	0	0	0	0	0	0	0	0	0	0	0	0	0	0	0	0	0	19
82HMB95D	0	0	0	0	34	7	0	0	0	0	0	0	0	0	0	0	0	0	0	0	0	0	0	0
82HM49F5D	0	0	0	0	18	2	0	0	0	0	0	0	0	0	0	0	0	0	0	0	0	0	0	3
82HMB10A5D	0	0	0	0	19	0	0	0	0	0	0	0	0	0	0	0	0	0	0	0	0	0	0	28
82HMB10B5D	0	0	0	0	56	0	0	0	0	0	0	0	0	0	0	0	0	0	0	0	0	0	0	12
82HMB10C5D	0	0	0	0	84	0	0	0	0	0	0	0	0	0	0	0	0	0	0	0	0	0	0	16
82HMB115D	0	0	0	0	128	0	0	0	0	0	0	0	0	0	0	0	0	0	0	0	0	0	0	2
82HMB125D	0	0	0	0	0	0	0	0	0	0	0	0	0	0	0	0	0	0	0	0	0	0	0	9
82HM1355D	0	0	0	0	0	0	0	0	0	4	0	0	0	0	0	0	0	0	0	0	0	0	0	58
82HMB135D	0	0	0	0	7	0	0	0	0	11	0	0	0	0	0	0	0	0	0	0	0	0	0	13
82HMB145D	0	0	0	0	0	2	0	0	0	0	0	0	0	0	0	0	0	0	0	0	0	0	0	3
82HMB155D	0	0	0	0	0	0	0	0	0	6	0	0	0	0	0	0	0	0	0	0	0	0	0	2
82HMB176D	0	0	0	0	10	0	0	0	0	0	0	0	0	0	0	0	0	0	0	0	0	0	0	3
82HMB186D	0	0	0	0	3	0	0	0	0	0	0	0	0	0	0	0	0	0	0	0	0	0	0	0
82HM19B6D	0	0	0	0	1	0	0	0	0	0	0	0	0	0	0	0	0	0	0	0	0	0	0	0
82HMB206D	0	0	0	0	0	0	0	0	0	0	0	0	0	0	0	0	0	0	0	0	0	0	0	0
82HMB216D	0	0	0	0	4	0	0	0	0	0	0	0	0	0	0	0	0	0	0	0	0	0	0	11
82HMB226D	0	0	0	0	2	0	0	0	0	1	0	0	0	0	0	0	0	0	0	0	0	0	0	8
82HMB236D	0	0	0	0	0	0	0	0	0	10	0	0	0	0	0	0	0	0	0	0	0	0	0	0
82HM23A6f	0	0	0	0	0	0	0	0	0	4	0	0	0	0	0	0	0	0	0	0	0	0	0	4
82HMB246D	0	0	0	0	0	0	0	0	0	4	0	0	0	0	0	0	0	0	0	0	0	0	0	0

	Rhynchotrema	*Rostricellula*	*Schizotreta*	*Strophomena*	*Sowerbyella*	*Zygospira*	*Inarticulata indet.*	*rhynchonellid indet.*	*Brachiopoda indet.*	*Ceraurus*	*Cryptolithus*	*Eomonorachus*	*Flexicalymene*	*Gravicalymene*	*Isotelus*	*Pterygometopus*	*Trilobita A*	*Trilobita indet.*	*Isotelus spines*	*Bellerophon*	*Bucania*	*Cyclonema*	*Hormotoma*	*Liospira*
82WK305D	0	0	0	0	0	0	0	0	0	0	0	0	0	0	0	0	0	0	0	0	0	0	0	0
82WK375D	0	0	0	0	0	0	0	0	0	0	0	0	0	0	0	0	0	0	0	0	0	0	0	0
82WK425D	0	0	0	0	0	0	0	0	0	0	0	0	0	0	0	0	0	0	0	0	0	0	0	0
82WK785D	0	0	0	0	0	0	0	0	0	0	0	0	0	0	0	0	0	0	0	0	0	0	0	0
82WK1305D	0	0	0	0	40	0	0	0	0	0	0	0	0	0	0	0	0	0	0	0	0	0	0	0
82WK1325D	0	0	0	0	44	0	0	0	0	0	0	0	0	0	0	0	0	0	0	0	0	0	0	0
82WK1405D	0	0	0	0	52	0	0	0	0	0	0	0	0	0	25	0	0	0	0	0	0	0	0	0
82W175A5D	0	0	0	0	0	0	0	0	0	0	0	0	0	0	2	0	0	0	0	0	1	0	0	0
82WK1856D	0	0	0	0	0	0	0	0	0	0	0	0	0	0	2	0	0	0	0	0	0	0	0	0
82WK2046D	0	0	0	0	0	0	0	0	0	0	0	0	0	0	9	0	0	0	0	0	0	0	0	0
82WK2116D	0	0	0	0	28	0	0	0	0	0	0	0	0	0	4	0	0	0	0	0	1	0	0	0
82WK2306D	0	0	0	0	92	0	0	0	0	0	0	0	0	0	5	0	0	0	0	0	0	0	0	0
82WK2506D	0	0	0	0	63	0	0	0	0	0	0	0	0	0	15	0	0	0	0	0	0	0	0	0
82W260S6D	0	0	0	0	0	0	0	0	0	0	0	0	0	0	1	0	0	0	0	0	0	0	0	0
82WK2606D	0	0	0	0	0	0	0	0	0	0	0	0	0	0	11	0	0	0	0	0	0	0	0	0
82WK2706D	0	0	0	0	42	0	0	0	0	0	0	0	0	0	12	0	0	0	0	0	0	0	0	0
82W270S6D	0	0	0	0	12	0	0	0	0	0	0	0	0	0	0	0	0	0	0	0	0	0	0	0
82WK3006D	0	0	0	0	0	0	0	0	0	0	0	0	0	0	16	0	0	0	0	0	0	0	0	0
82WK3126D	0	0	0	0	0	3	0	0	0	0	0	0	0	0	4	0	0	0	0	0	0	0	0	0
82WK3506D	0	0	0	0	0	45	0	0	0	0	0	0	0	0	1	0	0	0	0	0	0	0	0	0
82WK3656D	0	0	0	0	0	0	0	0	0	0	0	0	0	0	0	0	0	0	0	0	0	0	0	0
82WK3836D	0	0	0	0	11	5	0	0	0	0	0	0	0	0	11	0	0	0	0	0	0	0	0	0
82WM40B6D	0	0	0	0	13	20	0	0	0	0	0	0	0	0	2	0	0	0	0	0	0	0	0	0
82WM496D	0	0	0	0	165	18	0	0	0	0	0	0	0	0	6	0	0	0	0	0	0	0	0	0
82HMB15D	0	0	0	0	10	0	0	0	0	0	0	0	0	0	6	0	0	0	0	0	0	0	0	0
82HMB25D	0	0	0	0	0	0	0	0	0	0	0	0	0	0	3	0	0	0	0	0	0	0	0	0
82HMB35D	0	0	0	0	0	0	0	0	0	0	0	0	0	0	1	0	0	0	0	0	0	0	0	0
82HMB4A5D	0	0	0	0	0	0	0	0	0	0	0	0	0	0	11	0	0	0	0	0	0	0	0	0
82HMB4B5D	0	0	0	0	0	0	0	0	0	0	0	0	0	0	6	0	0	0	0	0	0	0	0	0
82HMB5A5D	0	0	0	0	7	0	0	0	0	0	0	0	0	0	2	0	0	0	0	0	0	0	0	0
82HMB5B5D	0	0	0	0	15	1	0	0	0	0	0	0	0	0	0	0	0	0	0	0	0	0	0	0
82HMB6A5D	0	0	0	0	0	1	0	0	0	0	0	0	0	0	0	0	0	0	0	0	0	0	0	0
82HMB6B5D	0	0	0	0	2	1	0	0	0	0	0	0	0	0	8	0	0	0	0	0	0	0	0	0
82HMB75D	0	0	0	0	10	0	0	0	0	0	0	0	0	0	0	0	0	0	0	0	0	0	0	0
82HMB8A5D	0	0	0	0	1	0	0	0	0	0	0	0	0	0	1	0	0	0	0	0	0	0	0	0
82HMB8B5D	0	0	0	0	7	2	0	0	0	0	0	0	0	0	0	0	0	0	0	0	0	0	0	0
82HMB8C5D	0	0	0	0	0	0	0	0	0	0	0	0	0	0	1	0	0	0	0	0	0	0	0	0
82HMB95D	0	0	0	0	37	0	0	0	0	0	0	0	0	0	0	0	0	0	0	0	0	0	0	0
82HM49F5D	0	0	0	0	6	0	0	0	0	0	0	0	0	0	0	0	0	0	0	0	0	0	0	0
82HMB10A5D	0	0	0	0	0	0	0	0	0	0	0	0	0	0	4	0	0	0	0	0	0	0	0	0
82HMB10B5D	27	0	0	0	0	0	0	0	0	0	0	0	0	0	1	0	0	0	0	0	0	0	0	0
82HMB10C5D	13	0	0	0	7	0	0	0	0	0	0	0	0	0	2	0	0	0	0	0	0	0	0	0
82HMB115D	0	0	0	0	0	0	0	0	0	0	0	0	0	0	6	0	0	0	0	0	0	0	0	0
82HMB125D	0	0	0	0	1	0	0	0	0	0	0	0	0	0	3	0	0	0	0	0	0	0	0	0
82HM1355D	0	0	0	0	0	2	0	0	0	0	0	0	0	0	0	0	0	0	0	0	0	0	0	0
82HMB135D	0	0	0	0	0	14	0	0	0	0	0	0	0	0	15	0	0	0	0	0	9	0	0	0
82HMB145D	0	0	0	0	0	2	0	0	0	0	0	0	0	0	1	0	0	0	0	0	0	0	0	0
82HMB155D	0	0	0	0	1	10	0	0	0	0	0	0	0	0	14	0	0	0	0	0	2	0	0	0
82HMB176D	0	0	0	0	15	29	0	0	0	0	0	0	0	0	9	0	0	0	0	0	0	0	0	0
82HMB186D	0	0	0	0	59	8	0	0	0	0	0	0	0	0	9	0	0	0	0	0	4	0	0	0
82HM19B6D	0	0	0	0	0	1	0	0	0	0	0	0	0	0	0	0	0	0	0	0	0	0	0	0
82HMB206D	0	0	0	0	0	39	0	0	0	0	0	0	0	0	0	0	0	0	0	0	0	0	0	0
82HMB216D	0	0	0	0	0	11	0	0	0	0	0	0	0	0	0	0	0	0	0	0	1	0	0	0
82HMB226D	0	0	0	0	0	2	0	0	0	0	0	0	0	0	0	0	0	0	0	0	0	0	0	0
82HMB236D	0	0	0	0	0	6	0	0	0	0	0	0	0	0	4	0	0	0	0	0	25	0	0	0
82HM23A6f	0	0	0	0	0	1	0	0	0	0	0	0	0	0	0	0	0	0	0	0	0	0	0	0
82HMB246D	0	0	0	0	0	6	0	0	0	0	0	0	0	0	6	0	0	0	0	0	0	0	0	0

	Lophospira	*Maclurites*	*Sinuites*	*Gastropoda indet.*	*Cyclora*	*Ambonychia*	*Ctenodonta*	*Cunemya*	*Cyrtodonta*	*Cyrtodontula*	*Deceptrix*	*Ischyrodonta*	*modiomorph*	*Lyrodesma*	*Paleoneilo*	*Whitella*	*Bivalvia indet.*	*leperditid ostracod*	*Columnaria*	*Streptelasma*	*Tetradium*	*Stromatoporoidea*	*Chasmatopora*	*Constellaria*
82WK305D	0	0	0	0	0	0	0	0	0	0	0	0	0	0	0	0	0	0	0	0	0	0	0	0
82WK375D	0	0	0	0	0	0	0	0	0	0	0	0	0	0	0	0	0	0	0	0	0	0	0	0
82WK425D	0	0	0	0	0	0	0	0	0	0	0	0	0	0	0	0	0	0	0	0	0	0	0	0
82WK785D	0	0	0	0	0	0	0	0	0	0	0	0	0	0	0	0	0	0	0	0	0	0	0	0
82WK1305D	0	0	0	0	0	0	0	0	0	0	0	0	0	0	0	0	0	0	0	0	0	0	0	0
82WK1325D	0	0	0	0	0	0	0	0	0	0	0	0	0	0	0	0	0	0	0	0	0	0	0	0
82WK1405D	0	0	0	0	0	0	0	0	0	0	0	0	0	0	0	0	0	0	0	0	0	0	0	0
82W175A5D	0	0	0	0	0	0	0	0	0	0	0	0	0	0	0	0	0	0	0	0	0	0	0	0
82WK1856D	0	0	0	0	0	0	0	0	0	0	0	0	0	0	0	0	0	0	0	0	0	0	0	0
82WK2046D	0	0	0	0	0	0	0	0	0	0	0	0	0	0	0	0	0	0	0	0	0	0	0	0
82WK2116D	0	0	0	0	0	0	0	0	0	0	0	0	0	0	0	0	0	0	0	0	0	0	0	0
82WK2306D	0	0	0	0	0	0	0	0	0	0	0	0	0	0	0	0	0	0	0	0	0	0	0	0
82WK2506D	0	0	0	0	0	0	0	0	0	0	0	0	0	0	0	0	0	0	0	0	0	0	0	0
82W260S6D	1	0	0	0	0	0	0	0	0	0	0	0	0	0	0	0	0	0	0	0	0	0	0	0
82WK2606D	0	0	0	0	0	0	0	0	0	0	0	0	0	0	0	0	0	0	0	0	0	0	0	0
82WK2706D	0	0	0	0	0	0	0	0	0	0	0	0	0	0	0	0	0	0	0	0	0	0	0	0
82W270S6D	0	0	0	0	0	0	0	0	0	0	0	0	0	0	0	0	0	0	0	0	0	0	0	0
82WK3006D	5	0	0	0	0	0	0	0	0	0	0	0	0	0	0	0	0	0	0	0	0	0	0	0
82WK3126D	0	0	0	0	0	0	0	0	0	0	0	0	0	0	0	0	0	0	0	0	0	0	0	0
82WK3506D	0	0	0	0	0	0	0	0	0	0	0	0	0	0	0	0	0	0	0	0	0	0	0	0
82WK3656D	1	0	0	0	0	0	0	0	0	0	0	0	0	0	0	0	0	0	0	0	0	0	0	0
82WK3836D	0	0	0	0	0	0	0	0	0	0	0	0	0	0	0	0	0	0	0	0	0	0	0	0
82WM40B6D	0	0	0	0	0	0	0	0	0	0	0	0	0	0	0	0	0	0	0	0	0	0	0	0
82WM496D	0	0	0	0	0	0	0	0	0	0	0	0	0	0	0	0	0	0	0	0	0	0	0	0
82HMB15D	1	0	0	0	0	0	0	0	0	0	0	0	0	0	0	0	0	0	0	0	0	0	0	0
82HMB25D	0	0	0	0	0	0	0	0	0	0	0	0	0	0	0	0	0	0	0	0	0	0	0	0
82HMB35D	1	0	0	0	0	0	0	0	0	0	0	0	0	0	0	0	0	0	0	0	0	0	0	0
82HMB4A5D	0	0	0	0	0	0	0	0	0	0	0	0	0	0	0	0	0	0	0	0	0	0	0	0
82HMB4B5D	1	0	0	0	0	0	0	0	0	0	0	0	0	0	0	0	0	0	0	0	0	0	0	0
82HMB5A5D	0	0	0	0	0	0	0	0	0	0	0	0	0	0	0	0	0	0	0	0	0	0	0	0
82HMB5B5D	0	0	0	0	0	0	0	0	0	0	0	0	0	0	0	0	0	0	0	0	0	0	0	0
82HMB6A5D	0	0	0	0	0	0	0	0	0	0	0	0	0	0	0	0	0	0	0	0	0	0	0	0
82HMB6B5D	0	0	0	0	0	0	0	0	0	0	0	0	0	0	0	0	0	0	0	0	0	0	0	0
82HMB75D	0	0	0	0	0	0	0	0	0	0	0	0	0	0	0	0	0	0	0	0	0	0	0	0
82HMB8A5D	0	0	0	0	0	0	0	0	0	0	0	0	0	0	0	0	0	0	0	0	0	0	0	0
82HMB8B5D	0	0	0	0	0	0	0	0	0	0	0	0	0	0	0	0	0	0	0	0	0	0	0	0
82HMB8C5D	0	0	0	0	0	0	0	0	0	0	0	0	0	0	0	0	0	0	0	0	0	0	0	0
82HMB95D	0	0	0	0	0	0	0	0	0	0	0	0	0	0	0	0	0	0	0	0	0	0	0	0
82HM49F5D	0	0	0	7	0	0	0	0	0	0	0	0	0	0	0	0	0	0	0	0	0	0	0	0
82HMB10A5D	0	0	0	18	0	0	0	0	0	0	0	0	0	0	0	0	0	0	0	0	0	0	0	0
82HMB10B5D	0	0	0	0	0	0	0	0	0	0	0	0	0	0	0	0	0	0	0	0	0	0	0	0
82HMB10C5D	0	0	0	0	0	0	0	0	0	0	0	0	0	0	0	0	0	0	0	0	0	0	0	0
82HMB115D	0	0	0	0	0	0	0	0	0	0	0	0	0	0	0	0	0	0	0	0	0	0	0	0
82HMB125D	0	0	0	0	0	0	0	0	0	0	0	0	0	0	0	0	0	0	0	0	0	0	0	0
82HM1355D	0	0	0	0	0	0	0	0	0	0	0	0	0	0	0	0	0	0	0	0	0	0	0	0
82HMB135D	0	0	0	0	0	0	0	0	0	0	0	0	0	0	0	0	0	0	0	0	0	0	0	0
82HMB145D	0	0	0	0	0	0	0	0	0	0	0	0	0	0	0	0	0	0	0	0	0	0	0	0
82HMB155D	0	0	0	0	0	0	0	0	0	0	0	0	0	0	0	0	0	0	0	0	0	0	0	0
82HMB176D	0	0	0	0	0	0	0	0	0	0	0	0	0	0	0	0	0	0	0	0	0	0	0	0
82HMB186D	0	0	0	0	0	0	0	0	0	0	0	0	0	0	0	0	0	0	0	0	0	0	0	0
82HM19B6D	0	0	0	0	0	0	0	0	0	0	0	0	0	0	0	0	0	0	0	0	0	0	0	0
82HMB206D	0	0	0	0	0	0	0	0	0	0	0	0	0	0	0	0	0	0	0	0	0	0	0	0
82HMB216D	0	0	0	0	0	0	0	0	0	0	0	0	0	0	0	0	0	0	0	0	0	0	0	0
82HMB226D	0	0	0	0	0	0	0	0	0	0	0	0	0	0	0	0	0	0	0	0	0	0	0	0
82HMB236D	10	0	0	0	0	0	0	0	0	0	0	0	0	0	0	0	0	0	0	0	0	0	0	0
82HM23A6f	0	0	0	0	0	0	0	0	0	0	0	0	0	0	0	0	0	0	0	0	0	0	0	0
82HMB246D	0	0	0	0	0	0	0	0	0	0	0	0	0	0	0	0	0	0	0	0	0	0	0	0

	Escharopora	*Heterotrypa*	*Prasopora*	*Rhindictya*	*massive trepostome*	*bifoliate bryozoan*	*bumpy ramose*	*encrusting bryozoan*	*thick ramose*	*thin ramose 1*	*thin ramose 2*	*cog crinoid*	*cog star crinoid*	*thin ring crinoid*	*thick ring crinoid*	*flower crinoid*	*pentagonal crinoid*	*stacked crinoid*	*star crinoid*	*inner star crinoid*	*striped crinoid*	*striped flower crinoid*	*striped star crinoid*	*crinoidea indet.*
82WK305D	0	0	0	0	0	0	0	0	2	0	12	0	0	0	0	0	0	0	0	0	0	0	0	20
82WK375D	0	0	0	0	0	0	0	0	0	0	14	0	0	0	0	0	0	0	0	0	0	0	0	20
82WK425D	0	0	0	0	0	0	0	0	0	0	4	0	0	0	0	0	0	0	0	0	0	0	0	0
82WK785D	0	0	0	0	0	0	0	0	0	0	0	0	0	0	0	0	0	0	0	0	0	0	0	1
82WK1305D	0	0	1	0	0	0	0	0	0	0	7	0	0	0	0	0	0	0	0	0	0	0	0	0
82WK1325D	0	0	0	0	0	0	0	0	0	0	2	0	0	0	0	0	0	0	0	0	0	0	0	0
82WK1405D	0	0	0	0	0	0	0	0	1	0	0	0	0	0	0	0	0	0	0	0	0	0	0	0
82W175A5D	0	0	0	0	0	0	0	0	1	0	0	0	0	0	0	0	0	0	0	0	0	0	0	0
82WK1856D	0	0	0	0	0	0	0	0	0	0	0	0	0	0	0	0	0	0	0	0	0	0	0	0
82WK2046D	0	0	0	0	0	0	0	0	0	0	0	0	0	0	0	0	0	0	0	0	0	0	0	0
82WK2116D	0	0	0	0	0	0	0	0	0	0	0	0	0	0	0	0	0	0	0	0	0	0	0	0
82WK2306D	0	0	5	0	0	0	0	0	0	0	0	0	0	0	0	0	0	0	0	0	0	0	0	0
82WK2506D	0	0	0	0	0	0	0	0	0	0	6	0	0	0	0	0	0	0	0	0	0	0	0	0
82W260S6D	0	0	11	0	0	0	0	0	1	0	4	0	0	0	0	0	0	0	0	0	0	0	0	0
82WK2606D	0	0	97	0	0	0	0	0	0	0	2	0	0	0	0	0	0	0	0	0	0	0	0	0
82WK2706D	0	0	0	0	0	0	0	0	0	0	1	0	0	0	0	0	0	0	0	0	0	0	0	0
82W270S6D	0	0	0	0	0	0	0	0	0	0	1	0	0	0	0	0	0	0	0	0	0	0	0	0
82WK3006D	0	0	0	0	0	0	0	0	0	0	0	0	0	0	0	0	0	0	0	0	0	0	0	0
82WK3126D	0	0	1	0	0	0	0	0	0	0	1	0	0	0	0	0	0	0	0	0	0	0	0	0
82WK3506D	0	0	0	0	0	0	0	0	0	0	1	0	0	0	0	0	0	0	0	0	0	0	0	0
82WK3656D	0	0	0	0	0	0	0	0	0	0	0	0	0	0	0	0	0	0	0	0	0	0	0	0
82WK3836D	0	0	0	0	0	0	0	0	0	0	0	0	0	0	0	0	0	0	0	0	0	0	0	0
82WM40B6D	0	0	2	0	0	0	0	0	0	0	0	0	0	0	0	0	0	0	0	0	0	0	0	0
82WM496D	0	0	0	0	0	0	0	0	0	0	2	0	0	0	0	0	0	0	0	0	0	0	0	0
82HMB15D	0	0	0	0	0	0	0	0	0	0	5	0	0	0	0	0	0	0	0	0	0	0	0	0
82HMB25D	0	0	0	0	0	0	0	0	0	0	3	0	0	0	0	0	0	0	0	0	0	0	0	0
82HMB35D	0	0	0	0	0	0	0	0	0	0	3	0	0	0	0	0	0	0	0	0	0	0	0	0
82HMB4A5D	0	0	0	0	0	0	0	1	0	0	1	0	0	0	0	0	0	0	0	0	0	0	0	1
82HMB4B5D	0	0	0	0	0	0	0	0	0	0	3	0	0	0	0	0	0	0	0	0	0	0	0	1
82HMB5A5D	0	0	0	0	0	0	0	0	0	0	1	0	0	0	0	0	0	0	0	0	0	0	0	0
82HMB5B5D	0	0	0	0	0	0	0	0	0	0	18	0	0	0	0	0	0	0	0	0	0	0	0	1
82HMB6A5D	0	0	0	0	0	0	0	0	0	0	0	0	0	0	0	0	0	0	0	0	0	0	0	1
82HMB6B5D	0	0	0	0	0	0	0	0	0	0	4	0	0	0	0	0	0	0	0	0	0	0	0	0
82HMB75D	0	0	1	0	0	0	0	0	0	0	2	0	0	0	0	0	0	0	0	0	0	0	0	2
82HMB8A5D	0	0	0	0	0	0	0	1	0	0	2	0	0	0	0	0	0	0	0	0	0	0	0	2
82HMB8B5D	0	0	4	0	0	0	0	2	12	0	0	0	0	0	0	0	0	0	0	0	0	0	0	0
82HMB8C5D	0	0	11	0	0	0	0	0	0	0	1	0	0	0	0	0	0	0	0	0	0	0	0	1
82HMB95D	0	0	11	0	0	0	0	0	7	0	0	0	0	0	0	0	0	0	0	0	0	0	0	0
82HM49F5D	0	0	2	0	0	0	0	0	0	0	4	0	0	0	0	0	0	0	0	0	0	0	0	1
82HMB10A5D	0	0	4	0	0	0	0	0	0	0	3	0	0	0	0	0	0	0	0	0	0	0	0	1
82HMB10B5D	0	0	8	0	0	0	0	1	16	0	8	0	0	0	0	0	0	0	0	0	0	0	0	3
82HMB10C5D	0	0	6	0	0	0	0	0	0	0	49	0	0	0	0	0	0	0	0	0	0	0	0	1
82HMB115D	0	0	0	0	0	0	0	0	0	0	42	0	0	0	0	0	0	0	0	0	0	0	0	1
82HMB125D	0	0	0	0	0	0	0	0	0	0	11	0	0	0	0	0	0	0	0	0	0	0	0	0
82HM1355D	0	0	0	0	0	0	0	0	0	0	6	0	0	0	0	0	0	0	0	0	0	0	0	4
82HMB135D	0	0	0	0	0	0	0	0	0	0	18	0	0	0	0	0	0	0	0	0	0	0	0	0
82HMB145D	0	0	0	0	0	0	0	0	2	0	0	0	0	0	0	0	0	0	0	0	0	0	0	0
82HMB155D	0	0	0	0	0	0	0	0	0	0	3	0	0	0	0	0	0	0	0	0	0	0	0	0
82HMB176D	0	0	0	0	0	0	0	0	0	0	9	0	0	0	0	0	0	0	0	0	0	0	0	1
82HMB186D	0	0	0	0	0	0	0	0	0	0	20	0	0	0	0	0	0	0	0	0	0	0	0	2
82HM19B6D	0	0	0	0	0	0	0	6	0	0	29	0	0	0	0	0	0	0	0	0	0	0	0	9
82HMB206D	0	0	0	0	0	0	0	0	5	0	1	0	0	0	0	0	0	0	0	0	0	0	0	0
82HMB216D	0	0	0	0	0	0	0	0	0	0	0	0	0	0	0	0	0	0	0	0	0	0	0	0
82HMB226D	0	0	0	0	0	0	0	0	21	0	11	0	0	0	0	0	0	0	0	0	0	0	0	0
82HMB236D	0	0	0	0	0	0	0	0	4	0	0	0	0	0	0	0	0	0	0	0	0	0	0	0
82HM23A6f	0	0	0	0	0	0	0	0	119	0	0	0	0	0	0	0	0	0	0	0	0	0	0	0
82HMB246D	0	0	0	0	0	0	0	0	9	0	0	0	0	0	0	0	0	0	0	0	0	0	0	0

	Echinodermata indet.	*orthoconic nautiloids*	*algal coating*	*Solenopora*	*Stromatoporoids*	*Chondrites*	*Diplocriterion*	*Cornulites*	*alga(Hindia?)*	*rhombiferan plate*	*graptolites*
82WK305D	0	0	0	0	0	0	0	0	0	0	0
82WK375D	0	0	0	0	0	0	0	0	0	0	0
82WK425D	0	0	0	0	0	0	0	0	0	0	0
82WK785D	0	0	0	0	0	0	0	0	0	0	0
82WK1305D	0	0	0	0	0	0	0	0	0	0	0
82WK1325D	0	0	0	0	0	0	0	0	0	0	0
82WK1405D	0	0	0	0	0	0	0	0	0	0	0
82W175A5D	0	0	0	0	0	0	0	0	0	0	0
82WK1856D	0	0	0	0	0	0	0	0	0	0	0
82WK2046D	0	0	0	0	0	0	0	0	0	0	0
82WK2116D	0	0	0	0	0	0	0	0	0	0	0
82WK2306D	0	0	0	0	0	0	0	0	0	0	0
82WK2506D	0	0	0	0	0	0	0	0	0	0	0
82W260S6D	0	0	0	0	0	0	0	0	0	0	0
82WK2606D	0	0	0	0	0	0	0	0	0	0	0
82WK2706D	0	0	0	0	0	0	0	0	0	0	0
82W270S6D	0	0	0	0	0	0	0	0	0	0	0
82WK3006D	0	0	0	0	0	0	0	0	0	0	0
82WK3126D	0	0	0	0	0	0	0	0	0	0	0
82WK3506D	0	0	0	0	0	0	0	0	0	0	0
82WK3656D	0	0	0	0	0	0	0	0	0	0	0
82WK3836D	0	0	0	0	0	0	0	0	0	0	0
82WM40B6D	0	0	0	0	0	0	0	0	0	0	0
82WM496D	0	0	0	0	0	0	0	0	0	0	0
82HMB15D	0	0	0	0	0	0	0	0	0	0	0
82HMB25D	0	0	0	0	0	0	0	0	0	0	0
82HMB35D	0	0	0	0	0	0	0	0	0	0	0
82HMB4A5D	0	0	0	0	0	0	0	0	0	0	0
82HMB4B5D	0	0	0	0	0	0	0	0	0	0	0
82HMB5A5D	0	0	0	0	0	0	0	0	0	0	0
82HMB5B5D	0	0	0	0	0	0	0	0	0	0	0
82HMB6A5D	0	0	0	0	0	0	0	0	0	0	0
82HMB6B5D	0	0	0	0	0	0	0	0	0	0	0
82HMB75D	0	0	0	0	0	0	0	0	0	0	0
82HMB8A5D	0	0	0	0	0	0	0	0	0	0	0
82HMB8B5D	0	0	0	0	0	0	0	0	0	0	0
82HMB8C5D	0	0	0	0	0	0	0	0	0	0	0
82HMB95D	0	0	0	0	0	0	0	0	0	0	0
82HM49F5D	0	0	0	0	0	0	0	0	0	0	0
82HMB10A5D	0	0	0	0	0	0	0	0	0	0	0
82HMB10B5D	0	0	0	0	0	0	0	0	0	0	0
82HMB10C5D	0	0	0	0	0	0	0	0	0	0	0
82HMB115D	0	0	0	0	0	0	0	0	0	0	0
82HMB125D	0	0	0	0	0	0	0	0	0	0	0
82HM1355D	0	0	0	0	0	0	0	0	0	0	0
82HMB135D	0	0	0	0	0	0	0	0	0	0	0
82HMB145D	0	0	0	0	0	0	0	0	0	0	0
82HMB155D	0	0	0	0	0	0	0	0	0	0	0
82HMB176D	0	0	0	0	0	0	0	0	0	0	0
82HMB186D	0	0	0	0	0	0	0	0	0	0	0
82HM19B6D	0	0	0	0	0	0	0	0	0	0	0
82HMB206D	0	0	0	0	0	0	0	0	0	0	0
82HMB216D	0	0	0	0	0	0	0	0	0	0	0
82HMB226D	0	0	0	0	0	0	0	0	0	0	0
82HMB236D	0	0	0	0	0	0	0	0	0	0	0
82HM23A6f	0	0	0	0	0	0	0	0	0	0	0
82HMB246D	0	0	0	0	0	0	0	0	0	0	0

	Anazyga	*Bilobia*	*Camerella*	*Christiana*	*Dalmanella*	*Dinorthis*	*Doleroides*	*Eoplectodonta*	*Glyptorthis*	*Hebertella*	*Hesperorthis*	*Heterorthina*	*Leptaena*	*Lingula*	*Multicostella*	*Oepikina*	*Orthorhyncula*	*Oxoplecia*	*Paucicrura*	*Paurorthis*	*Pionodema*	*Platystrophia*	*Plectocamara*	*Rafinesquina*
82HMB256D	0	0	0	0	0	0	0	0	0	48	0	0	0	0	0	0	0	0	0	0	0	0	0	0
82HMB266D	0	0	0	0	0	0	0	0	0	0	0	0	0	0	0	0	0	0	0	0	0	3	0	7
82HMB276D	0	0	0	0	0	0	0	0	0	8	0	0	0	0	0	0	0	0	0	0	0	0	0	46
82H062F5D	0	0	0	0	94	0	0	0	0	0	0	0	0	0	0	0	0	0	0	0	0	0	0	13
82DNR15D	0	0	0	0	21	0	0	0	0	0	0	0	0	0	0	0	0	0	0	0	0	0	0	15
82DNR25D	0	0	0	0	101	0	0	0	0	0	0	0	0	0	0	0	0	0	0	0	0	0	0	39
82DNR35D	0	0	0	0	40	0	0	0	0	0	0	0	0	0	0	0	0	0	0	0	0	0	0	4
82DNR45D	0	0	0	0	66	0	0	0	0	0	0	0	0	0	0	0	0	0	0	0	0	0	0	31
82DNR55D	0	0	0	0	6	0	0	0	0	0	0	0	0	0	0	0	0	0	0	0	0	0	0	42
82DNR65D	0	0	0	0	10	0	0	0	0	0	0	0	0	0	0	0	0	0	0	0	0	0	0	32
82DNR75D	0	0	0	0	9	0	0	0	0	0	0	0	0	0	0	0	0	0	0	0	0	0	0	8
82DNR105D	0	0	0	0	33	0	0	0	0	0	0	0	0	0	0	0	0	0	0	0	0	0	0	25
82DNR115D	0	0	0	0	17	0	0	0	0	0	0	0	0	0	0	0	0	0	0	0	0	0	0	14
82DNR125D	0	0	0	0	1	0	0	0	0	0	0	0	0	0	0	0	0	0	0	0	0	0	0	25
82DNR135D	0	0	0	0	20	0	0	0	0	0	0	0	0	0	0	0	0	0	0	0	0	0	0	0
82DNR146D	0	0	0	0	18	0	0	0	0	0	0	0	0	0	0	0	0	0	0	0	0	0	0	0
82DNR156D	0	0	0	0	0	0	0	0	0	0	0	0	0	0	0	0	0	0	0	0	0	0	0	69
82DNR166D	0	0	0	0	0	0	0	0	0	0	0	0	0	0	0	0	0	0	0	0	0	0	0	0
82DNR1756D	0	0	0	0	4	0	0	0	0	0	0	0	0	0	0	0	0	0	0	0	0	0	0	2
82DNR186D	0	0	0	0	10	0	0	0	0	0	0	0	0	0	0	0	0	0	0	0	0	0	0	1
82DNR196D	0	0	0	0	0	0	0	0	0	0	0	0	0	0	0	0	0	0	0	0	0	0	0	19
82DNR206D	0	0	0	0	36	0	0	0	0	0	0	0	0	0	0	0	0	0	0	0	0	0	0	12
82DNR226D	0	0	0	0	14	0	0	0	0	0	0	0	0	0	0	0	0	0	0	0	0	0	0	0
82DNR236D	0	0	0	0	57	0	0	0	0	0	0	0	0	0	0	0	0	0	0	0	0	0	0	4
82DNR246D	0	0	0	0	1	0	0	0	0	0	0	0	0	0	0	0	0	0	0	0	0	0	0	1
82DNR256D	0	0	0	0	44	0	0	0	0	0	0	0	0	0	0	0	0	0	0	0	0	0	0	4
82DNR26A6D	0	0	0	0	0	0	0	0	0	0	0	0	0	0	0	0	0	0	0	0	0	0	0	0
82DNR266D	0	0	0	0	23	0	0	0	0	0	0	0	0	0	0	0	0	0	0	0	0	0	0	12
82DNR276D	0	0	0	0	0	0	0	0	0	0	0	0	0	0	0	0	0	0	0	0	0	0	0	13
82DN28C6D	0	0	0	0	0	0	0	0	0	0	0	0	0	0	0	0	0	0	0	0	0	0	0	0
82DNR286D	0	0	0	0	3	0	0	0	0	0	0	0	0	0	0	0	0	0	0	0	0	0	0	1
82DNR306D	0	0	0	0	7	0	0	0	0	0	0	0	0	0	0	0	0	0	0	0	0	0	0	1
82DNR316D	0	0	0	0	1	0	0	0	0	0	0	0	0	0	0	0	0	0	0	0	0	0	0	7
82DNR326D	0	0	0	0	1	0	0	0	0	0	0	0	0	0	0	0	0	0	0	0	0	0	0	1
82DNR336D	0	0	0	0	17	0	0	0	0	0	0	0	0	0	0	0	0	0	0	0	0	0	0	0
82DNR346D	0	0	0	0	5	0	0	0	0	0	0	0	0	0	0	0	0	0	0	0	0	0	0	0
82DNR356D	0	0	0	0	6	0	0	0	0	0	0	0	0	0	0	0	0	0	0	0	0	0	0	0
82DNR406D	0	0	0	0	1	0	0	0	0	3	0	0	0	0	0	0	0	0	0	0	0	0	0	55
82DNR416D	0	0	0	0	0	0	0	0	0	0	0	0	0	0	0	0	0	0	0	0	0	0	0	5
82DN41A6D	0	0	0	0	3	0	0	0	0	0	0	0	0	0	0	0	0	0	0	0	0	0	0	1

	Rhynchotrema	*Rostricellula*	*Schizotreta*	*Strophomena*	*Sowerbyella*	*Zygospira*	*Inarticulata indet.*	*rhynchonellid indet.*	*Brachiopoda indet.*	*Ceraurus*	*Cryptolithus*	*Eomonorachus*	*Flexicalymene*	*Gravicalymene*	*Isotelus*	*Pterygometopus*	*Trilobita A*	*Trilobita indet.*	*Isotelus spines*	*Bellerophon*	*Bucania*	*Cyclonema*	*Hormotoma*	*Liospira*
82HMB256D	0	0	0	0	0	2	0	0	0	0	0	0	0	0	0	0	0	0	0	0	0	0	0	0
82HMB266D	0	0	0	0	0	3	0	0	0	0	0	0	0	0	2	0	0	0	0	0	0	0	0	0
82HMB276D	0	0	0	0	0	22	0	0	0	0	0	0	0	0	8	0	0	0	0	0	0	0	0	0
82H062F5D	1	0	0	0	5	0	0	0	0	0	0	0	0	0	1	0	0	0	0	0	0	0	0	0
82DNR15D	0	0	0	0	4	0	0	0	0	0	0	0	0	0	20	0	0	0	0	0	0	0	0	0
82DNR25D	0	0	0	0	43	0	0	0	0	0	0	0	2	0	12	0	0	0	0	0	0	0	0	0
82DNR35D	0	0	0	0	13	1	0	0	0	0	0	0	0	0	26	0	0	0	0	0	0	0	0	0
82DNR45D	0	0	0	0	20	0	0	0	0	0	0	0	0	0	5	0	0	0	0	0	0	0	0	0
82DNR55D	0	0	0	0	0	0	0	0	0	0	0	0	0	0	21	0	0	0	0	0	0	0	0	0
82DNR65D	0	0	0	0	0	0	0	0	0	0	0	0	0	0	10	0	0	0	0	0	0	0	0	0
82DNR75D	0	0	0	0	0	0	0	0	0	0	0	0	0	0	10	0	0	0	0	0	0	0	0	0
82DNR105D	0	0	0	0	3	0	0	0	0	0	0	0	0	0	20	0	0	0	0	0	0	0	0	0
82DNR115D	0	0	0	0	33	2	0	0	0	0	0	0	0	0	5	0	0	0	0	0	2	0	0	0
82DNR125D	0	0	0	0	30	0	0	0	0	0	0	0	0	0	20	0	0	0	0	0	0	0	0	0
82DNR135D	0	0	0	0	7	0	0	0	0	0	0	0	1	0	10	0	0	0	0	0	12	0	0	0
82DNR146D	0	0	0	0	15	0	0	0	0	0	0	0	0	0	16	0	0	0	0	0	0	0	0	0
82DNR156D	0	0	0	0	0	0	0	0	0	0	0	0	0	0	69	0	0	0	0	0	10	0	0	0
82DNR166D	0	0	0	0	0	0	0	0	0	0	0	0	0	0	0	0	0	0	0	0	3	0	0	0
82DNR1756D	0	0	0	0	0	0	0	0	0	0	0	0	0	0	4	0	0	0	0	0	13	0	0	0
82DNR186D	0	0	0	0	0	0	0	0	0	0	0	0	0	0	4	0	0	0	0	0	2	0	0	0
82DNR196D	0	0	0	0	7	18	0	0	0	0	0	0	0	0	10	0	0	0	0	0	0	0	0	0
82DNR206D	0	0	0	0	5	22	0	0	0	0	0	0	0	0	1	0	0	0	0	0	0	0	0	0
82DNR226D	0	0	0	0	36	12	0	0	0	0	0	0	0	0	1	0	0	0	0	0	0	0	0	0
82DNR236D	0	0	0	0	104	11	0	0	0	0	0	0	0	0	11	0	0	0	0	0	0	0	0	0
82DNR246D	0	0	0	0	8	19	0	0	0	0	0	0	0	0	0	0	0	0	0	0	10	0	0	0
82DNR256D	0	0	0	0	22	34	0	0	0	0	0	0	0	0	7	0	0	0	0	0	0	0	0	0
82DNR26A6D	0	0	0	0	20	10	0	0	0	0	0	0	0	0	0	0	0	0	0	0	0	0	0	0
82DNR266D	0	0	0	0	76	78	0	0	0	0	0	0	0	0	9	0	0	0	0	0	0	0	0	0
82DNR276D	0	0	0	0	0	182	0	0	0	0	0	0	0	0	13	0	0	0	0	0	0	0	0	0
82DN28C6D	0	0	0	0	1	46	0	0	0	0	0	0	0	0	2	0	0	0	0	0	3	0	0	0
82DNR286D	0	0	0	0	0	2	0	0	0	0	0	0	1	0	4	0	0	0	0	0	0	0	0	0
82DNR306D	0	0	0	0	114	12	0	0	0	0	0	0	0	0	8	0	0	0	0	0	0	0	0	0
82DNR316D	0	0	0	0	146	10	0	0	0	0	0	0	0	0	14	0	0	0	0	0	0	0	0	0
82DNR326D	0	0	0	0	215	9	0	0	0	0	0	0	0	0	20	0	0	0	0	0	0	0	0	0
82DNR336D	0	0	0	0	28	73	0	0	0	0	0	0	0	0	14	0	0	0	0	0	0	0	0	0
82DNR346D	0	0	0	0	75	10	0	0	0	0	0	0	0	0	0	0	0	0	0	0	0	0	0	0
82DNR356D	0	0	0	0	38	8	0	0	0	0	0	0	0	0	1	0	0	0	0	0	0	0	0	0
82DNR406D	0	0	0	0	0	0	0	0	0	0	0	0	0	0	29	0	0	0	0	0	0	0	0	0
82DNR416D	0	0	0	0	0	3	0	0	0	0	0	0	0	0	12	0	0	0	0	0	0	0	0	0
82DN41A6D	0	0	0	0	0	0	0	0	0	0	0	0	0	0	0	0	0	0	0	0	0	0	0	0

	Lophospira	*Maclurites*	*Sinuites*	*Gastropoda indet.*	*Cyclora*	*Ambonychia*	*Ctenodonta*	*Cunemya*	*Cyrtodonta*	*Cyrtodontula*	*Deceptrix*	*Ischyrodonta*	*modiomorph*	*Lyrodesma*	*Paleoneilo*	*Whitella*	*Bivalvia indet.*	*leperditid ostracod*	*Columnaria*	*Streptelasma*	*Tetradium*	*Stromatoporoidea*	*Chasmatopora*	*Constellaria*
82HMB256D	23	0	0	0	0	0	0	0	0	0	0	0	0	0	0	0	0	0	0	0	0	0	0	0
82HMB266D	0	0	0	0	0	1	0	0	0	0	0	0	0	0	0	0	0	0	0	0	0	0	0	0
82HMB276D	0	0	0	0	0	0	0	0	0	0	0	0	0	0	0	0	0	0	0	0	0	0	0	0
82H062F5D	0	0	0	0	0	0	0	0	0	0	0	0	0	0	0	0	0	0	0	0	0	0	0	0
82DNR15D	0	0	0	0	0	0	0	0	0	0	0	0	0	0	0	0	0	0	0	0	0	0	0	0
82DNR25D	4	0	0	0	0	0	0	0	0	0	0	0	0	0	0	0	0	0	0	0	0	0	0	0
82DNR35D	0	0	0	0	0	0	0	0	0	0	0	0	0	0	0	0	0	0	0	0	0	0	0	0
82DNR45D	0	0	0	0	0	0	0	0	0	0	0	0	0	0	0	0	0	0	0	0	0	0	0	0
82DNR55D	0	0	0	0	0	0	0	0	0	0	0	0	0	0	0	0	0	0	0	0	0	0	0	0
82DNR65D	0	0	0	0	0	0	0	0	0	0	0	0	0	0	0	0	0	0	0	0	0	0	0	0
82DNR75D	0	0	0	0	0	0	0	0	0	0	0	0	0	0	0	0	0	0	0	0	0	0	0	0
82DNR105D	0	0	0	0	0	0	0	0	0	0	0	0	0	0	0	0	0	0	0	0	0	0	0	0
82DNR115D	0	0	0	0	0	0	0	0	0	0	0	0	0	0	0	0	0	0	0	0	0	0	0	0
82DNR125D	0	0	0	0	0	0	0	0	0	0	0	0	0	0	0	0	0	0	0	0	0	0	0	0
82DNR135D	0	0	0	0	0	0	0	0	0	0	0	0	0	0	0	0	0	0	0	0	0	0	0	0
82DNR146D	0	0	0	0	0	0	0	0	0	0	0	0	0	0	0	0	0	0	0	0	0	0	0	0
82DNR156D	0	0	0	0	0	0	0	0	0	0	0	0	0	0	0	0	0	0	0	0	0	0	0	0
82DNR166D	30	0	0	0	0	0	0	0	0	0	0	0	0	0	0	0	0	0	0	0	0	0	0	0
82DNR1756D	0	0	0	0	0	0	0	0	0	0	0	0	0	0	0	0	0	0	0	0	0	0	0	0
82DNR186D	0	0	0	0	0	0	0	0	0	0	0	0	0	0	0	0	0	0	0	0	0	0	0	0
82DNR196D	0	0	0	0	0	0	0	0	0	0	0	0	0	0	0	0	0	0	0	0	0	0	0	0
82DNR206D	0	0	0	0	0	0	0	0	0	0	0	0	0	0	0	0	0	0	0	0	0	0	0	0
82DNR226D	0	0	0	0	0	0	0	0	0	0	0	0	0	0	0	0	0	0	0	0	0	0	0	0
82DNR236D	0	0	0	0	0	0	0	0	0	0	0	0	0	0	0	0	0	0	0	0	0	0	0	0
82DNR246D	1	0	0	0	0	0	0	0	0	0	0	0	0	0	0	0	0	0	0	0	0	0	0	0
82DNR256D	0	0	0	0	0	0	0	0	0	0	0	0	0	0	0	0	0	0	0	0	0	0	0	0
82DNR26A6D	0	0	0	0	0	0	0	0	0	0	0	0	0	0	0	0	0	0	0	0	0	0	0	0
82DNR266D	0	0	0	0	0	0	0	0	0	0	0	0	0	0	0	0	0	0	0	0	0	0	0	0
82DNR276D	0	0	0	0	0	0	0	0	0	0	0	0	0	0	0	0	0	0	0	0	0	0	0	0
82DN28C6D	24	0	0	0	0	0	0	0	0	0	0	0	0	0	0	0	0	0	0	0	0	0	0	0
82DNR286D	1	0	0	0	0	0	0	0	0	0	0	0	0	0	0	0	0	0	0	0	0	0	0	0
82DNR306D	0	0	0	0	0	0	0	0	0	0	0	0	0	0	0	0	0	0	0	0	0	0	0	0
82DNR316D	0	0	0	0	0	0	0	0	0	0	0	0	0	0	0	0	0	0	0	0	0	0	0	0
82DNR326D	0	0	0	0	0	0	0	0	0	0	0	0	0	0	0	0	0	0	0	0	0	0	0	0
82DNR336D	0	0	0	0	0	0	0	0	0	0	0	0	0	0	0	0	0	0	0	0	0	0	0	0
82DNR346D	0	0	0	0	0	0	0	0	0	0	0	0	0	0	0	0	0	0	0	0	0	0	0	0
82DNR356D	0	0	0	0	0	0	0	0	0	0	0	0	0	0	0	0	0	0	0	0	0	0	0	0
82DNR406D	0	0	0	0	0	0	0	0	0	0	0	0	0	0	0	0	0	0	0	0	0	0	0	0
82DNR416D	0	0	0	0	0	0	0	0	0	0	0	0	0	0	0	0	0	0	0	0	0	0	0	0
82DN41A6D	0	0	0	0	0	2	0	0	0	0	0	0	0	0	0	0	0	0	0	0	0	0	0	0

	Escharopora	*Heterotrypa*	*Prasopora*	*Rhindictya*	*massive trepostome*	*bifoliate bryozoan*	*bumpy ramose*	*encrusting bryozoan*	*thick ramose*	*thin ramose 1*	*thin ramose 2*	*cog crinoid*	*cog star crinoid*	*thin ring crinoid*	*thick ring crinoid*	*flower crinoid*	*pentagonal crinoid*	*stacked crinoid*	*star crinoid*	*inner star crinoid*	*striped crinoid*	*striped flower crinoid*	*striped star crinoid*	*crinoidea indet.*
82HMB256D	0	0	3	0	0	0	0	0	14	0	0	0	0	0	0	0	0	0	0	0	0	0	0	0
82HMB266D	0	0	0	0	0	0	0	0	20	0	0	0	0	0	0	0	0	0	0	0	0	0	0	0
82HMB276D	0	0	0	0	0	0	0	0	45	0	7	0	0	0	0	0	0	0	0	0	0	0	0	0
82H062F5D	0	0	2	0	0	0	0	0	0	0	38	0	0	0	0	0	0	0	0	0	0	0	0	1
82DNR15D	0	0	0	0	0	0	0	0	0	0	0	0	0	0	0	0	0	0	0	0	0	0	0	0
82DNR25D	0	0	0	0	0	0	0	0	0	0	0	0	0	0	0	0	0	0	0	0	0	0	0	0
82DNR35D	0	0	0	0	0	0	0	0	0	0	0	0	0	0	0	0	0	0	0	0	0	0	0	0
82DNR45D	0	0	0	0	0	0	0	0	0	0	0	0	0	0	0	0	0	0	0	0	0	0	0	0
82DNR55D	0	0	0	0	0	0	0	0	0	0	0	0	0	0	0	0	0	0	0	0	0	0	0	0
82DNR65D	0	0	0	0	0	0	0	0	0	0	0	0	0	0	0	0	0	0	0	0	0	0	0	0
82DNR75D	0	0	0	0	0	0	0	0	0	0	0	0	0	0	0	0	0	0	0	0	0	0	0	0
82DNR105D	0	0	0	0	0	0	0	0	0	0	16	0	0	0	0	0	0	0	0	0	0	0	0	0
82DNR115D	0	0	1	0	0	0	0	0	0	0	0	0	0	0	0	0	0	0	0	0	0	0	0	0
82DNR125D	0	0	0	0	0	0	0	0	0	0	1	0	0	0	0	0	0	0	0	0	0	0	0	3
82DNR135D	0	0	0	0	0	0	0	0	0	0	5	0	0	0	0	0	0	0	0	0	0	0	0	0
82DNR146D	0	0	0	0	0	0	0	0	0	0	1	0	0	0	0	0	0	0	0	0	0	0	0	0
82DNR156D	0	0	5	0	0	0	0	0	5	0	0	0	0	0	0	0	0	0	0	0	0	0	0	0
82DNR166D	0	0	0	0	0	0	0	0	0	0	0	0	0	0	0	0	0	0	0	0	0	0	0	0
82DNR1756D	0	0	2	0	0	0	0	0	0	0	4	0	0	0	0	0	0	0	0	0	0	0	0	0
82DNR186D	0	0	7	0	0	0	0	0	0	0	5	0	0	0	0	0	0	0	0	0	0	0	0	2
82DNR196D	0	0	0	0	0	0	0	0	0	0	6	0	0	0	0	0	0	0	0	0	0	0	0	0
82DNR206D	0	0	0	0	0	0	0	0	0	0	2	0	0	0	0	0	0	0	0	0	0	0	0	1
82DNR226D	0	0	9	0	0	0	0	0	0	0	0	0	0	0	0	0	0	0	0	0	0	0	0	3
82DNR236D	0	0	0	0	0	0	0	0	0	0	2	0	0	0	0	0	0	0	0	0	0	0	0	2
82DNR246D	0	0	1	0	0	0	0	0	0	0	4	0	0	0	0	0	0	0	0	0	0	0	0	0
82DNR256D	0	0	0	0	0	0	0	0	0	0	13	0	0	0	0	0	0	0	0	0	0	0	0	1
82DNR26A6D	0	0	0	0	0	0	0	0	0	0	0	0	0	0	0	0	0	0	0	0	0	0	0	0
82DNR266D	0	0	0	0	0	0	0	0	0	0	1	0	0	0	0	0	0	0	0	0	0	0	0	25
82DNR276D	0	0	0	0	0	0	0	0	9	0	0	0	0	0	0	0	0	0	0	0	0	0	0	0
82DN28C6D	0	0	0	0	0	0	0	0	2	0	0	0	0	0	0	0	0	0	0	0	0	0	0	0
82DNR286D	0	0	0	0	0	0	0	0	0	0	0	0	0	0	0	0	0	0	0	0	0	0	0	0
82DNR306D	0	0	1	0	0	0	0	0	0	0	0	0	0	0	0	0	0	0	0	0	0	0	0	0
82DNR316D	0	0	0	0	0	0	0	0	0	0	0	0	0	0	0	0	0	0	0	0	0	0	0	1
82DNR326D	0	0	0	0	0	0	0	0	0	0	0	0	0	0	0	0	0	0	0	0	0	0	0	1
82DNR336D	0	0	0	0	0	0	0	0	0	0	0	0	0	0	0	0	0	0	0	0	0	0	0	0
82DNR346D	0	0	2	0	0	0	0	0	0	0	1	0	0	0	0	0	0	0	0	0	0	0	0	0
82DNR356D	0	0	0	0	0	0	0	0	0	0	0	0	0	0	0	0	0	0	0	0	0	0	0	0
82DNR406D	0	0	0	0	0	0	0	0	0	0	16	0	0	0	0	0	0	0	0	0	0	0	0	1
82DNR416D	0	0	0	0	0	0	0	0	0	0	4	0	0	0	0	0	0	0	0	0	0	0	0	0
82DN41A6D	0	0	0	0	0	0	0	0	0	0	0	0	0	0	0	0	0	0	0	0	0	0	0	0

	Echinodermata indet.	*orthoconic nautiloids*	*algal coating*	*Solenopora*	*Stromatoporoids*	*Chondrites*	*Diplocriterion*	*Cornulites*	*alga(Hindia?)*	*rhombiferan plate*	*graptolites*
82HMB256D	0	0	0	0	0	0	0	0	0	0	0
82HMB266D	0	0	0	0	0	0	0	0	0	0	0
82HMB276D	0	0	0	0	0	0	0	0	0	0	0
82H062F5D	0	0	0	0	0	0	0	0	0	0	0
82DNR15D	0	0	0	0	0	0	0	0	0	0	0
82DNR25D	0	0	0	0	0	0	0	0	0	0	0
82DNR35D	0	0	0	0	0	0	0	0	0	0	0
82DNR45D	0	0	0	0	0	0	0	0	0	0	0
82DNR55D	0	0	0	0	0	0	0	0	0	0	0
82DNR65D	0	0	0	0	0	0	0	0	0	0	0
82DNR75D	0	0	0	0	0	0	0	0	0	0	0
82DNR105D	0	0	0	0	0	0	0	0	0	0	0
82DNR115D	0	0	0	0	0	0	0	0	0	0	0
82DNR125D	0	0	0	0	0	0	0	0	0	0	0
82DNR135D	0	0	0	0	0	0	0	0	0	0	0
82DNR146D	0	0	0	0	0	0	0	0	0	0	0
82DNR156D	0	0	0	0	0	0	0	0	0	0	0
82DNR166D	0	0	0	0	0	0	0	0	0	0	0
82DNR1756D	0	0	0	0	0	0	0	0	0	0	0
82DNR186D	0	0	0	0	0	0	0	0	0	0	0
82DNR196D	0	0	0	0	0	0	0	0	0	0	0
82DNR206D	0	0	0	0	0	0	0	0	0	0	0
82DNR226D	0	0	0	0	0	0	0	0	0	0	0
82DNR236D	0	0	0	0	0	0	0	0	0	0	0
82DNR246D	0	0	0	0	0	0	0	0	0	0	0
82DNR256D	0	0	0	0	0	0	0	0	0	0	0
82DNR26A6D	0	0	0	0	0	0	0	0	0	0	0
82DNR266D	0	0	0	0	0	0	0	0	0	0	0
82DNR276D	0	0	0	0	0	0	0	0	0	0	0
82DN28C6D	0	0	0	0	0	0	0	0	0	0	0
82DNR286D	0	0	0	0	0	0	0	0	0	0	0
82DNR306D	0	0	0	0	0	0	0	0	0	0	0
82DNR316D	0	0	0	0	0	0	0	0	0	0	0
82DNR326D	0	0	0	0	0	0	0	0	0	0	0
82DNR336D	0	0	0	0	0	0	0	0	0	0	0
82DNR346D	0	0	0	0	0	0	0	0	0	0	0
82DNR356D	0	0	0	0	0	0	0	0	0	0	0
82DNR406D	0	0	0	0	0	0	0	0	0	0	0
82DNR416D	0	0	0	0	0	0	0	0	0	0	0
82DN41A6D	0	0	0	0	0	0	0	0	0	0	0

APPENDIX E

Collector curves. Based on pilot work conducted during first summer of fieldwork.

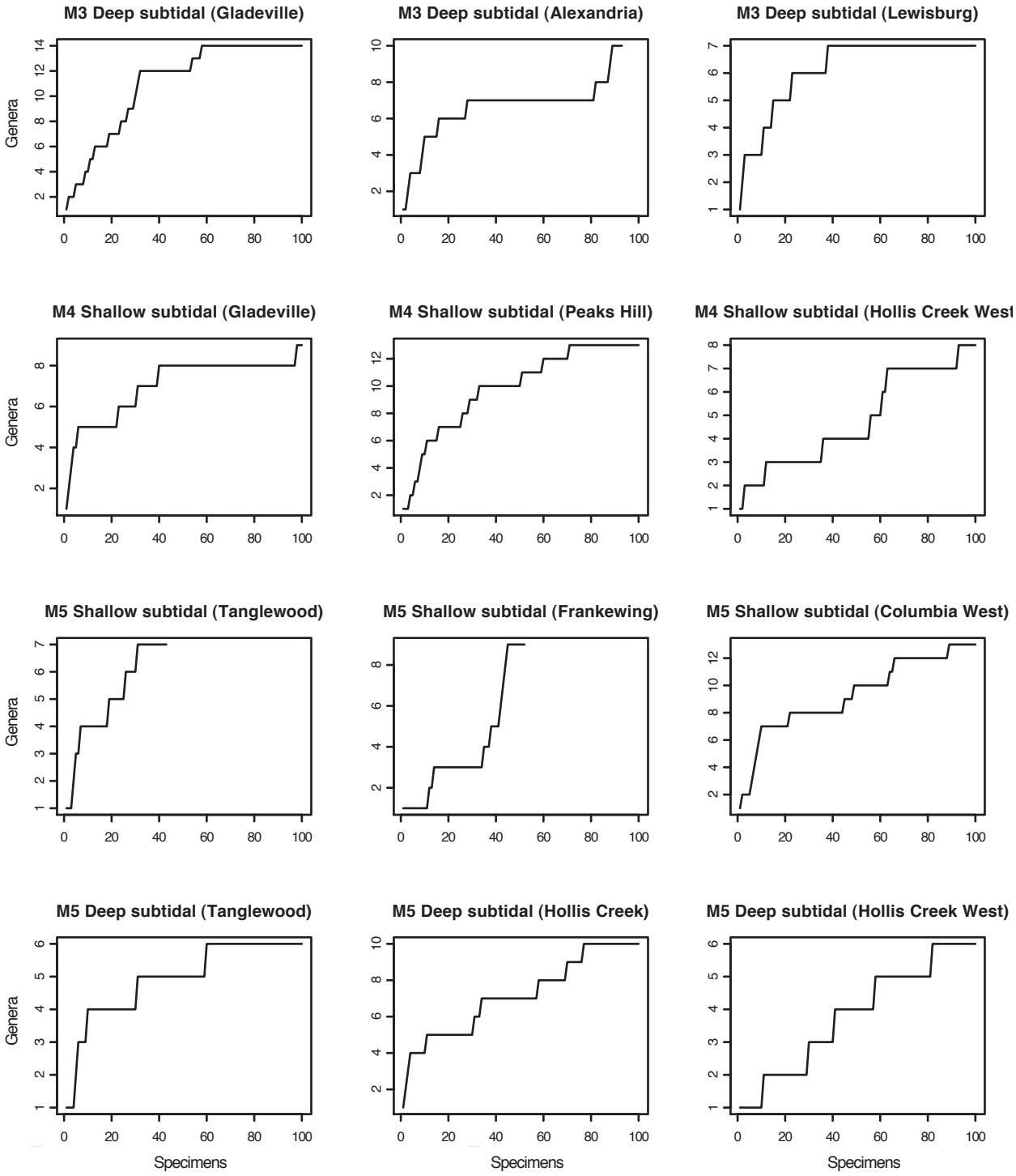
M3 Deep subtidal (Gladeville)
M3 Deep subtidal (Alexandria)
M3 Deep subtidal (Lewisburg)
M4 Shallow subtidal (Gladeville)
M4 Shallow subtidal (Peaks Hill)
M4 Shallow subtidal (Hollis Creek West
M5 Shallow subtidal (Tanglewood)
M5 Shallow subtidal (Frankewing)
M5 Shallow subtidal (Columbia West)
M5 Deep subtidal (Tanglewood)
M5 Deep subtidal (Hollis Creek)
M5 Deep subtidal (Hollis Creek West)
Genera
Specimens

APPENDIX F

Data analyses with bryozoans and crinoids excluded.

1. Changes in mean diversity and evenness metrics across the M4/M5 boundary based on subsampled subsets of field data, including holdovers and new taxa. 95% confidence limit reported is for difference of means. 95%UCL = 95% upper confidence limit; 95%LCL = 95% lower confidence limit; SS = all shallow subtidal samples; DS = all deep subtidal samples.

	S	*H*	*E*	Pielou's *J*	*PIE*
M3/4 (All)	25.003	2.488	0.486	0.774	0.845
M5 (All)	17.179	2.048	0.457	0.722	0.801
95%UCL	8.027	0.452	0.033	0.054	0.047
95%LCL	7.621	0.428	0.025	0.049	0.042
M3/4 (SS)	20.276	2.372	0.532	0.789	0.868
M5 (SS)	18.427	2.201	0.495	0.757	0.832
95%UCL	2.025	0.180	0.041	0.034	0.037
95%LCL	1.673	0.161	0.033	0.030	0.034
M3/4 (DS)	20.276	2.372	0.532	0.789	0.868
M5 (DS)	15.318	1.861	0.426	0.684	0.761
95%UCL	7.760	0.428	0.009	0.047	0.037
95%LCL	7.362	0.403	0.001	0.041	0.030

M3/4 (Tennessee)	17.777	2.028	0.432	0.706	0.764
M5 (Tennessee)	16.535	2.359	0.645	0.843	0.889
95%UCL	1.404	-0.320	-0.209	-0.134	-0.122
95%LCL	1.080	-0.340	-0.217	-0.140	-0.127
M3/4 (Kentucky)	13.755	1.940	0.509	0.741	0.776
M5 (Kentucky)	18.474	1.963	0.390	0.674	0.767
95%UCL	-4.561	-0.013	0.123	0.069	0.012
95%LCL	-4.877	-0.033	0.116	0.064	0.007
M3/4 (Virginia)	19.299	2.545	0.664	0.861	0.908
M5 (Virginia)	11.712	1.628	0.442	0.665	0.726
95%UCL	7.738	0.926	0.225	0.198	0.184
95%LCL	7.436	0.908	0.218	0.194	0.180

2. Changes in mean diversity and evenness metrics across the M5/M6 boundary based on subsampled subsets of field data, including holdovers and new taxa. 95% confidence limit reported is for difference of means. 95%UCL = 95% upper confidence limit; 95%LCL = 95% lower confidence limit; SS = all shallow subtidal samples; DS = all deep subtidal samples.

	S	*H*	*E*	Pielou's *J*	*PIE*
M5 (All)	17.179	2.048	0.457	0.722	0.801
M6 (All)	15.207	2.037	0.510	0.751	0.823
95%UCL	2.154	0.022	-0.050	-0.026	-0.020
95%LCL	1.790	0.001	-0.057	-0.031	-0.025
M5 (SS)	18.427	2.201	0.495	0.757	0.832
M6 (SS)	18.136	2.136	0.472	0.738	0.796
95%UCL	0.468	0.076	0.028	0.022	0.039
95%LCL	0.114	0.055	0.019	0.016	0.034
M5 (DS)	15.318	1.861	0.426	0.684	0.761
M6 (DS)	9.520	1.734	0.604	0.774	0.786
95%UCL	5.953	0.137	-0.173	-0.087	-0.023
95%LCL	5.643	0.117	-0.182	-0.093	-0.028

M5 (Tennessee)	16.535	2.359	0.645	0.843	0.889
M6 (Tennessee)	17.671	2.258	0.546	0.788	0.853
95%UCL	-0.972	0.110	0.103	0.057	0.038
95%LCL	-1.300	0.092	0.095	0.053	0.035
M5 (Kentucky)	18.474	1.963	0.390	0.674	0.767
M6 (Kentucky)	15.196	1.815	0.409	0.668	0.693
95%UCL	3.448	0.160	-0.016	0.010	0.077
95%LCL	3.108	0.136	-0.023	0.003	0.070
M5 (Virginia)	11.712	1.628	0.442	0.665	0.726
M6 (Virginia)	8.320	1.674	0.648	0.794	0.775
95%UCL	3.515	-0.037	-0.201	-0.126	-0.047
95%LCL	3.269	-0.055	-0.211	-0.132	-0.052

3. Changes in mean diversity and evenness metrics across the M4/M5 boundary based on subsampled subsets of field data, including holdovers only. 95% confidence limit reported is for difference of means. 95%UCL = 95% upper confidence limit; 95%LCL = 95% lower confidence limit; SS = all shallow subtidal samples; DS = all deep subtidal samples.

	S	*H*	*E*	Pielou's *J*	*PIE*
M3/4 (All)	25.003	2.488	0.486	0.774	0.845
M5 (All)	13.513	1.726	0.422	0.665	0.705
95%UCL	11.678	0.775	0.069	0.112	0.144
95%LCL	11.302	0.750	0.060	0.106	0.137
M3/4 (SS)	22.947	2.618	0.601	0.836	0.899
M5 (SS)	15.499	1.853	0.417	0.678	0.732
95%UCL	7.611	0.774	0.188	0.161	0.170
95%LCL	7.285	0.754	0.180	0.156	0.165
M3/4 (DS)	26.129	2.759	0.608	0.847	0.912
M5 (DS)	10.110	1.398	0.408	0.608	0.613
95%UCL	16.199	1.371	0.204	0.242	0.302
95%LCL	15.839	1.350	0.196	0.236	0.296

M3/4 (Tennessee)	21.629	2.587	0.619	0.843	0.900
M5 (Tennessee)	14.135	2.152	0.615	0.815	0.859
95%UCL	7.660	0.443	0.008	0.030	0.042
95%LCL	7.328	0.426	0.000	0.025	0.039
M3/4 (Kentucky)	15.837	2.452	0.712	0.877	0.901
M5 (Kentucky)	8.497	0.700	0.242	0.328	0.277
95%UCL	7.445	1.728	0.472	0.551	0.626
95%LCL	7.235	1.711	0.467	0.546	0.620
M3/4 (Virginia)	23.437	2.762	0.679	0.877	0.927
M5 (Virginia)	4.737	1.073	0.627	0.697	0.602
95%UCL	18.823	1.696	0.057	0.183	0.327
95%LCL	18.577	1.682	0.047	0.176	0.323

4. Changes in mean diversity and evenness metrics across the M5/M6 boundary based on subsampled subsets of field data, including holdovers only. 95% confidence limit reported is for difference of means. 95%UCL = 95% upper confidence limit; 95%LCL = 95% lower confidence limit; SS = all shallow subtidal samples; DS = all deep subtidal samples.

	S	*H*	*E*	Pielou's *J*	*PIE*
M5 (All)	13.513	1.726	0.422	0.665	0.705
M6 (All)	13.115	1.945	0.540	0.759	0.813
95%UCL	0.552	-0.209	-0.114	-0.091	-0.105
95%LCL	0.244	-0.230	-0.123	-0.097	-0.111
M5 (SS)	15.499	1.853	0.417	0.678	0.732
M6 (SS)	13.178	1.797	0.464	0.699	0.733
95%UCL	2.473	0.068	-0.043	-0.018	0.002
95%LCL	2.169	0.046	-0.052	-0.025	-0.005
M5 (DS)	10.110	1.398	0.408	0.608	0.613
M6 (DS)	9.024	1.713	0.623	0.783	0.783
95%UCL	1.201	-0.306	-0.210	-0.172	-0.167
95%LCL	0.971	-0.324	-0.220	-0.179	-0.174

M5 (Tennessee)	14.135	2.152	0.615	0.815	0.859
M6 (Tennessee)	12.721	1.956	0.563	0.773	0.814
95%UCL	1.554	0.202	0.056	0.045	0.047
95%LCL	1.274	0.186	0.047	0.040	0.044
M5 (Kentucky)	8.497	0.700	0.242	0.328	0.277
M6 (Kentucky)	11.430	1.463	0.384	0.602	0.597
95%UCL	-2.811	-0.752	-0.138	-0.270	-0.315
95%LCL	-3.055	-0.755	-0.145	-0.279	-0.324
M5 (Virginia)	4.737	1.073	0.627	0.697	0.602
M6 (Virginia)	8.148	1.668	0.657	0.798	0.775
95%UCL	-3.345	-0.588	-0.024	-0.097	-0.170
95%LCL	-3.477	-0.601	-0.036	-0.105	-0.175

APPENDIX G

Tables of most abundant taxa by sequence for each facies and region.

1. Ten most abundant taxa in the shallow subtidal facies within each sequence ranked by relative abundance. Thin ramose 1, thin ramose 2, thick ramose, and trepostome refer to distinct bryozoan morphologies.

M4		M5		M6	
Strophomena	0.15	Thick ramose	0.22	Thick ramose	0.20
Leperditid ostracod	0.10	Thin ramose 2	0.15	*Zygospira*	0.19
Escharopora	0.10	*Zygospira*	0.13	Thin ramose 1	0.12
Tetradium	0.08	*Hebertella*	0.06	*Hebertella*	0.08
Rhindictya	0.06	Trepostome	0.05	*Escharopora*	0.07
Lophospira	0.05	*Rhindictya*	0.05	*Rhynchotrema*	0.05
Thin ring crinoid	0.05	*Rafinesquina*	0.04	*Rafinesquina*	0.04
Thick ring crinoid	0.04	*Escharopora*	0.04	*Constellaria*	0.04
Thin ramose 2	0.03	*Prasopora*	0.03	*Platystrophia*	0.03
Maclurites	0.03	*Lophospira*	0.03	Thick ring crin.	0.02
TOTAL	0.69	TOTAL	0.80	TOTAL	0.84

2. Ten most abundant taxa in the deep subtidal facies within each sequence ranked by relative abundance. Thin ramose 1, thin ramose 2 and thick ramose refer to distinct bryozoan morphologies.

M4		M5		M6	
Leperditid ostracod	0.27	*Dalmanella*	0.34	*Sowerbyella*	0.28
Escharopora	0.15	*Rafinesquina*	0.18	*Zygospira*	0.20
Rhindictya	0.06	*Sowerbyella*	0.07	*Rafinesquina*	0.11
Thin ramose 2	0.05	Thin ramose 1	0.06	*Dalmanella*	0.10
Thick ramose	0.05	*Isotelus*	0.06	*Isotelus*	0.07
Pionodema	0.05	Thin ramose 2	0.05	Thin ramose 1	0.06
Hesperorthis	0.03	*Zygospira*	0.05	Thick ramose	0.05
Trilobita indet.	0.03	*Deceptrix*	0.04	*Prasopora*	0.03
Strophomena	0.03	Thick ramose	0.02	*Lophospira*	0.02
Rostricellula	0.03	Trilobita indet.	0.02	*Hebertella*	0.01
TOTAL	0.75	TOTAL	0.89	TOTAL	0.93

3. Ten most abundant taxa in Tennessee within each sequence ranked by relative abundance. Thin ramose 1, thin ramose 2, thick ramose, and trepostome refer to distinct bryozoan morphologies.

M4		M5		M6	
Leperditid ostracod	0.26	Thick ramose	0.25	Thick ramose	0.20
Escharopora	0.16	*Deceptrix*	0.09	Thin ramose 1	0.19
Strophomena	0.07	*Dalmanella*	0.09	*Zygospira*	0.12
Rhindictya	0.06	Thin ramose 1	0.08	*Hebertella*	0.08
Thin ramose 1	0.05	*Hebertella*	0.07	*Escharopora*	0.07
Thick ramose	0.05	Trepostome	0.06	*Rafinesquina*	0.05
Pionodema	0.04	*Tetradium*	0.05	*Platystrophia*	0.04
Hesperorthis	0.03	*Escharopora*	0.04	*Constellaria*	0.04
Rostricellula	0.03	*Zygospira*	0.04	*Lophospira*	0.03
Thin ring crinoid	0.03	*Rhynchotrema*	0.04	*Rhynchotrema*	0.02
TOTAL	0.78	TOTAL	0.81	TOTAL	0.84

4. Ten most abundant taxa in Kentucky within each sequence ranked by relative abundance. Thin ramose 1, thin ramose 2, thick ramose, encrusting, and bifoliate refer to distinct bryozoan morphologies.

M4		M5		M6	
Tetradium	0.29	Thin ramose 1	0.23	*Zygospira*	0.32
Trepostome	0.09	*Zygospira*	0.18	Thick ramose	0.19
Lophospira	0.08	Thick ramose	0.08	Thin ramose 1	0.05
Strophomena	0.07	*Dalmanella*	0.08	*Rhynchotrema*	0.03
Thick ramose	0.07	*Rhindictya*	0.06	Bifoliate bryo	0.03
Thin ring crinoid	0.05	*Rafinesquina*	0.05	*Hebertella*	0.03
Zygospira	0.05	*Escharopora*	0.05	Stromatoporoid	0.03
Ortho. nautiloids	0.04	*Prasopora*	0.04	*Rafinesquina*	0.03
Maclurites	0.03	Encrusting bryo.	0.04	*Orthorhyncula*	0.03
Leperditid ostracod	0.03	Thick ring crinoid	0.03	Thin ramose 2	0.02
TOTAL	0.80	TOTAL	0.84	TOTAL	0.76

5. Ten most abundant taxa in Virginia within each sequence ranked by relative abundance. Thin ramose 1, thin ramose 2 and thick ramose refer to distinct bryozoan morphologies.

M4		M5		M6	
Gastropoda indet.	0.14	*Dalmanella*	0.39	*Sowerbyella*	0.31
Sowerbyella	0.11	*Rafinesquina*	0.22	*Zygospira*	0.18
Trilobita indet.	0.11	*Sowerbyella*	0.10	*Rafinesquina*	0.11
Rhindictya	0.08	Thin ramose 2	0.08	*Dalmanella*	0.11
Eoplectodonta	0.07	*Isotelus*	0.06	*Isotelus*	0.07
Bilobia	0.06	Trilobita indet.	0.02	Thin ramose 2	0.06
Christiana	0.06	*Bucania*	0.02	Thick ramose	0.05
Brachiopoda indet.	0.05	Crinoidea indet.	0.02	*Prasopora*	0.03
Paucicrura	0.05	*Prasopora*	0.01	*Lophospira*	0.02
Escharopora	0.03	*Rhynchotrema*	0.01	*Hebertella*	0.01
TOTAL	0.76	TOTAL	0.93	TOTAL	0.95